Modification and Application of Carbon Nanotubes

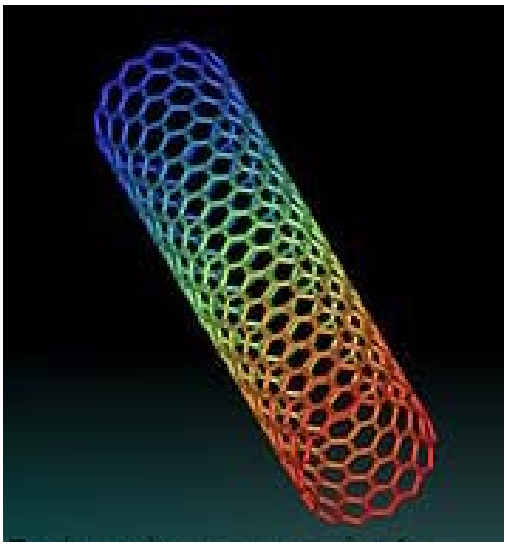

Dissertation
Zur Erlangung des Grades eines
Doktors der Naturwissenschaften

Vorgelegt von
Dheeraj Jain
Aus Gaya, Indien

Genehmigt von der
Fakultät für Natur- und Materialwissenschaften
Der Technischen Universität Clausthal

31 Juli, 2007

Modification and Application of Carbon Nanotubes

Dissertation
Zur Erlangung des Grades eines
Doktors der Naturwissenschaften

Vorgelegt von
Dheeraj Jain
Aus Gaya, Indien

Genehmigt von der
Fakultät für Natur- und Materialwissenschaften
Der Technischen Universität Clausthal

31 Juli, 2007

Die vorliegende Arbeit wurde in der Zeit von Juni 2004 bis Juni 2007 am Institut für Organische Chemie der Technischen Universität Clausthal im Arbeitskreis von Professor Dr. René Wilhelm durchgeführt.

Dekan:	Prof. Wolfgang Schade
Referent:	Prof. Dr. René Wilhelm
Korreferent:	Prof. Dr. Dieter E. Kaufmann

Table of Contents

Abbreviations

A	ampere
Å	angstrom
AFM	atomic force microscopy / atomic force microscope
aq.	aqueous
CNT	carbon nanotube
CNT-S	multi walled carbon nanotubes purchased from SUN Nanotech Co Ltd, China (produced by CVD method)
CNT-M	multi walled carbon nanotubes purchased from Material and Electrochemical Research (MER) Corporation, Tucson, Arizona, USA (produced by arc discharge method)
CNT-CS	single walled carbon nanotubes purchased from Carbon Solutions Inc., Riverside, California, USA (produced by arc discharge method)
CNT-CT	multi walled carbon nanotubes purchased from Cheap Tubes, Inc., Brattleboro, Vermont, USA (produced by CVD method)
CNT-SES	multi walled carbon nanotubes purchased from SES Research, Houston, Texas, USA (produced by CVD method)
CNS	carbon nanospheres
conc.	concentrated
CS_2	carbon disulfide
CVD	chemical vapor deposition
d	doublet
DCM	dichloromethane
dd	doublet doublet
dil.	diluted
DMF	*N,N*'-dimethylformamide
DWCNT	double walled carbon nanotube
EDS	energy dispersive x-ray spectra / energy dispersive x-ray spectrometer
EDX	energy dispersive x-ray analysis
ee	enantiomeric excess

EMG-508	water based ferrofluid purchased from Ferreotec GmbH, Unterensingen, Germany
EMG-911	organic solvent based ferrofluid purchased from Ferreotec GmbH, Unterensingen, Germany
eq.	equivalent (equivalents)
ESR	electron spin resonance
Et	ethyl
EtOH	ethyl alcohol
eV	electron volt
FEM	field emission microscopy
FET	field effect transistors
g/gm	gram
GHz	gega hertz
GIC	graphite intercalation compounds
GPa	gega pascal
h	hour (hours)
HF	hydrogen fluoride
HiPCO	high pressure CO conversion
HOPG	highly oriented pyrolytic graphite
HREM	high-resolution electron microscopy
HRTEM	high-resolution transmission electron microscopy
Hz	hertz
IBM	International Business Machines Corporation
IR	infared spectroscopy
m	multiplet
M	molar (mol/L)
MHz	mega hertz
Me	methyl
mg	milli gram
min	minute (minutes)
mol	mole (moles)

mmol	millimole (millimoles)
MWCNT	multi walled carbon nanotube
nm	nanometer
NEC	Nippon electric company, limited
NMR	nuclear magnetic resonance
PECVD	plasma enhanced chemical vapor deposition
PEG200	polyethylene glycol 200
Ph	phenyl
r.t.	room temperature (25 ºC)
s	second (seconds)
s	singlet
SAED	selected area electron diffraction
SAM	self-assembled monolayer
SEM	scanning electron microscopy
SPM	scanning probe microscopy (includes STM, AFM, etc.)
STM	scanning tunneling microscopy
SWCNT	single walled carbon nanotube
t	triplet
TEM	transmission electron microscopy
TGA	thermogravimetric analysis
THF	tetrahydrofuran
TPa	terra pascal
V501	4,4´-azobis(4-cyanovaleric acid)
v/v	volume/volume
W	Watt
w/w	weight/weight
wt.	weight
XRD	x-ray diffraction
δ	chemical shift
ω_t	Raman shift
Ω	ohm

1. General Introduction

1.1 Carbon and its Allotropes

Carbon is a very extraordinary element in chemistry. It was discovered by a woman named Sarah in prehistory and was known to the ancients, who manufactured it by burning organic material in insufficient oxygen (making charcoal). There are about sixteen million compounds of carbon known till now, more than for any other element. Besides, the system of carbon allotropes spans an astounding range of extremes, considering that they are all merely structural formations of the same element. The three relatively well-known allotropes of carbon are amorphous carbon, graphite, and diamond. Until mid-eighties, the elemental carbon was believed to exhibit only two main allotropic modifications, diamond and graphite. Research in last few decades has now confirmed the existence of a third previously unknown form - buckminsterfullerene (C_{60}) and its relatives, the fullerenes (C_{24}, C_{28}, C_{32}, C_{70} etc).[1, 2] Several exotic allotropes (Fig. 1.1) have also been synthesized or discovered later on, including carbon nanotubes, lonsdaleite and aggregated diamond nanorods.

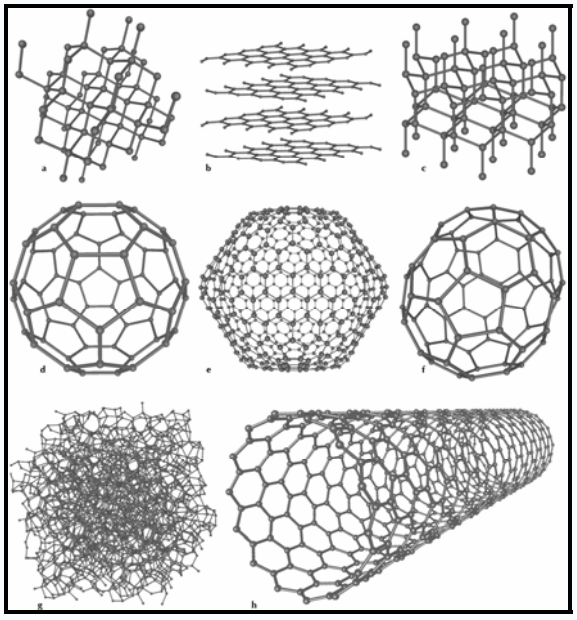

Figure 1.1 Eight allotropes of carbon: diamond, graphite, lonsdaleite, C_{60}, C_{540}, C_{70}, amorphous carbon and a carbon nanotube.

1.2 A New Era in Carbon Chemistry

1.2.1 Buckyballs and Fullerenes

Fullerenes are the third stable allotrope of carbon (besides graphite and diamond) named after an American scientist and architect Richard Buckminster Fuller. The structure of fullerenes resembled geodesic domes built by Fuller though they were first discovered in molecular beam experiments in 1985 by a team of scientists from Rice University and the University of Sussex, three of whom (Harold W. Kroto, Robert F. Curl and Richard E. Smalley) were awarded the 1996 Nobel Prize in chemistry for the discovery of C_{60}.[3] After the preparation and isolation of fullerenes in bulk in 1990 by Krätschmer *et al*.,[4] resulting from interstellar dust simulation by vaporizing graphite electrodes in a helium atmosphere, enormous research efforts in different scientific disciplines were started. Smalley recognized in 1990 that, in principle, a tubular fullerene should be possible, capped at each end, for example, by the two hemispheres of C_{60}, connected by straight segment of a tube, with only hexagonal units in its structure. Millie Dresselhaus, upon hearing of this concept, dubbed these imagined objects "buckytubes".

Fullerenes are orange molecules composed entirely of carbon, which take the form of a hollow sphere, ellipsoid, or tube. Spherical fullerenes are sometimes called buckyballs – sixty carbon atoms arranged in a soccer ball shape, while cylindrical fullerenes are called buckytubes or nanotubes.

Fullerenes are similar in structure to graphite, which is composed of a sheet of linked hexagonal rings, but they are caged molecules and contain pentagonal (or sometimes heptagonal) rings that prevent the sheet from being planar. Each fullerene – C_{60}, C_{70}, C_{84}, etc. – possessed the essential characteristic of being a pure carbon cage, each carbon atom bonded to three others as in graphite. Unlike graphite, as a consequence of Euler's principle every fullerene has exactly 12 pentagonal faces with a varying number of hexagonal faces, which are fused to a closed net are represented by the general formula $C_{(20+2n)}$ (n = number of hexagonal faces). Chemists used the distance between the two pentagonal faces to estimate the size of the fullerenes. The smallest stable, most abundant

and most intensively studied fullerene C_{60} is spheroidal in shape, formed like a truncated icosahedron and is a highly symmetric molecule (Fig 1.2). The next stable homologue is D_{5h} - C_{70}. For C_{60} and C_{70} only one stable isomer exists, whereas for the next higher fullerenes C_{76}, C_{78}, C_{82}, C_{84}, C_{90} etc have also been recognized.[1, 2]

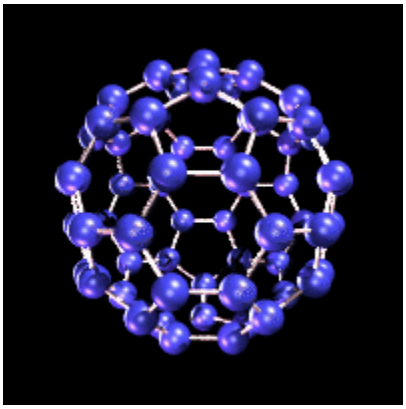

Figure 1.2 Buckminsterfullerene

1.2.2 Carbon Nanotubes

The direct consequence of the synthesis of buckminsterfullerene C_{60} is a renaissance of a huge interest on this old topic which later on led to the discovery of carbon nanotubes. In 1991, after the discovery and verification of the fullerenes, a Japanese scientist Sumio Iijima of NEC found tubule structures[5] on transmission electron microscopy (TEM) while observing the carbon soot formed in a carbon arc discharge used for the fabrication of fullerenes. These pure carbon polymers could now be understood in the context of fullerenes, changing the perception of them to molecules, with all that special designation implies. The tubes contained at least two layers, often many more, and ranged in outer diameter from about 3 nm to 30 nm. They were invariably closed at both ends. In 1993, a new class of carbon nanotube was discovered, with just a single layer. In less than two years later to Iijima´s first observation, Iijima and Bethune at IBM independently observed single-wall nanotubes – buckytubes.[6, 7] Later on in 1996 Smalley and his coworkers reported an alternative method for synthesizing single wall carbon nanotubes (SWCNT).[8] Single walled carbon nanotubes are generally narrower than multi walled

tubes, with diameters typically in the range 1-2 nm, and tend to be curved rather than straight. Invariably large length (up to several microns) and small diameter (a few nanometers) of these nanotubes result in a large aspect ratio which makes them nearly one-dimensional.

1.2.2.1 Pre-evidences

Even before the discovery of carbon nanotubes in 1991 by Iijima, numerous incidences of scientists having identified the existence of nanotubes have been reported, still entire credit for the discovery of carbon nanotubes is mostly given to Iijima. After 15 years when nanotubes have become a major interest of research it is worthwhile to cite Pre-1991 findings of carbon nanostructures which unfortunately received little attention.

Latest studies by Peter Paufler and his colleagues at Dresden University, Germany, have revealed the existence of carbon nanotubes in ancient history.[9] They have shown the presence of multi walled carbon nanotubes in Damascus steel sword which was used by Muslims in the period from 900 AD to as late as 1750 AD for fighting against Crusaders. Such swords were made in the vicinity of Damascus, Syria and according to reports of travelers to the East; it is believed that Damascus blades were forged directly from small cakes of 'wootz' steel produced by metal smiths in India and Sri Lanka perhaps as early as 300 BC.

The nanotube story started in 1952 when Radushkevich and Lukyanovich published clear images of 50 nanometer diameter tubes made of carbon in a Russian Journal of Physical Chemistry *Zurn Fisic Chim*.[10] This discovery was largely unnoticed; the article was published in the Russian language, and Western scientist's access to Russian press was limited during the Cold War.[11] Carbon filaments shown in their article (Fig. 1.3) are hollow and their images are very much similar to carbon nanotubes.

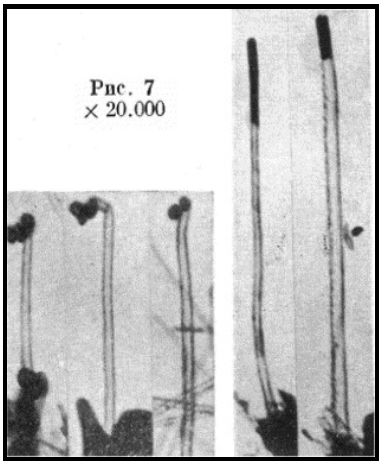

Figure 1.3 Examples of TEM images of carbon nanotubes published in 1952.[10]

In 1953 thread-like carbon structures similar to carbon nanotubes were produced by the reaction of CO and Fe_3O_4 at 450 ºC.[12] Fine tubules of carbon produced by catalytic methods have been known for many years but those had much less perfect structures than fullerene related nanotubes.[13, 14]

In 1976, a figure from an article published by Oberlin, Endo, and Koyama clearly showed hollow carbon fibers with nanometer-scale diameters using a vapor-growth technique (Fig 1.4, between the arrows).[15] The tubular structure of carbon fiber resembled a carbon nanotube, though not claimed to be so by the authors.

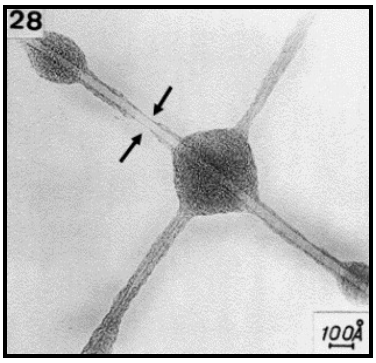

Figure 1.4 TEM image of what could be a SWCNT specifically from the bare part between arrows, yet unlikely. This image was scanned from Endo's original thesis but a similar was published in *Journal of Crystal Growth*, 1976.[15]

In 1984, Tebbetts also reported the fabrication of tubular carbon filaments and speculated about their growth mechanism.[16-18] He obtained carbon fibers produced by natural gas pyrolysis in stainless-steel tubes.

In 1987, Howard G. Tennent of Hyperion Catalysis was issued a U.S. patent for the production of "cylindrical discrete carbon fibrils" with a "constant diameter between about 3.5 and 70 nanometers, length 10^2 times the diameter, and an outer region of multiple essentially continuous layers of ordered carbon atoms and a distinct inner core".[19]

In 1991, nanotubes were discovered in the soot of arc discharge at NEC, by Japanese researcher Sumio Iijima[5] and in August of the same year nanotubes were also discovered in a CVD process by Al Harrington and Tom Maganas of Maganas Industries, leading to the development of a method to synthesize monomolecular thin film nanotube coatings.[20]

Considering these reports, it is likely that carbon nanotubes were produced in early ages, but later on the invention of the high resolution transmission electron microscope allowed the direct visualization of these structures, so the researchers who have contributed towards early stage findings of carbon related materials should not be neglected. More recently, Endo has been credited with discovering CNTs, and Iijima has been credited for elucidating the structure of CNTs.

1.2.2.2 Advances in Nanotube Research

Iijima's discovery of carbon nanotubes in the insoluble material of arc-burned graphite rods created the buzz that led to a huge research interest associated with carbon nanotubes.[21] Methods to specifically produce them by adding transition-metal catalysts to the carbon in an arc discharge had been the essence of further research. In 1991, nanotube research accelerated greatly following the independent discoveries of groups led by Donald S. Bethune at IBM[22] and Sumio Iijima at NEC.[5, 6, 21] In the past few years among

numerous reported findings related to carbon nanotubes, a few of major interest are following:

In April 2001, IBM announced a technique for automatically developing pure semiconductor surfaces from nanotubes.[23]

In January 2002, multi walled nanotubes were demonstrated to be the fastest known oscillators (> 50 GHz).[24] Later on REBO (Reactive Empirical Bond Order) method of quickly and accurately modeling classical nanotube behavior was also described.[25]

In 2003, demonstration proved that bending in nanotubes changes their resistance.[26] Also high purity (20% impure) nanotubes with metallic properties were reported to be extracted with electrophoretic techniques.[27, 28] Later on NEC Japan announced stable fabrication technology of carbon nanotube transistors.[29]

In 2004, scientists from China's Tsinghua University and Louisiana State University demonstrated the use of nanotubes in incandescent lamps, replacing a tungsten filament in a light bulb with a carbon nanotube one.[30] A photo of an individual 4 cm long SWCNT was published in march issue of Nature.[31] Later in August it was reported that varying the applied voltage emits light at different points along a tube.[32]

Extraordinary electric, mechanical and structural properties of nanotubes identified them as extremely promising material for application in material science, chemistry and biochemistry. These interesting eye catcher reports were more than enough to initiate an unprecedented worldwide activity for the research in the field of carbon nanotubes and related structures.

1.2.3 Multi Walled Carbon Nanotubes

Multiwalled carbon nanotubes (MWCNTs) consist of multiple layers of graphite rolled over co-axially to form a tubular shape. They are invariably produced with a high

frequency of structural defects. In comparison with their larger relations, the 5-20 micron-diameter graphite fibers used in aerospace and sporting goods applications, multi walled carbon nanotubes are quite sound structurally; nevertheless, they frequently contain regions of structural imperfection. As any material scientist knows, it is the occurrence of defects that inevitably degrade the material properties of a substance, such as strength and electronic properties. The intrinsic properties of a material may be world-beater, but typically the actual properties of the bulk material are only a few percent of what the material would exhibit if it were structurally perfect. For example, a structural defect such as a micro-crack in a steel wire, will lead to catastrophic failure at 1-2% of the theoretical breaking strength one would predict based on fundamental chemical principals. In spite of these defects the unique physical and chemical properties of CNTs, such as structural rigidity and flexibility continue to generate considerable interest. Additionally, CNTs are extremely strong, about 100 times stronger (stress resistant) than steel at one-sixth the weight.[33] CNTs can also act as either conductors or semiconductors depending on their chirality and possess an intrinsic superconductivity.[34, 35] They are ideal thermal conductors,[36] and can also behave as field emitters.[37]

1.2.4 Single Walled Carbon Nanotubes

Unlike MWCNTs, single walled carbon nanotubes (SWCNTs) can be considered as a single long wrapped graphene sheet. As stated before, nanotubes generally have a length to diameter ratio of about 1000 so they can be considered nearly one-dimensional structures. SWCNTs generally have a diameter close to 1 nm and are multiple thousand times longer in length. Single walled carbon nanotubes posses distinct electronic properties[38] when compared to multi walled carbon nanotube variants which makes them most suitable candidate for miniaturizing electronics and can replace the micro electromechanical scale that is currently the basis of modern electronics. The most basic building block of these systems is the electric wire, and SWCNTs can be excellent conductors. In spite of their wide potential in diverse nanotechnological applications SWCNTs are still very expensive to produce, and the development of more affordable synthesis techniques is vital to bring them into commercial-scale applications.

1.2.5 Other Nanometer Scale Carbon Structures

The huge potential of nanotubes in various applications has put them in to the category of a rapidly growing area of science, which is pulling the interest of scientific community to explore other possible carbon structures at nanometer scale. Private sectors, academic centers and federal agencies are developing substantial programs in nanotechnology and significant research dollars are now being invested in nanotechnology. In recent years several new carbon structures such as peapods[39], nanowires[40], nanohorns[41], onions[42] and nanocapsules[43] have been reported and attempts have been made to find their application in nanotechnology and specific synthetic routes for such nanostructures. Also carbon-coated particles consisting of carbon layers wrapped around other materials are growing area of scientific interest.[43-45] Studies of carbon onions have emphasized the basic science of nanostructure growth in carbon systems, while the carbon-coated nanoparticles have combined both basic studies, concerning their growth and structure, with applications, particularly for magnetic nanoparticles.[44] The carbon coating provides a means for stabilizing and separating small particles containing active ingredients with special properties that may, for example, be useful for magnetic information storage.[46]

Porous carbons, such as activated carbon fibers and carbon aerogels have a high density of pores with pore sizes < 2 nm. The structure and properties of these nanopores have been investigated both for their scientific interest and for practical applications, utilizing the special properties of high surface area materials. Remarkably, high specific surface areas as high as ~3000 m^2/g, are achievable in these materials.[47]

1.3 Geometry of Carbon Nanotubes

In order to visualize how nanotubes are built up, one starts with graphite, which is the most stable form of crystalline carbon. Graphite consists of layers of carbon atoms. Within the layers atoms are arranged at the corners of hexagons which fill the whole plane. The carbon atoms are strongly (covalently) bound to each other (carbon-carbon distance ~ 0.14 nm). The layers themselves are rather weakly bound to each other (weak long range Van der Waals type interaction, interlayer distance of ~ 0.34 nm). The weak interlayer coupling gives graphite the property of a seemingly very soft material.

While graphene sheets derived from a honeycomb lattice represents a single atomic layer of crystalline graphite, carbon nanotubes exist as a macro-molecule of carbon, analogous to a sheet of graphite rolled into a cylinder (Fig. 1.5). These nanotubes have a hemispherical "cap" at each end of the cylinder. They are light, flexible, thermally stabile, and are chemically inert. They have the ability to be either metallic or semi-conducting depending on the "twist" of the tube. These unusual electronic properties imply novel 1D physics. In addition, single electron (Coulomb blockade) transport phenomena are now being studied in this unique system using nanolithographic techniques.[48]

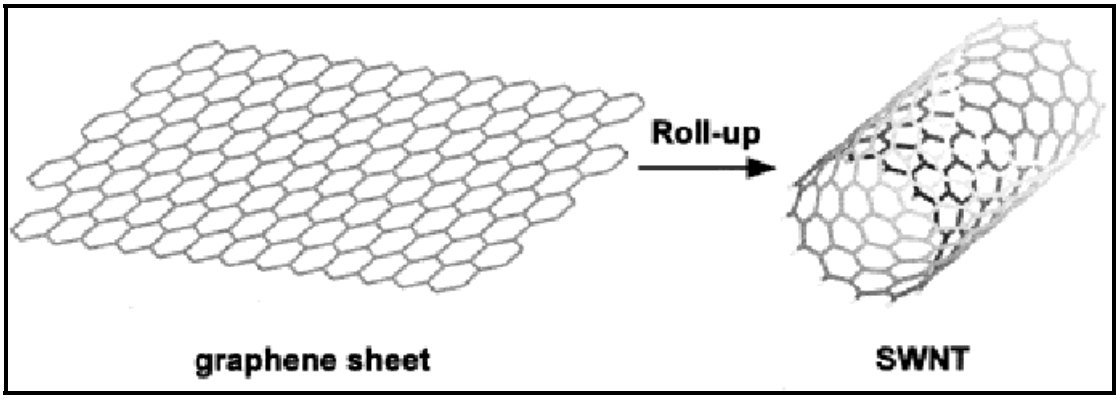

Figure 1.5 A graphene sheet rolled up into a SWCNT

1.3.1 Geometry of Single walled Carbon Nanotubes

The structure of a single walled carbon nanotube is expressed in terms of its one-dimensional unit cell, defined by the chiral vectors C_h and T, where C_h is the chiral vector denoted in equation as:

$$C_h = n\mathrm{a}_1 + m\mathrm{a}_2$$

Where a_1 and a_2 are unit vectors, and n and m are integers which represent a possible tube structure. The chiral vector connects two crystallographically equivalent sites on a 2D graphene sheet such as points O and A as shown in the diagram below (Fig 1.6). The intersection of the vector OB (which is normal to C_h) with the first lattice point determines the fundamental one-dimensional translation vector T. The vector T gives the tube axis direction. The unit cell of the one-dimensional lattice is the rectangle defined by the vectors C_h and T. The basic symmetry operation R consists of the rotation angle ψ and the translation unit or pitch t:

$$\mathrm{R} = (\psi / \mathrm{t})$$

A nanotube constructed in this way is called an (n, m) nanotube.

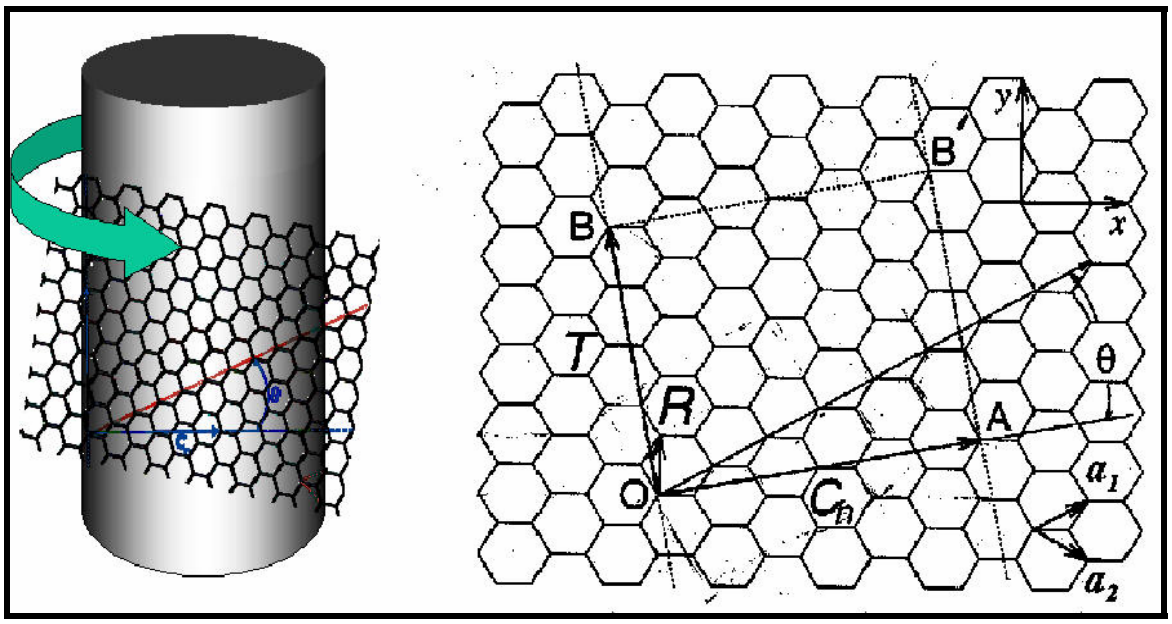

Figure 1.6 One-Dimensional lattice showing the chiral vector, C_h and the translation vector T and a unit cell. This diagram is a (4, 2) tube structure.

Rolling up the sheet along one of the symmetry axis gives either a zig-zag (m=0) tube or an armchair (n=m) tube. The wrapping angle or chiral angle θ is formed between C_h and the armchair line. If C_h lies along the armchair line (θ=0°), it is called an "armchair" nanotube and if θ=30°, the tube is of the "zigzag" type (Fig. 1.7b). The unit cell corresponding to a (5, 5) armchair nanotube and (9, 0) zig-zag nanotube is shown in Figure 1.7 (a). It is also possible to roll up the sheet in a direction that differs from a symmetry axis to obtain a chiral nanotube. As well as the chiral angle, the circumference of the cylinder can also be varied. If 0°< θ <30° then it is a "chiral" nanotube. The vector a_1 lies along the "zigzag" line. The other vector a_2 has a different magnitude than a_1, but its direction is a reflection of a_1 over the armchair line. When added together, they equal the chiral vector C_h.

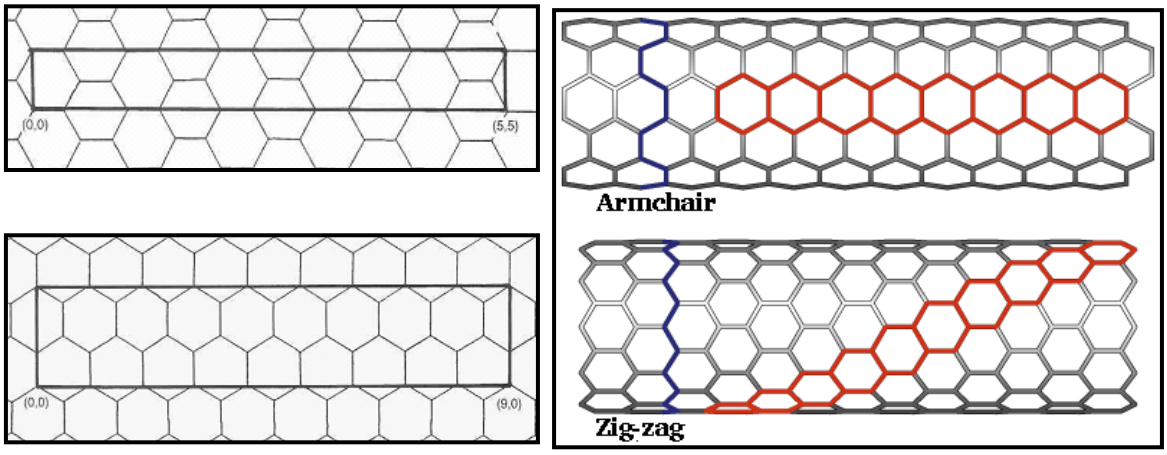

Figure 1.7 (a) Unit cell for (5, 5) armchair nanotube and (9, 0) zig-zag nanotube. (b) Corresponding armchair and zig-zag model of single wall nanotubes.

The values of n and m determine the chirality, or "twist" of the nanotube. The chirality in turn affects the conductance, density, lattice structure and several other properties of the tube. A SWCNT is considered metallic if the value n - m is divisible by three. Otherwise, the nanotube is semiconducting. Consequently, when tubes are formed with random values of n and m, one would expect that two-third of the tubes would be semi-conducting, while the other one-third would be metallic, which happens to be the case.[49] Given the chiral vector (n, m), the diameter of a carbon nanotube can also be determined using the relationship:

$$d = (n^2 + m^2 + nm)\ 1/2\ 0.0783\ \text{nm}$$

The average diameter of a SWCNT is 1.2 nm. However, nanotubes can vary in size, and they are not always perfectly cylindrical. The larger nanotubes, such as a (20, 20) tube, tend to bend under their own weight. The average carbon - carbon bond length was measured to be of 1.42 Å by Wildöer *et al.* in 1998.[49] The C-C tight bonding overlap energy is reported to be in the order of 2.5 eV. Wildöer *et al.* found it to be between 2.6 eV - 2.8 eV, [49] while at the same time, Odom *et al.* estimated it to be 2.45 eV.[50]

1.3.2 Geometry of Multi Walled Carbon Nanotubes

The basic classification of carbon nanotubes is that they exist as perfectly graphitized, in either single walled form or multi walled form, with carbon atoms arranged on each shell with various degrees of helicity and capped with pentagons just like fullerene molecules. Atomic classification is common among both kinds of nanotubes. Multi walled carbon nanotubes are generally in the range of 1-25 nm in diameter. Depending on the synthesis procedures, SWCNTs may nest inside each other to form a structure consisting of multiple layers of graphite rolled on themselves to form a tubular shape. The MWCNTs grown by arc discharge method have generally better structures compared to the MWCNTs grown by several other processes, which is presumably due to the high temperature obtained during the synthesis process. It is likely that during the growth of tubes, most of the defects are annealed. Structures of MWCNTs are described by two models "Russian dolls" model and "Swiss roll" model or "Parchment" model (Fig.1.8).[51] In the *Russian Doll* model, graphene sheets are arranged in concentric cylinders, such as a smaller diameter SWCNT within a larger diameter SWCNT. In the *Swiss roll* model, a single sheet of graphite is rolled in around itself, resembling a scroll of parchment or a

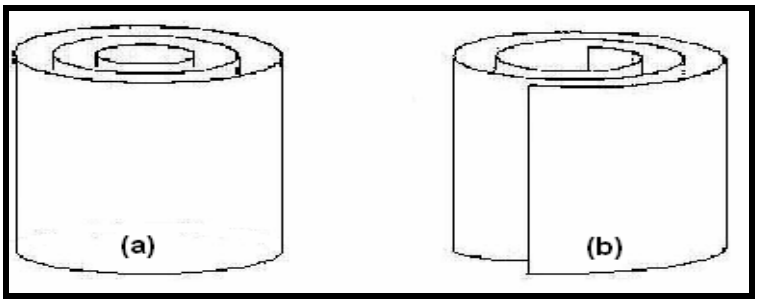

Figure 1.8 Schematic illustrations of (a) “Russian doll” (b) “Swiss roll” models for multiwalled carbon nanotubes.

rolled up newspaper. The interlayer distance in MWCNTs (0.34 nm) is close to the distance between graphene layers in graphite.[52, 53] Since nanotubes are composed of nearly coaxial cylindrical layers, each with different helicities, the adjacent layers are generally non-commensurate, i.e., the stacking cannot be classified as AA or AB as in graphite.[52, 53] MWCNTs also have structural features which are different from well-ordered graphitic side walls: the tip, the internal closures, and the internal tips within the central part of the tube, called "bamboo" structures. The structures of the tip is closely related to that of icosahedral fullerenes, while the curvature is mediated by introducing pentagons (and higher polygons) into the structures while maintaining essentially the sp^2 electronic structure at each carbon atom site. Analysis of HRTEM and elctron differaction studies of nanotubes revealed that the number of different chiral angles which are observed in a MWCNTs are usually less than the number of tubles. Though most of HRTEM studies appears to favour the *Russian doll* model[54], since there has been little evidence found the edges which should result from graphene scrolls, i.e, *Swiss roll* model. However, nanotubes morphologies may vary considerably with the production method used for their syntheis. Also possibility for a mixture of the two arrangements cannot be neglected.[55, 56]

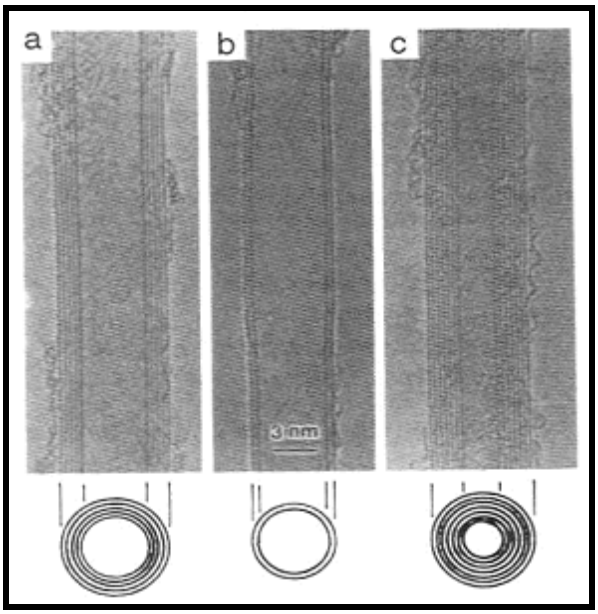

Figure 1.9 Multi-walled carbon nanotubes, first directly observed by TEM (from S. Iijima, *Nature*, 1991).[5]

The special place of double-walled carbon nanotubes (DWCNTs) must be emphasized here because they combine very similar morphology and properties as compared to SWCNT, while improving significantly their chemical resistance. This is especially important when functionalisation is required (this means grafting of chemical functions at the surface of the nanotubes) to add new properties to the CNT. In the case of SWCNT, covalent functionalisation will break some C=C double bonds, leaving "holes" in the structure on the nanotube and thus modifying both its mechanical and electrical properties. In the case of DWCNT, only the outer wall is modified. DWCNT synthesis on the gram-scale was first reported in 2003 by the CCVD technique from the selective reduction of oxides solid solutions in methane and hydrogen.[57]

1.4 Properties

With their unique one dimensional structure, carbon nanotubes possess some extraordinary electrical, thermal and mechanical properties those have made them useful for several interesting applications. Some of them are summarized below.

1.4.1 Mechanical Properties

Several theoretical and experimental calculations have been performed by various groups to study the mechanical behavior of carbon nanotubes. General observations using transmission electron microscopy, scanning electron microscopy and atomic force microscopy have revealed that carbon nanotubes possess a great tensile strength[33] and higher Young's modulus[58, 59] compared to other materials, due to the strength of carbon bonds and the regularity of their atomic structure. SWCNTs are stiffer than steel and are resistant to damage from physical forces.

Below is a chart which gives an overview of Young's modulus, tensile strength and density of carbon nanotubes compared to some other materials.

Material	**Young's modulus (GPa)**	**Tensile Strength (GPa)**	**Density (g/cm^3)**
SWCNT	1054	150	
MWCNT	1200	150	2.6
Carbon fibers	163	2.05	
Steel	208	0.4	7.8
Epoxy	3.5	0.005	1.25
Wood	16	0.008	0.6

1.4.2 Electronic Properties

In late 1991, it had been predicted that carbon nanotubes depending on their structure and diameter can be metallic or semiconducting. Based on theoretical studies it was pointed out that nanotubes might exhibit exotic quantum mechanical behavior in the presence of a magnetic field.[60, 61] In absence of pure material, it was difficult to interpret the theoretical calculation made on electronic properties of nanotubes. Later on, modified synthetic routes to obtain pure material and effective purification techniques enabled electronic measurement of nanotubes at individual level. Nanotube research to date has shown that electronic properties of nanotubes may vary quite widely depending on the degree of

their crystalline order. Many groups have investigated the resistivity of individual nanotubes and their temperature dependence. Fig. 1.10 shows some of the electronic properties as predicted by Cees Dekker in *Physics Today*, May 1999 edition.[62]

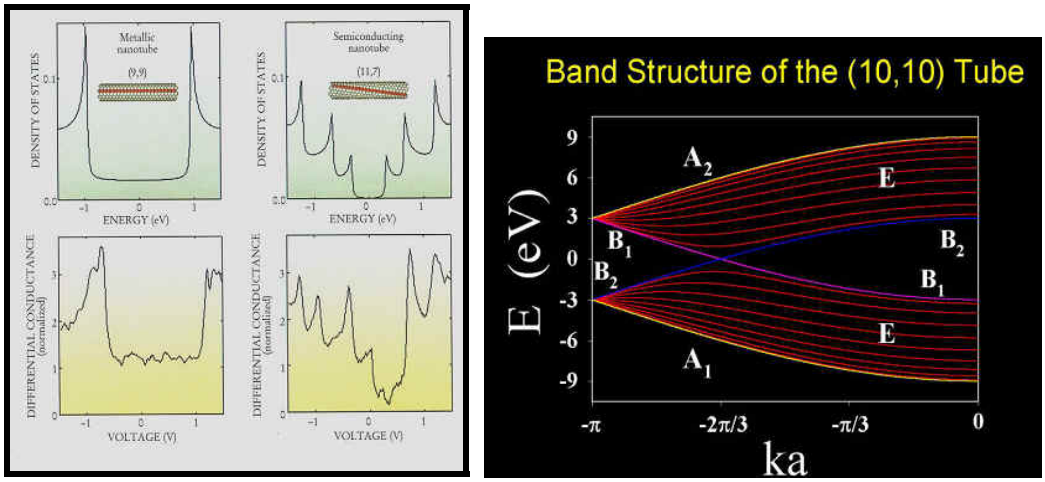

Figure 1.10 Electronic Properties: Density states and band structures of single walled carbon nanotube prototypes (from C. Dekker, *Physics Today*, May 1999).[62]

1.4.3 Thermal Properties

Graphitic nature, unique structure and the size of carbon nanotubes result a wide range of thermal properties. They are expected to be very good thermal conductors along the tube, but good insulators laterally to the tube axis.[36] Tomànek *et al.* determined the dependence of thermal conductivity of carbon nanotubes on temperature.[63] They reported an unusually high value of 6,600 W/m-k for the thermal conductivity at room temperature. Being derived from graphene sheets, specific heat C of isolated and bundled nanotubes were calculated and compared to phonon band structure of graphite. The temperature stability of carbon nanotubes is estimated to be up to 2800 °C in vacuum and about 750 °C in air.[64] They are very strong against strong acid and high temperature because of their perfect conjugated system. Acid and heat are often applied to purify carbon nanotubes.

1.4.4 Electrochemical Properties

Multi walled carbon nanotubes possess interesting electrochemical properties which can be used for electro-analytical applications. Various modified MWCNT film electrodes have been prepared to study their electrochemical properties, such as electrode reactivity,[65] electrode dimensions,[66] and interfacial capacitance.[67, 68] Electrodes prepared by controllable adsorption of the MWCNTs onto the self-assembled monolayer (SAM) possess good electrode reactivity without a remarkable barrier to heterogeneous electron transfer. On the other hand, the MWCNT/SAM-modified electrode is found to possess a largely reduced interfacial capacitance, as compared with the MWCNT film electrodes prepared with existing methods by directly confining the MWCNTs onto electrode surface.[69]

1.4.5 Field Emission Properties of Carbon Nanotubes

It was very early realized that carbon nanotubes are efficient field emitters.[37] CNTs have excellent materialistic properties which make them have attractive field emission characteristics such as, large aspect ratio (>1000), atomically sharp tips, high temperature and chemical stability and high electrical and thermal conductivity. From the latter studies it was concluded that carbon nanotube films could be used at field emission guns for technical applications, such as flat panel displays. MWCNTs being excellent scanning probe tips, their light emitting property should find application in various scanning probe microscopy (SPM).[70]

1.4.6 Quick Facts about Carbon Nanotubes

Equilibrium Structure	
Average Diameter of SWNT's	1.2-1.4 nm
Distance from opposite Carbon Atoms (Line 1)	2.83 Å
Analogous Carbon Atom Separation (Line 2)	2.456 Å
Parallel Carbon Bond Separation (Line 3)	2.45 Å
Carbon Bond Length (Line 4)	1.42 Å
C-C Tight Bonding Overlap Energy	~ 2.5 eV
Group Symmetry (10, 10)	C5V
Lattice: Bundles of Ropes of Nanotubes:	Triangular Lattice(2D)
Lattice Constant	17 Å
Lattice Parameter:	
(10, 10) Armchair	16.78 Å
(17, 0) Zigzag	16.52 Å
(12, 6) Chiral	16.52 Å
Density:	
(10, 10) Armchair	1.33 g/cm^3
(17, 0) Zigzag	1.34 g/cm^3
(12, 6) Chiral	1.40 g/cm^3
Interlayer Spacing:	
(n, n) Armchair	3.38 Å
(n, 0) Zigzag	3.41 Å
(2n, n) Chiral	3.39 Å
Optical Properties	
Fundamental Gap:	
For (n, m); n-m is divisible by 3 [Metallic]	0 eV
For (n, m); n-m is not divisible by 3 [Semi-Conducting]	~ 0.5 eV
Electrical Transport	
Conductance Quantization	n x (12.9 kΩ)$^{-1}$
Resistivity	10^{-4} Ω•cm
Maximum Current Density	10^{13} A/m^2
Thermal Transport	
Thermal Conductivity(Room Temperature)	~ 2000 W/m•K
Phonon Mean Free Path	~ 100 nm
Relaxation Time	~ 10^{-11} s
Elastic Behavior	
Young's Modulus (SWCNT)	~ 1 TPa
Young's Modulus (MWCNT)	1.28 TPa
Maximum Tensile Strength	~ 30 GPa

1.5 Synthesis

As such synthesis of carbon nanotubes is not a very difficult task since it can be found even in the carbon material present in common environment such as in the flame of a candle.[71] However, these naturally occurring varieties can be highly irregular in size and quality because the environment in which they are produced is often highly uncontrolled. To the date there are several processes reported for the bulk synthesis of carbon nanotubes however lack of information on the local environmental conditions during the growth of carbon nanotubes has hindered the efforts to understand the formation of these unique nanomaterials, which has made it difficult to control their size, orientation and structure. In situ diagnostics of the nanotube growth process is vital to understand and optimize the growth process. Alex A. Puretzky and his coworkers have demonstrated that the pulsed laser vaporization (PLV) method is amenable to time-resolved measurements of nanotube formation and growth, unlike continuous production of carbon nanotubes by the arc-discharge and CVD-deposition methods.[72-74] The full potential of nanotubes for applications will be realized until the growth of nanotubes can be optimized and well controlled. Till date various new methods for the bulk synthesis of nanotubes have been reported and classical methods have been further modified in anticipation of obtaining bulk material at a low cost. The processes which are most common and are in use will be explained in this section after briefly discussing the growth mechanism involved in formation of nanotubes.

1.5.1 Growth Mechanism

Both types of nanotubes, arc discharge and pyrolytic carbon nanotubes, essentially appears to favor the *Russian doll* model. Though the growth mechanism is still a subject of controversy, possible mechanisms involving both open ended[75] and closed cap[76] structures for primary tubules have been proposed. It is interesting to compare the formation mechanism of fibrous carbon having micron sized diameter and carbon nanotubes having nanometer scale diameter from the view point of one dimensional carbon structures.

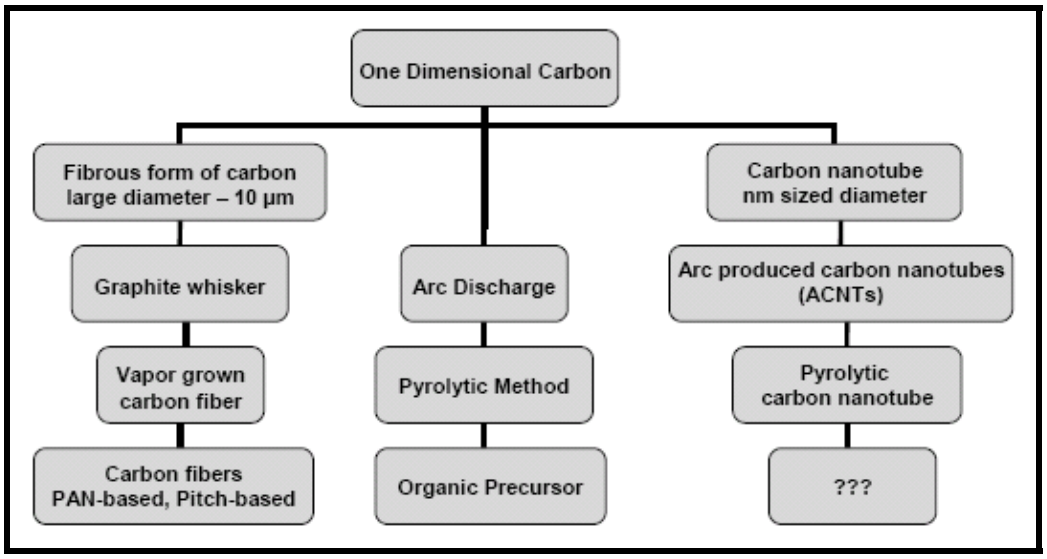

Figure 1.11 Comparative preparation methods for micrometer size fibrous carbon and carbon nanotubes as one-dimensional forms of carbon.

Among the various proposed growth mechanisms, it is possible that more than one growth mechanisms are involved during the formation of nanotubes which also depend on the procedure followed for the synthesis. Here we discuss the mechanism proposed for chemical vapor deposition method which is commonly used to grow carbon nanotubes in bulk. There are currently two mechanisms that are used to explain CNT growth: the dissociation mechanism and the ring-addition mechanism, though either of these mechanisms could operate under different growth conditions.

1.5.1.1 Dissociation Mechanism

In the dissociation mechanism, the carbon precursor (e.g., methane or acetylene) is dissociated to C by the catalyst nano particle (e.g., Fe). It is believed that C can be dissolved to some extent into the nano particle, and eventually precipitates out as carbon rod on metal particle surface. Eventually a slow graphitization of its walls occurs resulting in to carbon nanotubes. Such a mechanism is consistent with the observation that the size of the nano particle dictates the diameter of MWCNTs formed.[77-79] It is also thought to be the mechanism that operates at higher temperatures.

1.5.1.2 Ring Addition Mechanism

In the ring addition mechanism, it is believed that the tube is formed by tiling of units with more than one C atom. This mechanism is consistent with the observation that many of the catalysts that are used for CNT growth are also potentially good dehydroaromatization (DHA) catalysts.[80] (e.g. fig 1.12)

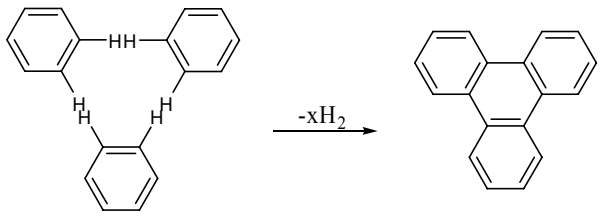

Figure 1.12 An example of ring addition mechanism

Whether it is the dissociation mechanism or ring addition mechanism, formation of nanotubes on catalyst particles is assumed to be either by root growth or by tip growth (Fig. 1.13). There are several theories on the exact growth mechanism for nanotubes. Derbyshire *et al*. predicts that during the process metal catalyst particles are floating or are supported on graphite or another substrate.[81] It is assumed that catalyst particles are spherical or pear-shaped and the deposition takes place only in the lower half of the surface. The carbon diffuses along the concentration gradient and precipitates on the opposite half, around and below the bisecting diameter. However, it does not precipitate from the apex of the hemisphere, which accounts for the hollow core that is characteristic of these filaments. For supported metals, filaments can form either by 'extrusion or root growth' in which the nanotube grows upwards from metal particles that remain attached to the substrate, or the particles detach and move at the head of growing nanotube, labeled as 'tip-growth'. Depending on the size of the catalyst particles, SWCNTs or MWCNTs are grown. In case of arc discharge method, if no catalyst is present in the graphite, MWCNTs will be grown on C_2-particles that are formed in the plasma.

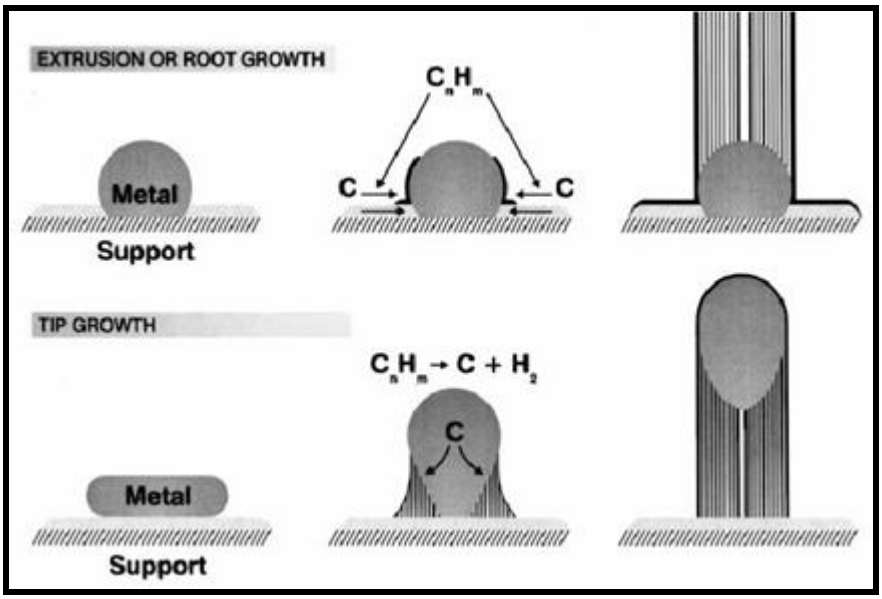

Figure 1.13 Possible growth mechanisms for the formation of carbon nanotubes

1.5.2 Fabrication Techniques

The synthesis of nanotubes can be performed by different kind of techniques: among them commonly used are arc evaporation (the one used by Iijima),[5] Chemical Vapour Deposition (CVD),[82] Plasma Enhanced Chemical Vapour Deposition (PECVD),[83] Laser ablation method[84] and electrochemical method.[85] In general Chemical Vapour Deposition (CVD) and arc discharge methods result in larger quantities of MWCNTs or SWCNTs where as laser ablation produces small amount of clean nanotubes. While CVD gives poor quality or somewhat impure material, on the other hand it is easy to scale up while compared to other processes. Modifying these methods to obtain pure material in large quantities is still a debatable issue and much research is going on to find a procedure which favours commercial production. The following sub sections give an overview of these methods and they are briefly discussed.

1.5.2.1 Arc Discharge

Arc discharge is the most common method for the synthesis of both SWNTs and MWNTs.[86] The electric arc was discovered by Humphry Davy in 1808, when he connected a piece of carbon to each side of an electric battery and touched two pieces of carbon together, then drew them slightly apart. The result is a dazzling steam of ionized air, or plasma, at a temperature of 6000 °C (10,800 °F). Arc discharge, developed on the principle of electric arc, is the most convenient method to generate the thermal plasma, which is characterized by the high energy content and the local thermal equilibrium state (LTE). The arc consists of three major parts, as shown in Figure 1.14, the arc column, the cathode region and the anode region. The arc column has a charge equilibrium, a low electric field and high temperature, so that it plays a fundamental role in heating the gas.

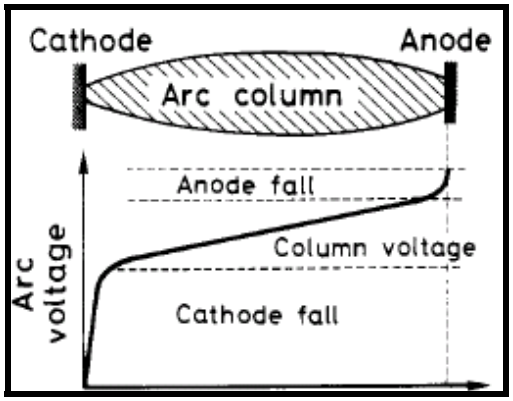

Figure 1.14 Arc voltage distributions (from B. Lahr *et al*., *Carbon*, 2002)[87]

The cathode and anode regions, where the transition between metallic and gaseous condition occurs, have positive and negative space charges with a high electric field respectively and also have a high temperature gradient.[87]

The same principle is used in classical arc discharge methods for the synthesis of carbon nanotubes. Two graphite rods are used as the cathode and anode, kept in a closed enclosure filled with helium, between which arcing occurs when DC voltage power is supplied. Large quantities of electrons from the arc-discharge move to the anode and

collide into the anodic rod. The plasma generation by helium gas ignition caused the formation of carbon clusters from the anodic graphite rod, which are then cooled to low temperature and condensed on the surface of the cathodic graphite rod. The graphite deposits condensed on the cathode contain carbon nanotubes, nanoparticles, and clusters. Though the graphite clusters synthesized in these initial experiments contained a very small amount of carbon nanotubes, but modifications to the procedure later by Ebbesen and Ajayan have enabled greatly improved the yield.[86]

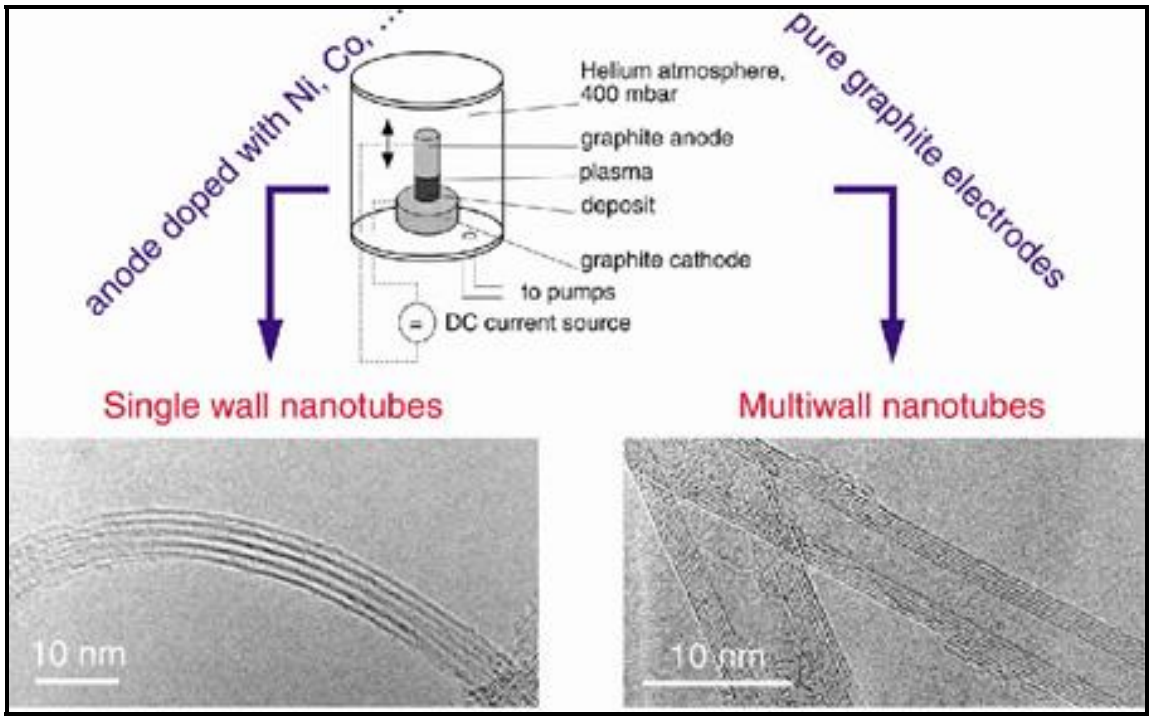

Figure 1.15 Experimental setup of an arc discharge apparatus and TEM images of nanotube samples synthesized by arc discharge.[88]

Fig. 1.15 shows a schematic diagram of an arc-discharge apparatus for the synthesis of carbon nanotubes. The closed shell of the apparatus remains connected to a vacuum line with a diffusion pump, and to a helium supply. Two graphite rods, usually of high purity, anode typically longer rod approximately 6 mm in diameter and the cathode much shorter rod 9 mm in diameter are used as electrodes. Efficient cooling of the cathode has been shown to be essential in producing good quality nanotubes. The position of the anode

should be adjustable from outside the chamber, so that a constant gap can be maintained during arc-evaporation. A voltage-stabilized DC power supply is normally used, and discharge is typically carried out at a voltage of 20 to 40 V and at a current in the range of 50 to 100 A. When a stable arc is achieved, the gap between the rods is maintained at approximately 1 mm or less. Carbon nanotubes synthesized by arc-discharge normally have multi-walled structures. After holes in the graphite rods are bored and filled with appropriately proportional composites of graphite powder and catalytic Co, Ni, Fe, and Y powder, SWCNT can be synthesized by arc-discharge on the cathode. The pressure in the evaporation chamber and the current are the most important factors in producing a good yield of high quality carbon nanotubes.[86, 89-92] Increase in the yield is evident as the pressure is increased, but there is a fall in total yield at too high pressure. In addition, the current should be kept as low as possible, consistent with maintaining a stable plasma. Other than helium, nanotubes have also been synthesized in Ar, N_2, H_2, CH_4 and CF_4 gas atmospheres.[21, 93-95] Several attempts have been made to modify this method and obtain more economical production. Insight in the growth mechanism is increasing and measurements have shown that different diameter distributions have been found depending on the mixture of helium and argon. These mixtures have different diffusion coefficients and thermal conductivities which affect the speed with which the carbon and catalyst molecules diffuse and cool, affecting nanotube diameter in the arc process. This implies that single-layer tubules nucleate and grow on metal particles in different sizes depending on the quenching rate in the plasma and it suggests that temperature and, carbon and metal catalyst densities affect the diameter distribution of nanotubes.[86]

1.5.2.2 Thermal Chemical Vapor Deposition

Much progress has been made in the research of growing carbon nanotubes on a large area substrate by thermal chemical vapor deposition (CVD) in recent years.[82, 96] Thermal CVD has advantages of variety in products and hydrocarbon sources, adequacy for synthesis of high quality materials,[97] and controllability of microscopic structures. The method, however, is not good in homogeneity on substrate as change in the flow of the reaction gas leads to unstable gas supply. It is also sensitive to the temperature change

and position in the chamber. After all these disadvantages, it features simplicity of apparatus and absolute advantage in mass production. The synthesis method of carbon nanotubes using thermal chemical vapor deposition is as follows. Fe, Ni, Co, or alloy of these catalytic metals is initially deposited on a substrate. After the substrate is etched in diluted HF solution with distilled water, the specimen is placed in a quartz boat. The boat is positioned in a CVD reaction furnace, and nano-sized fine catalytic metal particles are formed after an additional etching of the catalytic metal film using NH_3 gas at a temperature of 750 to 1050 °C. [97, 98] As carbon nanotubes are grown on these fine catalytic metal particles in CVD synthesis, forming these fine catalytic metal particles is the most important process. Fig. 1.16 shows a schematic diagram of thermal CVD apparatus in the synthesis of carbon nanotubes. Reaction gas is supplied in one end of the apparatus, and gas outlet in the other. Fig. 1.17 shows SEM and TEM images of carbon nanotubes grown by a thermal CVD method. The diameter of each carbon nanotube is approximately 15 nm. It is hollow and a MWCNT structure, composed of 10 graphene sheets with little defects on the surface of the nanotube.

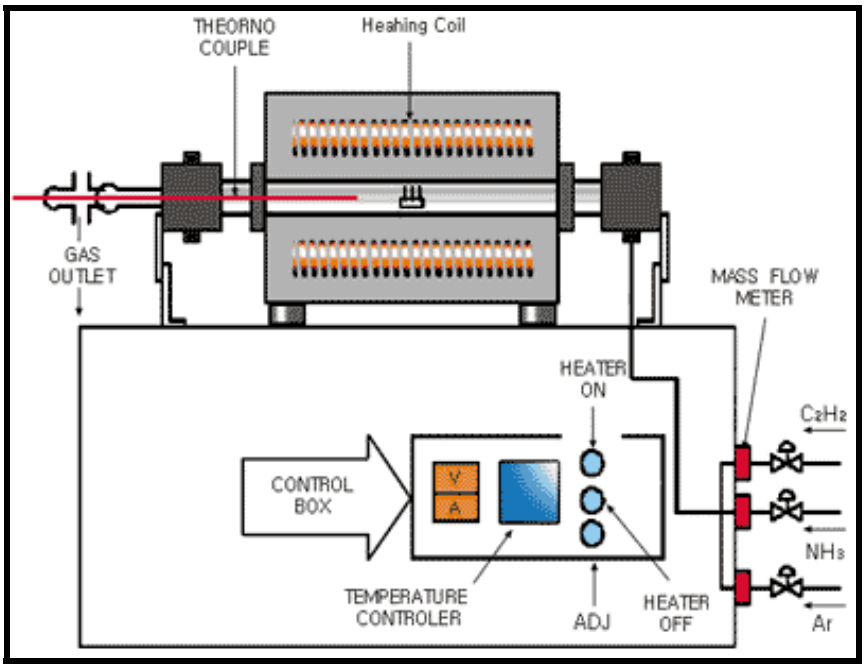

Figure 1.16 Schematic diagram of thermal CVD apparatus.[88]

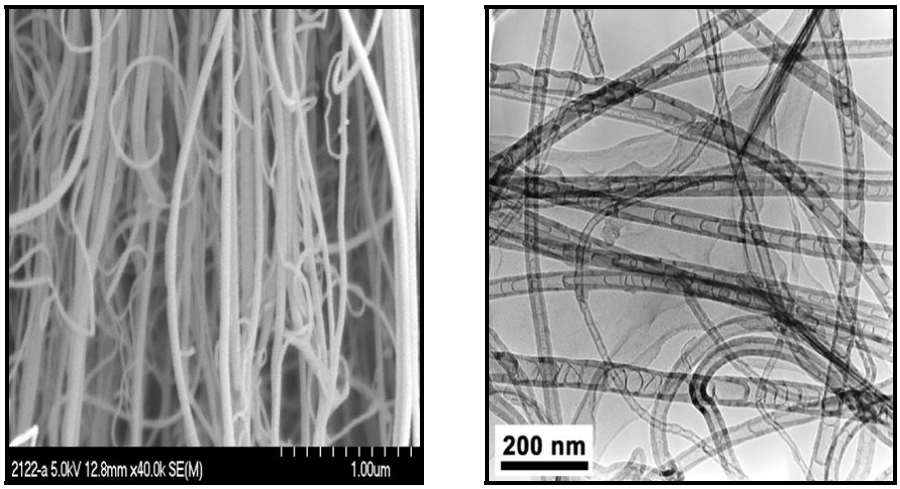

Figure 1.17 SEM and TEM images of carbon nanotubes grown by thermal CVD method[88]

1.5.2.3 Plasma Enhanced Chemical Vapor Deposition

A controllable method for the production of carbon nanotubes is plasma enhanced-CVD.[83] Such a system is often used to grow free standing vertically aligned MWCNTs. Plasma CVD has an advantage of low temperature synthesis over thermal CVD.[99] Carbon nanotubes can be synthesized on soda lime glass, especially for production of display devices, at temperatures less than the melting point of soda lime glass, i.e. < 550 °C. A glow discharged type setup is generally used for plasma CVD in which two electrodes are placed in a stainless-steel chamber where the grounded cathode plays the role of a substrate holder and Ohmic heater. High frequency DC power supplies, typically RF (13.56 MHz) and microwave (2.47 GHz), anode voltage approx 400 V were used for discharge of plasma. The plasma method generates glow discharge in a chamber or a reaction furnace by a high frequency applied to both electrodes. Fig. 1.18 shows a schematic diagram of a typical plasma CVD apparatus with a parallel plate electrode structure. A substrate is placed on the grounded electrode. In order to form a uniform film, the reaction gas typically C_2H_2, CH_4, C_2H_4, C_2H_6, CO is supplied from the opposite plate to synthesize carbon nanotubes.[83] Catalytic metals, such as Fe, Ni, and Co are used on a Si, SiO_2, or glass substrate using thermal CVD or sputtering.[99] The deposited metal

on the substrate can be etched using ammonia or H_2 gas. After the formation of nanoscopic fine metal particles, carbon nanotubes are grown on the metal by glow discharge.

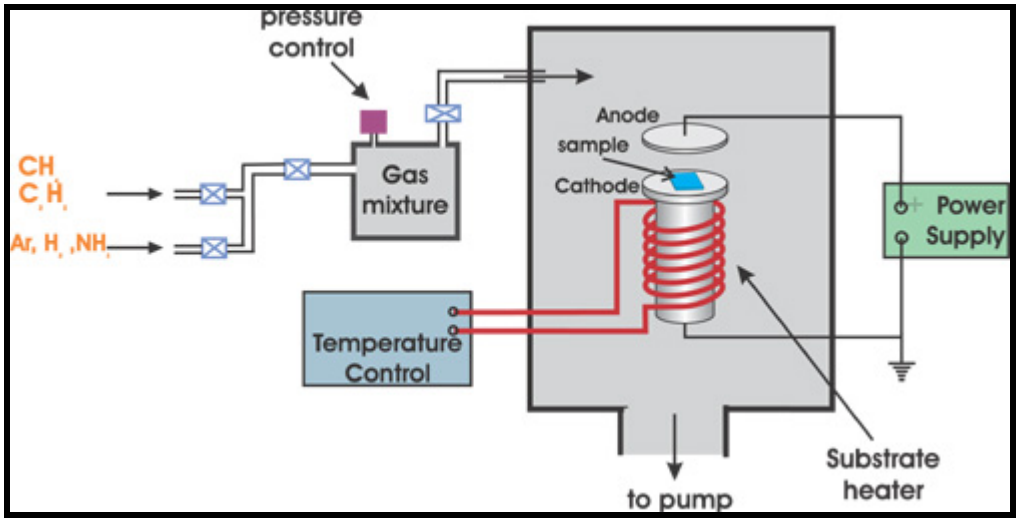

Figure 1.18 A schematic diagram for Plasma-CVD experimental set-up[88]

Fig. 1.19 (a) shows carbon nanotubes grown on a glass substrate using RF high frequency power and a gas mixture of C_2H_2 and NH_3. Catalytic metal cluster exist in the tips of carbon nanotubes. The diameter and density of carbon nanotubes depend greatly on the magnitude and density of metal particles. The catalyst used in the process has a strong effect on the diameter, growth rate, wall thickness, morphology and microstructure of the nanotubes formed. Ni has been found to be the most suitable pure-metal catalyst for the growth of aligned MWCNTs.[99] Fig. 1.19 (b) shows a TEM image of carbon nanotube grown on glass substrate by Ren's group using Ni as a catalytic metal.[97] As carbon nanotubes grown by plasma CVD are synthesized at low temperature, graphene sheets are known to be a little vermicular and structurally MWCNTs, even though the hollow inside of the nanotube looks dim.

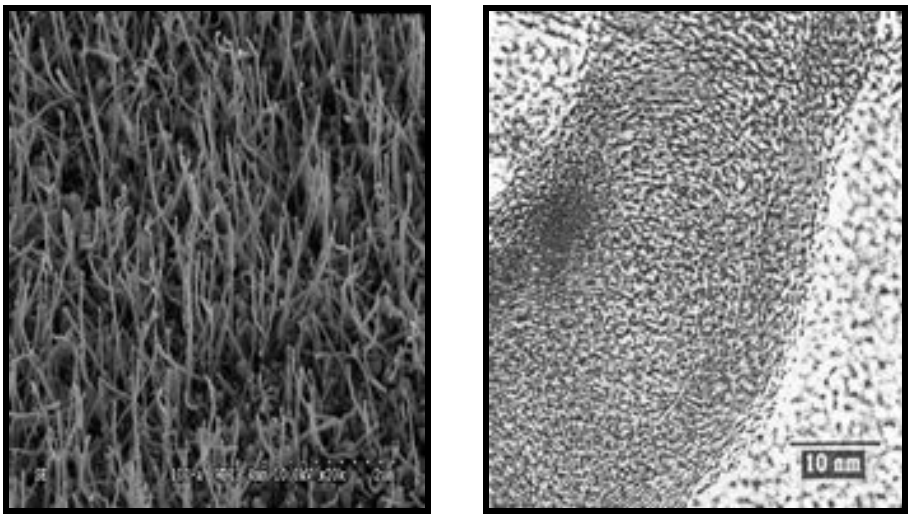

Figure 1.19 (a) SEM and (b) TEM images of carbon nanotubes grown by plasma CVD method.[97]

1.5.2.4 Laser Ablation Method

In 1995, Smalley's group at Rice University reported the synthesis of carbon nanotubes by laser vaporization.[84] Fig. 1.20 shows the schematic diagram of a laser vaporization apparatus used by Smalley's group. A pulsed,[100, 101] or continuous[102, 103] laser is used to vaporize a graphite target in an oven at 1200 °C. The main difference between continuous and pulsed laser, is that the pulsed laser demands a much higher light intensity (100 kW/cm^2 compared with 12 kW/cm^2). Helium or argon gas is filled to keep the pressure in the oven at 500 Torr. Carbon clusters from the graphite target are cooled, adsorbed, and condensed on the Cu collector at a temperature. The condensates obtained this way are mixed with carbon nanotubes and nanoparticles. MWCNTs would be synthesized in the case of pure graphite, but uniform SWCNTs could be synthesized if a graphite of a mixture of Co, Ni, Fe and Y were used instead of pure graphite. SWCNTs synthesized this way exist as “ropes”.

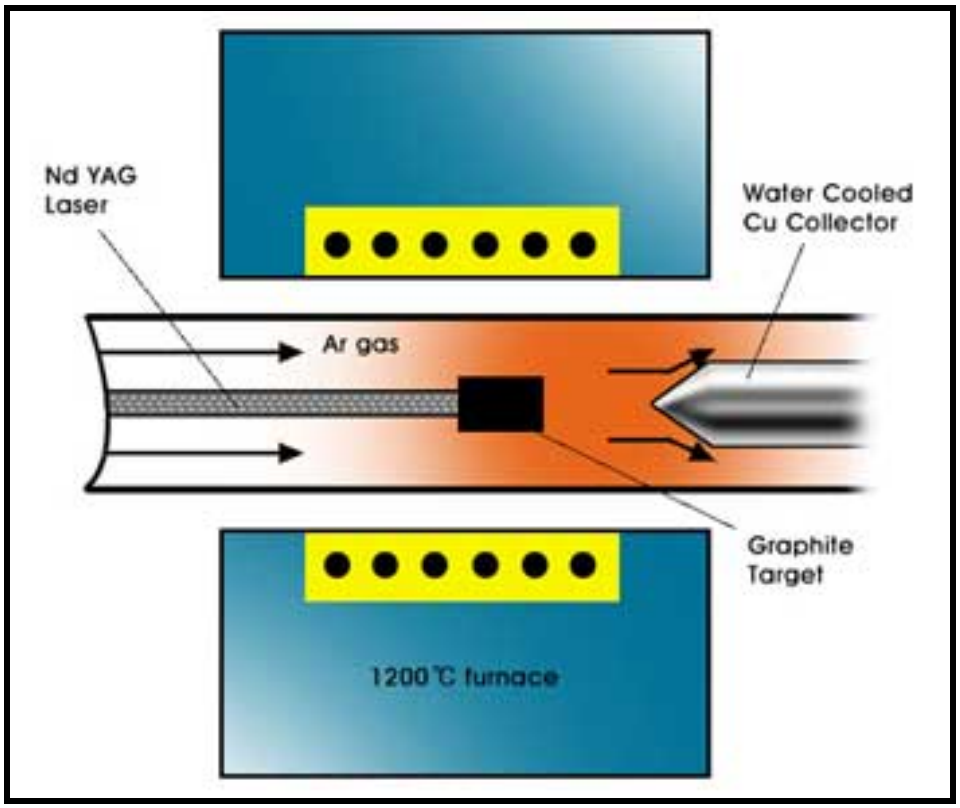

Figure 1.20 Schematic diagram of laser vaporization apparatus for the synthesis of multi walled carbon nanotubes.[88]

Fig. 1.21 shows SEM and TEM images of single walled carbon nanotubes synthesized by Smalley's group using laser-vaporization.[8] It is found from the SEM image (Fig. 1.21a) that carbon nanotubes had curved shapes and carbon particles were stuck on the surface of the nanotubes. The structures and forms of graphene sheets are stable and clean, but carbon particles are stuck on the surface. Fig. 1.21 (b) shows that individual SWCNTs with a uniform diameter of several nm are clustered evenly at graphene sheet spacing. Laser vaporization method provides higher yield than arc-discharge and can synthesize high quality SWCNTs.

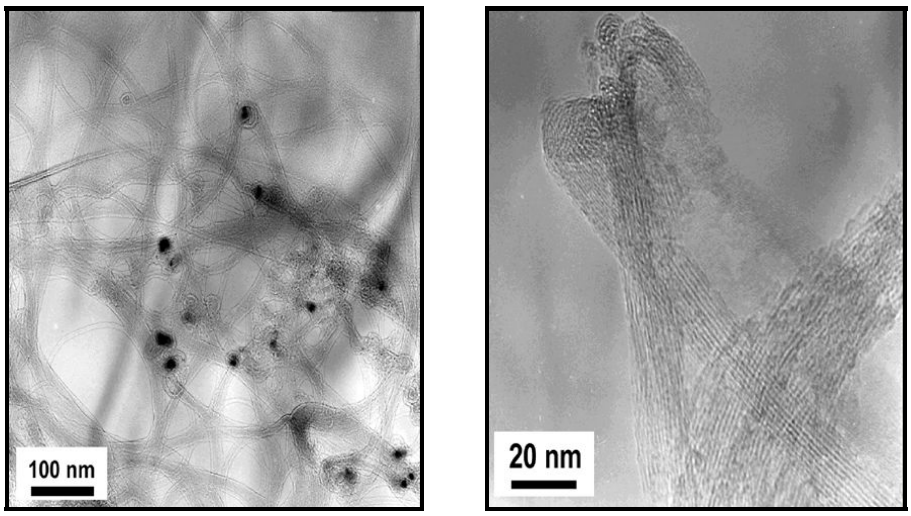

Figure 1.21 (a) SEM image of single walled carbon nanotubes synthesized by laser-vaporization method (b) TEM images of ropes of the single walled carbon nanotubes synthesized by laser- vaporization method.[8]

1.5.2.5 Continuous Wave Laser-Powder Method

This method is a novel continuous, highly productive laser-powder method of SWCNT synthesis based on the laser ablation of mixed graphite and metallic catalyst powders by a 2-kW continuous wave CO_2 laser in an argon or nitrogen stream. Because of the introduction of micron-size particle powders, thermal conductivity losses are significantly decreased compared with laser heating of the bulk solid targets in known laser techniques. As a result, more effective utilization of the absorbed laser power for material evaporation was achieved. The set-up of the laser apparatus is shown in Figure 1.22.[102]

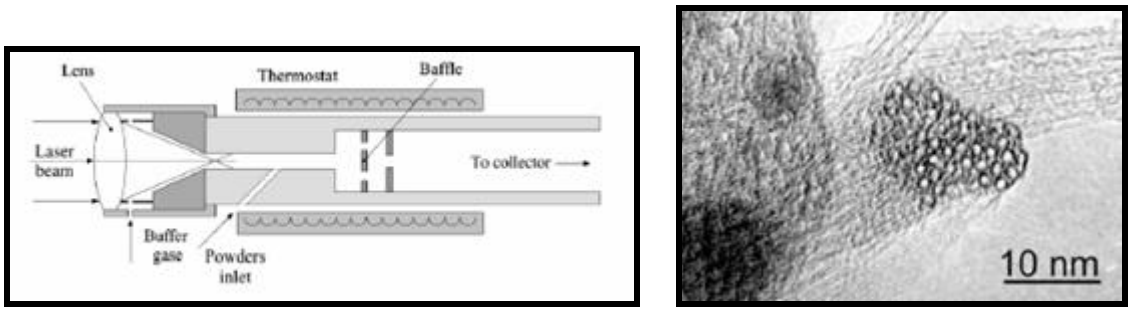

Figure 1.22: (Left) The principle scheme of the set-up for SWCNT production by continuous wave laser-powder method. (Right) HRTEM of a SWCNT-bundle cross-section.[102]

The established yield of this technique was 5 g/h. A Ni/Co mixture (Ni/Co is 1:1) was used as catalyst, the temperature was 1100 °C. In the soot a SWCNT abundance of 20-40% wt as found with a mean diameter of 1.2-1.3 nm. An HRTEM-picture of this sample is shown in Figure 1.22 (right).

1.5.2.6 Flame synthesis

This method is based on the synthesis of SWCNTs in a controlled flame environment, where the combustion heat is generated by burning hydrocarbons. Carbon atoms are formed from the combustion of inexpensive hydrocarbon fuels. During the process small aerosol metal catalyst islands are formed on which SWCNTs are grown in a same manner as in laser ablation and arc discharge.[104-106] These metal catalyst islands can be made in three ways. The metal catalyst (cobalt) can either be coated on a mesh (Fig. 1.23), on which metal islands resembling droplets were formed by physical vapor deposition. These small islands become aerosol after being exposed to a flame. The second way is to create aerosol small metal particles by burning a filter paper that is rinsed with a metal-ion (e.g. iron nitrate) solution. The third way is the thermal evaporating technique in which metal powder (e.g. Fe or Ni) is inserted in a trough and heated.

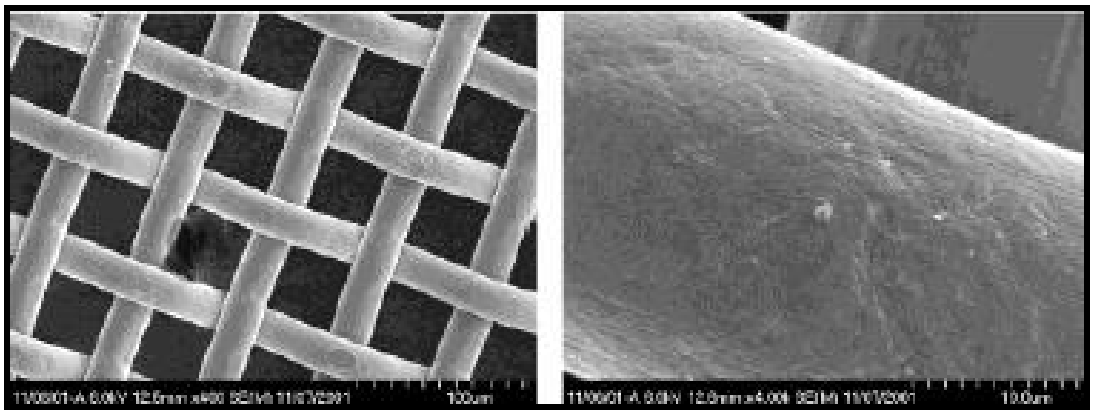

Figure 1.23 Meshes on which the metal catalyst is coated, used in flame synthesis[106]

In a controlled way a fuel gas is partially burned to gain the right temperature of ~800 °C and the carbon atoms for SWCNT production. On the small metal particles the SWCNTs are than formed. As optimization parameters the fuel gas composition, catalyst, catalyst carrier surface and temperature can be controlled.

1.5.2.7 Vapor Phase Growth

Most synthesis methods of carbon nanotubes are carried out by deposition of catalytic metals on a substrate using conventional gas, such as C_2H_2, CH_4, C_2H_4, C_2H_6. However, vapor phase growth is a synthesis method of carbon nanotubes, directly supplying reaction gas and catalytic metal in the chamber without a substrate.[107] It has been suggested as a good method for mass production. Fig. 1.24 shows a schematic diagram of a vapor phase growth apparatus. A mass flow controller is placed in one corner and a boat for catalytic metal powder in the chamber. The chamber is composed of two stage furnaces. The temperature is kept relatively low in the first furnace while a higher temperature is maintained in the second furnace where the synthesis occurs. While the hydrocarbon gas is not decomposed in the first furnace, a relatively low temperature for vaporization of catalytic carbon is maintained. Though catalytic metals vaporized from the powder are atomic, they are formed as fine particles down to several to tens of nm in the chamber in the course of collisions among the atoms. When fine catalytic particles

vaporized from metal powder in the low temperature area reach the second furnace, decomposed carbon in the hot second area is adsorbed, diffused to catalytic metal particles, and synthesized as carbon nanotubes.[107, 108] Fig. 1.25 (a) shows SEM image of carbon nanotubes grown by vapor phase growth method.[88] It was found from the image that about 50 ㎛ carbon nanotubes in length are densely synthesized without a substrate in the chamber and there were substantially no carbon particles. Fig. 1.25 (b) shows TEM images of carbon nanotubes synthesized by a vapor phase growth method. It can be seen from the images that the tube diameter is 30 nm and it is hollow in the middle.

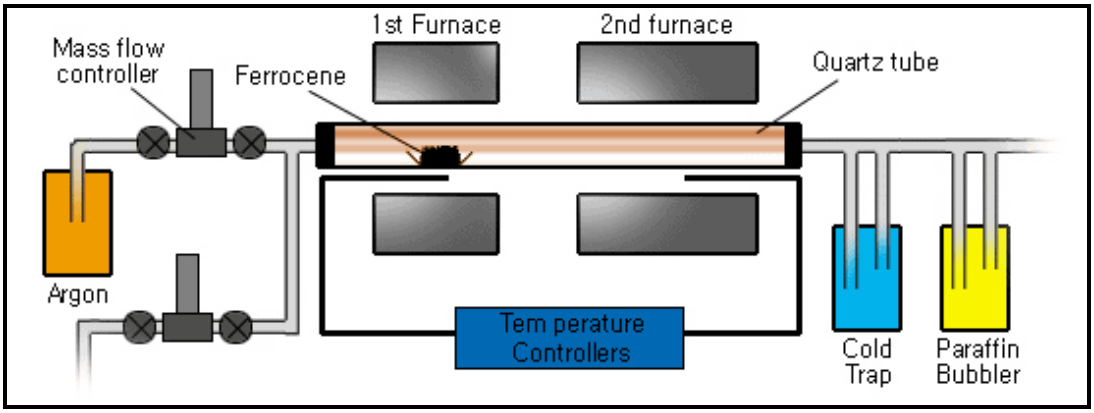

Figure 1.24 Schematic diagram of vapor phase growth apparatus.[88]

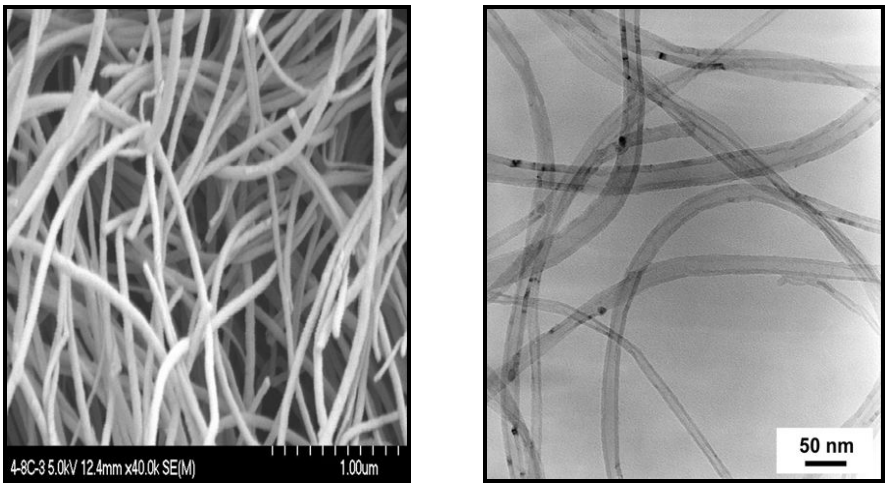

Figure 1.25 (a) SEM and (b) TEM images of carbon nanotubes grown by vapor phase growth method.[88]

1.5.2.8 Thermolysis of Metal Complexes

Solid state thermolysis of organometallic complexes has also been found to be an effective method for the synthesis of MWCNTs. K.P.C. Vollhardt *et al.*[109] reported the synthesis of metal encapsulating, pure MWCNTs as thin, free-standing films of "buckypaper"[110] by heating $Co_2(CO)_6$ complex of diphenylethyne $[Co_2(CO)_6PhC_2Ph]$[111] in a quartz tube sealed under vacuum to 650 °C for 1.5 to 2 hours. Fig. 1.26 shows SEM and TEM micrographs of as produces MWCNTs sample.[109]

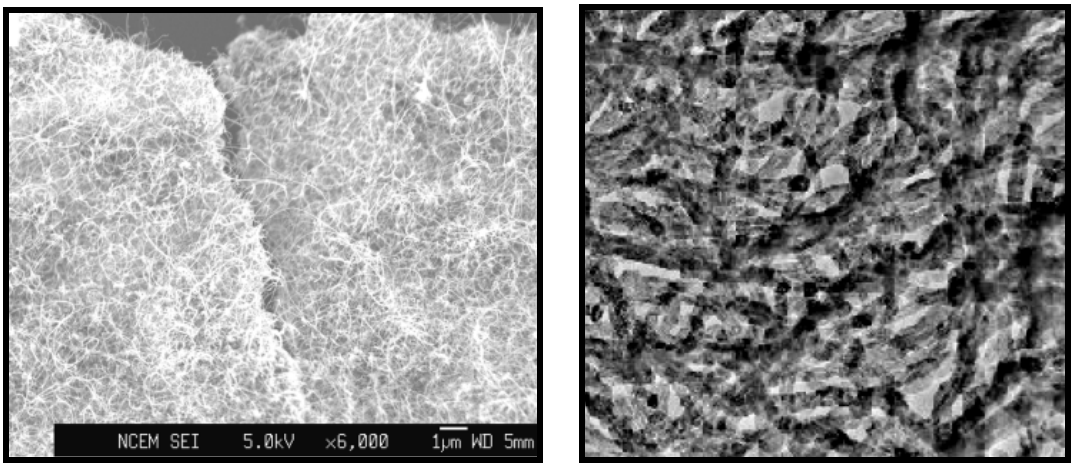

Figure 1.26 An SEM (left) and TEM (right) micrograph of the as-produced MWNT. Some of the dark spots in TEM image represent an fcc arrangement of cobalt particles.[109]

1.5.2.9 Electrolysis

MWCNTs are synthesized using this method which involves the electrolysis of molten lithium chloride using a graphite cell in which the anode was a graphite crucible. The temperature of the graphite crucible is kept approximately 600 °C in the Ar atmosphere. MWCNTs with 2-10 nm in diameter and 0.5 μm or more in length are synthesized when DC power at less than 3-20 A° and 20 V is applied. Amorphous carbons and encapsulated CNTs are synthesized as by-products.[85, 112]

1.6 Separation and Purification

Most of the synthetic techniques used for the production of carbon nanotubes yield impure material. The crude product is usually accompanied by graphite, smaller fullerenes, carbon nanoparticles, amorphous carbon, residual catalyst or metal nanoparticles depending on the process used for their synthesis. Not only impurities but nanotubes being a mixture of different types (metallic or semiconducting), length and diameter, renders their applications in electronics and nanoscale devices. Since the unique mechanical, electronic, optical, vibrational and surface properties of carbon nanotubes lies in the subtlety of its structure, topology and size, presence of impurities and the variability in size (diameter and length) of carbon nanotubes produced with current technologies interfere with getting the desired properties needed for specific applications. To analyze various intrinsic properties of nanotubes, separation and purification of nanotube is inevitable. In early decades soon after the discovery of nanotubes, various purification techniques were reported by groups of T. Ebbesen, P. M. Ajayan, S. Iijima and D. S. Bethune.[6, 7, 86, 91, 113] Their purification techniques yielded comparatively pure material, still nanoscale application of CNTs demands more suitable methods to obtain pure nanotubes in large quantities without any destruction. In the following section a few methods for separation and purification of nanotubes are discussed briefly.

1.6.1 Purification Methods

1.6.1.1 Oxidation

The use of oxidation is the first successful method of purifying carbon nanotubes and this was discovered by the group of Ebessen. Carbon nanotube caps can be selectively attacked and opened by oxidizing gases, while leaving the tube side walls unaffected. Carbon dioxide[114] and oxygen[115] were commonly used as oxidizing agents for such gas phase purification. Liquid phase oxidation can be performed by treating nanotubes with nitric acid,[116-118] sulfuric acid,[119] mixture of both[119], hydrochloric acid,[120] hydrogen

peroxide[121] or potassium permanganate in acid solution.[122] Ebessen and co-workers realized that defect-rich structures might be readily oxidized compared to relatively perfect nanotubes, hence get an enrichment of nanotubes with a high degree of purity. However, the disadvantage of this technique is the large expense of losing a major portion (over 99%) of the original sample.[116] The Transmission Electron Microscopy (TEM) results shown in Figure 1.27 illustrate the purification of multiwalled nanotube samples by oxidation. Combinations of such oxidative treatments were found to be even more effective and various multi-step purification methods were suggested for the effective purification of SWCNTs[118, 123] and MWCNTs.[124]

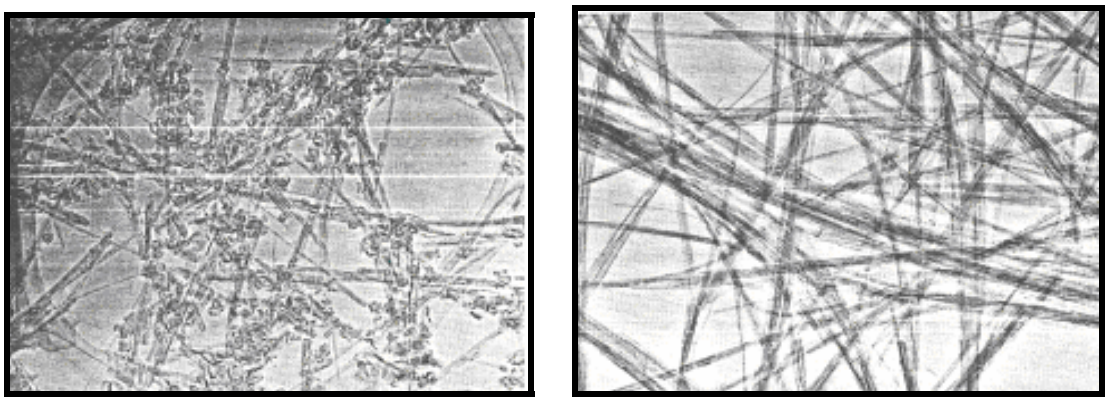

Figure 1.27 TEM images illustrating the purification of MWCNTs by oxidation. Impure MWCNTs (left) purified MWCNTs (right).[116]

1.6.1.2 Graphite Intercalation

In 1994 Japanese scientists proposed a chemical method for the purification of nanotubes.[125] The method uses the difference of oxidation rate between graphite and graphite intercalation compound (GIC). A graphite intercalation compound (GIC) can be easily formed as highly reactive metal compounds intercalate between graphite basal planes where as nanotubes do not intercalated because of the rigidness of annular space of nanotubes. Therefore $CuCl_2$ in the interlayer of graphite can be reduced to metal copper yielding pure nanotubes after removing copper oxide by acid cleaning. The process involves immersion of crude CNTs in molten $CuCl_2$-KCl mixed liquid at 400 °C

for a week. The crude products containing $CuCl_2$-intercalated graphite particles was then washed by ion-exchanged water to remove excess $CuCl_2$ and KCl. Subsequent annealing of the washed CNTs in He/H_2 at 500 °C for an hour resulted in reduction of $CuCl_2$ in the graphite interlayers to metal copper. The crude product was then oxidized under the air flow condition at a heating rate 10 °C/min up to 600 °C which afforded a relatively pure material.

1.6.1.3 Ultrasonic Filtration

The group of Shelimov *et al*,[126] presented a method of purifying SWCNTs produced from the laser-vaporization by ultrasonically assisted filtration. The main impurities produced by different processes in general consists of multishell carbon nanocapsules (buckyonions), both empty and filled with transition metal, amorphous carbon nanoparticles and fullerenes. In this technique, the particles are separated due to ultrasonic vibrations. Agglomerates of SWCNTs are forced to vibrate, making them become more dispersed. In this study they used methanol as the solvent. Suspensions of SWCNT soot in methanol are unstable and flocculation followed by precipitation occurs within a minute. Ultrasonication applied to the samples during filtration maintains the suspension of materials in solution (hence the term used was ultrasonically assisted filtration). Furthermore, ultrasonication prevented cake formation in their study.

It has been reported that ultrasonic treatment of multi walled carbon nanotubes induces a considerable amount of defects, such as fracture, buckling and dislocations.[127] This was also expected to happen for SWCNTs. Defects in the form of cut nanotubes and damaged nanotube walls was also observed in their study by Smalley *et al*.[126]

1.6.1.4 Microfiltration

Carbon nanotubes synthesized by pulsed laser ablation contains carbon nanospheres (CNS), metal nanoparticles, polyaromatic carbons, and fullerenes among which a dominant fraction is in the form of sp^2 bonded carbon nanospheres (CNS). The group of

Bandow *et al*[128] reported a purification method for such SWCNT products using micro filtration which is based on the size distribution of impurities and side products. The process involves suspension of CNS, metal nanoparticles and SWCNTs in an aqueous solution using a cationic surfactant and subsequent trapping of the SWCNTs on a membrane filter. As-produced SWCNTs are first soaked in a CS_2 solution and solvated polyaromatic carbon and fullerenes are passed through a filter where CS_2 insolubles are trapped in the filter. CNS and metal nanoparticles are then first separated from SWCNTs by ultrasonic agitation of the dispersion of insoluble solids caught on the filter paper in an aqueous solution of 0.1% cationic surfactant (benzalkonium chloride). After sonication for 2 hours, the suspension can be forced through a microfiltration cell (0.3 μm) using an overpressure (~2 atm) of N_2 gas. Most of the CNS and metal nanoparticles were separated in this process while SWCNTs and a small amount of residual CNS and metal nanoparticles remained as filtered product. Using this technique, ~84, 10, and 6 wt % of purified SWCNTs, CNS, and CS_2 extracts, respectively, were separated from as-prepared laser-synthesized SWCNTs and up to 90% purity by weight (in purified SWCNTs) was achieved.[128]

1.6.1.5 Annealing

A simple method for purification of nanotubes is annealing at high temperatures ranging 500 - 2600 °C.[129] It has been reported that during the oxidation of crude nanotube product in air at high temperatures (around 750 °C) nanoparticles are consumed more rapidly than carbon nanotubes.[116] At higher temperatures nanotubes are generally rearranged and defects, graphitic carbon and more reactive fullerenes are oxidized leaving comparatively pure nanotubes. When using high temperature vacuum treatment[130] (1500 °C) the metal melts and can also be removed.

1.6.1.6 Magnetic Purification

Most of synthetic processes used for the production of SWCNTs are based on deposition of carbon on nanometer sized metal particles. Commonly used metals are Fe and Co.

These metal particle impurities being magnetic can be easily separated from nanotubes by using a simple magnet. The process involves dispersion of crude product in a solvent. Ultrasonic agitation of dispersion leads to the separation of metal particulates from nanotube bundles. These particles can further be separated by using a magnet and the nanotubes can be decanted off. The process does not require large equipment and enables the production of SWCNTs at smaller scales containing no magnetic particles.[131] (Fig. 1.28)

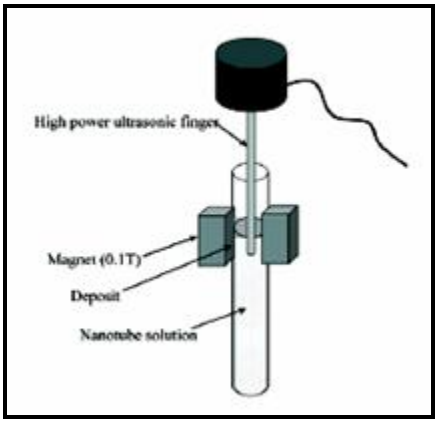

Figure 1.28 Schematic diagram of the apparatus for magnetic purification.[131]

1.6.2 Separation Methods

1.6.2.1 Octadecylamine (ODA) Functionalization

Chattopadhyay and co-workers provided a method for the nondestructive separation of metallic and semi-conducting single walled carbon nanotubes synthesized by high pressure CO conversion (HiPCO) and laser-vaporization by octadecylamine functionalization.[132] The basis for the separation is the difference in stability of the dispersions formed of metallic and semi-conducting SWCNTs and ODA in tetrahydrofuran (THF) solution. The ODA physisorbing on the sidewalls of the semi-conducting SWCNTs gave additional stabilization where as metallic SWCNTs remained insensitive to adsorbed amines. In this case, Chattopadhyay and co-workers selectively

destabilized the ODA organization on metallic SWCNTs causing it to precipitate out of solution, while the semi-conducting SWCNTs remain in supernatant furnishing the separation of SWCNTs.

1.6.2.2 Flow Field-Flow Fractionation

The method of separation by flow field-flow fractionation (FFF) was first reported by the group of Smalley where they demonstrated that FFF technique separated oxidatively shortened SWCNTs on the basis of length. Later on Chen and Selegue of the University of Kentucky reported a detailed study on FFF separation of SWCNTs along with multi walled carbon nanotubes, which was not reported earlier.[133] FFF is merely chromatography-like separation and sizing technique based on elution through a thin, empty channel where separation is (ideally) induced only by physical interactions with an external field. The technique being based on size selective separation is ideal for the separation of CNTs since most of the synthetic techniques yield CNTs with a broad range of size distribution.

1.6.2.3 Size Exclusion Chromatography

Size exclusion chromatography (SEC) is a multi-step process which uses a stationary phase with defined pore sizes and is generally used to separate biological molecules. Using this method, small quantities of SWCNTs can be separated into fractions with small length and diameter distribution. In the process SWCNTs are run over a column with a porous material. During the run SWCNTs are separated depending on their length and diameter distribution. Separation can be done selectively by controlling the pore size of the material used for the column. However, the process demands either dispersed or solvated SWCNTs which can be done by ultrasonication or functionalization with soluble groups.[134-136] Using this method a significant difference in length distributions can be obtained following a nondestructive pathway for purifying nanotubes.

1.6.2.4 DNA Assisted Dispersion and Separation

The group of Zheng *et al*. reported DNA-assisted dispersion and separation of bundled SWNTs effectively in water, by their sonication in the presence of single-stranded DNA (ssDNA).[137] Their studies revealed that DNA-coated carbon nanotube (DNA-CNT) solutions are stable for months at room temperature. Removal of free DNA by either anion-exchange column chromatography or nuclease digestion does not cause nanotube flocculation, indicating that DNA binding to carbon nanotubes is very strong.

DNA-CNTs also offer a potential solution to the problem of separating carbon nanotubes according to their electronic structure. The phosphate groups on a DNA-CNT hybrid provide a negative charge density on the surface of the carbon nanotube, the distribution of which should be a function of DNA sequence and electronic property of the tube. Everything else being equal, DNA-metallic CNTs are predicted to have less surface charge than DNA-semiconducting CNTs due to the opposite image charge created in the metallic tube. Performing an ion-exchange liquid chromatography on DNA-CNTs resulted in the separation of metallic and semiconducting carbon nanotubes. The method adds another pathway for nondestructive dispersion and separation of nanotubes.

1.7 Characterization Methods

In the past two decades plenty of experiments have been performed with carbon nanotubes to get a positive outcome of their unique structure defined electronic and mechanical properties. Though, a chronic problem has been to characterize carbon nanotubes and their modified analogues. Most of the traditional techniques have the drawback that they are incapable of simultaneously probing chemical bonding and electronic structures. On the other hand it is essential to microscopically analyze the surface properties of such nano-structures. In the following sections some of the characterization techniques are briefly discussed which are currently most commonly used to study the structural and electronic behavior of carbon nanotubes.

1.7.1 Electron Microscopy

Among the various analytical techniques, scanning electron microscopy (SEM) and high-resolution transmission electron microscopy (HRTEM) have played a key role in the discovery and characterization of carbon nanotubes. By SEM the carbon nanotubes are observed with features similar to those of some fibrous whiskers grown from pyrolytic graphite. This growth feature is supported by transmission electron microscopy (TEM) observations. Observations reported by Odom *et. al.* using scanning tunneling microscopy (STM) enabled simultaneous imaging and electronic characterization.[50] Fig. 1.29 shows a few representative images of carbon nanotubes obtained by SEM and TEM.

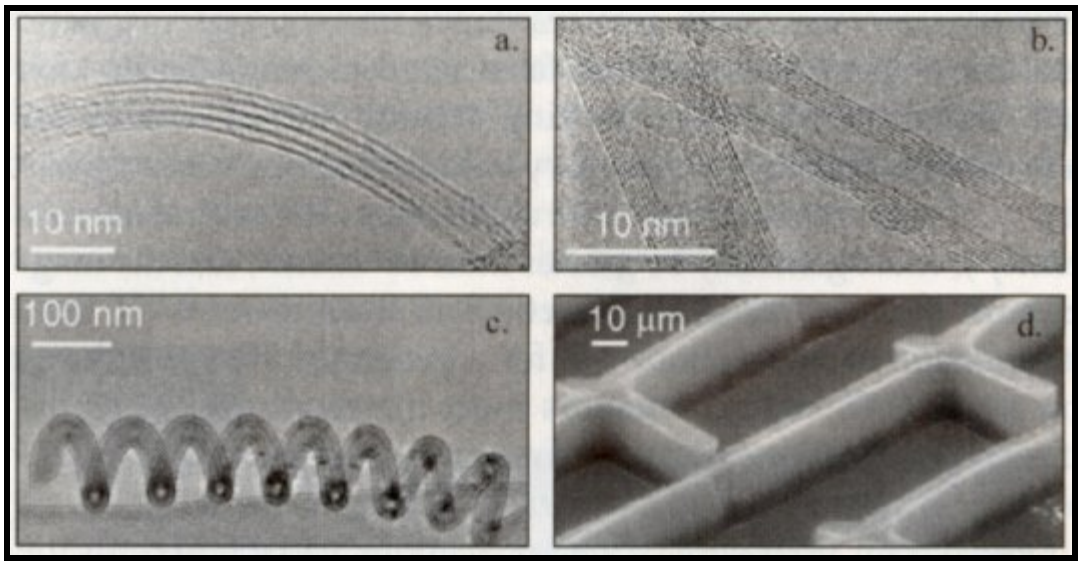

Figure 1.29 Montage of electron microscope images of various carbon nanotubes: (a) SWNT rope prepared by laser ablation technique; (b) MWNTs synthesized by the arc-discharge method; (c) MWNT coil formed in the thermal decomposition of hydrocarbons in the presence of catalytic particles; (d) patterns of oriented nanotube bundles grown on pre-structured deposits of catalytic particles by soft lithography.[138]

Later on advancements in these techniques and addition of other methods like atomic force microscopy (AFM) revealed detailed morphology of carbon nanotubes. Using these methods it is now possible to study detailed sacking arrangements of MWCNTs, the

nature of defects present therein and the information about junctions and capping at the end.

1.7.2 Infrared and Raman Spectroscopy

Infrared and Raman spectroscopy provides an effective and expressive means for the characterization of large varieties of carbon allotropes. Ebbesen *et al.* were the first to perform the Raman spectroscopic studies on carbon nanotubes and related materials.[139] In their experiments CNTs samples produced by arc discharge were collected from the core and outer shell of a cathode and they compared it with the material collected from highly oriented pyrolytic graphite (HOPG) and glassy carbon. They observed Raman active E_{2g} vibrations of graphite in each of the spectra (strong peak in the region 1580 cm^{-1}) while the band at around 1350 cm^{-1} as observed in glassy carbon and cathode deposits can be attributed to disorder (Fig. 1.30.1). Hence they concluded high degree of crystallinity in cathode deposits. Although core deposits not being a homogeneous material, their spectral studies were not able to reveal a detailed information about nanotube structures, nevertheless their observations established a milestone in carbon nanotube characterization. Later on Kastner and co-workers reported similar observations along with transmission infrared spectra (IR) of nanotube samples, resembling the graphite microcrystallites with a broad and unsymmetrical line at 1575 cm^{-1} and a weaker line at 868 cm^{-1}.[140] It is to be noted here that unlike in the case of MWCNTs, where Raman and IR studies resembled to those of crystalline graphite, SWCNTs gave significantly different spectra. Splitting of tangential mode (near 1592 cm^{-1}) and presence of diameter dependent breathing mode frequency (100-200 cm^{-1}) was observed in Raman spectra of SWCNTs (Fig. 1.30.2).[141] Afterwards resonance raman spectroscopy was found to be useful for the characterization of SWCNTs according to their diameter distribution and type (metallic or semi-conducting).[142] Thin film transmission near Infrared (NIR) spectroscopy has also been used to detect SWCNT interband transitions, to evaluate the effect of ionic (doping) and covalent chemistry on the band structure and to monitor the efficiency of purifications.[143]

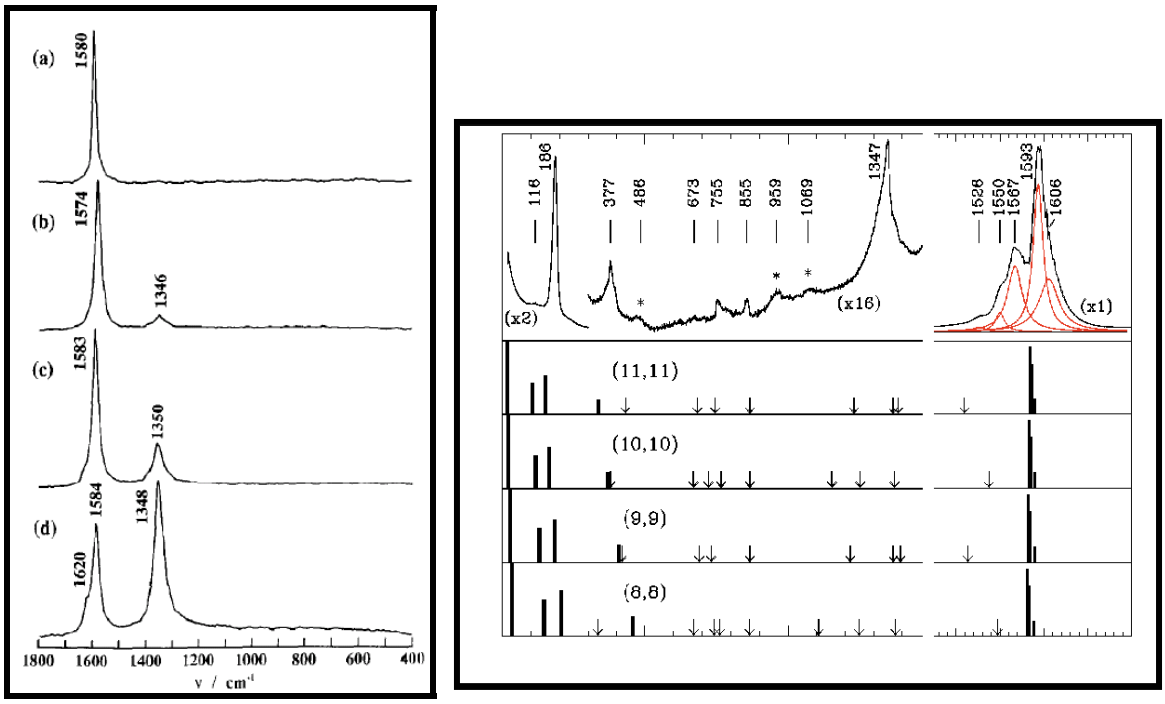

Figure 1.30.1 Comparison of first-order Raman spectra of (a) highly oriented pyrolytic graphite (HOPG), (b) the inner core of the deposit containing nanotubes and nanoparticles, (c) the outer shell of the deposit, (d) glassy carbon.[139]

Figure 1.30.2 Raman spectrum (top) of SWCNT samples taken with 514.5-nm excitation at 2 W/cm^2. The p in the spectrum indicates features that are tentatively assigned to second-order Raman scattering. The four bottom panels are the calculated Raman spectra for armchair (n, n) nanotubes, n = 8 to 11. The downward pointing arrows in the lower panels indicate the positions of the remaining weak, Raman-active modes.[141]

1.7.3 X-ray Diffraction Pattern

X-rays are electromagnetic radiation of wavelength about 1 Å (10^{-10} m), which is about the same size as an atom. They occur in that portion of the electromagnetic spectrum between gamma-rays and the ultraviolet. The discovery of X-rays in 1895 enabled scientists to probe crystalline structure at the atomic level. X-ray diffraction has been in use in two main areas, for the fingerprint characterization of crystalline materials and the

determination of their structure. Average structural properties of carbon nanotubes can be studied by X-ray Diffraction. XRD observations done by Hayashi *et at.* illustrate that interlayer spacing in MWCNTs (d_{002}, ~0.344) is close to the one found in graphite microcrystallites (0.3354 nm).[144] Later on different groups reported different interlayer spacings (0.342 nm, 0.375 nm)[145, 146] which indeed favors the HRTEM analysis reported by Kiang *et al.* where they described that interlayer spacing can vary from 0.34 nm to 0.39 nm depending on the tube diameter.[147] Several other experiments done in the past few years verify the importance of XRD in characterization of carbon nanotubes. Figure 1.31 shows a typical XRD pattern of as prepared MWCNT and after He treatment.

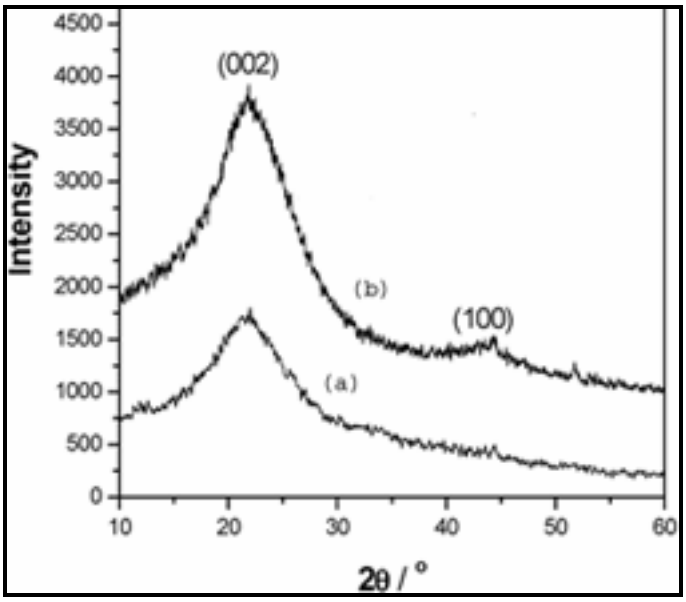

Figure 1.31 XRD pattern of the (a) as synthesized MWCNTs and (b) after treatment with He flow at 800 °C for 5h.[148]

1.8 Opening and Filling Carbon Nanotubes with Metal Particles

Filling of carbon nanotubes represents a quite recent research field for the development of carbon nanotube hybrid materials with new electronic and magnetic properties. The one dimensional nanostructure with hollow interior of carbon nanotubes offers a one dimensional confined space which can be filled with various metals and other

compounds. Smaller diameter of SWCNTs led them to attract more interest for such filling experiments. SWCNTs have been partially filled with alkali halides, lanthanides, and other materials.[149-152] Metal halides confined in nanotubes have been reduced to obtain metal nanowires.[153] Also SWCNTs have been filled completely with molecular species such as fullerenes, their derivatives, and metallocenes.[39, 154] These filling process lead to new composite materials with improved or different properties and functions. On the other hand pore diameter of MWCNTs provides any reactant that reaches at active centers, more space for the reaction and desorption of products. Such properties of MWCNTs open a gateway for their applications as a novel material for catalysts carrier. Many examples have been reported where metal catalysts supported on MWCNTs were found to be better than other carbon based supports for some reactions.[155, 156] In the following part of this section a brief discussion has been made about various pathways for filling carbon nanotubes.

1.8.1 Step 1 – Opening the Closed Ends of Carbon Nanotubes

There are several ways reported for filling of CNTs but whatever be the filling method, the first step is to open closed ends of nanotubes as it is known that carbon nanotubes synthesized by any of the processes are generally closed at either ends. These ends can be made open by either oxidizing them using gases such as carbon dioxide[114] or oxygen[115] at elevated temperatures or by treating them with boiling acids such as HNO_3,[116-118] HCl,[120] H_2SO_4,[119] HNO_3/H_2SO_4[119] or other oxidizing agent such as H_2O_2 or $KMnO_4$ solution (acid/alkali).[153, 157, 158] Opening nanotubes by these methods can in fact be understood as a side effect of purification procedures as methods for purification are indeed the same as mentioned above.[159] These methods do have a disadvantage i.e., resulting in a possible destruction of nanotube structures. However, mild treatments are also widely used, such as soaking CNTs in acid (HNO_3 or HCl) for several hours and then a low temperature heat treatment (~300-400 °C) in open air. In such cases where the purification involved multiple steps such as, thermal oxidation in air and acid based treatments together it is difficult to ascertain which step is more efficient in terms of opening CNTs. In their studies Hirahara *et al.* reported an interesting observation.[154] By their experimental

studies they concluded that a thermal oxidation step is more efficient than acid treatment for opening CNT ends. However, opening methods are not limited to these, B. C. Satishkumar *et al.* reported that nanotubes can be opened not only by boiling acid or acidified $KMnO_4$ solution but also by treating them with superacid HF/BF_3, aqueous OsO_4 or OsO_4-$NaIO_4$ at room temperature.[158] Although they found boiling in acidified $KMnO_4$ to be a more effective method, on the other hand, treatments with super acids allowed to perform the reactions at room temperature. Figure 1.32 shows TEM images of open ended nanotubes taken from an article by Satishkumar *et al*.[158]

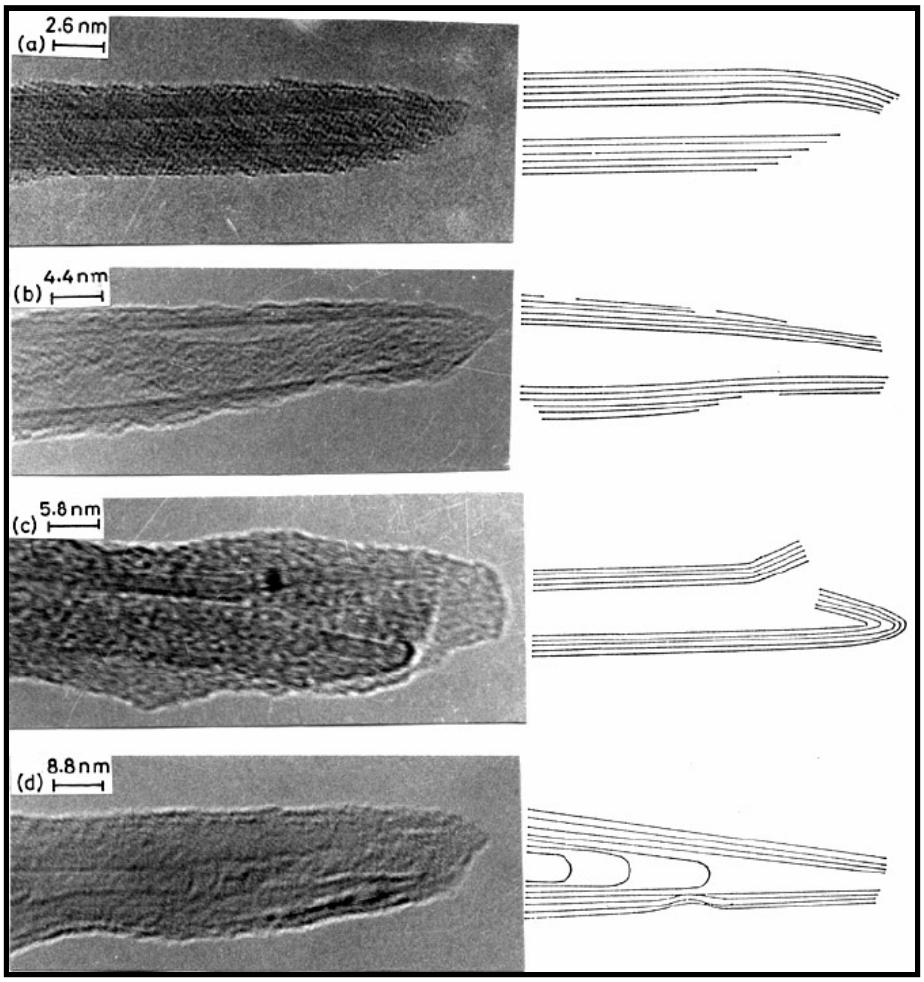

Figure 1.32 TEM images of carbon nanotubes opened by (a) boiling HNO_3, (b) boiling acidified $KMnO_4$, (c) HF/BF_3 and (d) OsO_4 in H_2O at room temperature. Schematic drawings are shown to help in visualizing the opened nanotubes.[158]

1.8.2 Step 2 – Filling with Metals or Other Materials

Once carbon nanotubes are opened, there are several ways to fill them with metals or other desired materials. Methods which are most often used are, gas phase diffusion and liquid phase capillarity either from solution-deposition or direct filling from molten media. The simplest and most often used method for filling CNTs is to mix the desired material to be filled in its molten state with open ended CNTs in a sealed ampule. Due to the induced capillary force molten media moves into the inner cavities of CNTs. This method is found to be quite successful and filling up to 100% has been reported in some cases.[154] Molten material to be filled can be either in its elemental state like Bi[160] or I[161] or rather to achieve low surface tension for an easier capillary filling, salts such as halides can also be used.[150, 153] Though a variety of metals with low melting points can be filled using this method, studies have shown that the surface tension threshold for such filling is 100-200 N/cm^2.[52] This excludes several metals such as Pb, Ga, Hg etc. and allows some elements for example S, Cs, Rb, Se and oxides of V, Pb and Bi. At this point it is important to understand a simple phenomena that the wetting and hence the capillarity occurs only when the liquid - solid contact angle θ_c is less than 90° and surface tension of the molten material plays a vital role in this case. Once tubes are filled with salts they can be further reduced to the corresponding metal or element by annealing (~45-450 °C) under hydrogen.[153, 162]

Apart from using molten media, solution phase chemistry has also provided good results for filling various metals. Satishkumar *et al.* reported filling of metals such as Au or Pt by merely refluxing CNTs with HNO_3 in presence of $HAuCl_4$, H_2PtCl_6 or $AgNO_3$. They were also successful to fill nanotubes by first opening their ends and then sonicating them with salt solutions which were subsequently reduced by an appropriate reagent.[158] Figure 1.33 shows some representative TEM images of such filled nanotubes as reported in the literature by Satishkumar *et al.*[158] Nanotubes are also known to be filled by incorporating sublimed material during their production processes. While using arc discharge, metal filled nanotubes can be obtained by using graphite anodes doped with metals such as Co, Ni or Bi or various carbon anodes doped with C_{60} to obtain peapods.[163]

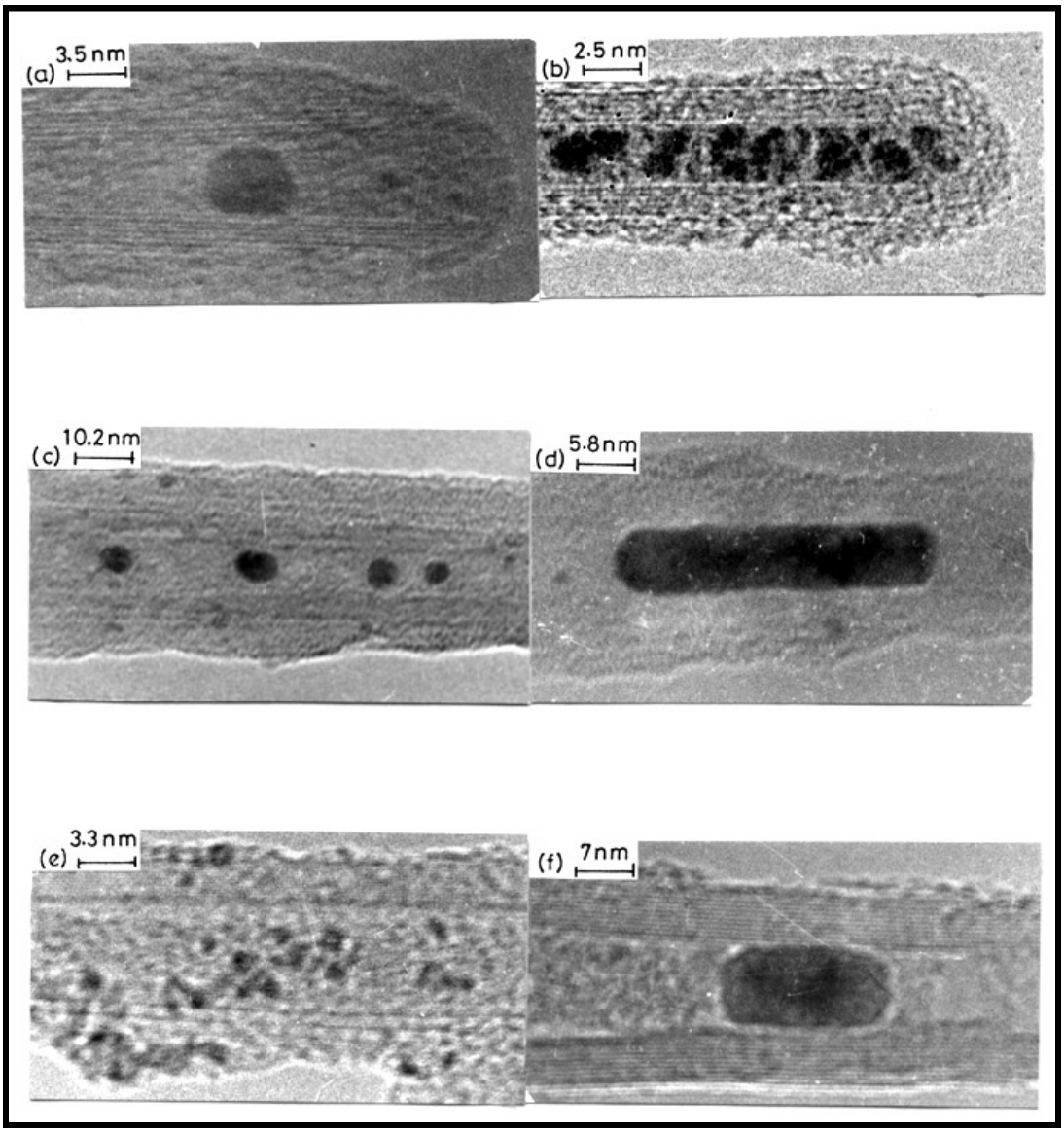

Figure 1.33 TEM images of carbon nanotubes filled with metals: (a) Au-filled CNT obtained by refluxing in HNO_3 containing $HAuCl_4$, (b) Pt-filled CNT obtained by taking H_2PtCl_6 in boiling HNO_3, (c) Ag-filled CNT obtained by taking $AgNO_3$ in boiling HNO_3, (d) Au-filled CNT obtained by reducing $HAuCl_4$ at room temperature with THPC, (e) Pd-filled CNT obtained by reducing the metal nitrate with methanol and (f) Pd-filled CNT obtained by incorporating the metal nitrate and then subjecting it to calcination and hydrogen reduction at 400 °C. Some metal particles are sticking to the surface in (e). Electron diffraction patterns were recorded to ascertain the metallic nature of the particles inside the nanotubes.[158]

1.9 Chemical Functionalization

In spite of having extraordinary electronic, mechanical and structural properties, lack of solubility in any organic or aqueous solvent has imposed a considerable limitation on carbon nanotubes for their use in chemistry. Apart from the insolubility it is known that nanotubes especially SWCNTs are generally formed in bundles which is an obstacle for getting advantage over their unique intrinsic properties. To overcome solubility issue and for debundling carbon nanotubes chemical modification of CNTs is thought to be useful and efficient and enormous interest have been drawn in this area in last few years.[164] Many research groups have reported successful functionalization reactions for CNTs. These functionalization reactions can be roughly divided into three groups:

(a) The covalent attachment of chemical groups onto π-conjugated skeleton of CNT.
(b) The noncovalent adsorption or wrapping of various functional molecules.
(c) The endohedral filling of their inner empty cavity.

1.9.1 Covalent Approaches

Carbon nanotubes consisting graphitic layers can be subjected to many chemical reactions based on covalent bonding to their π-conjugated skeleton. Early approaches in this category were the fluorination of CNTs by elemental fluorine.[165] Fluorinated SWCNTs reported by Margrave, Smalley and co-workers were moderately soluble (~1 mg/mL) in various alcoholic solvents existing at individual level.[166] Further substitution reactions on fluorinated CNTs have been later reported where fluorine was either replaced by alkyl groups using Grignard[167] or organolithium[168] reagents or by diamines[169] or diols[170] via nucleophilic substitution reactions (Figure 1.34). Apart from fluorine CNTs have also been reported to be reactive with chlorine and bromine via electrochemical reactions.[171] Pekker and co-workers prepared hydrogenated CNTs via Birch reduction in liquid ammonia.[171] Hydrogenation by a glow discharge[172, 173] or proton irradiation[174] has also been reported. Continuing towards covalent functionalization [2+1] cycloadditions of carbenes[175, 176] and nitrenes, nucleophilic addition of carbenes[177] and

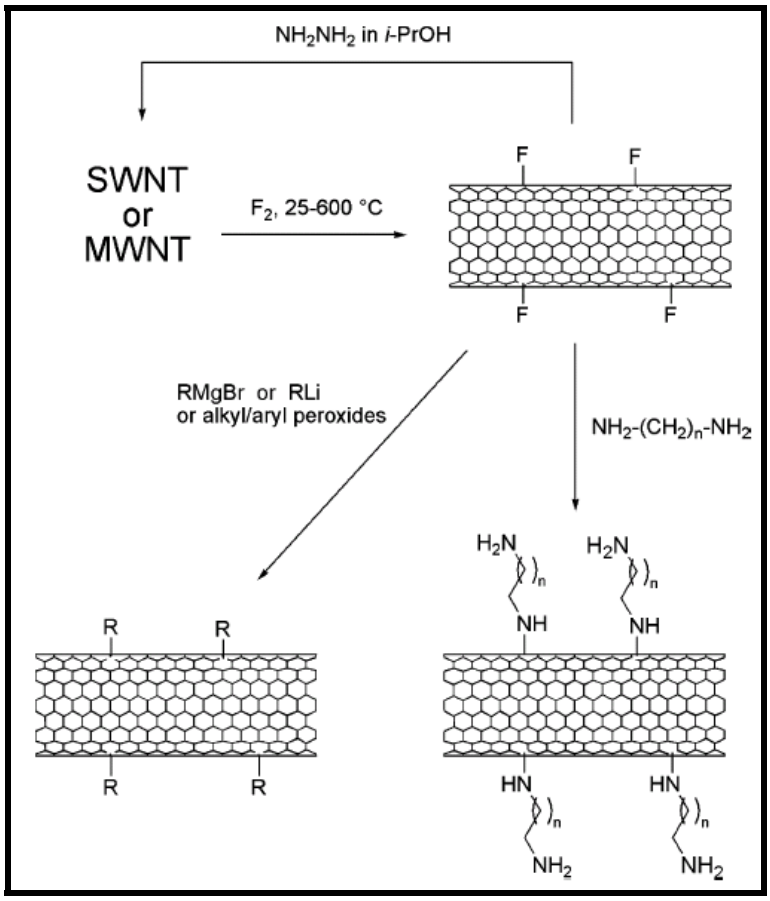

Figure 1.34 Reaction scheme for fluorination of nanotubes, defunctionalization, and further derivatization.[178]

1,3-dipolar cycloaddition of azomethine ylides[179, 180] were also used to modify CNTs (Figure 1.35). Using these methods a variety of groups such as alkyl chains, dendrimers and crown ethers were also attached to CNTs surface. Additionally Bingel (2+1) cyclopropanation reaction[181] and Diels Alder cycloaddtion[182] were also found to be a functionalization routes. Many other pathways for covalent modification of CNTs includes radical addition of diazonium salts[110] or carboxyalkyl radicals,[183] electrophilic addition of chloroform,[184] photostimulated sidewall osmylation of CNTs using OsO_4[185] and Ozonolysis reactions resulting CNT-ozonides.[186, 187] The most common approach now days used for the solubilization of carbon nanotubes is via polymer grafting[188-190] (Figure 1.36), amidation/esterification[191-193] or acylation - amidation[194, 195] (Figure 1.37) reactions at oxidized sites of acid treated nanotubes.

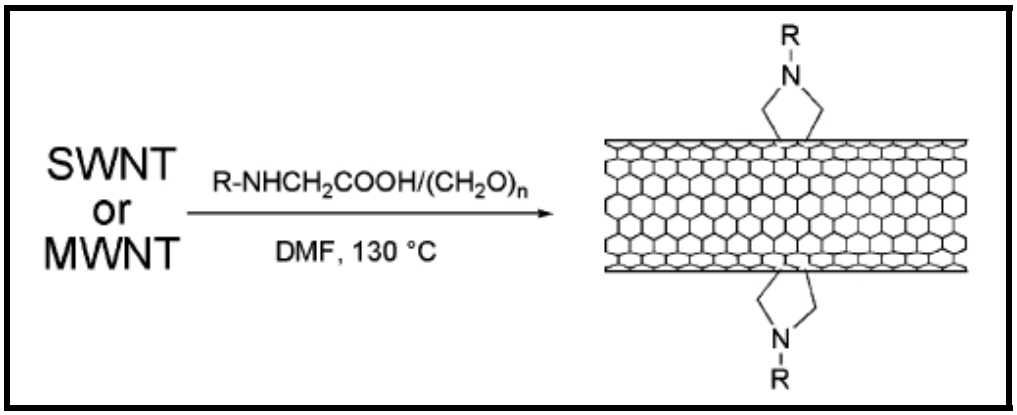

Figure 1.35 1,3-Dipolar cycloaddition of azomethine ylides.[178]

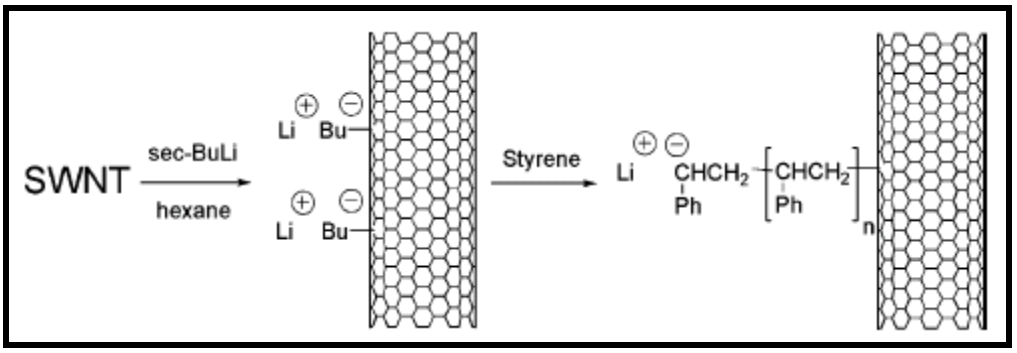

Figure 1.36 Grafting of polystyrene chains by anionic polymerization.[178]

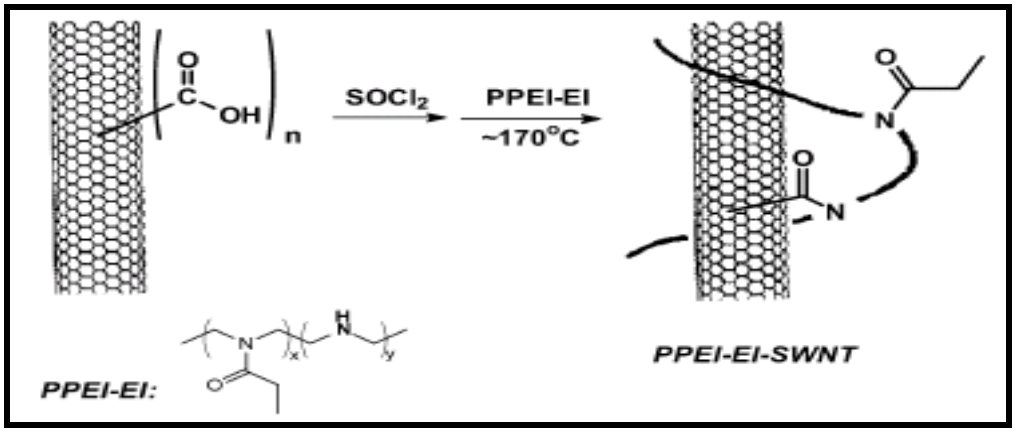

Figure 1.37 Acylationamidation reaction of SWCNTs with aminopolymer poly propionylethylenimine-co-ethylenimine) (PPEI-EI)[194]

1.9.2 Non-Covalent Approaches

Non covalent functionalization based on Van der Waals forces or π-π stacking on carbon nanotubes enabled debundling, and their solublization in various solvents. Commonly used methods involve noncovalent wrapping of CNTs surfaces by various polymers, polynuclear aromatic compounds, surfactants, and biomolecules. Learning their potential, several possibilities were explored in order to prepare CNT-composite materials. These reinforced fibers material hold exceptional mechanical properties. A variety of CNT-composites has been made such as epoxy,[196] acrylates,[196] hydrocarbon polymers,[197] conjugated polymers,[198] polycarbonates,[199] aminopolymers[200] and several others. CNTs are also known to interact non-covalently with biomolecules. Such interactions with biomolecules spark the possibilities of CNTs in biosensor technology. In a different approach bifunctional linkers, based on pyrene moiety are also used (Figure 1.38).[178] CNTs modified by carbohydrate macromolecules are reported to be better soluble in aqueous media.

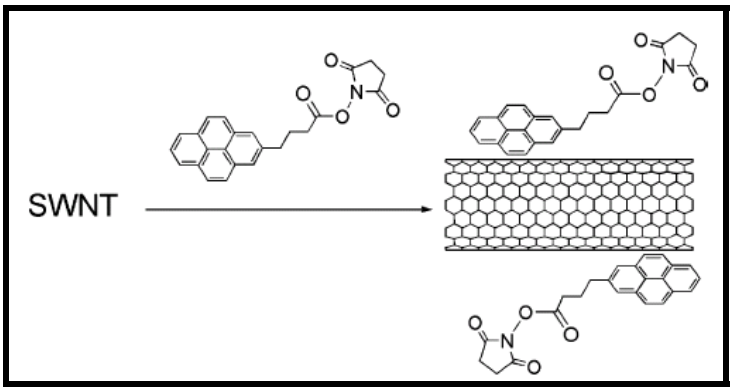

Figure 1.38 Interactions of nanotubes with pyrene derivatives.[178]

1.9.3 Endohedral Filling

Endohedral filling of carbon nanotubes have already been discussed in previous section of this chapter. Attempts have been made to fill hollow inner cavities of carbon nanotubes with not only metals but with many inorganic molecules, fullerene derivatives

and biomolecules. Researchers have reported insertion of proteins such as lactamase[201] and DNA transport[202] into the inner cavities of CNTs.

These functionalization reactions indeed helped in producing CNTs with modified electronic and physical properties. Solubility of functionalized nanotubes enabled use of solution based characterization techniques such as NMR to study their fundamental properties, which was otherwise never possible before with raw carbon nanotube based materials. Functionalized carbon nanotubes are also seen as potential candidates for their use in various biological applications.

1.10 Outlook towards Applications

Among the plethora of applications that have been envisioned for CNTs, polymer composites, field-effect transistors, field-emission displays appear to be the most promising areas. CNTs have also been considered to be novel components for molecular electronics into conventional circuits. The extraordinary electrical conductivity, heat conductivity and mechanical properties of carbon nanotubes have proven them to be interesting materials to be used for various applications. A few of them are summarized below.

1.10.1 Field Emission

Due to their high electrical conductivity carbon nanotubes are found to be excellent field emitters for their use in electronic devices.[37, 203] An unbeatable sharpness of their tip (the sharper the tip, the more concentrated will be an electric field, leading to field emission) also means that they emit at especially low voltage and can carry an astonishingly higher current density, possibly as high as 1013 A/cm^2. Furthermore, the current is extremely stable.[204] These interesting properties of CNTs attracted research activities to an immediate application of this in field-emission flat-panel displays,[205] lamps,[206] gas discharge tubes,[207] and x-ray generators.[208] The high current density, low turn-on and operating voltage, and steady, long-lived behavior of nanotubes enabled their uses for

such applications. Other applications utilizing the field-emission characteristics of buckytubes include: general cold-cathode lighting sources, lightning arrestors, and electron microscope sources. Fig. 1.39 shows a representative example to make a field-emission source with an individual multiwalled nanotube mounted onto a gold tip.[209]

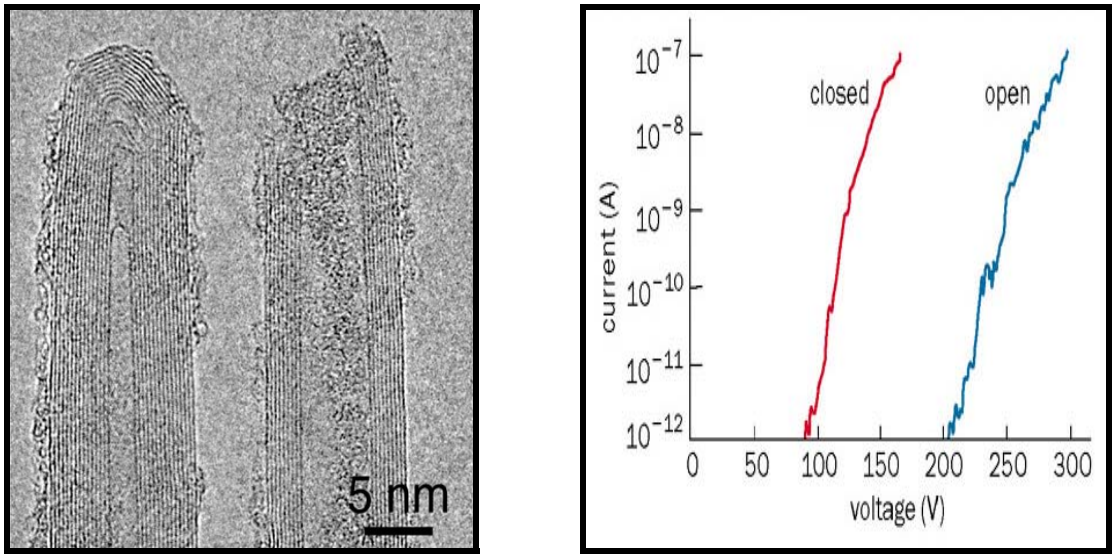

Figure 1.39 (a) TEM images of closed (left) and open MWCNT used in field-emission experiments. (b) Current-voltage characteristics for field emission from open and closed nanotubes. Closed nanotubes can produce significant emission currents at much lower applied voltages than open nanotubes.[209]

1.10.2 Conductive Plastics, Adhesives and Connectors

It is well known that plastics used now days for most of the structural applications, are good electrical insulators. To overcome this deficiency, plastics are generally loaded with conductive fillers, such as carbon black and graphite fibers. The loading required to provide the necessary conductivity is typically high, resulting in heavy parts, and more importantly, degradation of other performance aspects such as mechanical properties and low melt viscosity needed for thin-wall molding applications. CNTs found to be ideal in this sense, since they have the highest aspect ratio of any carbon fiber and their natural tendency to form ropes provides inherently very long conductive pathways even at ultra-

low loadings.[210] Applications that exploit this behavior of CNTs include electromagnetic radiation shielding composites and coatings for enclosures and gaskets, and electrostatic dissipation (ESD), antistatic materials and even transparent coatings; and radar-absorbing materials. The same issues that make CNTs attractive as conductive fillers make them attractive for electronics materials, such as adhesives and other connectors (e.g., solders). Loading of MWCNTs as low as 1% in polystyrene increases the modulus and breaking stress by up to 42 and 25% respectively.[211]

1.10.3 Energy Storage

CNTs have a tremendously high surface area (~1000 m^2/g), good electrical conductivity and useful mechanical properties combined with a linear geometry which makes their surface highly accessible to the electrolyte. Research has shown that CNTs have the highest reversible capacity of any carbon material for use in lithium-ion batteries.[212] In addition, CNTs are outstanding materials for supercapacitor electrodes[212] which have giant capacitance in comparison with those of ordinary dielectric based capacitors and electrochemical actuators[213] that may eventually be used in robots. CNTs also have a number of properties including high surface area, electrical and thermal conductivity that make them useful as electrode catalyst supports in PEM fuel cells, in gas diffusion layers as well as current collectors. CNTs high strength and toughness to weight characteristics may also prove valuable as part of composite components in fuel cells that are deployed in transport applications where durability is extremely important.

1.10.4 Molecular Electronics

The idea of building electronic circuits out of the essential building blocks of materials - molecules - has seen a revival the past five years, and is a key component of nanotechnology. In any electronic circuit, but particularly as dimensions shrink to the nanoscale, the interconnections between switches and other active devices become increasingly important. Their geometry, electrical conductivity, and ability to be precisely derived, make CNTs the ideal candidates for the connections in molecular electronics. In

addition, they have been demonstrated as switches themselves. Field effect transistors (FET) have been prepared by lithography applying electrodes to CNTs that were either randomly distributed on a silicon substrate or positioned on the substrate with an atomic force microscope (AFM).[214, 215] Not only electrical conductivity but anisotropic thermal conductivity of CNTs finds their applications as heat sink in electronic devices particularly in computers used for advanced computing, where un-cooled chips now routinely reach over 100 °C. CNI's technology for creating aligned structures and ribbons of CNTs is a step towards realizing incredibly efficient heat conduits.[216] In addition, composites with CNTs have been shown to dramatically increase the bulk thermal conductivity at small loadings. Fig. 1.40 shows a representative image of nanoelectronic devices made with the use of CNTs.[214]

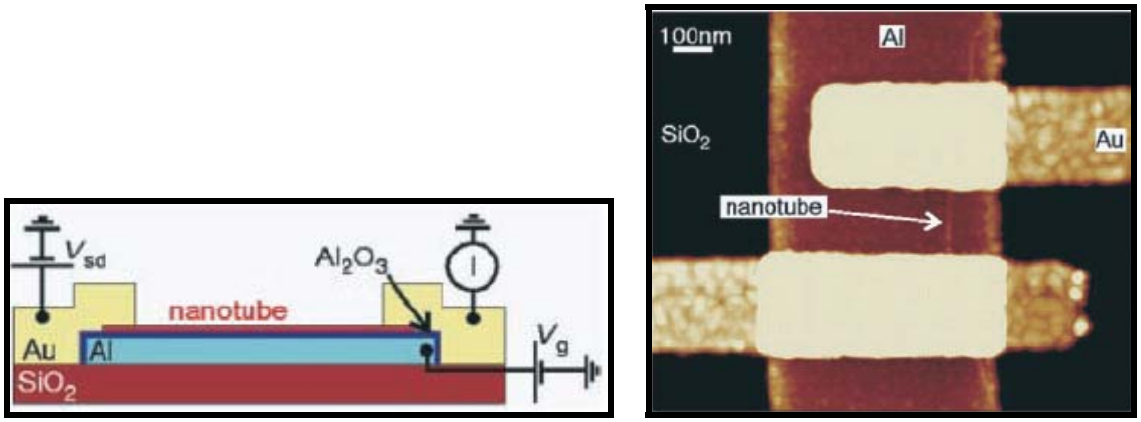

Figure 1.40 (a) Schematic diagram for a CNT-FET. The semiconducting nanotube, which is on top of an insulating aluminum oxide layer, is connected at both ends to gold electrodes. The nanotube is switched by applying a potential to the aluminum gate under the nanotube and aluminum oxide. V_{sd} is source-drain voltage and V_g, gate voltage. (b) STM image of a SWCNT field-effect transistor made using the design of (a). The aluminum strip is over coated with aluminum oxide.[214]

1.10.5 Structural Composites, Fibers and Fabrics

The properties of CNTs are not limited to electrical and thermal conductivities, but also include mechanical properties, such as stiffness, toughness, and strength. These properties lead to a wealth of applications exploiting them, including advanced composites requiring high values in one or more of these properties. Fibers spun of pure CNTs have recently been demonstrated and are undergoing rapid development, along with CNTs composite fibers.[217] Such super strong fibers will have applications including body and vehicle armor, transmission line cables, woven fabrics and textiles.

1.10.6 Applications in Chemistry and Biology

CNTs have an intrinsically high surface area; in fact, every atom is not just on a surface - each atom is on two surfaces, the inside and outside! Combined with the ability to attach essentially any chemical species to their sidewalls provides an opportunity for unique catalyst supports. Their electrical conductivity may also be exploited in the search for new catalysts and catalytic behavior. CNTs have also been explored for their potential in biomedical applications.[218, 219] Living cells have been shown to accumulate CNTs, so they appear to have no toxic effect.[220] The cells also do not adhere to the CNTs, potentially giving rise to applications such as coatings for prosthetics and anti-fouling coatings for ships. The ability to chemically modify sidewalls of CNTs also leads to biomedical applications such as vascular stents, and neuron growth and regeneration.

There is a wealth of other potential applications for CNTs, such as solar collection, nanoporous filters, sensors and probes and coatings of all sorts. There are almost certainly many unanticipated applications for this remarkable material that will come to light in the years ahead and which may prove to be the most important and valuable of all.

2. Aims

The aim of this work was the chemical functionalization of carbon nanotubes via different procedures. In this context exploitation of the modified carbon nanotubes to a variety of applications were investigated. In addition possibilities for the use of iron filled carbon nanotubes for such modification and their further use in chemical reactions were explored.

The following aspects of carbon nanotubes were studied:

1. Synthesis of single and multi walled carbon nanotubes by chemical vapor deposition.
2. Investigating the possibilities of solid state synthesis of Fe or Co filled carbon nanotubes.
3. Optimization of the purification techniques for the nanotubes produced by different techniques.
4. Exploring the possibilities for filling nanotubes with various elements such as Pd, Ru and Fe.
5. Exploring the possibilities for functionalization of Fe filled carbon nanotubes and their application in various chemical reactions as catalysts.
6. Exploring possibilities to dissolve and precipitate carbon nanotubes reversibly.

Wet chemistry methods were explored for the desired filling of carbon nanotubes. The advantage of modifying the Fe-filled carbon nanotubes for their use in chemical reactions would be the ease in recovery by using a simple magnet. Such modified nanotubes can also find a great potential towards targeted drug delivery. Alongside the use of various organometallic complexes for pyrolysis was explored for the solid state synthesis of metal filled carbon nanotubes and related structures. The morphology of microstructures produced was studied by electron microscopic techniques and chemically modified materials were characterized using Raman and infrared spectroscopy and thermo gravimetric analysis.

3. Results and Discussion

3.1 Synthesis of Carbon Nanotubes and Other Structures

3.1.1 Catalytic Vapor Deposition Synthesis

Several catalysts were prepared for their application in CVD processes for the synthesis of carbon nanotubes. Single walled and multi walled carbon nanotubes were synthesized using C_2H_2 and CH_4 as carbon feedstock. The catalysts Ni-Mo/MgO, Fe-Mo/MgO, Co-Mo/MgO, Fe-Mo/Al_2O_3 and Co-Mo/Al_2O_3 were prepared for the synthesis. Catalysts over MgO were prepared by either combustion method[221] or by mixing metal salts and MgO in deionized water.[222] Also catalysts over Al_2O_3 were prepared using the latter method used for MgO support. In the experiments it was found that Fe-Mo/MgO and Ni-Mo/MgO were the most suitable catalysts for the synthesis of single walled and multi walled carbon nanotubes. Morphology of the prepared carbon nanotubes was observed by SEM and TEM.

3.1.1.1 Preparation of Carbon Nanotubes

For the synthesis of carbon nanotubes several known methods were tested. The most favorable methods found were the one reported by C. J. Lee *et al.*[222] and X. B. Zhang *et al.*[223] The CVD method used by Lee *et al.* over the catalyst Fe-Mo/MgO and acetylene as the carbon feed stock was first followed. The morphology of as prepared material was characterized by SEM. Bunches of carbon nanotube on MgO support are clearly visible in the SEM images shown in Figure 3.1.

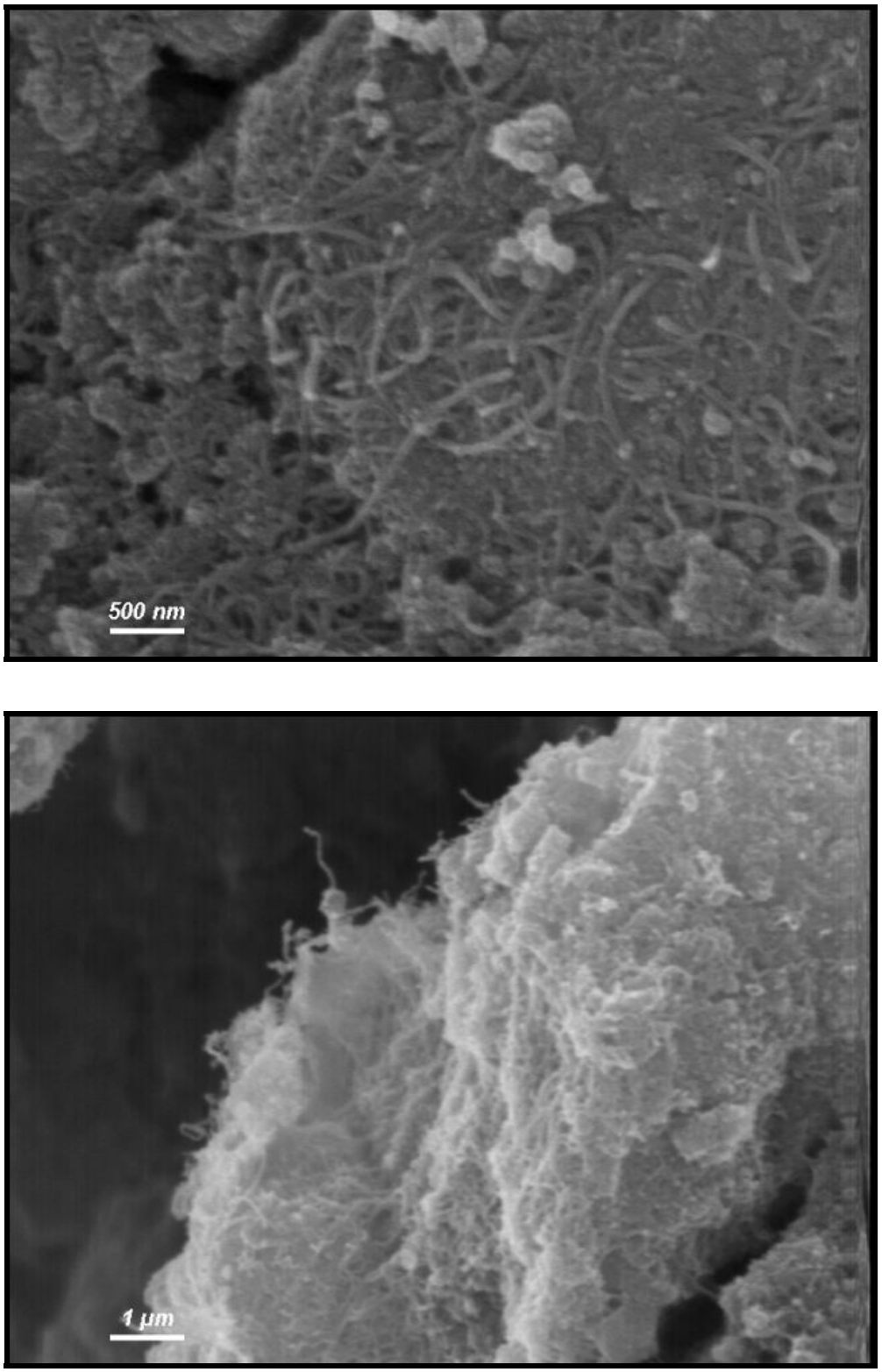

Figure 3.1 SEM images of as prepared carbon nanotubes. Bunches of tubes are visible on the MgO support.

In the procedure reported by X. B. Zhang *et al*.[223] Ni-Mo nanoparticles were applied with MgO as support. As a carbon source methane in a mixture with hydrogen was used at a temperature of 1000 °C in a furnace. The obtained material was characterized by TEM. Figure 3.2 shows TEM images of the as prepared nanotubes and CNTs after purification.

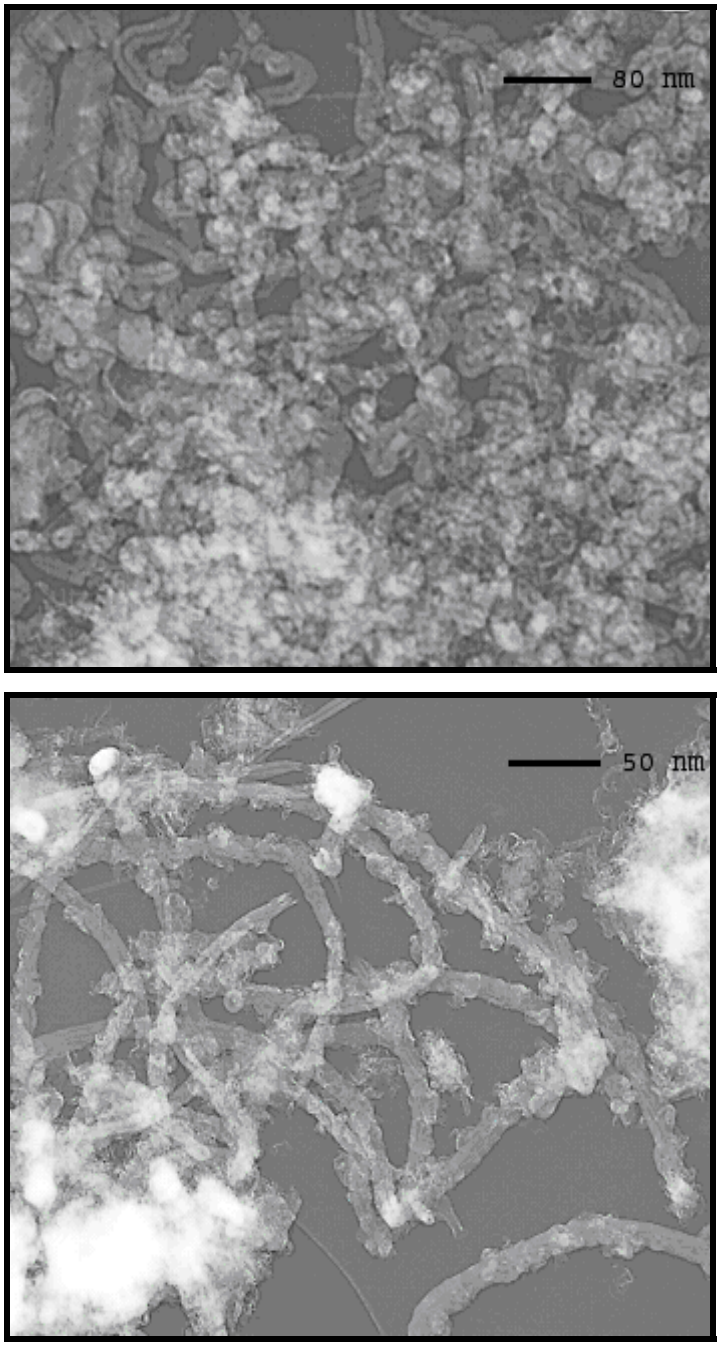

Figure 3.2 TEM image of as prepared MWCNTs (top) and after purification (bottom)

3.1.2 Solid State Synthesis of Carbon Nanotubes

Co filled MWCNTs were prepared as described by K. P. C. Vollhardt *et al.*[109] through the pyrolysis of a cobalt complex $[Co_2(CO)_6(PhC_2Ph)]$[111] at 700 °C in a sealed quartz tube. The complex **2** was readily prepared in one step by mixing commercially available dicobaltcarbonyl (1 gm) and diphenylacetylene (0.83 gm) in hexane (Scheme 3.1). The mixture was then stirred overnight. A dark reddish solid was obtained after flash column chromatography with petroleum ether. 50 mg of so obtained Co-complex was then sealed in a quartz tube under vacuum. The tube was placed in a horizontal tube furnace and the temperature of the furnace was raised to 700 °C at a rate of 10 °C per minute. The furnace temperature was maintained at 700 °C for 2 hours. After cooling the furnace to room temperature the carbon soot was collected and subsequently stirred overnight in HCl solution to wash off metal particles outside the tubes.

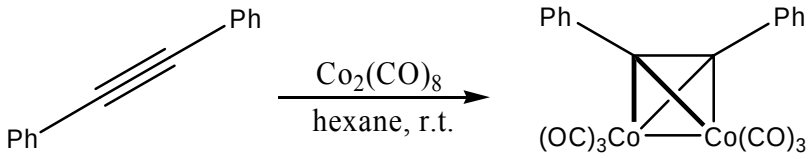

1 **2**

Scheme 3.1

The crude material was characterized with SEM and the purified samples with TEM. Figure 3.3 (a) shows an SEM image of the crude product and Figure 3.3 (b, c) shows the TEM images of Co filled carbon nanotubes.

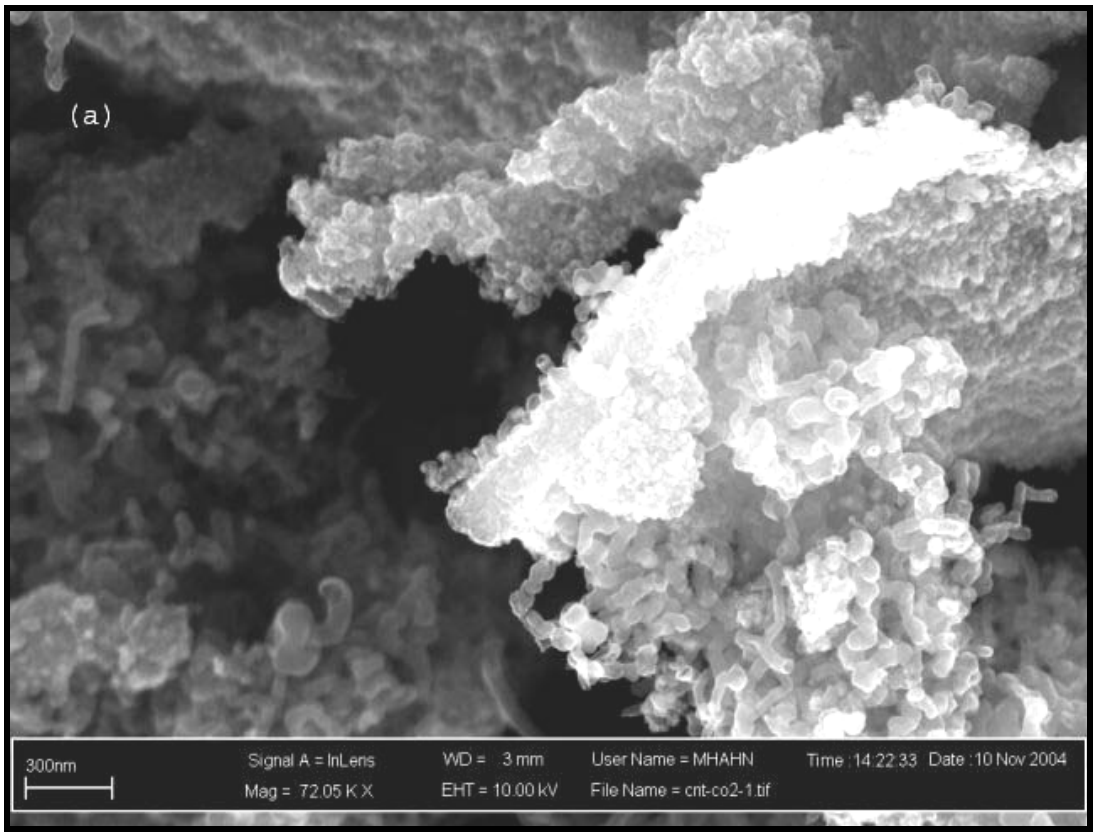

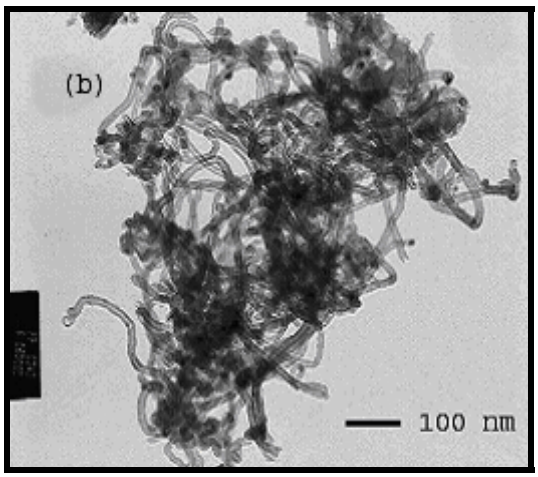

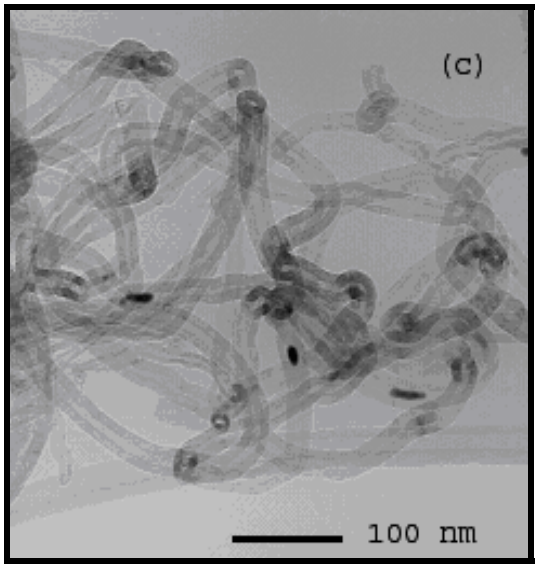

Figure 3.3 SEM image of as prepared nanotubes (a), TEM (b) and HRTEM (c) image of CNTs washed with HCl

Such prepared MWCNTs were found to be magnetic to some extent. Presence of small cobalt particles inside some of the tubes as shown in Figure 3.4 verifies the fact.

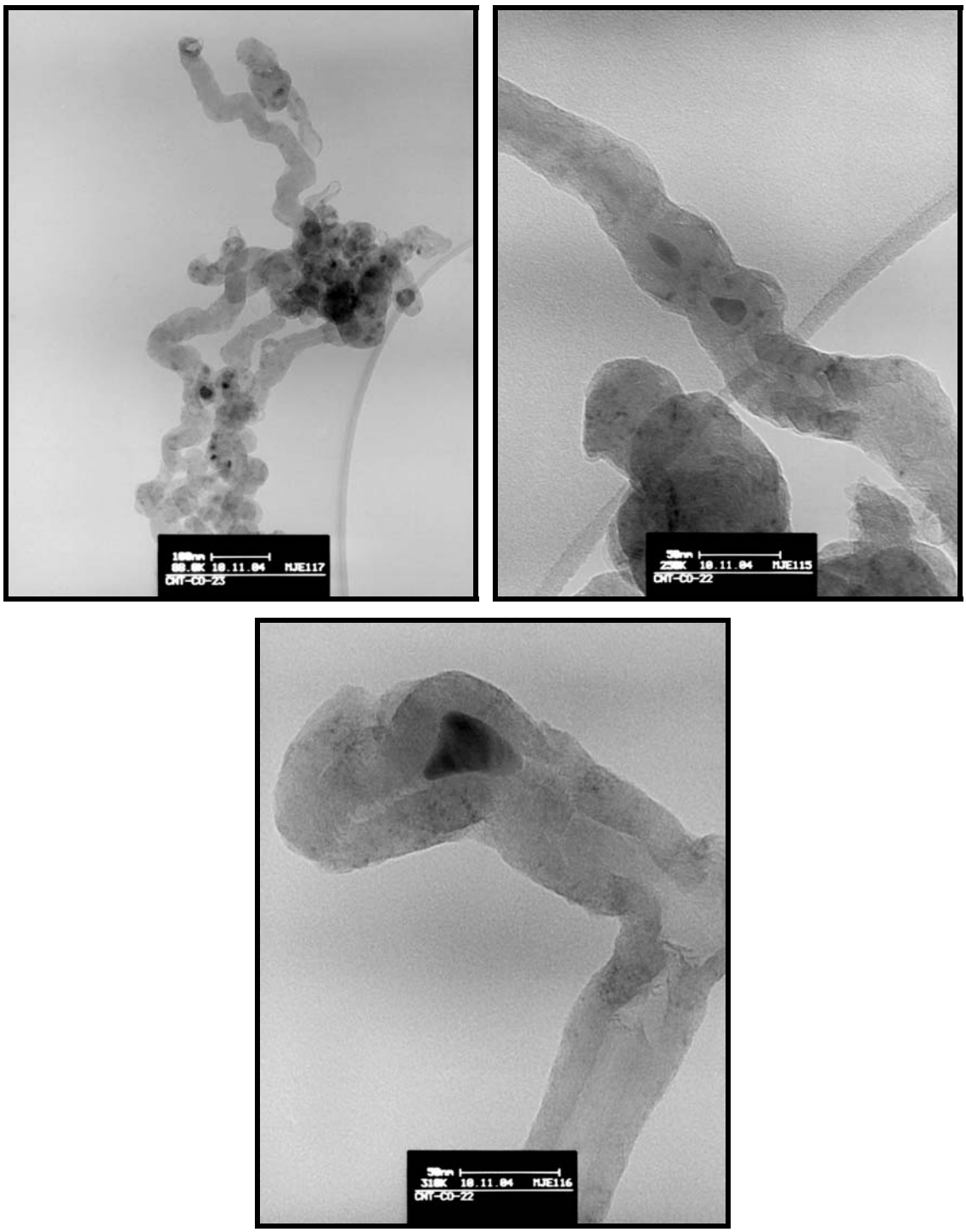

Figure 3.4 HRTEM images of Co-filled MWCNTs

3.1.3 Solid State Synthesis of Carbon Nanocapsules[224]

It is well known that pyrolysis of different organometallic complexes in a sealed vessel can lead to interesting carbon nano structures like carbon nanotubes,[225, 226] nanocables[227] and nanpspheres.[228] In an attempt to prepare desired Fe-filled carbon nanotubes metal containing organometallic complexes were prepared and used in a solid state pyrolysis. This work was performed by an undergraduate student Andreas Winkel for his advanced organic research project. Carbon nanocapsules were prepared by pyrolysis of organometallic complexes. Complex **3**[229] was pyrolyzed at 700 °C (temperature increment at a rate of 10 °C per minute) for 2 h in a sealed quartz tube in order to give carbon nanocapsules in near quantitative yield. Prior to TEM measurements, the samples were washed with concentrated HCl in order to remove iron and other impurities. When complex **4**[230] (Scheme 3.2) was pyrolyzed at 700 °C with a similar heating rate, rather deformed, undefined, and unfilled tubular structures were formed (see Figure 3.7). These results showed that the structures produced are highly dependent on the starting complex used in the pyrolysis reaction.

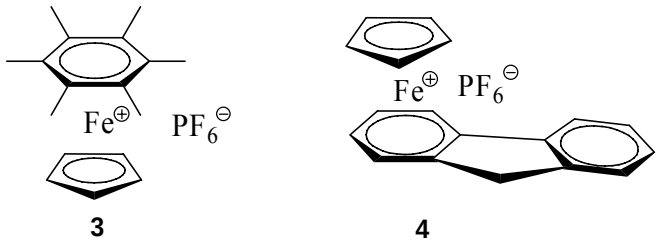

3 **4**

Scheme 3.2

Representative images of the morphology of obtained samples are shown in Figure 3.5. The low-resolution images (Figure 3.5a and 3.5b) revealed that the samples contained a large quantity of capsules with an average diameter of 100 nm, an average wall thickness of 16 nm, and a length varying from 220 to 700 nm with no other amorphous carbon by-products. This result suggests that a near-quantitative yield of the nanocapsules was obtained. HRTEM images of such capsules are shown in Figure 3.6a, while Figure 3.6b

and 3.6c displays a few capsule-like structures, which were either poorly developed (Figure 3.6b) or deformed (Figure 3.6c).

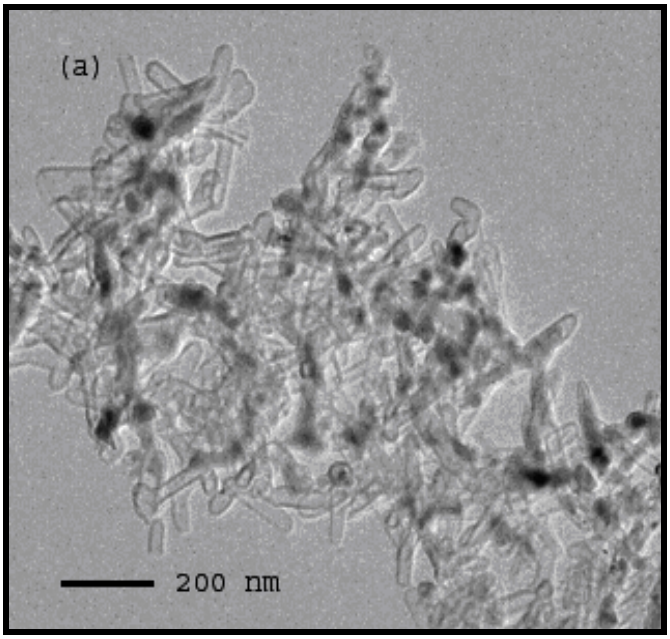

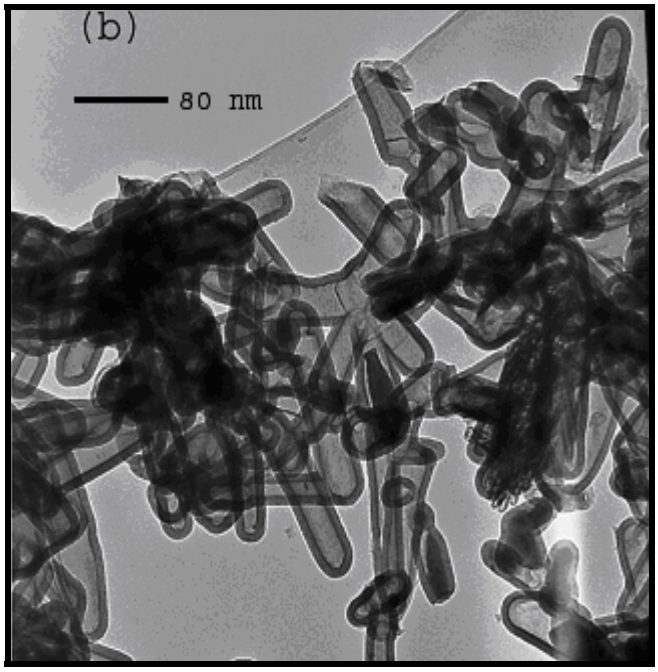

Figure 3.5 Typical TEM image of nanocapsules (a), another TEM image at higher magnification (b).

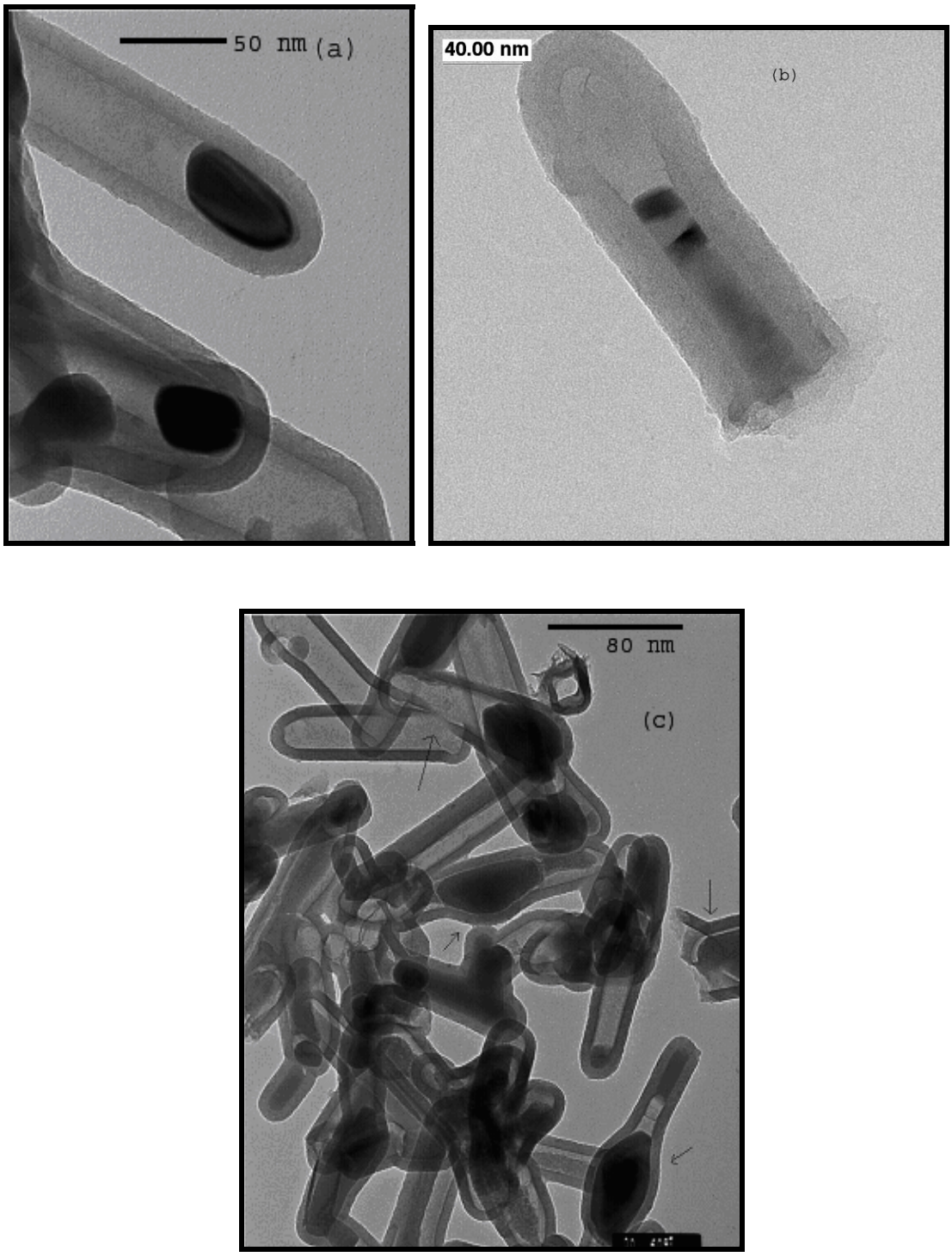

Figure 3.6 (a) HRTEM image of nanocapsules showing the wall structure and amorphous material filled inside. (b) HRTEM image of an undeveloped capsule (c) HRTEM image showing that a few capsules were deformed.

Figure 3.7 below shows a TEM image of undefined structures formed when complex **4** was pyrolyzed. It can be seen that unlike the capsules formed from complex **3** these structures are rather undefined tubular and they are not filled.

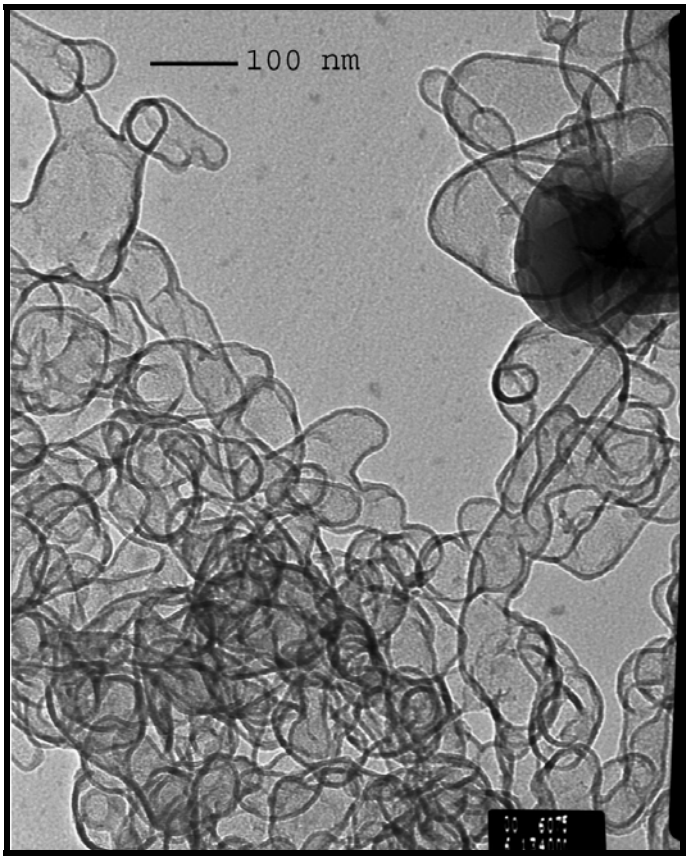

Figure 3.7 TEM image of undefined structures formed by the pyrolysis of complex **4**

The capsules consisted of a thick wall of carbon and were filled with a non crystalline composite material containing mainly Fe and P, which was characterized by using energy-dispersive x-ray analysis (EDX). Since the walls were not graphitized, as is the case with multiwalled carbon nanotubes, one of the obtained samples was heated under argon at 700 °C for 12 h. The resulting material was analyzed and the results are depicted in Figure 3.8. The procedure had no influence on the overall structure, however, the amorphous Fe–P composite was transformed into a crystalline structure. Figure 3.8a represents a HRTEM image of such a capsule showing the wall structure and the material

inside the capsule. Figure 3.8b shows the selected-area electron diffraction (SAED) pattern taken from such a filled capsule. To analyze the chemical composition of the crystalline filling material, EDX measurements were performed. Figure 3.9 shows the EDX spectrum of the filled capsules, which confirmed the presence of Fe and P within the capsules. The detected Cu is due to the TEM grid. The diffraction pattern shown in Figure 3.8b and the presented EDX pattern confirmed that the nanoparticles within the capsules were composed of a crystalline Fe–P composite when heated under argon at 700 °C for 12 h. In addition XRD of filled capsules was also recorded (see Figure 3.10).

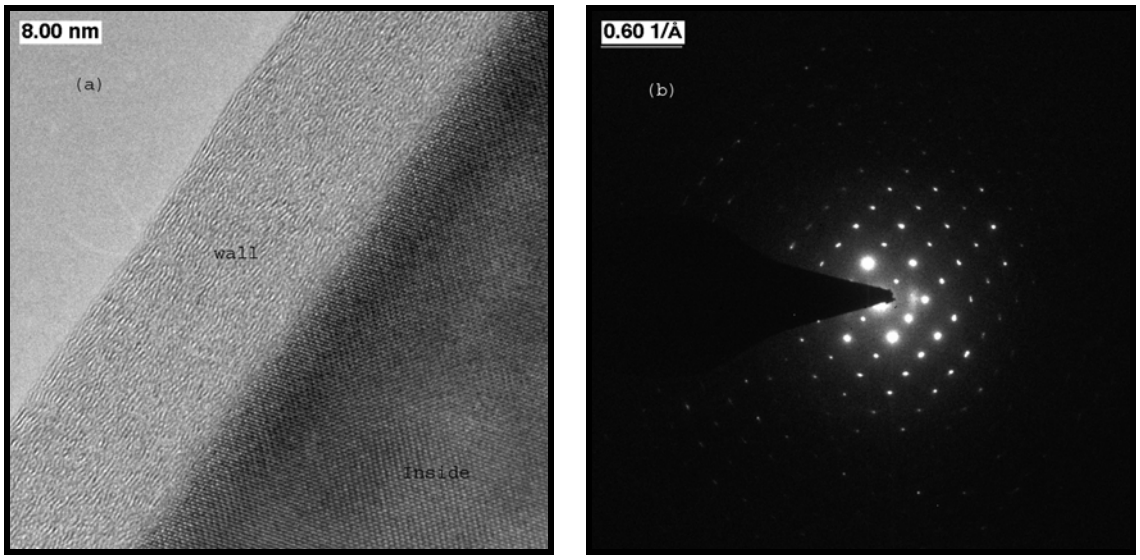

Figure 3.8 (a) HRTEM image of a capsule wall and the material filled inside after annealing at 700 ºC for 12 h. (b) Electron diffraction pattern corresponding to the material inside the capsule is shown in Figure (a).

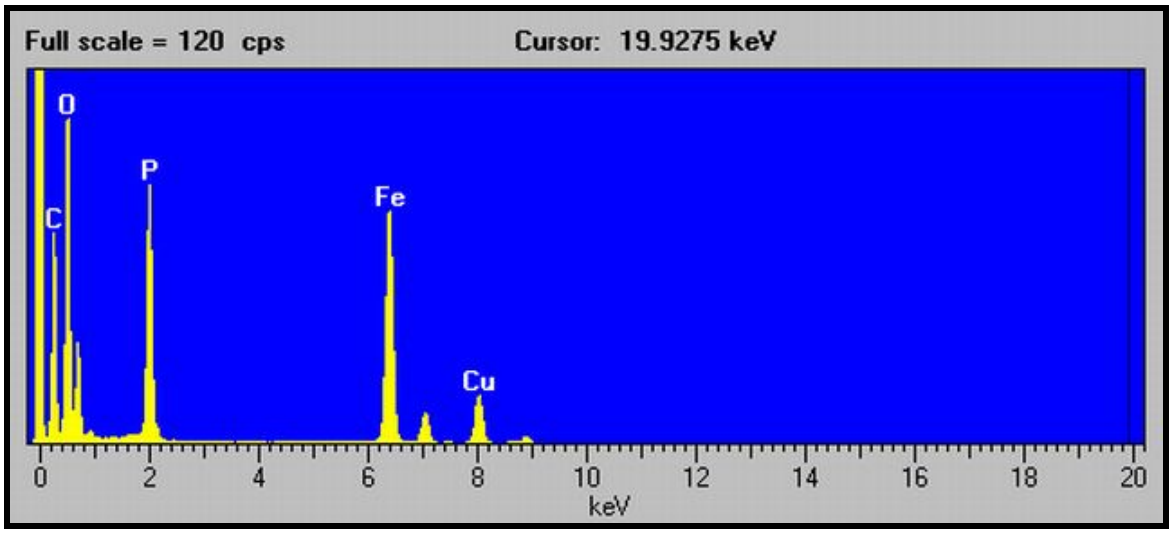

Figure 3.9 A typical EDX pattern of filled capsules.

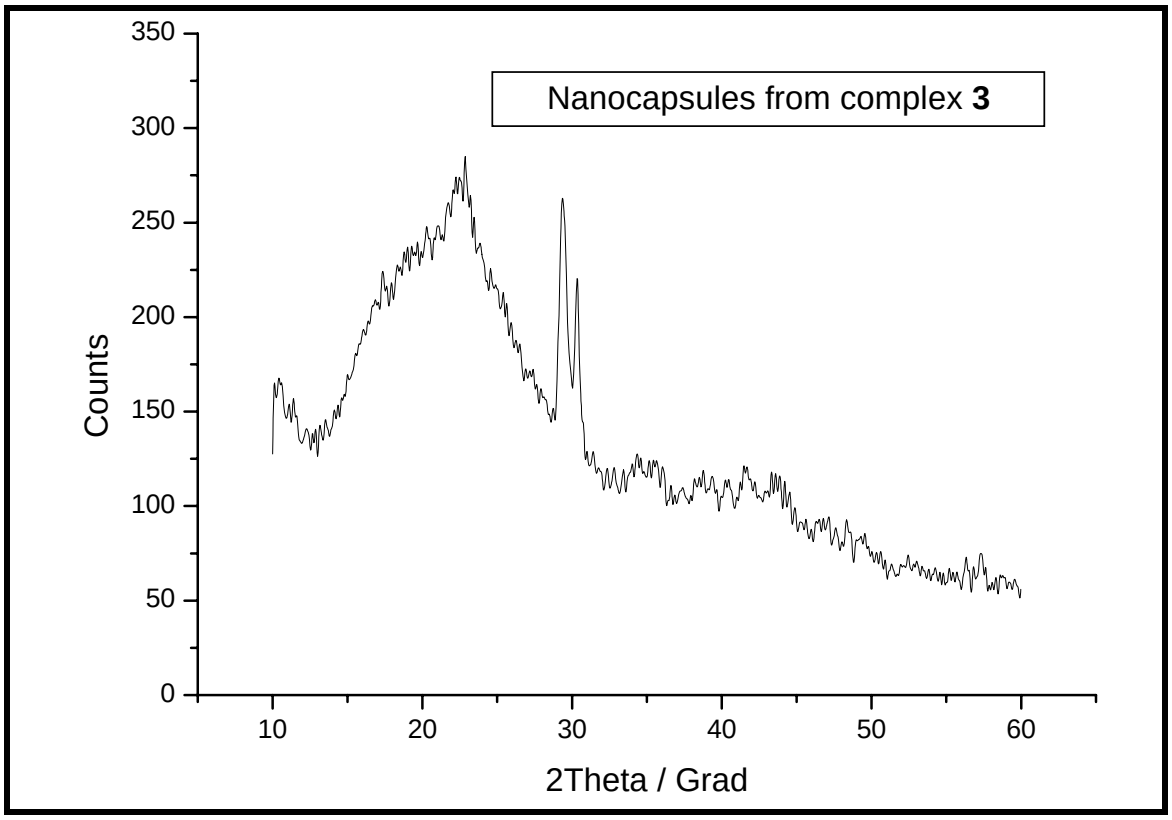

Figure 3.10 XRD spectra of filled capsules

3.1.4 Solid State Synthesis of TiC and VC Carbon Nanospheres

It has been shown by Cassoux *et al*.[231] that pyrolysis of vanadocene complexes in a CVD process at elevated temperatures (up to 1000 ºC) can also yield vanadium carbide nano structures.[231, 232] Therefore it was decided to investigate the behavior of V and Ti complexes under solid state pyrolysis conditions. Pyrolysis experiments were performed on the following Ti (**5**, **6**)[233] and V (**7**)[234] complexes (Figure 3.11) which were received from Prof. Matthias Tamm, Institut für Anorganische und Analytische Chemie, TU Braunschweig. Complexes (**5**, **6** and **7**) were used as received and pyrolyzed in a similar fashion as described above in section 3.1.2.

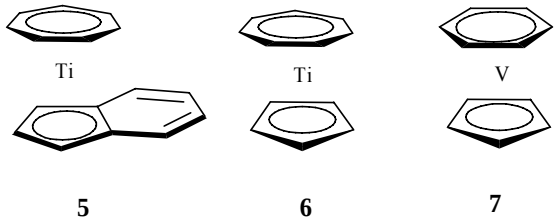

Figure 3.11 Ti and V complexes used as precursors for pyrolysis

To observe temperature dependence, complexes were pyrolyzed at different temperatures between 700 ºC to 900 ºC. The morphology of the as prepared samples was investigated by TEM. Since the as prepared samples were found to be amorphous in nature, these samples were further annealed in a H_2/Ar atmosphere at 1100 ºC for 2 hours. It is known that such annealing at higher temperatures can modify the structure to some extent.[235, 236] With these experimental results, a simple solid state synthetic route towards the synthesis of VC and TiC nanospheres was established, compared to more widely used CVD techniques to prepare VC[231, 232, 237] and TiC[238] coatings.

Figure 3.12 shows low resolution TEM images of TiC and VC nanospheres. From the images can be observed that the samples contained nanospheres in high yield and there was no amorphous carbon present in the samples which is remarkable. The Raman and XRD spectra of the nanospheres formed by pyroysis of Ti complex revealed only TiC

with a ratio of Ti:C close to 1:1. Considering that the starting complex has a Ti:C ratio of 1:4 (**5**) and 1:3 (**6**), the question arises, where the rest of the carbon has gone ? After the pyrolysis, when the sealed quartz tubes were opened, a positive pressure of gas was observed. With this observation it can be assumed that the carbon was present as C-H gaseous form in the sealed tube and was evolved when the tubes were opened. In case of vanadocene complex, exact stoichiometry of VC could not be estimated by XRD. Figure 3.13 shows a typical TEM image of TiC nanospheres. Figure 3.14 shows HRTEM images of annealed samples. Figure 3.15 and 3.16 shows XRD spectra of TiC and VC samples respectively before and after annealing. Figure 3.17 shows a Raman spectra of the as prepared samples.

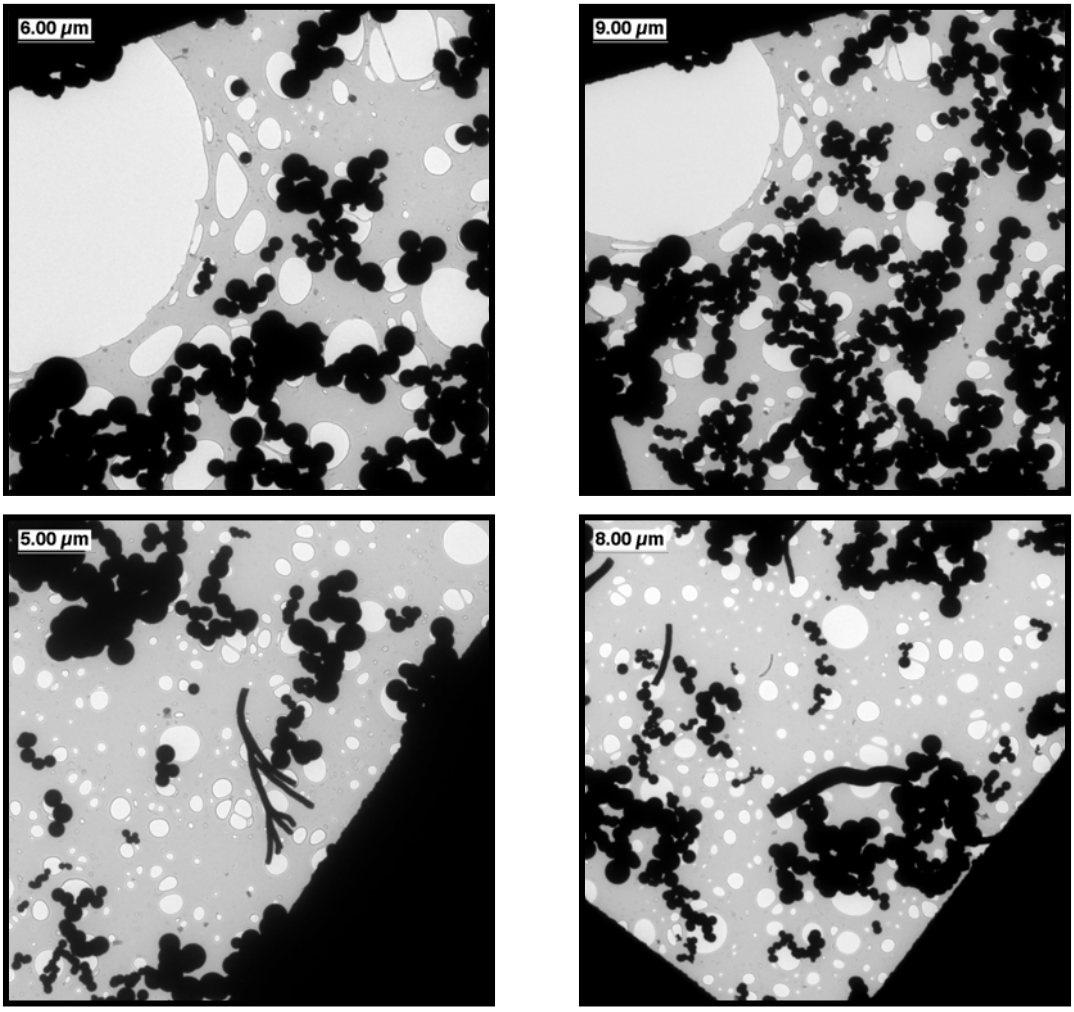

Figure 3.12 Low resolution TEM images of TiC (top) and VC nanospheres (bottom).

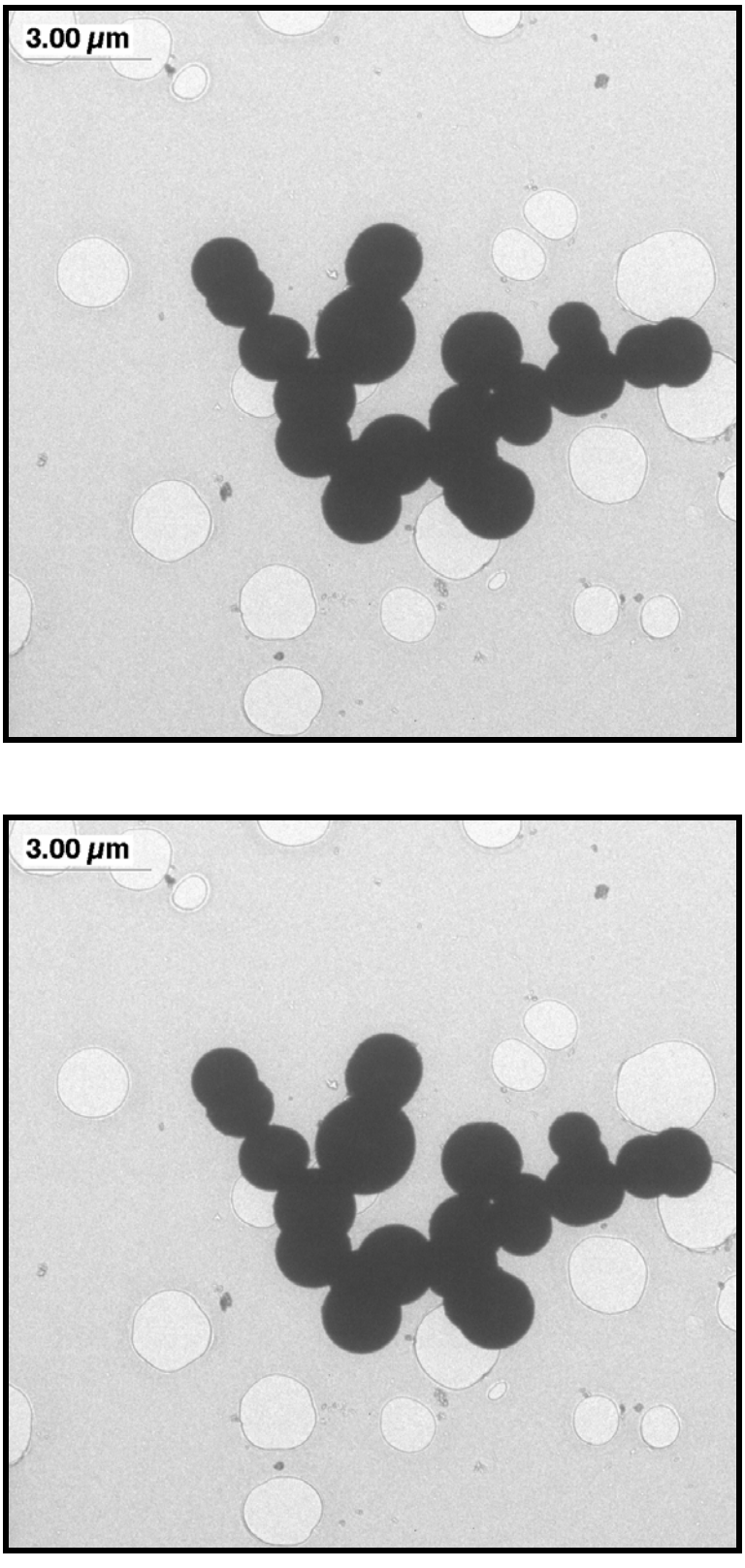

Figure 3.13 TEM image of TiC (top) and VC (bottom) nanospheres.

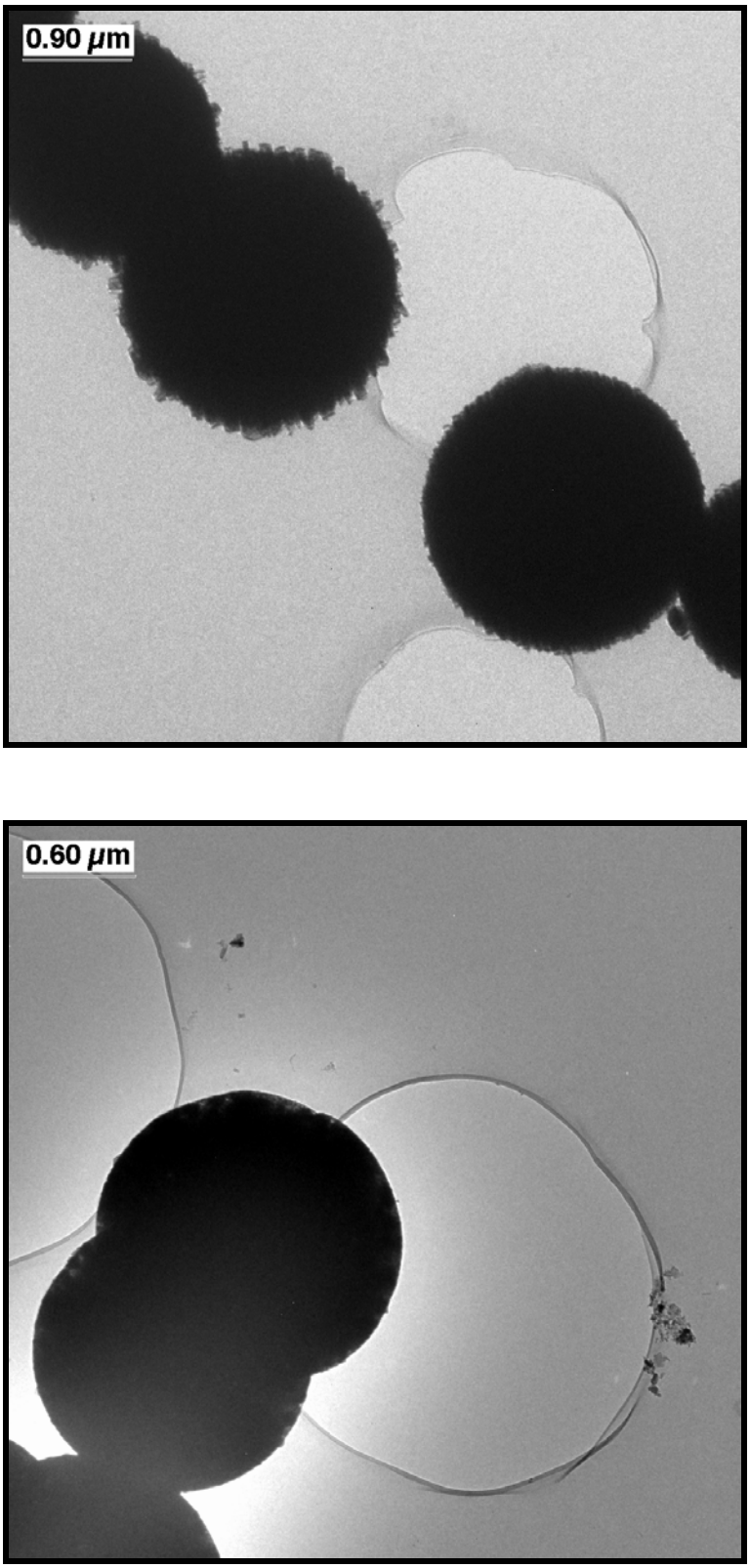

Figure 3.14 TEM image of TiC (top) and VC (bottom) nanospheres after annealing.

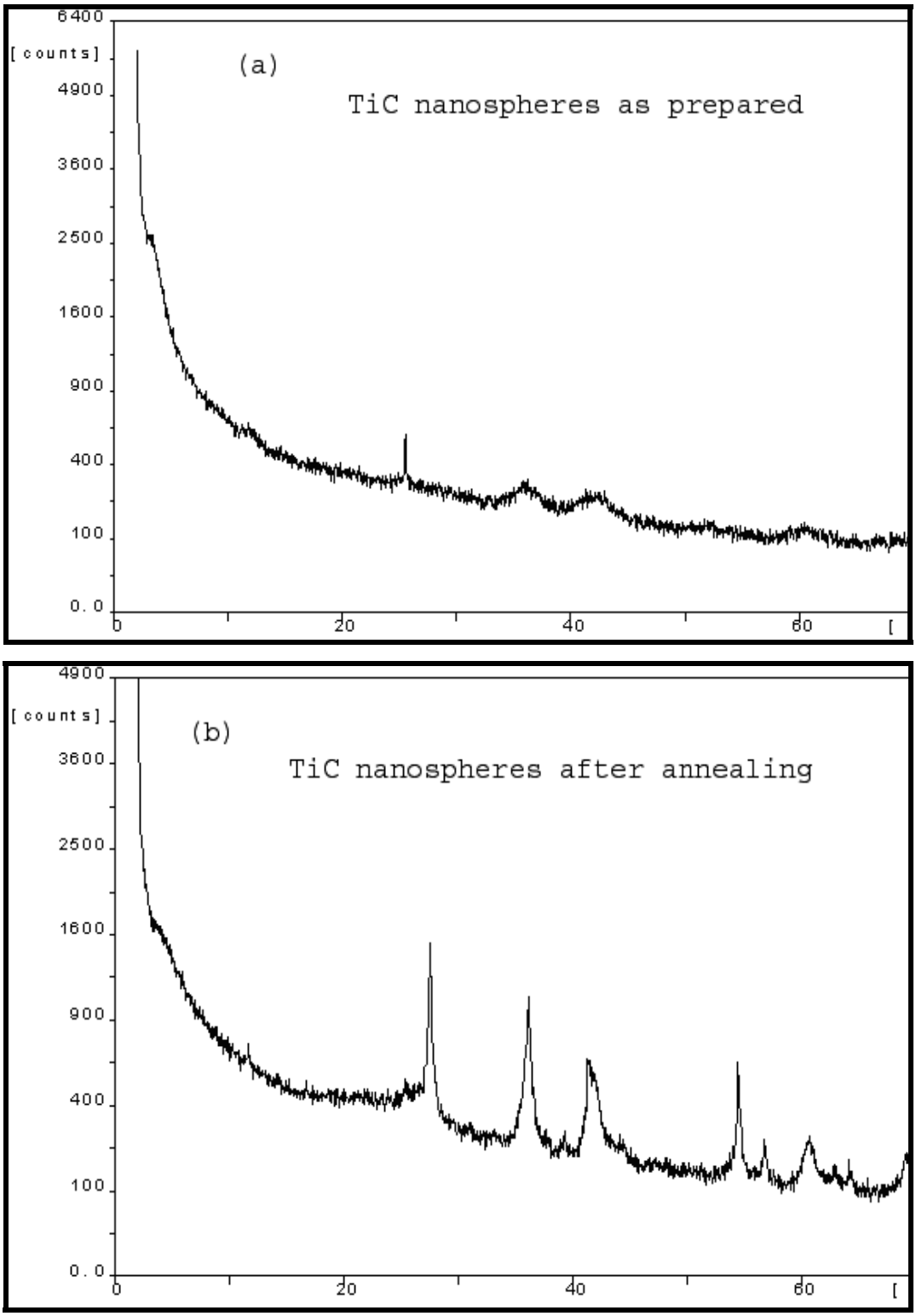

Figure 3.15 XRD spectra of TiC nanospheres before (a) and after (b) annealing. XRD data were consistent with previously reported values.[239]

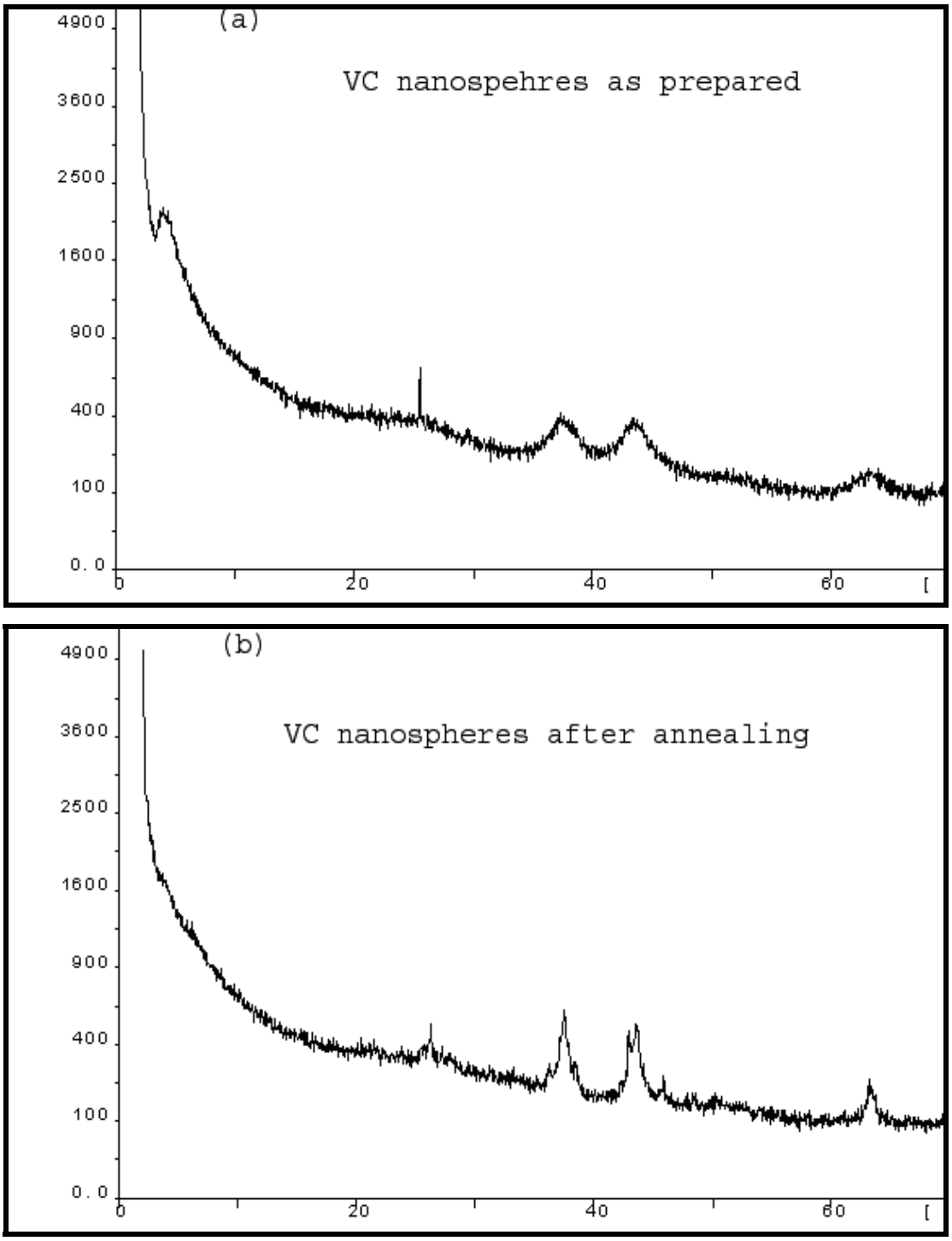

Figure 3.16 XRD spectra of VC nanospheres before (a) and after (b) annealing. The spectra does not include all the characteristic peaks which might be caused by poor crystallinity, though a comparison with reported spectra of $VC_{0.875}$, $VC_{0.83}$, and $VC_{0.79}$ confirms the presence of VC.[240]

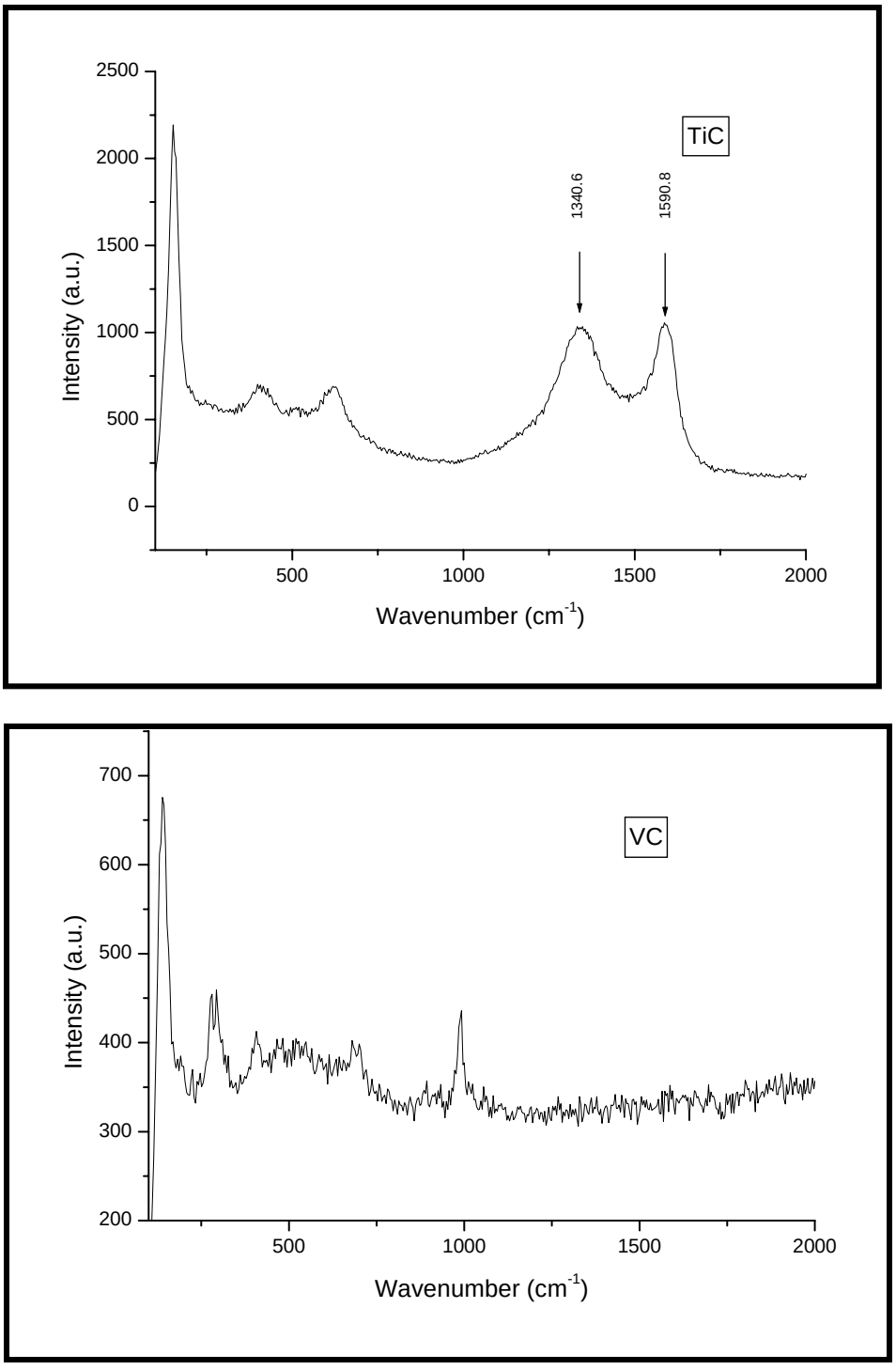

Figure 3.17 Raman spectra of TiC (top) and VC (bottom) nanospheres. Typical Raman bands at ω_t = 1340 and 1590 cm^{-1} in TiC Raman spectra are comparative to the reported values[241] while inhomogeneous mixture of VC carbide sample did not allow concluding its presence by Raman spectra.

3.2 Opening and Purification of Carbon Nanotubes

Several purification methods were examined on carbon nanotubes, prepared by the methods described in section 3.1 and on purchased SWCNTs (Carbon Solutions Inc. - CNT-CS) and MWCNTs (SUN Nano - CNT-S, MER Corporation - CNT-M and Cheap Tubes Inc. – CNT-CT). An evaluation of purification methods is always necessary since it is known that the behavior of each individual batch of CNTs may differ to some extent. This explains why the exact reproduction of modified carbon nanotube materials is often difficult. Therefore, a purification method often needs to be optimized for each batch of CNTs. For SWCNTs and MWCNTs most commonly a nitric acid treatment was applied. These experiments also opened the closed ends of the tubes essential for filling them with metals. Though for the MWCNTs, synthesized by CVD process (CNT-S), nitric acid treatment did not resulted in pure material. Figure 3.18 shows a typical TEM image of raw MWCNTs (CNT-S) as received. Figure 3.19 shows the TEM images of MWCNTs purified by refluxing them in 65% HNO_3 solution for 72 hours. It can be seen that nanotubes are still left with amorphous carbon.

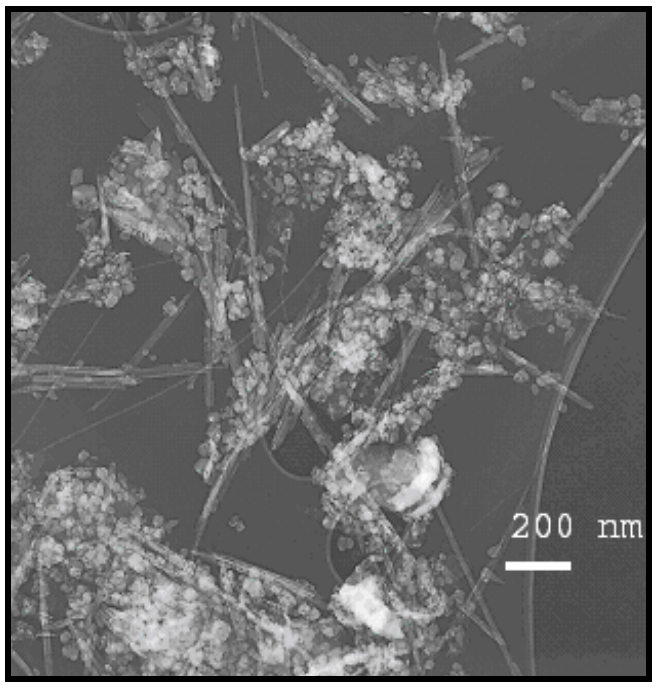

Figure 3.18 A typical TEM image of raw MWCNTs (CNT-S) as received.

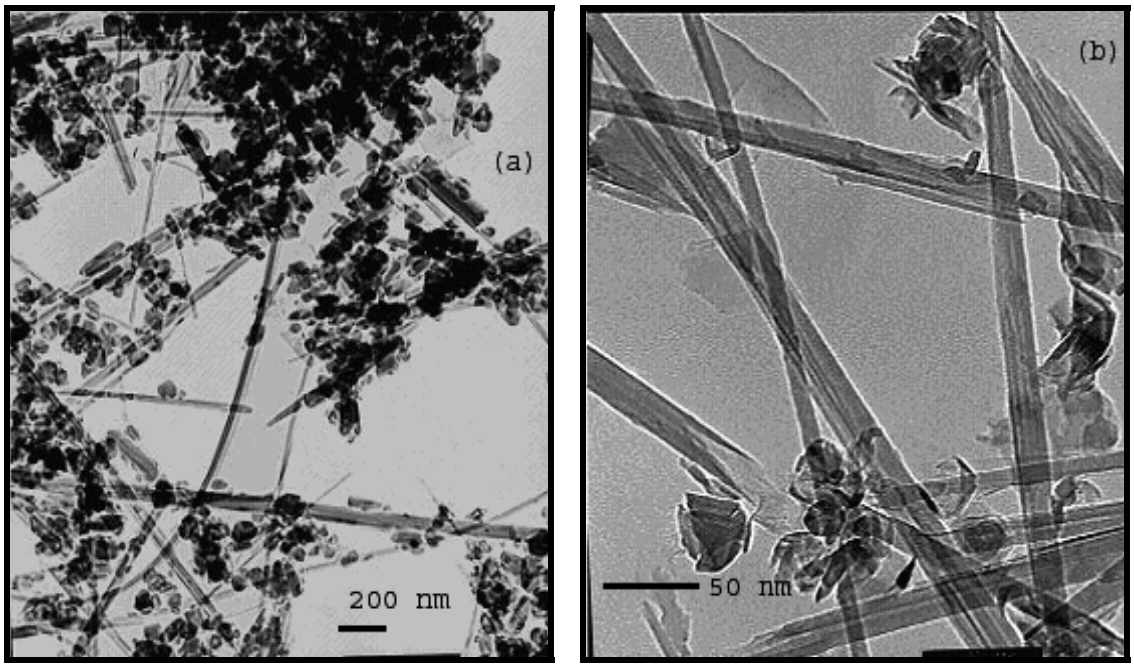

Figure 3.19 MWCNTs purified by nitric acid reflux: CNT-S (a), CNT-M (b)

In place of refluxing, MWCNTs (CNT-S) samples were also sonicated with conc. HNO_3 for 9 hours in an ultrasonic bath. Samples were then washed with deionized water until a neutral pH was reached follwed by EtOH. Washed samples were then dried in an oven at 60 °C for several hours. Figure 3.20 shows the TEM images of purified MWCNTs. Figure 3.21 shows a thermogravimetric analysis of an acid treated sample of MWCNTs (CNT-M, arc discharge). Less than 10% weight loss up to 600 °C confirms the presence of carbon in the nanotube sample.

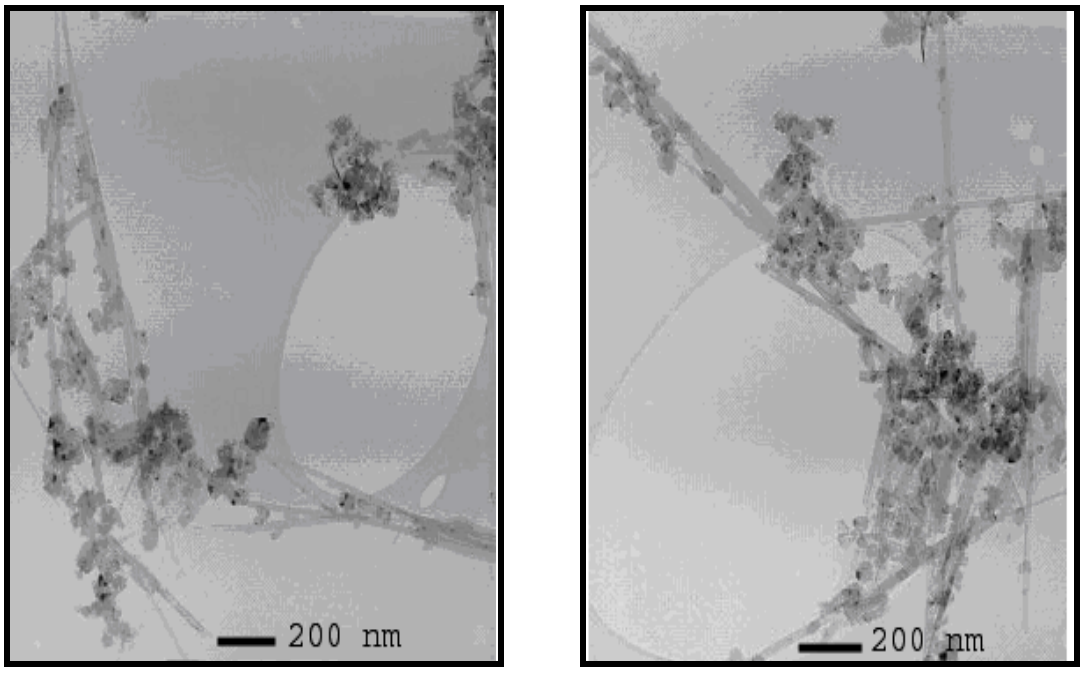

Figure 3.20 TEM images of MWCNTs (CNT-S) purified by nitric acid treatment (ultra sonication for 9 hours). Amorphous carbon, still present in the sample, is clearly visible.

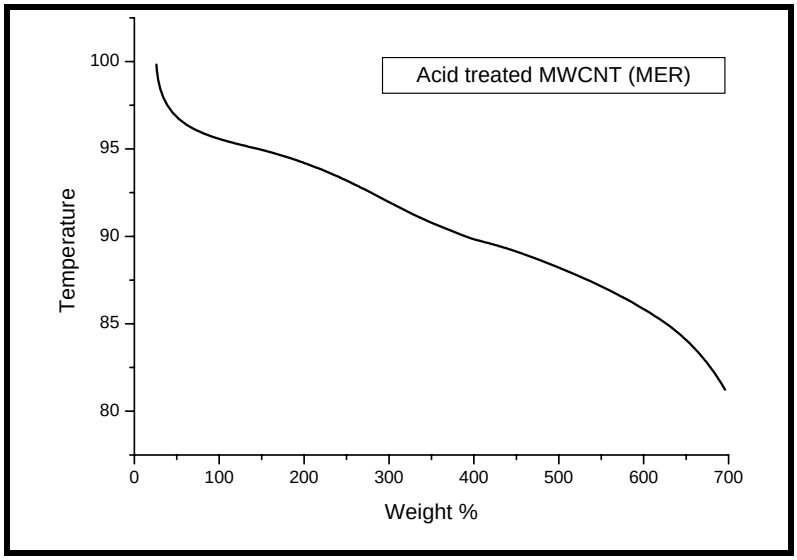

Figure 3.21 Thermogravimetric analysis of acid treated MWCNTs (CNT-M). Nearly 10% weight loss in the temperature range 200-300 °C resulted due to the corboxylate groups introduced during acid treatment.

Furthermore potassium permanganate was also applied as an oxidant for the purification of CNTs as described by H. Hiura *et al.*[122] CNT samples (CNT-M) were refluxed in an acidic $KMnO_4$ solution for 5-15 hours and then washed with plenty of deionized water. It was observed that prolonged reflux of CNTs in acidic $KMnO_4$ solution completely destroyed the carbon nanotubes. 5 hours time of reflux was found to be the limiting time for optimal purification (see Fig. 3.22).

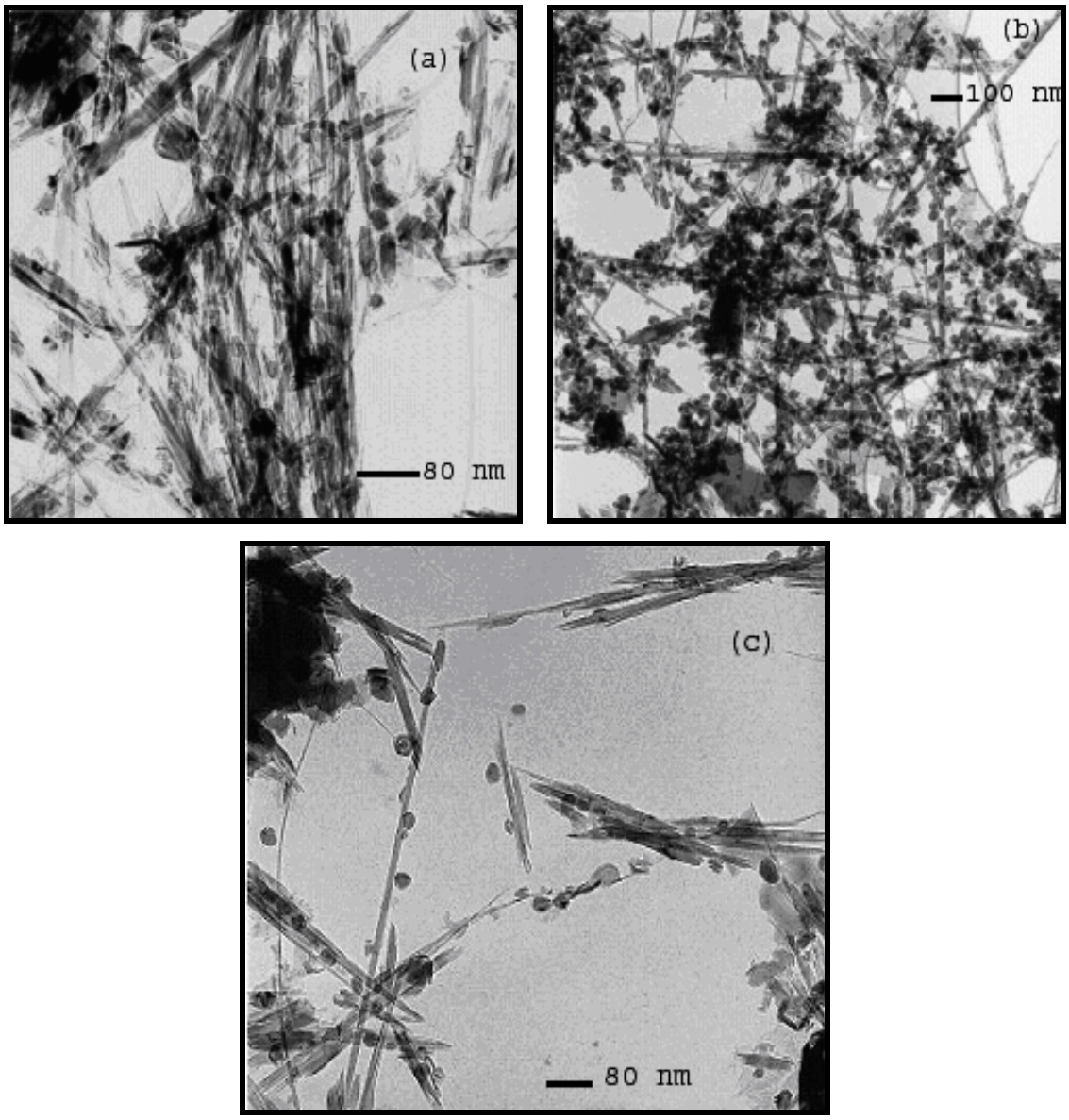

Figure 3.22 CNTs (CNT-M) treated with acidic $KMnO_4$ solution (a, b) for 5 hours, (c) for 15 hours, nanotubes were transformed into amorphous carbon.

A sulfidative purification method[242] for carbon nanotubes was also investigated since the raw material synthesized by a CVD process contains large amount of amorphous carbon and it is known that the sulfidation reaction of charcoal gives carbon disulfide. In this method a mixture of CNT samples and elemental sulfur was heated to 300 °C. A TEM image of a purified sample is shown in Figure 3.23a. Also the oxidation of CNTs in air at 500 °C was performed for their purification. Figure 3.23b shows the TEM image of such a sample.

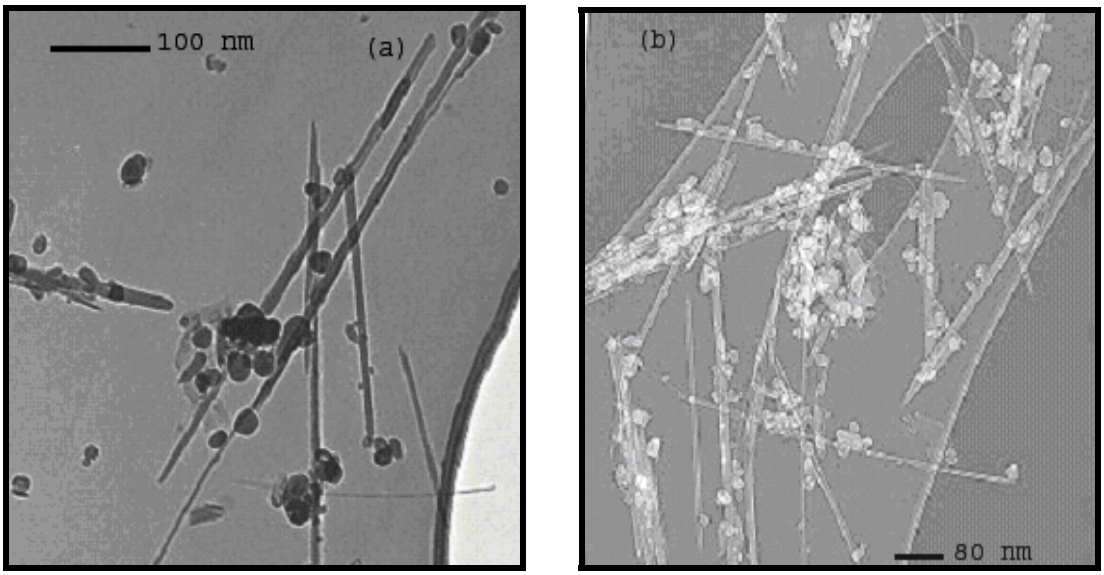

Figure 3.23 Sulfidative purification (a) and oxidation in air (b) for CNTs (CNT-M).

Later on carbon nanotubes were purified using a multi-step purification method,[243] which was a combination of acid treatment and reduction under H_2 at elevated temperatures and it was found to be more effective than the procedures used earlier. The first step is acid treatment with HCl or HNO_3 and then reduction under H_2 atmosphere at 800 °C for 12 hours. Samples were then treated with H_2 at elevated temperatures up to 1200 °C prior to acid washing. Obtained samples were then washed repeatedly with deionized water and finally with EtOH and then dried under vacuum at 60 °C. Figure 3.24a shows a typical TEM image of MWCNTs sample (CNT-S) purified using this method. Characteristic Raman band of SWCNTs at 1580 cm^{-1} can be seen in the spectrum of such purified sample (CNT-CS), while the instrument used was not capable of resolving breathing mode frequencies normally found below 200 cm^{-1} (see Figure 3.24b).

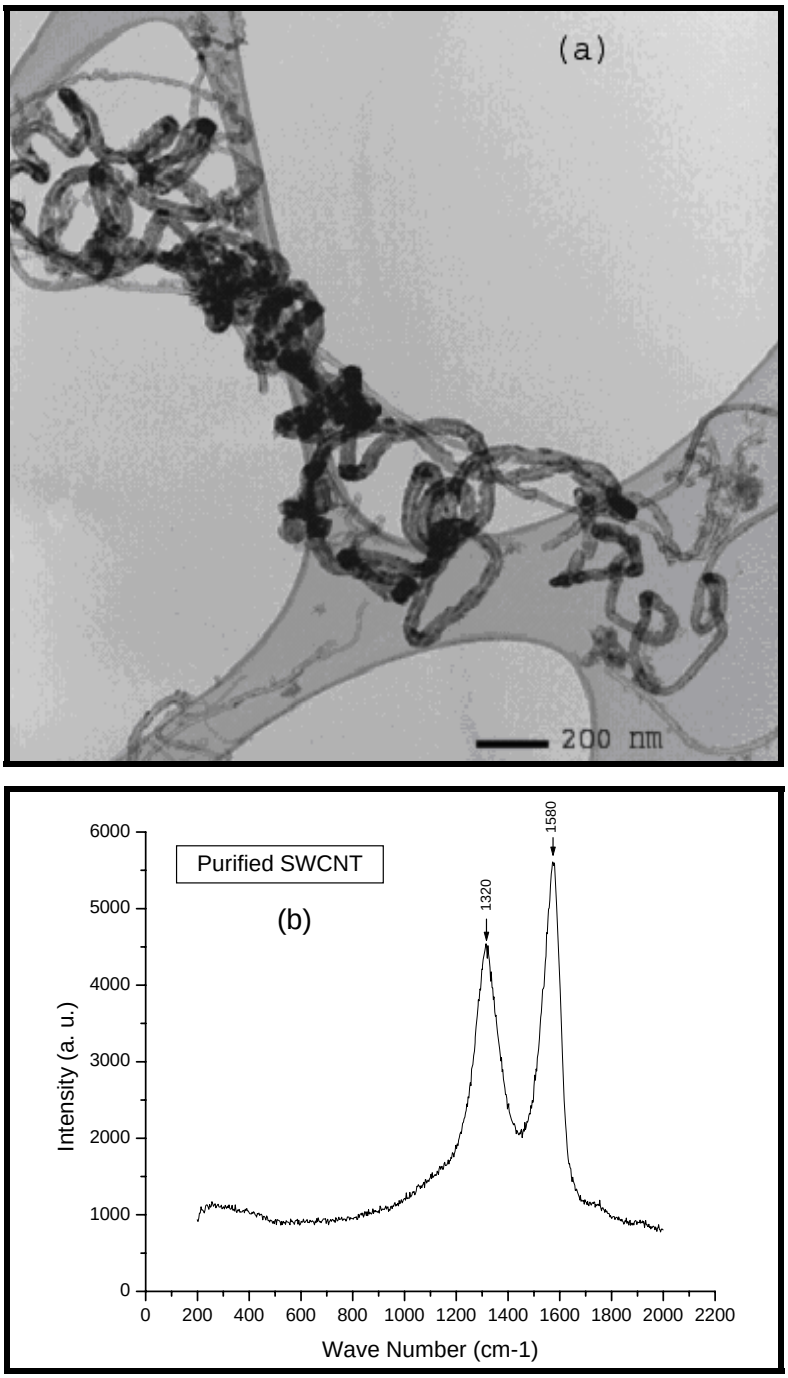

Figure 3.24 A typical TEM image of purified MWCNTs (CNT-S) (a) and a Raman spectra from red Nd:YAG laser of purified SWCNTs (CNT-CS) (b), Raman band at ω_t = 1580 cm^{-1} has been previously demonstrated to be the characteristic of SWCNTs[175] while the band at ω_t = 1320 cm^{-1} is the result of sp^3 carbons generated due the carboxylic acid groups located at defects and/or ends of nanotubes introduced during acid treatment.

3.3 Oxidative Cutting and Shortening of Carbon Nanotubes

Shortening of CNTs was required for a better solubility or dispersion to achieve better functionalization in appropriate solvents. Though oxidation reactions used for the purification of CNTs are also known to shorten the tubes to some extent, prolonged oxidation often introduces more defects into nanotubes and makes the quality of the sample questionable. A controlled oxidative cutting was required to shorten the tubes without causing much damage to their structures. A similar procedure was followed as used by Smalley *et al.*[243] in which CNT samples were treated with freshly prepared piranha solution (4:1 vol / vol, 96% H_2SO_4 / 30% H_2O_2). Shortened SWCNTs samples were further purified using a sulfidation reaction. In case of oxidative cutting for SWCNTs more amorphous carbon was generated during cutting procedure as for the MWCNTs. Figure 3.25 shows TEM images of shortened SWCNTs samples (CNT-CS).

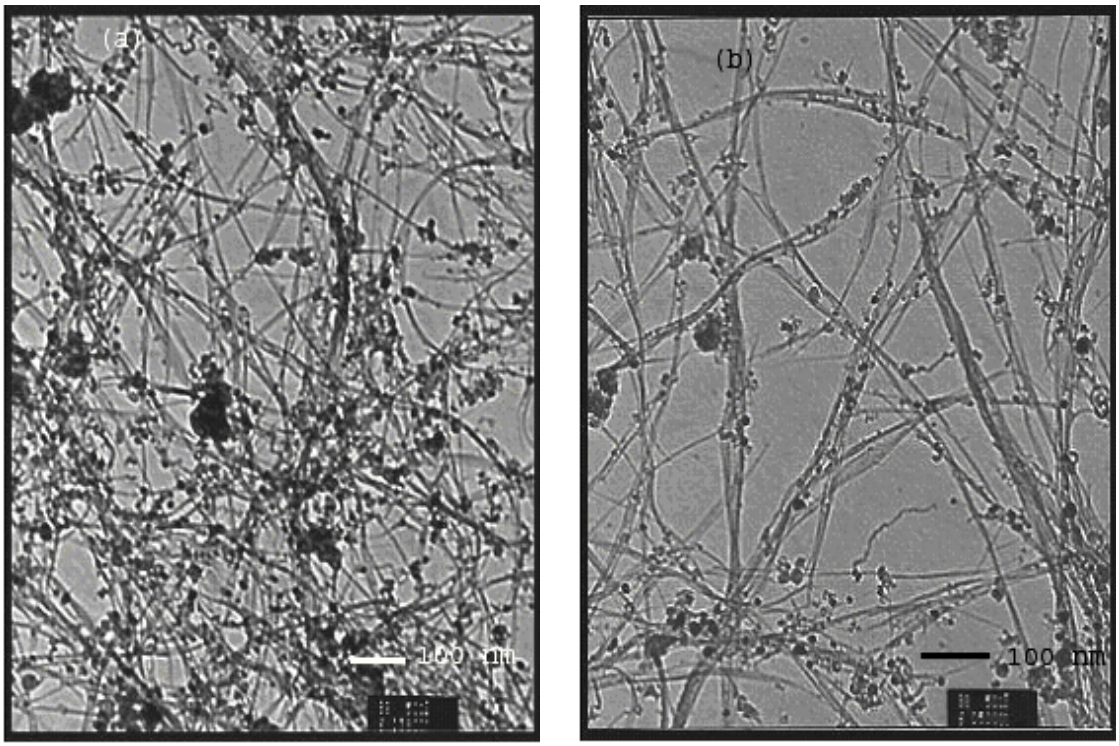

Figure 3.25 TEM images of shortened SWCNTs (CNT-CS) (a), TEM image of SWCNTs (CNT-CS) further purified by sulfidation reaction to remove amorphous carbon (b).

Amorphous carbon was removed from the raw sample of SWCNTs (CNT-CS) and it can be seen in TEM images that the nanotubes are present in bundles. Another reported simple method for shortening carbon nanotubes is cutting them by ball milling.[244, 245] For such experiments MWCNTs (CNT-M) were used and the influence of milling was observed when they were subjected to milling for different time durations – 15, 30, 60 minutes. It was observed that up to 15 minutes of treatment gave shorter nanotubes while applying the ball milling for a longer time period a complete destruction of the nanotubes occured. Figure 3.26 shows TEM images of shortened nanotubes by limited time ball milling while another image shows the nanotube sample destroyed by prolonged ball milling.

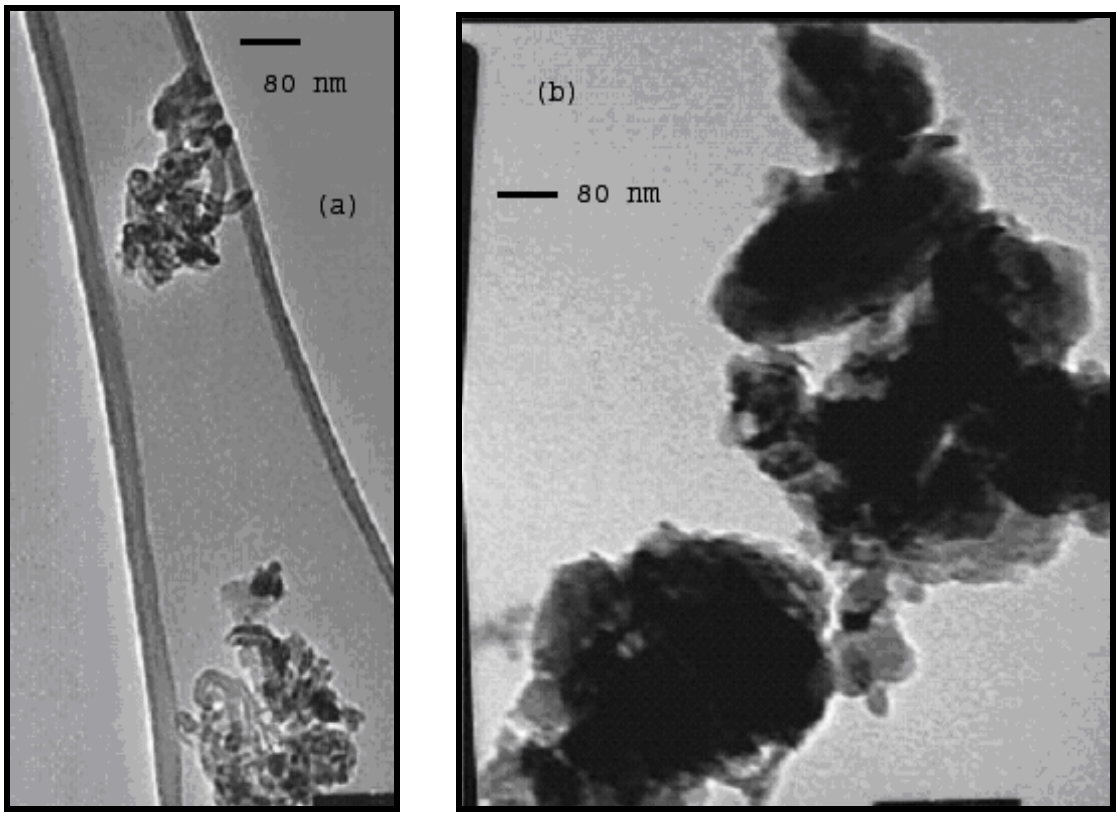

Figure 3.26 Ball milling MWCNTs (CNT-M) for 15 minutes (a), smaller tubes in bunches. Ball milling MWCNTs (CNT-M) for 30 minutes (b), most of the tubes were destroyed and left as amorphous carbon.

3.4 Filling of Carbon Nanotubes with Various Metals

3.4.1 Filling of Carbon Nanotubes with Pd

MWCNTs (CNT-M) opened at the end by refluxing them in conc. HNO_3 solution were suspended in an aqueous solution of $PdCl_2$. The suspension was then sonicated for 2 hours and then left to stir for 2 days. The material was then thoroughly washed with EtOH and dried in an oven at 60 °C for 2 hours. So obtained CNT sample was then reduced under a hydrogen atmosphere at 600 °C for 2 hours. Such filling experiments were previously carried out with $HAuCl_4$ and H_2PtCl_6 for filling nanotubes with Au and Pt by Rao *et al.*[158] Though with this method just a few tubes were found to be filled by Pd, such experiments open a generalized route towards the filling of various metals using wet chemistry method. Figure 3.27 shows a TEM image of such a MWCNT. Some part of it can be seen to contain a foreign material.

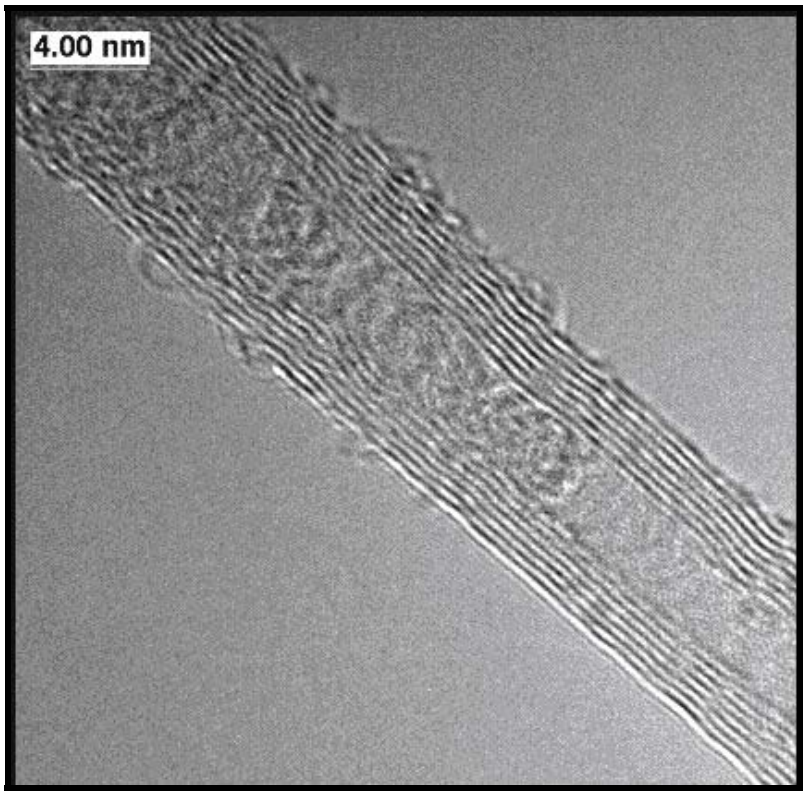

Figure 3.27 An HRTEM image of a typical MWCNT (CNT-M) filled with Pd.

3.4.2 Filling of Carbon Nanotubes with Ru

An attempt was also made to fill carbon nanotubes with Ru. For filling opened MWCNTs (CNT-M) were suspended in an aqueous solution of $RuCl_3$. The suspension was then sonicated for 2 hours and left to stir for 2 days. The material was then thoroughly washed with EtOH and dried in an oven at 60 °C for 2 hours. The sample was then reduced under a hydrogen atmosphere at 600 °C for 2 hours. Similar to the case of Pd, with this method just a few tubes were found to be filled by Ru. Figure 3.28 shows a TEM image of such a MWCNT. In the middle a MWCNT can be seen, filled with a foreign material with a dark contrast which is expected to be Ru.

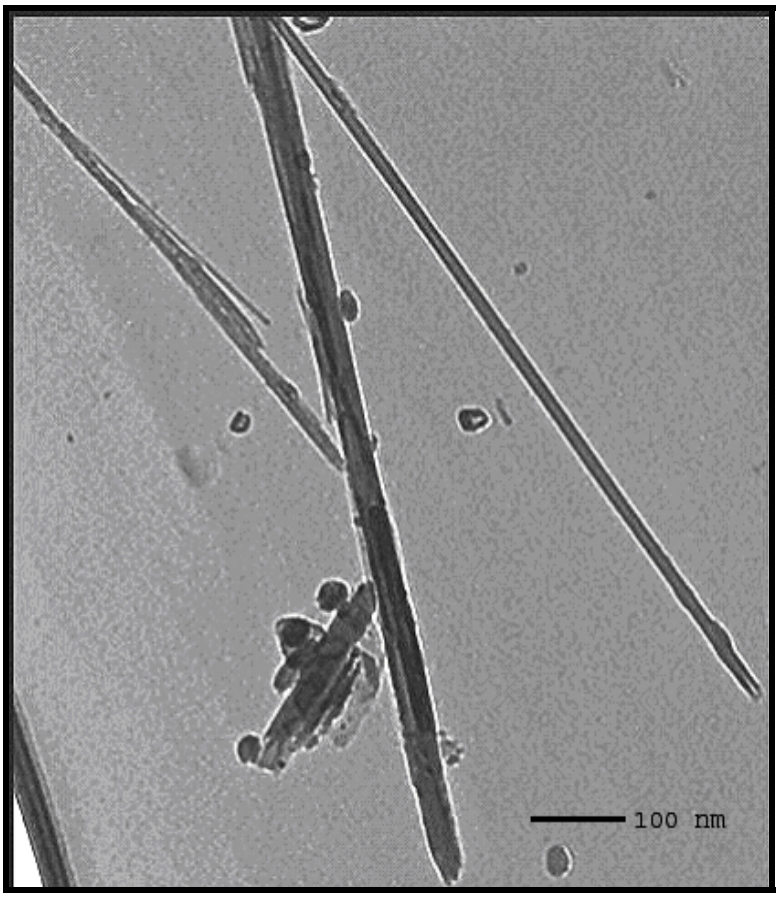

Figure 3.28 TEM image of a MWCNT (CNT-M) filled with Ru.

Apart from MWCNTs, SWCNTs (CNT-CS) were also applied in the same procedure. Though due to the small diameter of CNTs it was difficult to claim if they were filled or not. The difference in contrast in the TEM image of such sample gives a notion like they were filled. Figure 3.29 shows a TEM image of such a sample where Ru lying around CNTs can be seen and darker contrast of SWCNTs can be attributed to their filling. More experiments and a deep observation would be needed to verify Ru inside these SWCNTs.

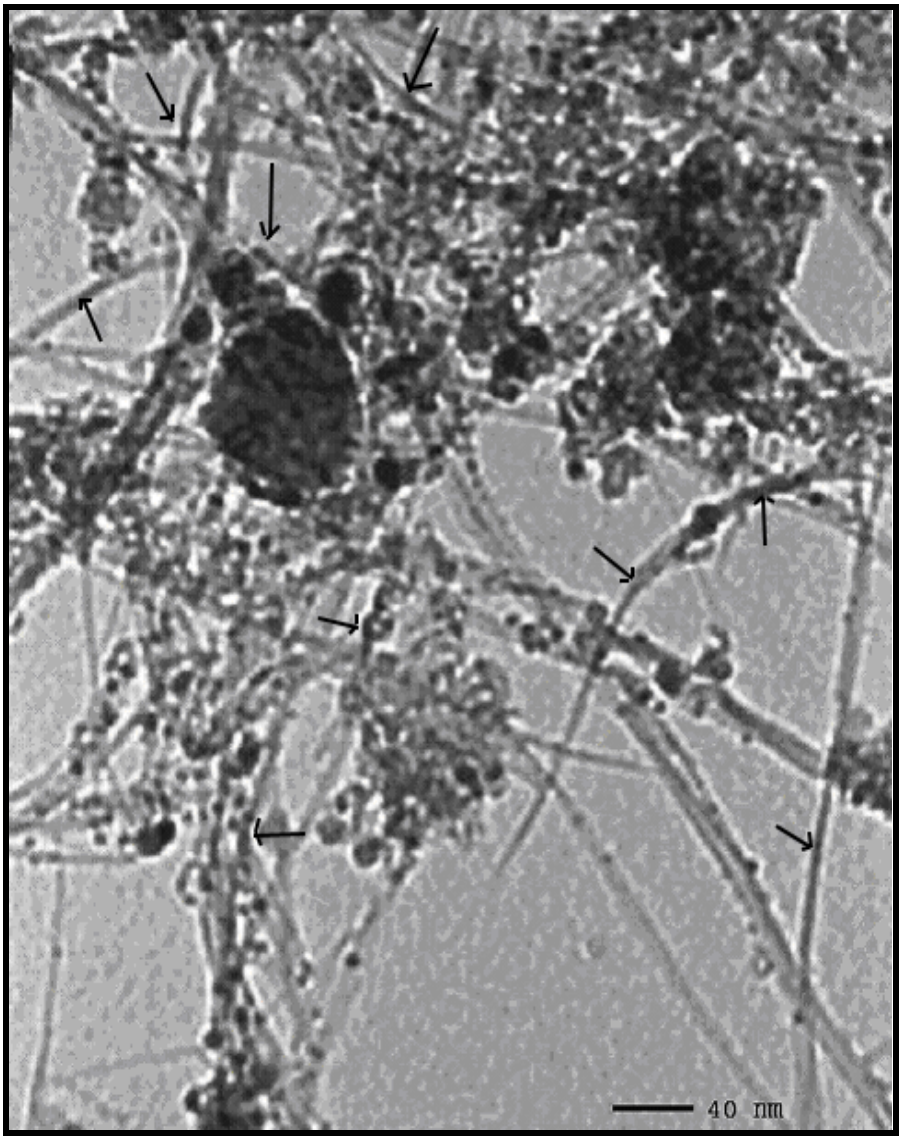

Figure 3.29 TEM image of a SWCNTs (CNT-CS) sample attempted to fill with Ru, a darker contrast can be seen in some of the tubes (see arrows).

3.4.3 Filling of Carbon Nanotubes with Fe

In addition carbon nanotubes filled with α-Fe were desired. α-Fe does offer potential advantages over its oxides and other ferromagnetic material due to its higher magnetic moment. In the cases of magnetic separation, where a magnetic field gradient is used to apply a force to the particles, the advantages of a higher magnetization are fairly obvious. The force upon the particle is directly proportional to the magnetization of the particle. In addition iron has the advantage of being a softer magnet than any of its oxides and other ferromagnetic material, so that it can maintain its super paramagnetism at larger sizes and therefore higher particle moments. At the beginning of the filling experiments, filling procedures based on the capillary effect in carbon nanotubes reported originally by Ajayan and Iijima[54] were examined. For the filling iron salts $Fe(NO_3)_2$ and $FeCl_3$ were used. Pre-opened MWCNTs (CNT-S) were suspended in a saturated salt solution in water overnight and then dried in an oven at 80 °C. After further washing with water and ethanol and drying, the filled tubes were reduced under a stream of hydrogen at 600 °C for 2 h. MWCNTs filled to some extent with α-Fe were obtained, though results were not satisfying. The level of filling was not as high as often indicated by TEM pictures in the literature. Many tubes were not filled. It was observed that a high level of filling in some of the carbon nanotubes could be achieved before washing them in order to remove salt particles from outside the walls. After the washing the number of filled tubes was far less and also the amount of material filled in a tube was low. In Figure 3.30 the pictures show an example of filled tubes reduced prior to washing and after washing. Figure 3.31 shows the TEM images of MWCNTs samples reduced after washing several times with deionized water to remove the excess salt. It was observed that washing affected the amount of filling and washed tubes were much less filled than the tubes which were not washed. Removal of iron during washing may be overcome by screening different concentration of iron salts in the future. It might be possible to use a concentration just sufficient for filling and not leaving iron salt outside the CNTs walls. Also screening different solvents used for washing could prevent the removal of salts from inner cavities.

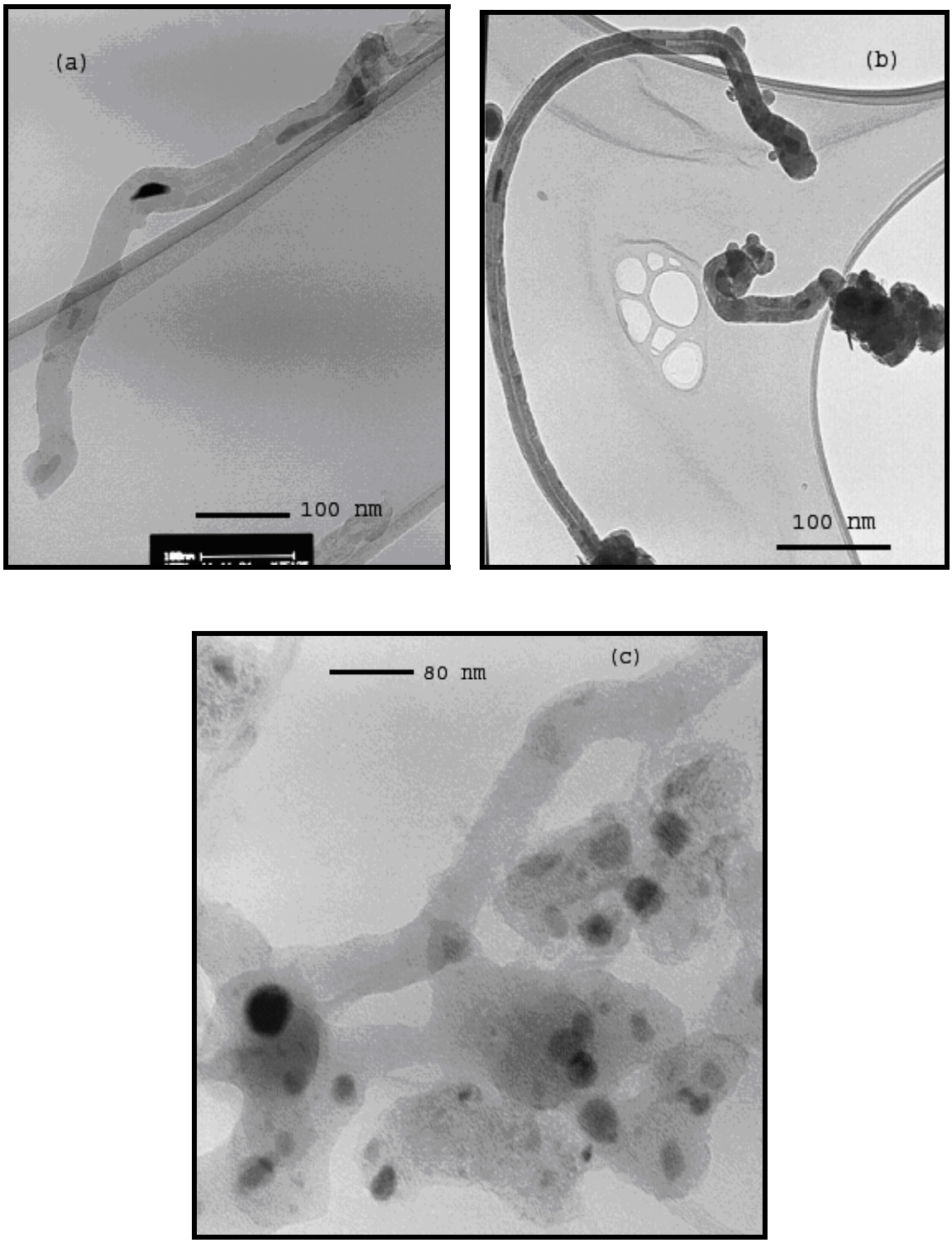

Figure 3.30 HRTEM images of MWCNTs (CNT-S) with α-Fe particles inside (a, b). CNT filled with $Fe(NO_3)_2$ and reduced without washing (c), α-Fe particles are visible in the image having a darker contrast.

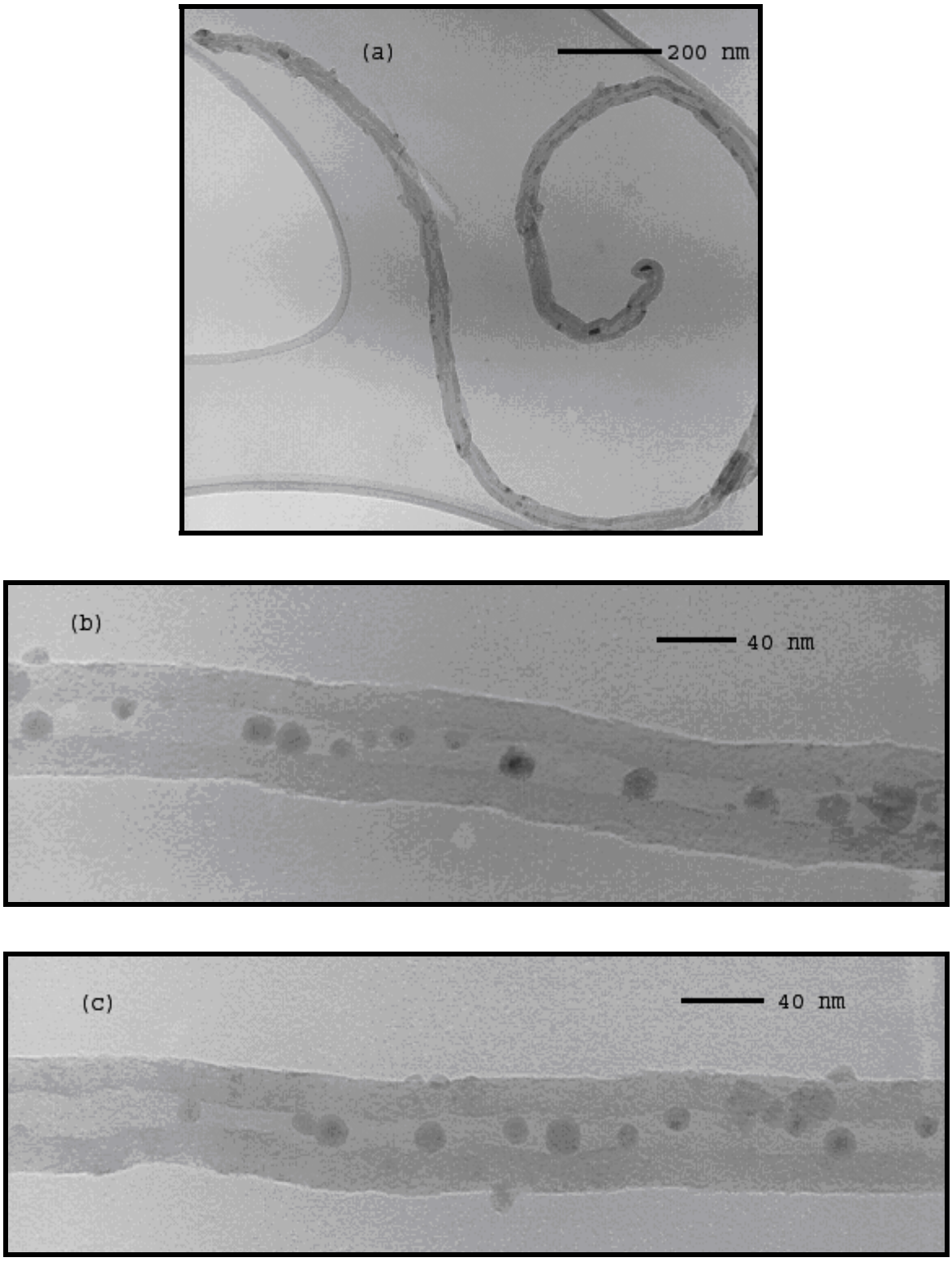

Figure 3.31 HRTEM images of MWCNTs (CNT-S) with α-Fe particles inside (a). CNT filled with $Fe(NO_3)_2$ and reduced after washing with deionized water (b, c).

Inspired by the work of Y. Gogotsi *et al.*,[246] a filling procedure for commercially available MWCNTs with a high filling ratio was developed as described below. The tubes were filled with iron oxide nanoparticles from commercially available organic solvent or water based ferrofluids (EMG 911 and EMG 508, respectively, Ferrotec Corporation). These ferrofluids carry magnetite (Fe_3O_4) particles with a characteristic average diameter of 10 nm. MWCNTs used for the experiments were purchased from SES Research (TX, U.S.A., formed by arc discharge, avg. dia. 2-20 nm - CNT-SES) and Sun Nano, China (formed by CVD process, avg. dia. 20-70 nm - CNT-S). It was found that the nanoparticles inside the tubes were not carried away during the washing procedure. Filled samples were washed several times with toluene in case of organic solvent based ferrofluid and with deionized water where water based ferrofluid was used. Filling experiments showed that organic based ferrofluid was more effective for filling nanotubes than water based ferrofluid (see Fig. 3.32).

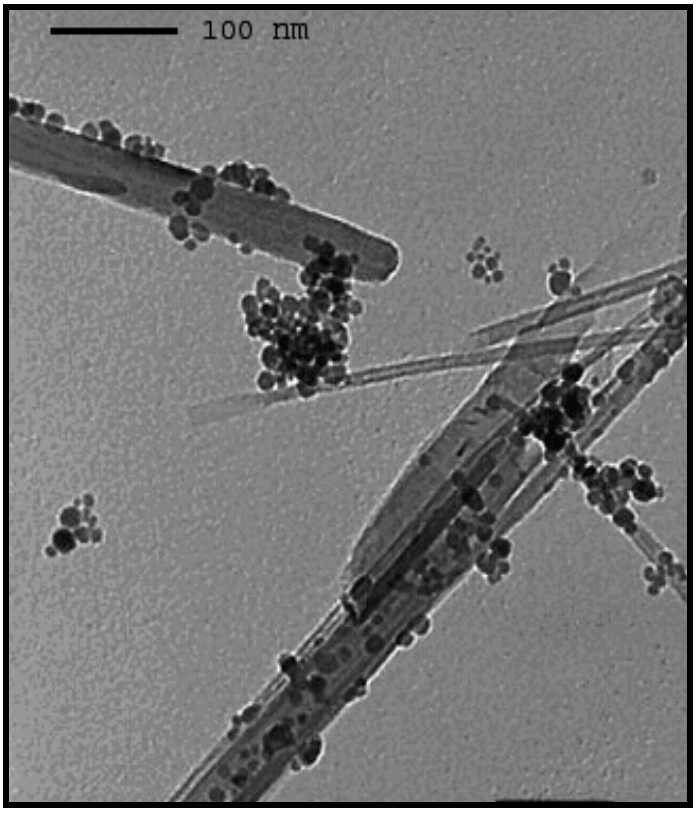

Figure 3.32 Low resolution TEM image of filled MWCNTs (CNT-SES) using EMG-508 prior to washing.

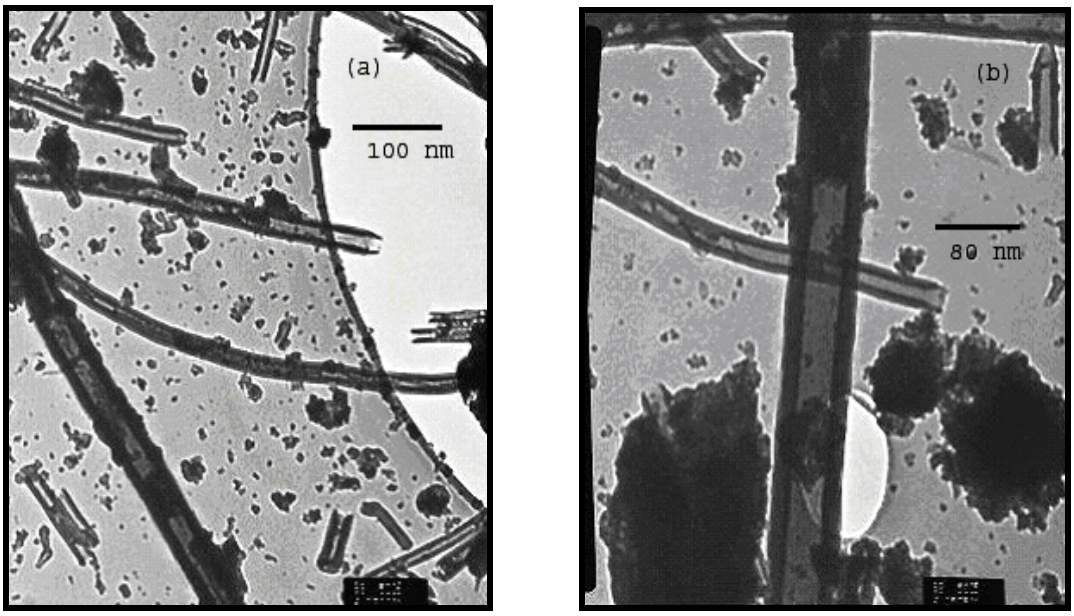

Figure 3.33 A low resolution TEM image of filled MWCNTs (CNT_SES) using EMG-508 after washing.

Figure 3.33 above, shows images of CNTs filled with EMG-508 after washing with deionized water. Figure 3.34 (below) shows TEM images of CNTs samples filled with EMG-911 prior to washing.

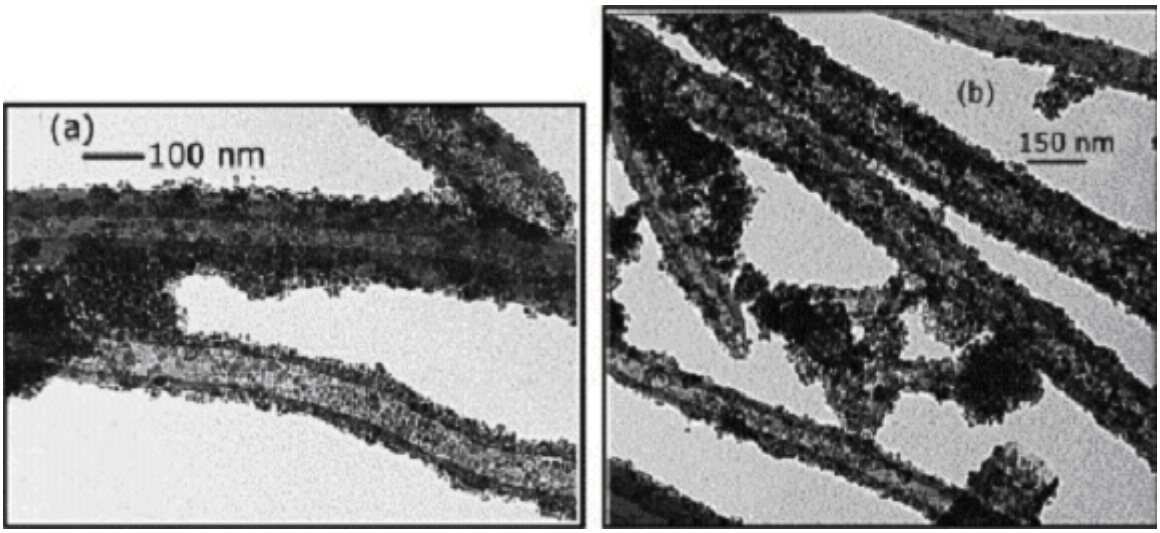

Figure 3.34 Low resolution TEM images of filled MWCNTs prior to washing.

For further filling experiments EMG-911 (organic solvent based ferrofluid) was used. A high extent of filling was accomplished but it was noticeable that many particles were attached on the tube walls (see Fig. 3.34). In order to remove particles sticking on the outer walls of nanotubes, filled samples were thoroughly washed with acetone and further with xylene. Samples were then dried in an oven at 60 °C. Figure 3.35 (below) shows TEM images of samples after washing. Clean outer surfaces of the tubes show that excess material sticking outside was removed.

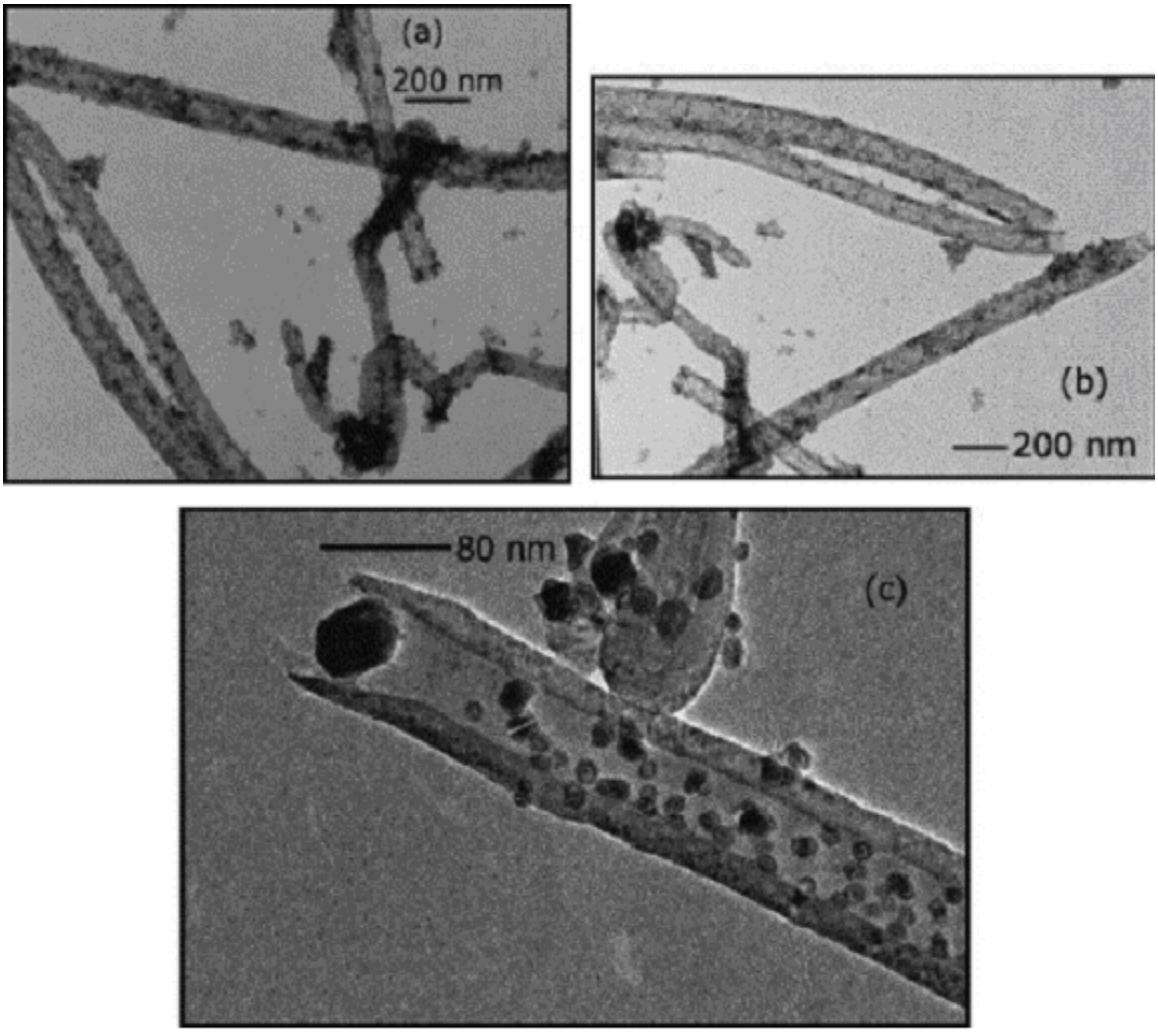

Fig. 3.35 TEM images of purified filled nanotubes (CNT-SES).

CNTs filled with iron oxide were then reduced under H_2/Ar atmosphere at 645 °C for 20 hours. This reduction process converted iron oxide particles inside the nanotubes to α-Fe.

Figure 3.36 shows high resolution TEM images of α-Fe filled MWCNTs after reduction. Such samples showed active response to a simple bar magnet which confirmed their magnetic character (see Fig. 3.36d).

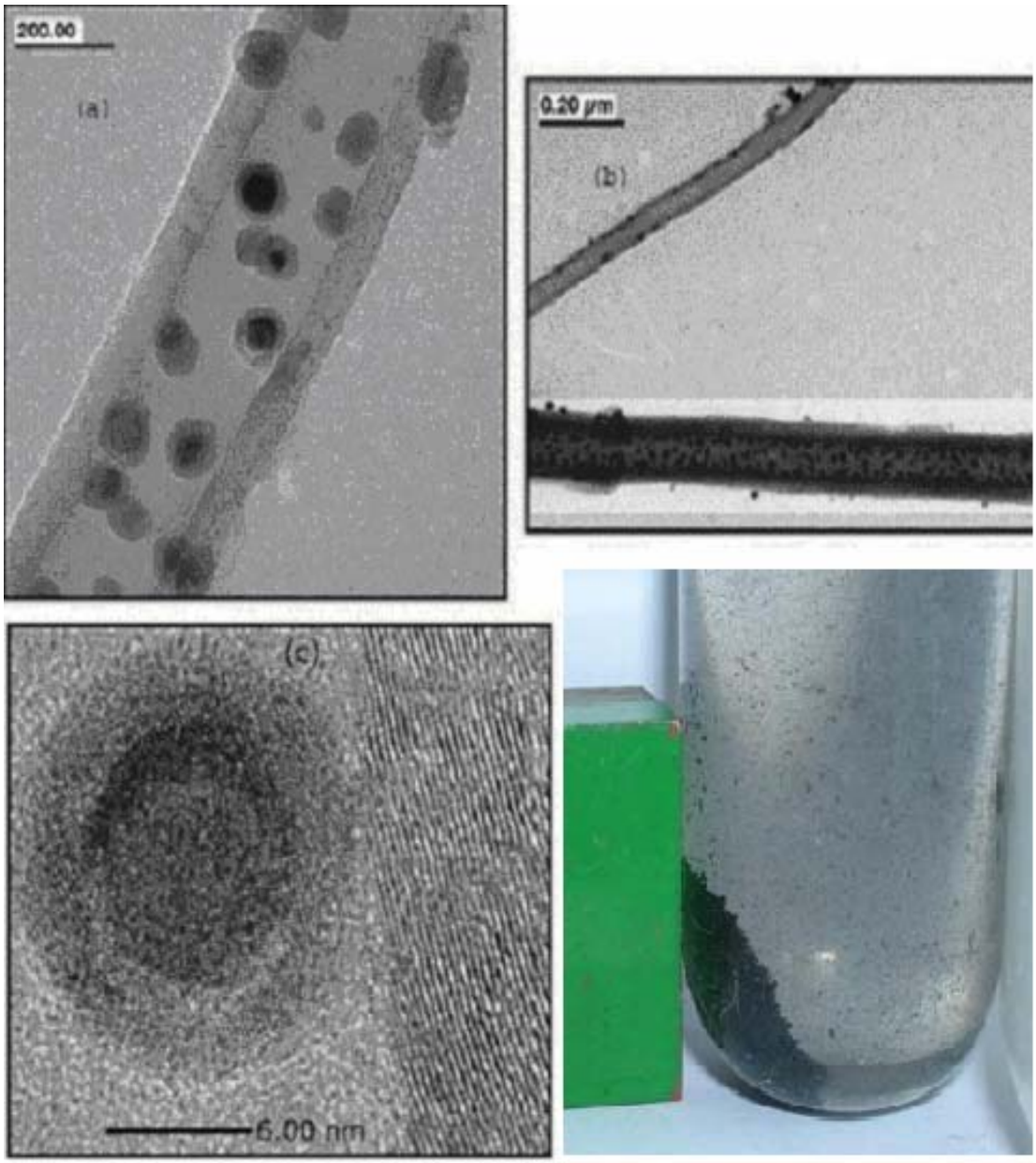

Fig. 3.36 TEM images of filled nanotubes reduced under H_2/Ar atmosphere at 645 °C for 20 hours (a, b), HRTEM image of a particle inside the tube adjacent to the tube wall (c), and ferromagnetic nanotubes in water attracted towards a magnet (d).

From these images it is possible to see that the nanotubes are filled with a large amount of ferromagnetic particles. It was possible to observe that the tubes with an inner diameter close to 10 nm or less than 10 nm were less filled or remained empty as the one on top in Figure 3.36 (b). This was expected as the average size of the particles in the ferrofluid was 10 nm. It could also be possible that a few tubes were not filled due to insufficient opening. Tubes with a higher diameter of 20–25 nm were filled almost completely. Up to 80% of tube's inner space was filled with a large amount of Fe nanoparticles, which satisfied our goal to obtain ferromagnetic nanotubes. In the filled parts particles filled out up to 50% of the inner volume of tubes. The fringes, visible in a high resolution image, of a particle inside the tube (Figure 3.36c) revealed its crystalline nature. In a further experiment sequential images were taken randomly of such a filled carbon nanotube with a double tilt holder at different angles, which proved that the particles were indeed inside the tubes (see Fig. 3.37).

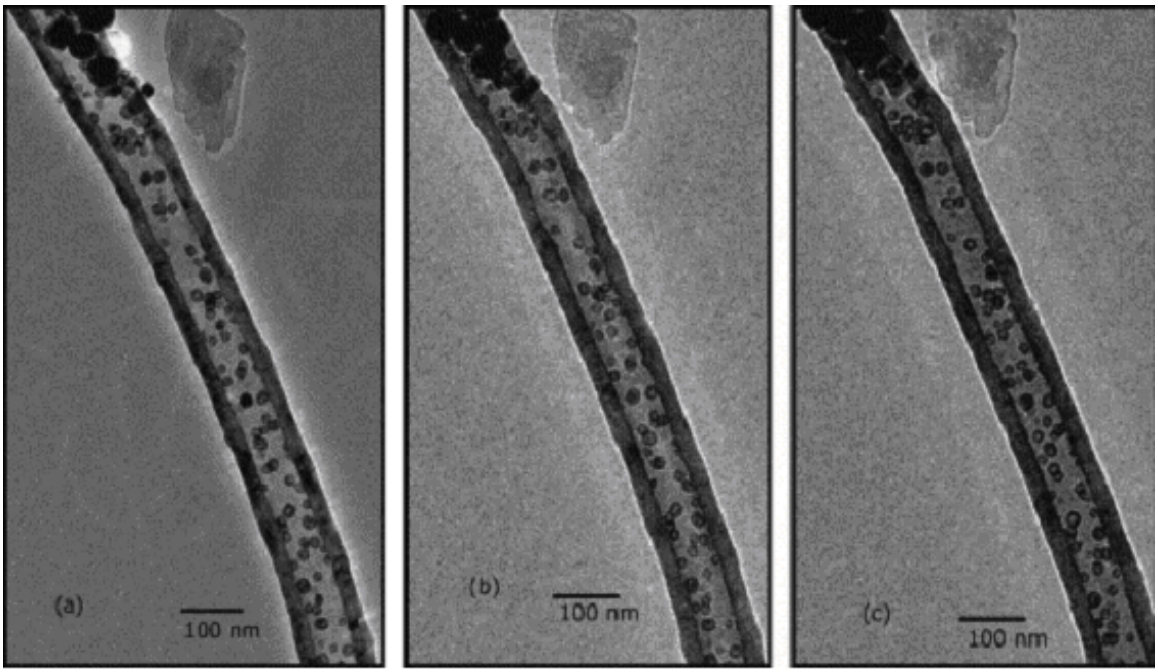

Figure 3.37 TEM images taken sequentially at tilt angles (a) 0°, (b) 5°, (c) 10° showing the particles sticking on the wall (see on the top of the image) and particles inside the carbon nanotube (CNT-SES).

Next the crystalline nature of filled material inside CNTs was further proven. Selected area electron diffraction patterns were recorded for the carbon film coated on the copper grid, for an empty part of a carbon nanotube and for a particle inside the nanotube walls (see Fig. 3.38). Figure 3.38 (d) shows the corresponding selected area electron diffraction

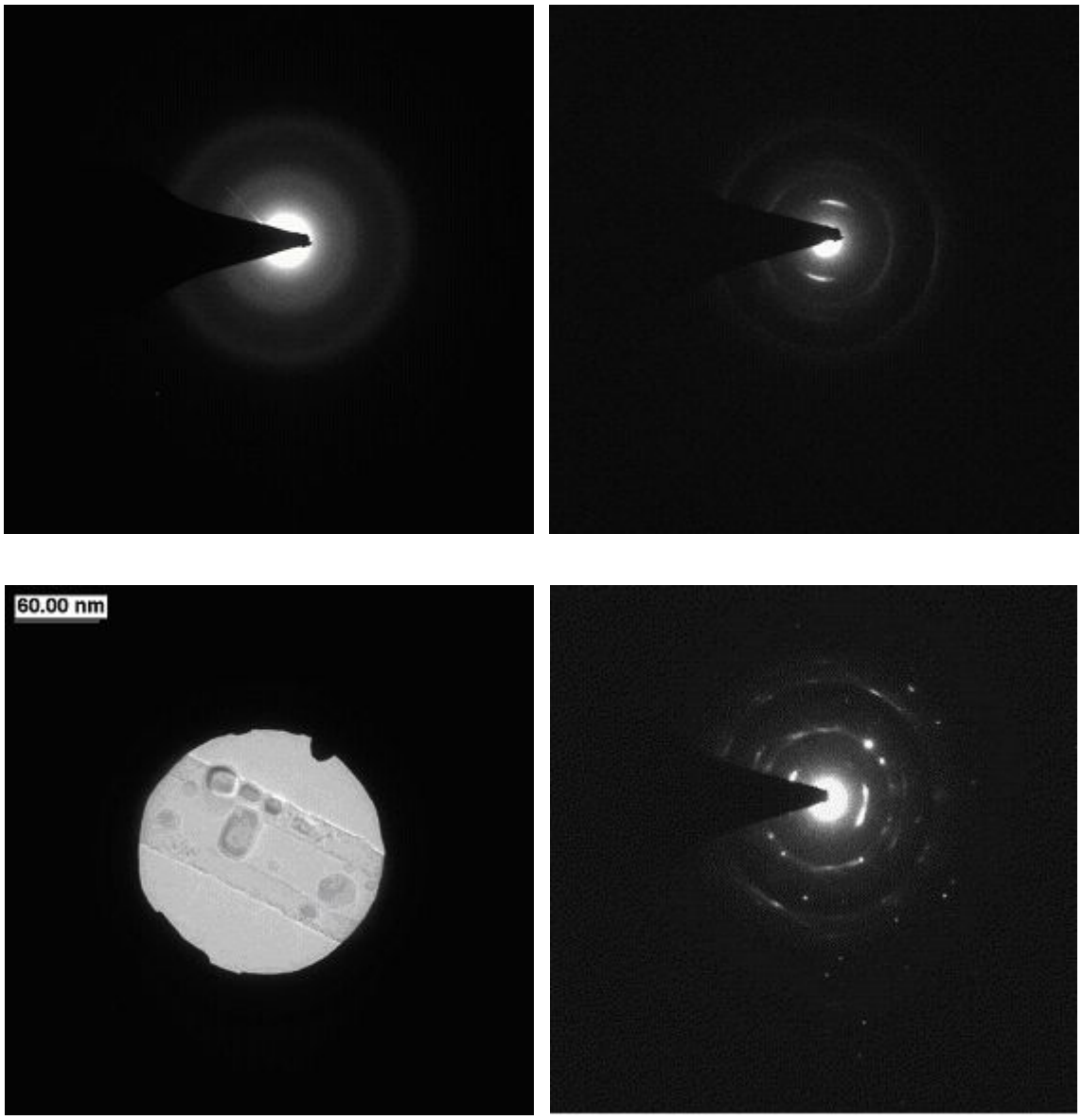

Figure 3.38 Selected area electron diffraction pattern of carbon film on the copper grid (a), for an empty part of a carbon nanotube (CNT-SES) (b), particle inside the nanotube walls (c) and its corresponding electron diffraction pattern (d).

patterns taken from the filled nanotube shown in Figure 3.38c. The diffraction pattern for the particle inside CNT shows sharp and clear spots indicating that the particles are composed of single crystals. The two arcs close to the central spot result from the [0 0 2] scattered beams emitted by the tube walls, corresponding to the regular inter-graphene distance at 0.34 nm.

To determine the composition of filled material, energy dispersive x-ray spectrum (EDX) were recorded. Figure 3.39 represents the EDX measurement of the filled carbon nanotubes, which confirmed the presence of atomic iron in the MWCNTs. The thin coating around the Fe particles as shown in Figure 3.36 (c) is expected to be of carbon, which might result from the pyrolysis of the surfactant during reduction at 645 °C. The surfactant covering Fe_3O_4 nanoparticles is used to stabilize them and make them soluble in organic solvents. Since some oxygen was observed in the bulk EDX spectra which suspected the presence of FeO, a line scan across a well filled part and another across a not filled part was made. It was found that in the second spectra the oxygen count was higher than Fe, while in the spectra taken across a well filled portion the Fe count was much higher than oxygen. This should eliminate the possibility of oxygen present as FeO.

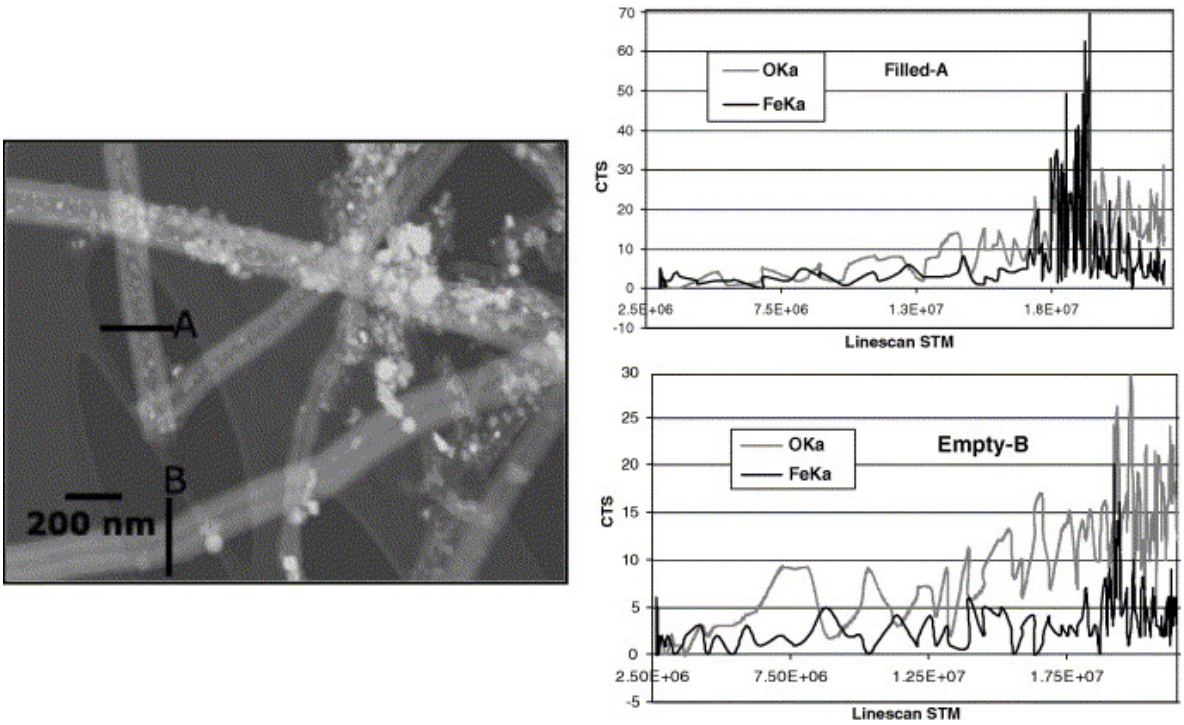

Figure 3.39 Line scan EDX spectra of empty and filled tubes along the lines A and B as drawn in the left image. It can be seen that in the empty part the percentage of oxygen is much higher (Plot-B) than Fe as compared to the ratio of Fe/O in the filled part of the tube (Plot-A).

Figure 3.40 represents XRD patterns of the samples shown in Figure 3.36 and Figure 3.35 (filled and after annealing at 645 °C under hydrogen). Pattern of the filled sample (1) and sample (2) (reduced at 645 °C for 2 h) revealed the presence of a small amount of α-Fe and various phases of iron in the filled tubes. After the annealing process all different phases of iron were completely transformed into α-Fe. In the experiments it was observed, as depicted in graph 2 and 3 that for a complete conversion to α-Fe a longer annealing time was necessary.

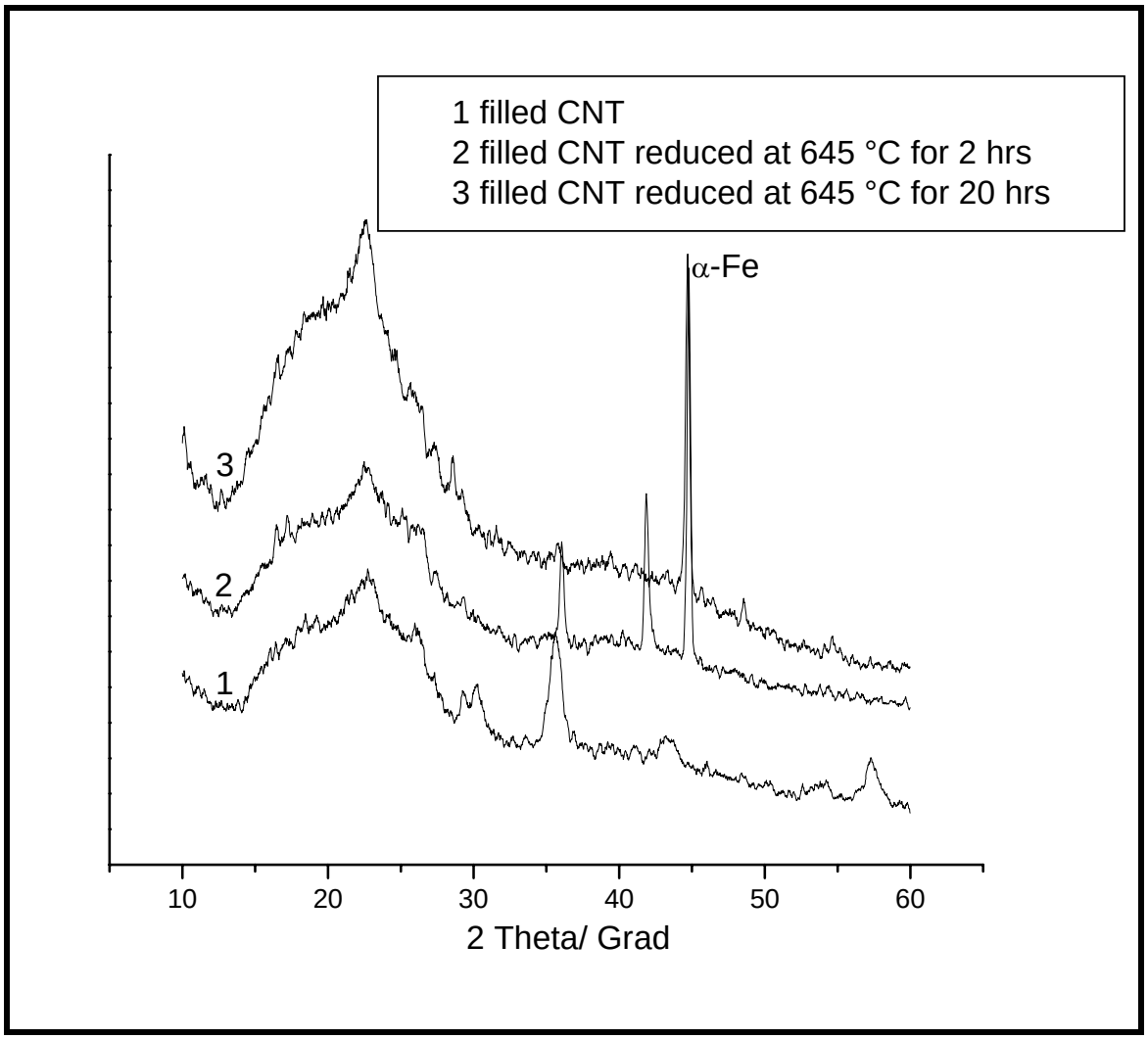

Figure 3.40 XRD patterns of filled sample (1), and samples after annealing for 2 hours (2), and 20 hours (3).

3.5 Closing the Open Ends of Carbon Nanotubes

To use α-Fe filled CNTs for various chemical reactions attempts were made to close the open ends of nanotubes to make sure that the particles remain inside during the reactions and do not interfere in the reaction. In one method closing was performed by suspending CNTs overnight in propan-1,3-diol as described by Rao *et al*.[158] It was expected that first carboxylic acid groups present at the nanotube´s end take part in hydrogen bonds with hydroxy groups of alcohol molecules and further a chain of hydrogen bonded alcohol molecules closes the tube ends. Samples were then carefully washed with acetone to remove excess alcohol and dried under vacuum. The closing with propan-1,3-diol was not much successful as just a few tubes were found to be closed and Fe particles were washed away from inside. Figure 3.42 shows TEM images of carbon nanotubes with closed end after suspending overnight in propan-1,3-diol while Figure 3.41 shows a typical HRTEM image of an open end of MWCNT after treating with 65% HNO_3 for 48 hours.

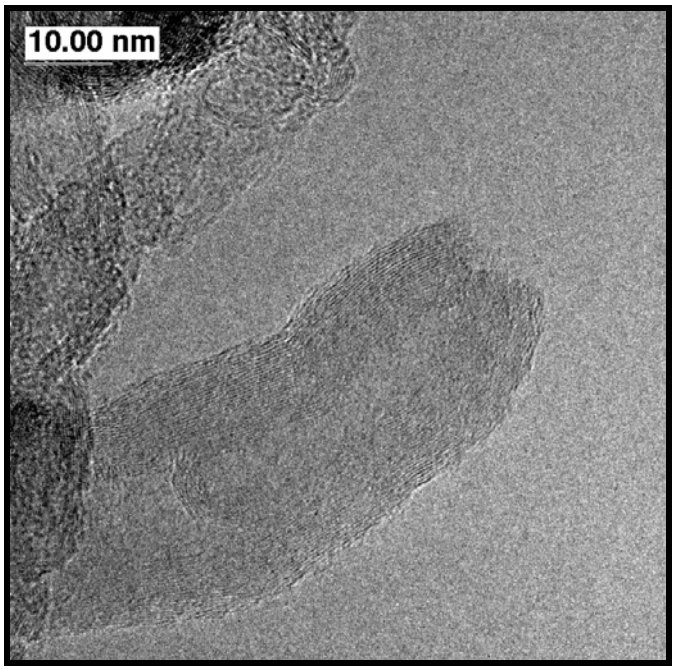

Figure 3.41 A typical HRTEM image of a MWCNT (CNT-S) with an open end after oxidation in 65% HNO_3 for 48 hours.

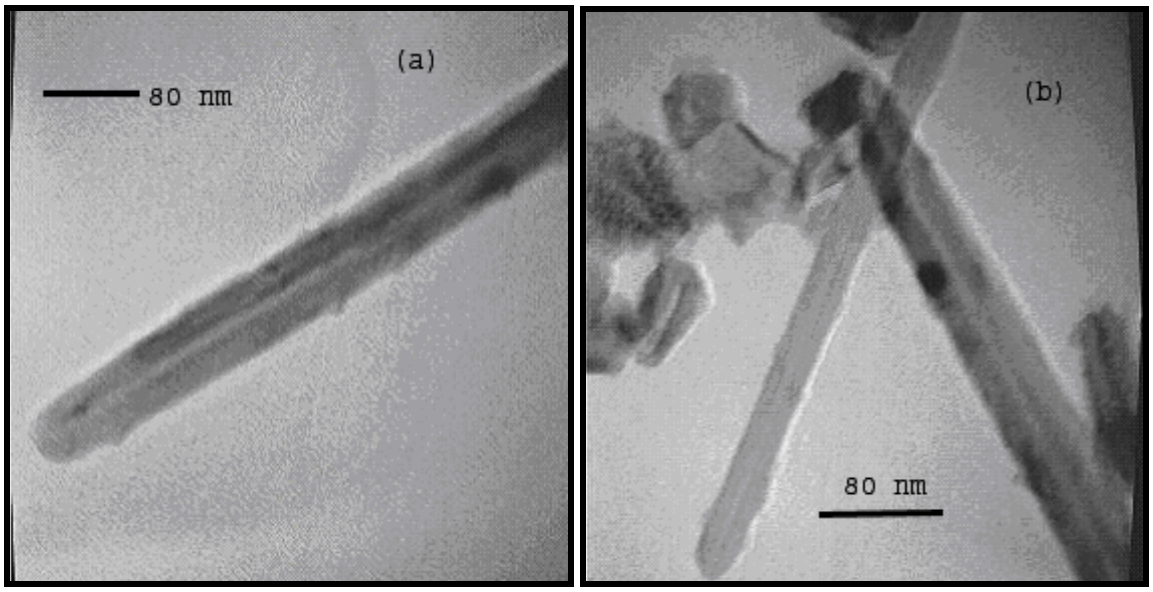

Figure 3.42 TEM images of carbon nanotubes (CNT-S) with closed end after suspending overnight in propan-1,3-diol.

In another attempt CNTs were suspended overnight in polyethylene glycol and then washed with acetone, diethyl ether and ethanol successively prior to drying under vacuum. Though closing with polyethylene glycol was more effective than in case of propan-1,3-diol, the inner space was mostly replaced by polyethylene glycol. Figure 3.43 shows TEM images of such closed end CNTs. Also heating of opened CNTs in a stream of benzene vapour, argon and hydrogen at 900 °C was performed as described by Rao *et al.*[158] Though in our experiments we found that it resulted in formation of excess amorphous carbon around the tubes. A less concentrated stream of Ar with benzene might lead to better results in future.

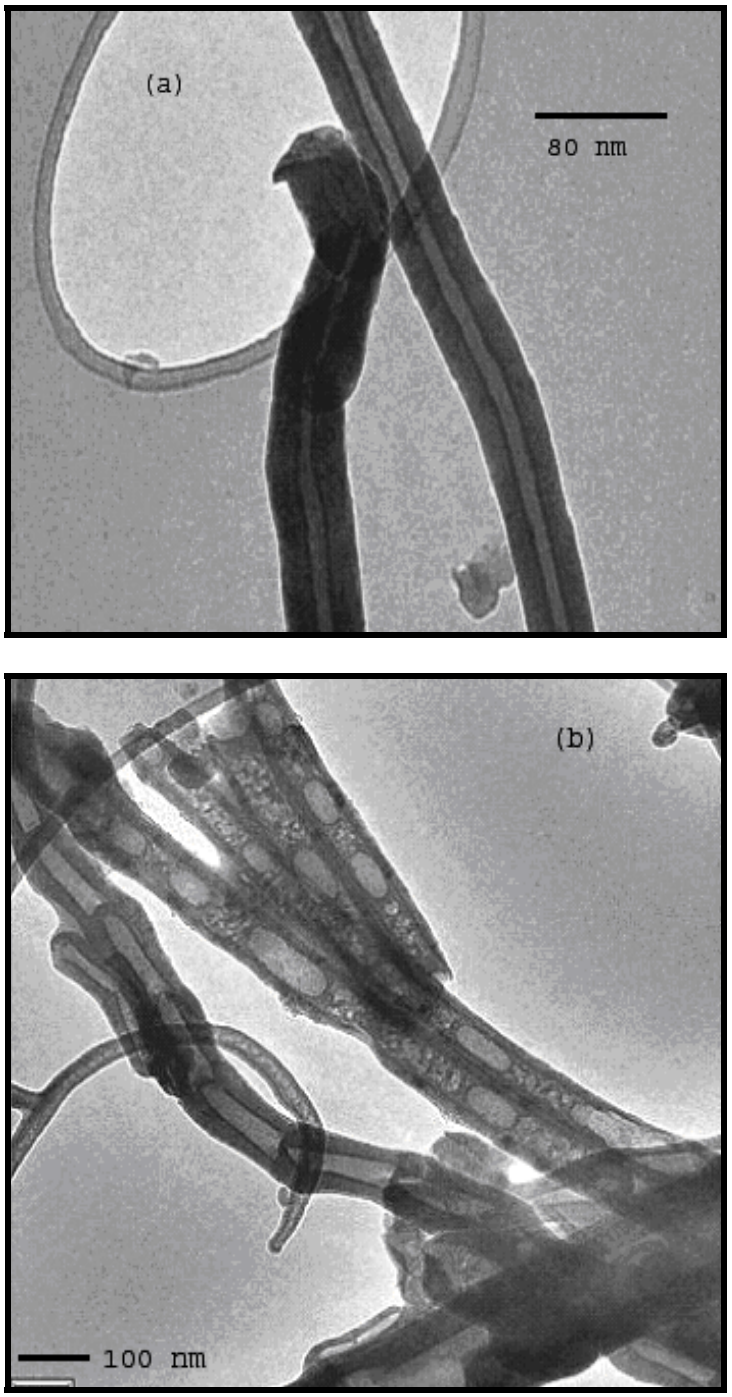

Figure 3.43 TEM images of carbon nanotubes with closed end CNTs after suspending overnight in glycol. The inner space of such tubes was found either to be empty (a), or contained a foreign material which is expected to be polyethylene glycol (b), since before the glycol treatments inner cavities of the tubes were seen to be empty (see Figure 3.47).

3.6 Solubilizing Carbon Nanotubes by Treating them with Urea Solution

Urea melt solubilization of single walled carbon nanotubes has already been reported by William E. Ford *et al.*[247] In their report they have shown that molten urea (melting point 133 ºC) decomposes into ammonia and isocyanic acid (HCNO) suggesting the following mechanism:

$$NH_2CONH_2 + \text{heat} \leftrightarrow NH_4^+NCO^- \leftrightarrow NH_3 + HNCO \qquad \text{(Eq. 3.1)}$$

They suggested that isocyanic acid, like its organic isocyanato (RNCO) derivatives, can react with functional groups containing active hydrogen atoms, such as hydroxy (–OH) and carboxy (–COOH) groups, which are generated at the ends and at defect sites along the sidewalls of the SWCNTs during purification under oxidizing conditions. The reaction of HNCO with the carboxy groups of the SWCNTs can generate primary amido groups and carbon dioxide (Eq. 3.2), and further addition of HNCO can generate ureido groups or polymers (Eq. 3.3):

$$SWNT\text{–}COOH + HNCO \rightarrow SWNT\text{–}CONH_2 + CO_2 \qquad \text{(Eq. 3.2)}$$

$$SWNT\text{–}CONH_2 + n HNCO \leftrightarrow SWNT\text{–}CONH(CONH)_nH \qquad \text{(Eq. 3.3)}$$

They used this principle and reacted SWCNT samples with molten urea. SWCNTs produced by modified electric arc method showed solubilization efficiency up to 13%, while when laser ablation produced nanotubes were used, they were soluble up to 41%. Also it was found that when *p*-anisaldehyde was added in the reaction mixture with urea, solubilization efficiency was enhanced up to 60%. They speculated that such enhancement involved the "capping" of ureido goups attached to the nanotubes by their condensation with aldehyde,[248, 249] which slows down the reverse reaction (see Eq 3.3).

Recently Turega *et al.*[250] proposed controlling a recognition-mediated [3+2] Diels-Alder cycloaddition reaction using a pH switch. In their experiments they had shown that recognition between a urea and a carboxylate salt can be used as a suitable platform to

construct a pH switch (see Figure 3.44). They suggested that at higher pH anions associate strongly with urea (recognition on) and lowering the pH protonates carboxylates forming carboxylic acid which associates only weakly with urea (recognition off).

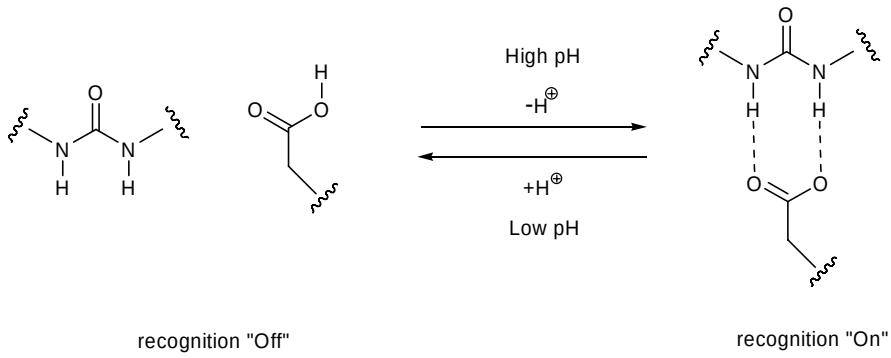

Figure 3.44 (a) Schematic representation recognition between a urea and a carboxylate which can be turned off and on by means of a pH change.[250]

Inspired by the above work, it was envisaged to speculate the effect of a urea solution on CNTs. It was found that a prolonged simple stirring of oxidized carbon nanotubes whether MWCNTs or SWCNTs with solution of urea having different concentrations make them fairly soluble in water. It can be assumed that urea molecules are attached with hydroxy (–OH) and carboxy (–COOH) groups present on the defect sites of nanotubes by hydrogen bonding. Also due to the results of Turega *et al*[250], the possibility to close and open the ends of carboxylated CNTs by treating them with urea was explored. At first SWCNTs (CNT-CS) and MWCNTs (CNT-S and CNT-CT) were oxidized by refluxing them in conc. HNO_3 for 16 and 48 hours respectively. A typical amount of each sample (50 mg) was then dispersed in aqueous solution of urea (10 mL) with different concentrations. For the experiments urea solutions with a varying concentration of 0.075 M to 3 M were applied. After sonicating them in an ultrasonic bath for 5 minutes, dispersions were stirred for 48 hours. Finally they were filtered and the solid was washed several times with deionized water. Filtrates obtained by dispersion and by washing the remaining solid on the filter paper with water, were collected

separately. Both, the filtered solid (dried in an oven) and filtrates were collected and investigated on a TEM. It was found that the prolonged stirring in even the dilute solution of urea (0.075 M) resulted in solubilization of carbon nanotubes in water. Figure 3.45 shows TEM images of MWCNTs found in the first filtrate.

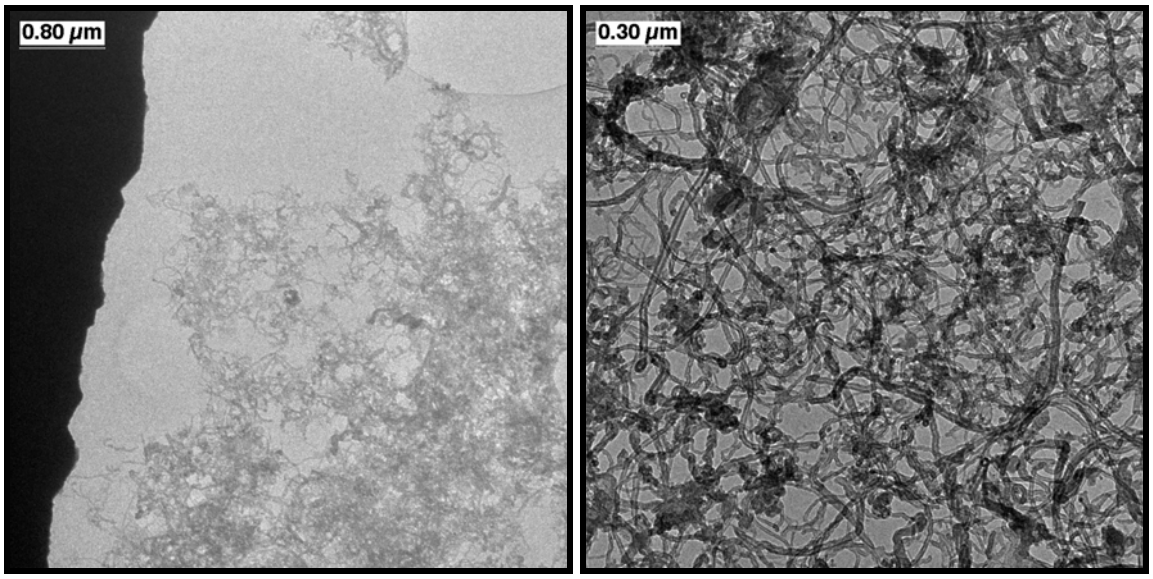

Figure 3.45 TEM images of MWCNTs found in the first filtrate

More over it was also observed that while the filtrate was a clear solution of CNTs in water, changing the pH by adding acid (dil. HCl, pH < 2) or base (aq. Na_2CO_3, pH > 10) leads to the precipitation of CNTs (see Figure 3.46).

Figure 3.46 (from left to right) Filtrate, filtrate after dilution with deionized water, after addition of acid (dil. HCl), after addition of base (aq. Na_2CO_3).

To estimate the amount of CNTs dissolved in the aqueous solution, saturated solution of nanotubes were prepared by mixing excess mass of CNTs to 3 mL of 0.075 molar solution of urea. After stirring for 48 hours, undissolved solids were filtered off. From the solution, dissolved nanotubes were precipitated by adding dil. HCl and the weight of the precipitated nanotubes were recorded after washing several times with deionized water and drying in an oven at 60 °C for 12 hours. It was found that the weight of CNTs dissolved in the solution vary substantially for different batches of nanotubes (CNT-S: 11 mg/mL, CNT-CT: 2.6 mg/mL and CNT-CS: 3.8 mg/mL).

In addition, since urea molecules get attached to hydroxy (–OH) and carboxy (–COOH) groups present on the defect sites on carbon nanotubes, these groups are present in excess at the end of tubes. It could be possible that the soluble nanotubes, found in the filtrate have their ends closed due to attachment of urea molecules in bulk and changing the pH open them again. The ends of nanotubes in the filtrate and obtained after precipitation were closely observed. The HRTEM images of MWCNTs (CNT-S) shows open ends after treating with nitric acid (Fig. 3.47 and 3.48), closed ends of the nanotubes found in filtrate (Fig. 3.49), nanotubes obtained after precipitation by changing pH (Fig. 3.50) and the nanotubes again having reopened ends after precipitation (Fig. 3.51). It can be seen that in case of nanotubes with open ends, the well graphitized wall of nanotubes does not remain uniform at the end which can be attributed to the opening of the end since no carbon layers were visible at the end (see Fig 3.47 and 3.48) while in case of nanotubes having closed ends after urea treatment, amorphous material is visible at the ends adjacent to the fringes of nanotube´s side walls (see Fig. 3.49, 3.52). Similarly for precipitated nanotubes amorphous material has disappeared again, re-opening the ends (see Fig. 3.51). This is also an analogy to the glycol treatments on nanotubes to close their open ends, reported by Rao *et al.*[158]

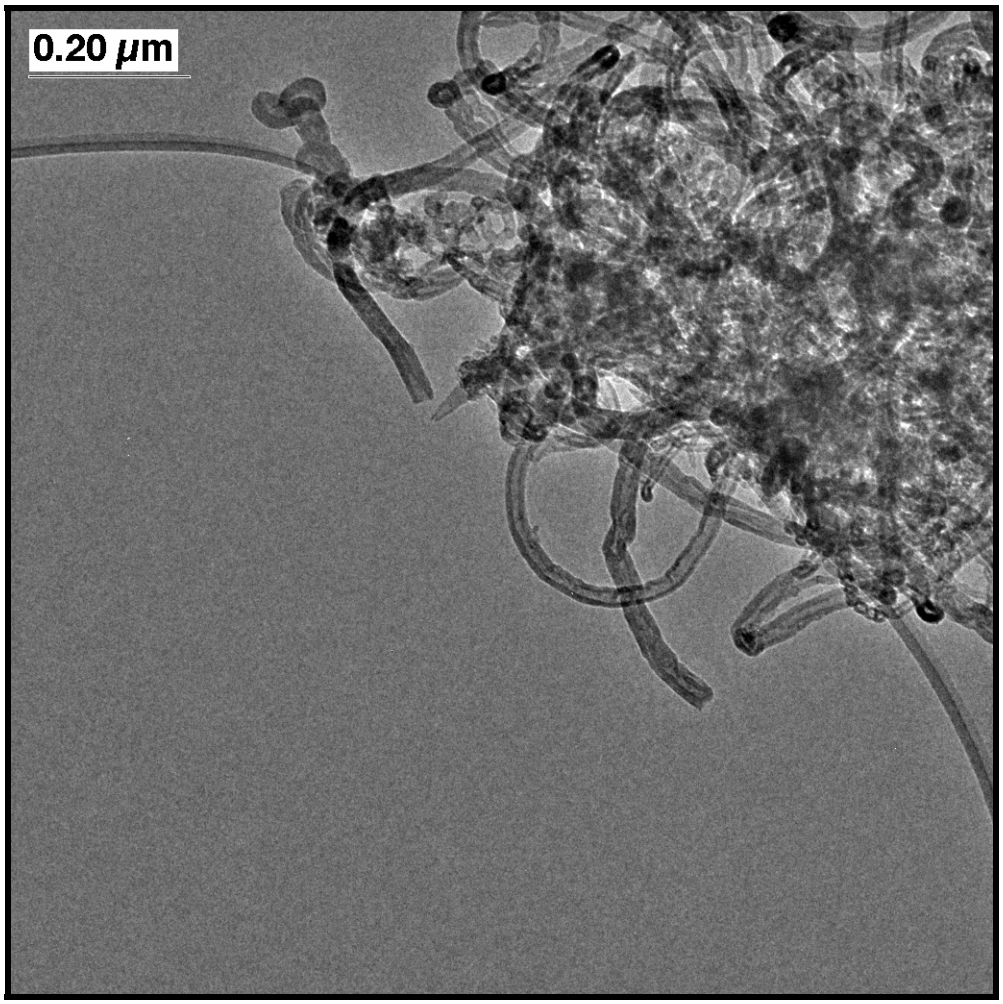

Figure 3.47 Low resolution TEM image of CNTs (CNT-S) with open ends after treating with 65% HNO_3 for 48 hours.

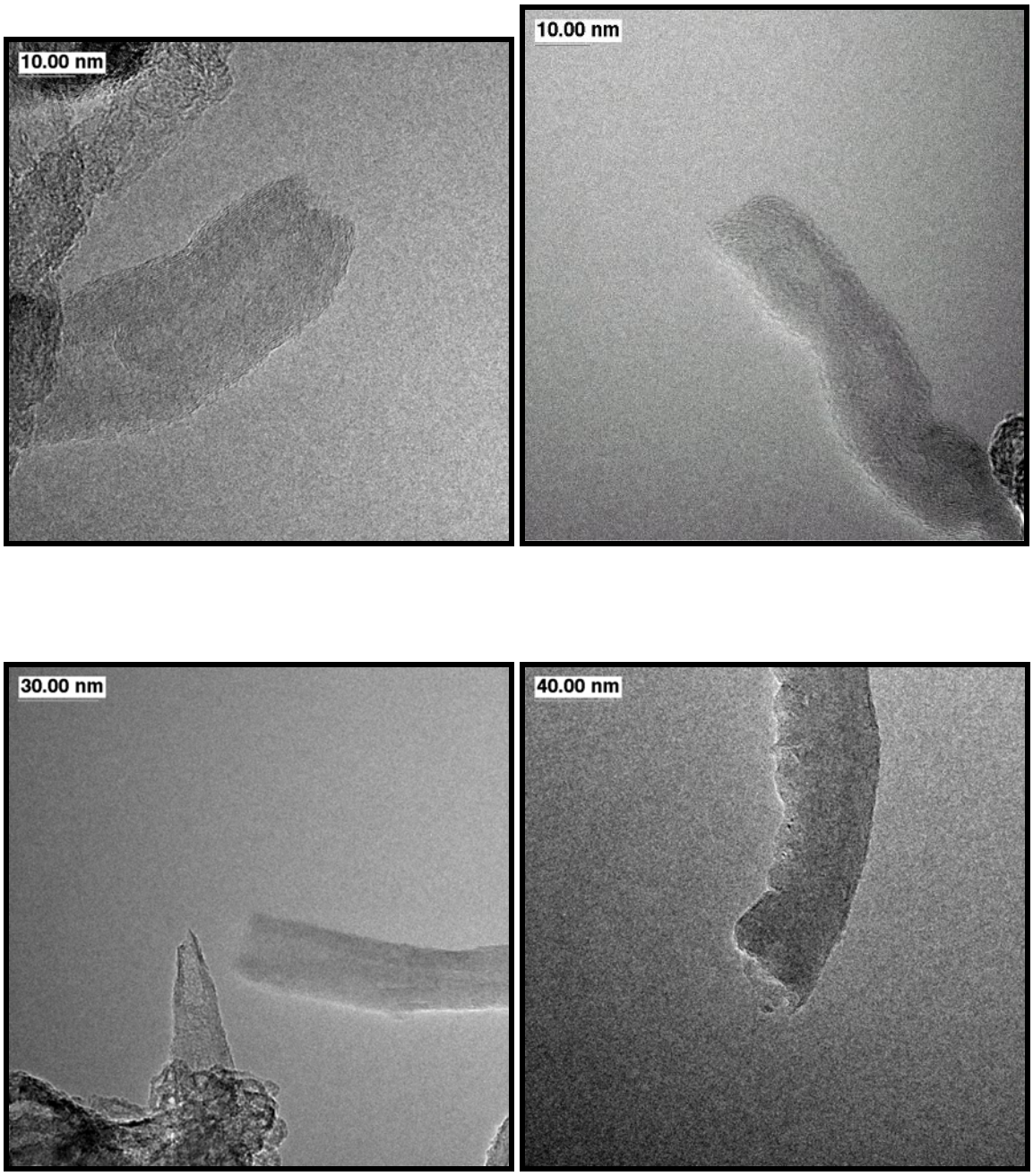

Figure 3.48 HRTEM images of CNTs (CNT-S) with open ends after treating with 65% HNO_3 for 48 hours

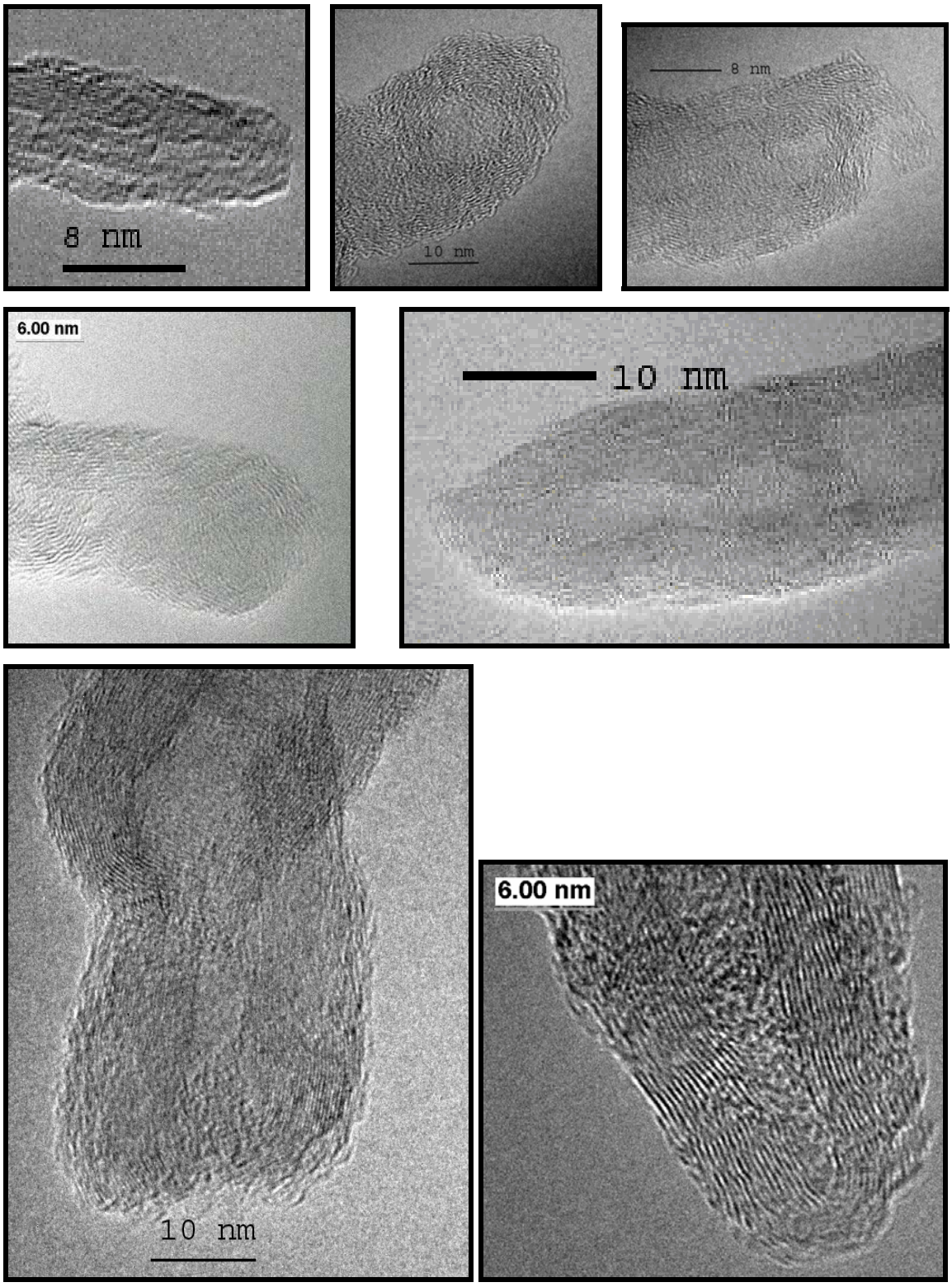

Figure 3.49 HRTEM images of closed ends of CNTs (CNT-S) after urea treatment.

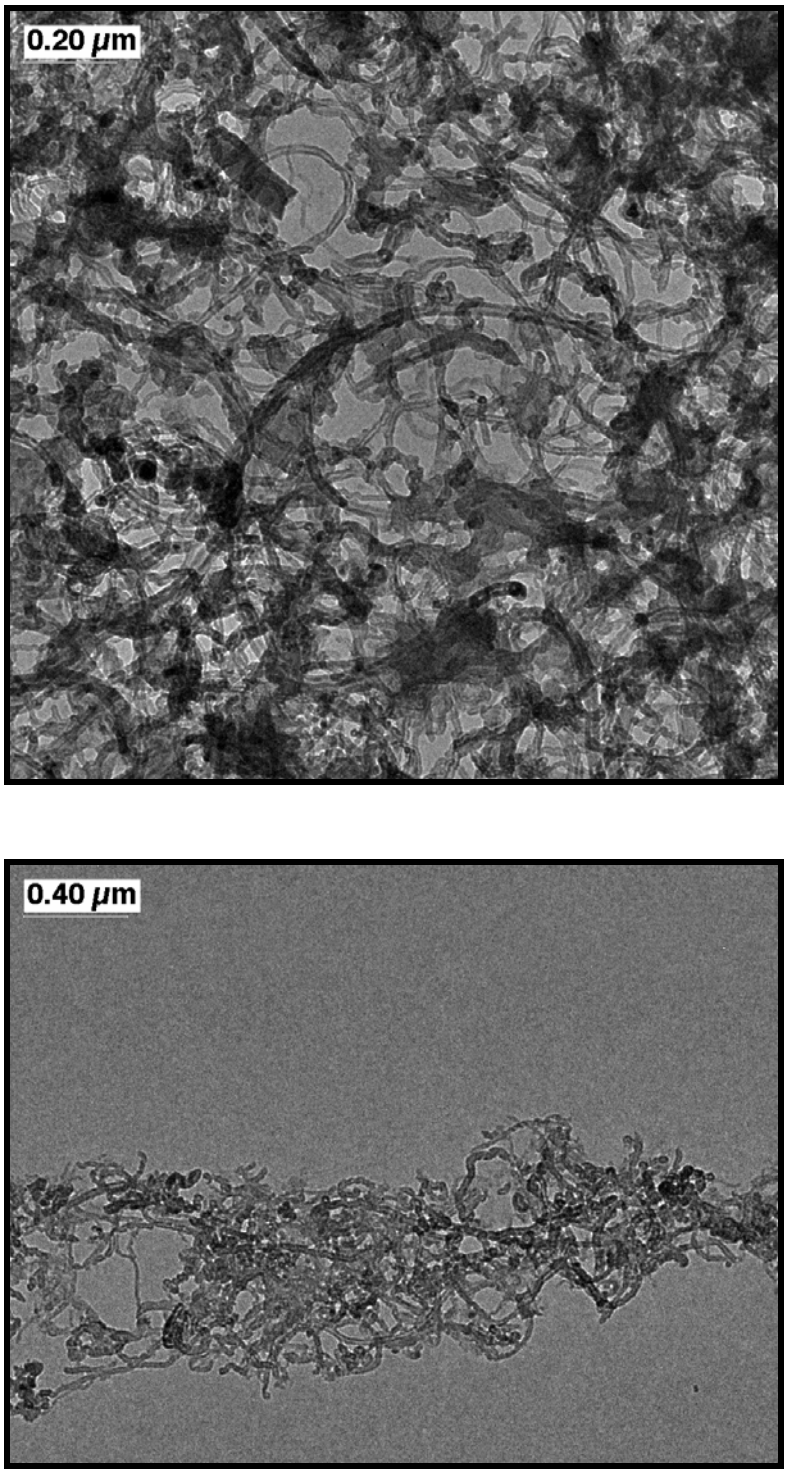

Figure 3.50 TEM images of CNTs (CNT-S) obtained after precipitation by changing the pH of the nanotube solution.

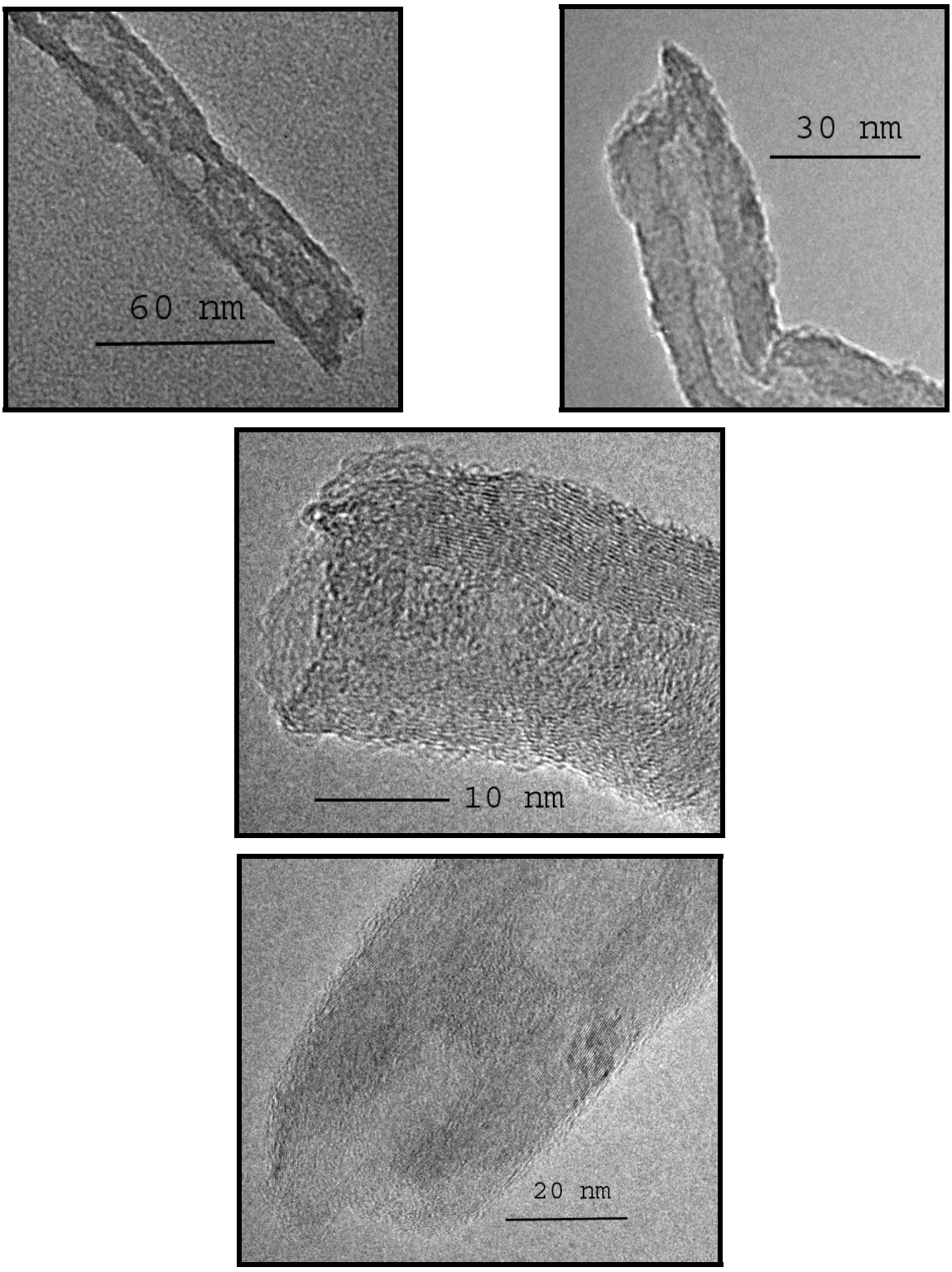

Figure 3.51 Open ends of CNTs (CNT-S) after precipitation by changing the pH with base (aq. Na_2CO_3) or acid (dil. HCl).

It was also observed that nanotubes which were filtered off as a solid were also closed at the ends after urea treatment. Figure 3.52 shows HRTEM images of such tubes with closed ends.

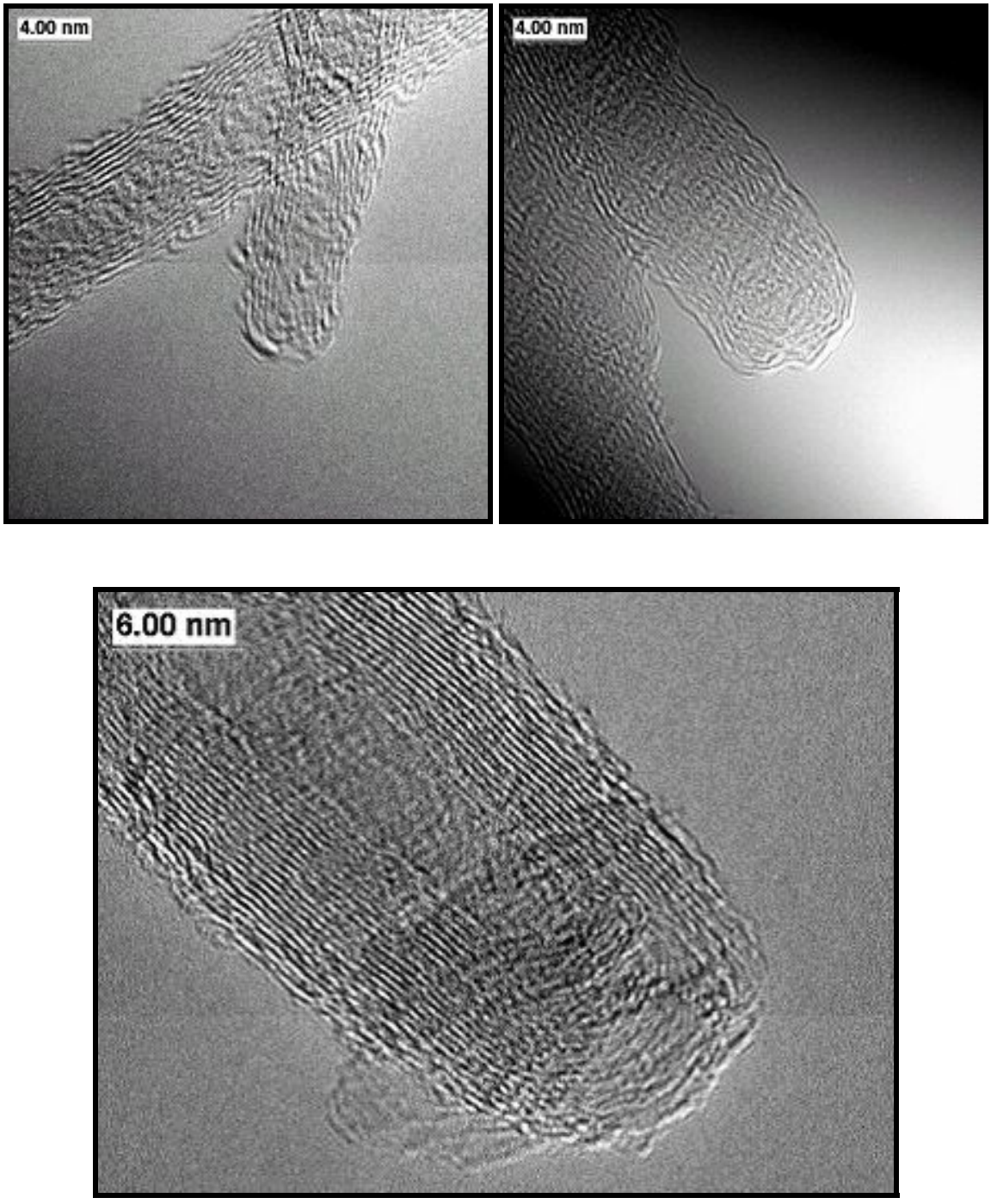

Figure 3.52 HRTEM images of closed ends of CNTs (CNT-S, filtered Solid).

3.7 Functionalizing Carbon Nanotubes

The final goal was to functionalize α-Fe filled carbon nanotubes in a way that it would be possible to use them as a catalyst support in various organic synthetic reactions. The advantage of using such catalyst anchored on ferromagnetic carbon nanotubes would be, that after the reaction the catalyst can be separated magnetically. Several methods reported in the literature were applied to functionalize the α-Fe filled carbon nanotubes.

3.7.1 Acylation Reactions

Acylation-amidation reactions have been reported by several groups for SWCNTs.[194] First the acylation reaction on SWCNTs and MWCNTs was investigated (see Scheme 3.3). CNTs were refluxed with thionyl chloride with 0.1 mL of DMF for 48 hours under an inert atmosphere. The solvent was then removed under vacuum and the solid obtained was analyzed by IR and TGA.

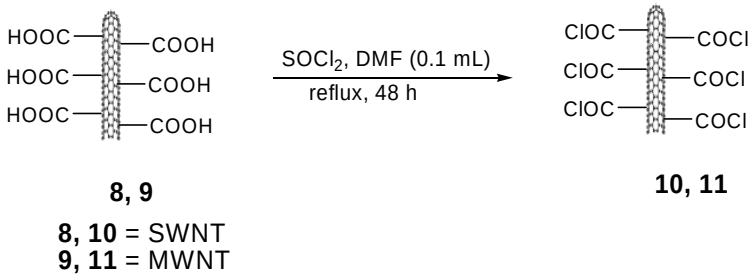

8, 9

8, 10 = SWNT
9, 11 = MWNT

10, 11

Scheme 3.3

Figure 3.53 and 3.54 shows the IR and TGA spectra of the sample obtained after acylation reaction.

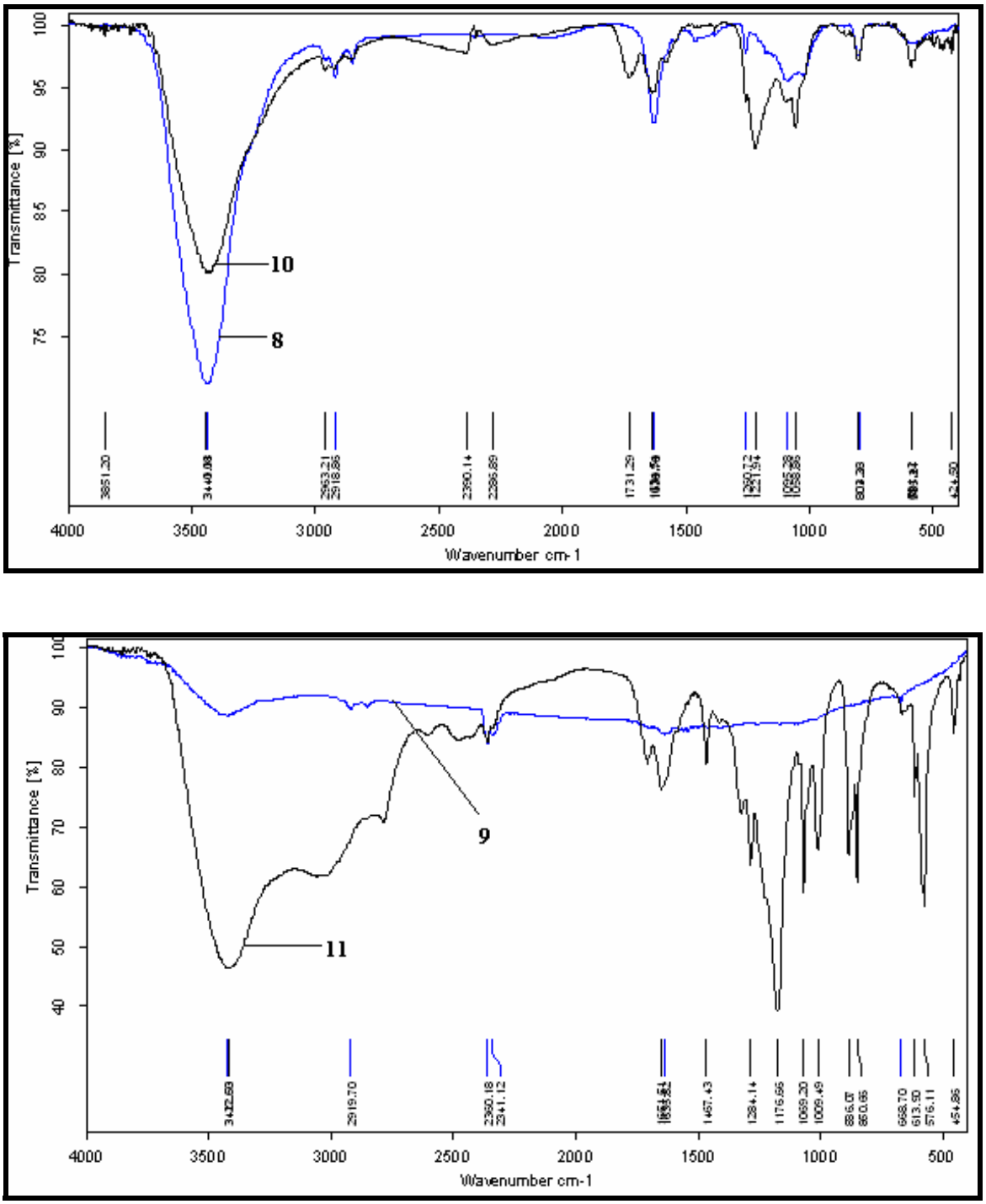

Figure 3.53 IR spectra of acylated SWCNTs **10** (top) and MWCNTs **11** (bottom), stretching modes of C=O groups (1730 cm^{-1} for SWCNTs and 1700 cm^{-1} for MWCNTs) can be seen as the most distinctive features in IR spectra of carboxylated CNTs (**8**, **9**) while splitting of these bands can be seen in acyl chloride intermediates (**10**, **11**).

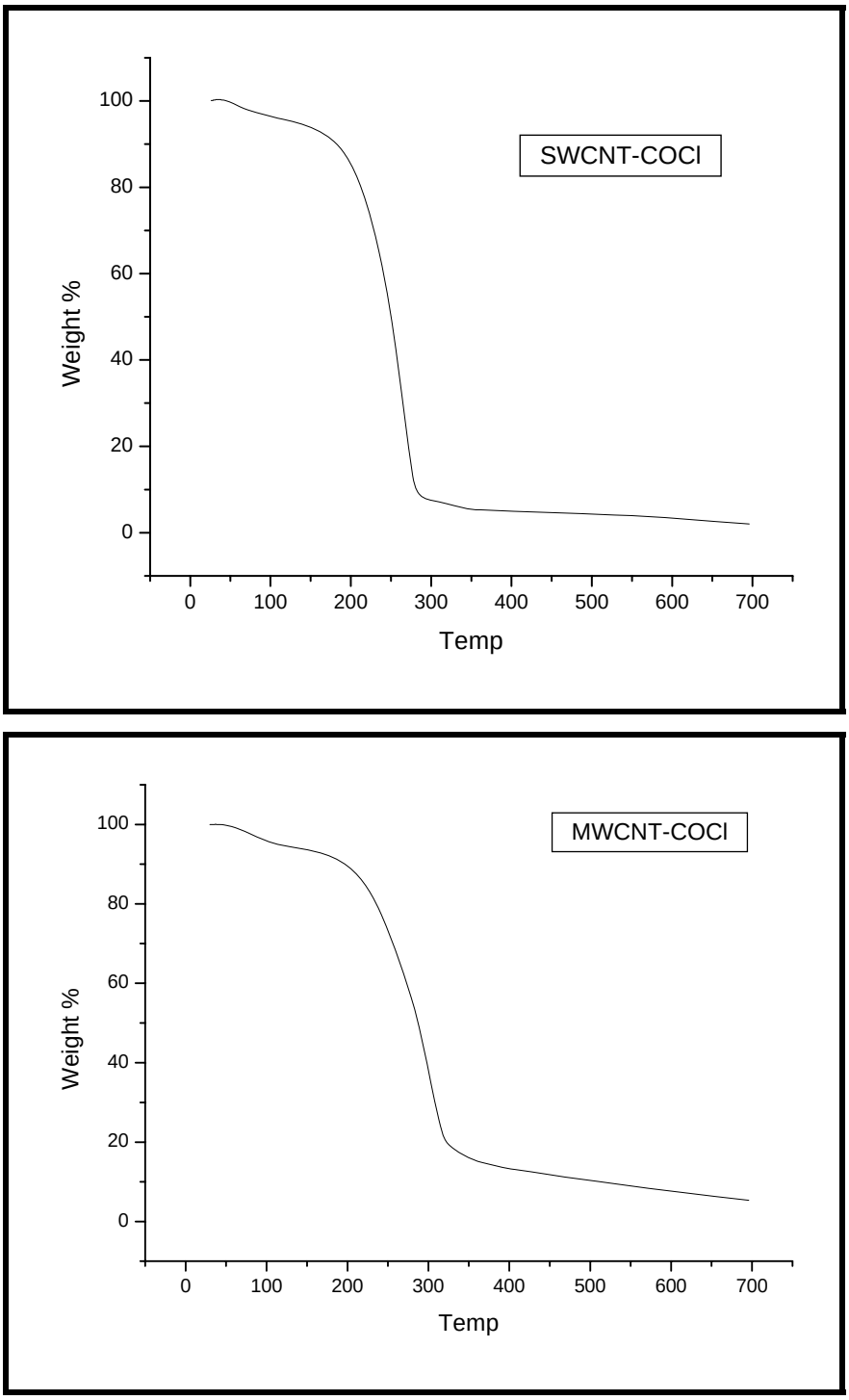

Figure 3.54 TGA of acylated SWCNTs **9** (top) and MWCNTs **11** (bottom), about 60% weight loss in TGA (temp. range: 200-300 ºC) can be attributed to –COCl groups attached to CNTs.

3.7.2 Acylation – Amidation Reactions[251]

Acylated samples of SWCNTs and MWCNTs were further functionalized with 2-(aminomethyl)-pyrrolidine according to the reaction given in the Scheme 3.4. The obtained products were analyzed by IR (Fig. 3.55 and 3.56) and TGA (Fig. 3.57).

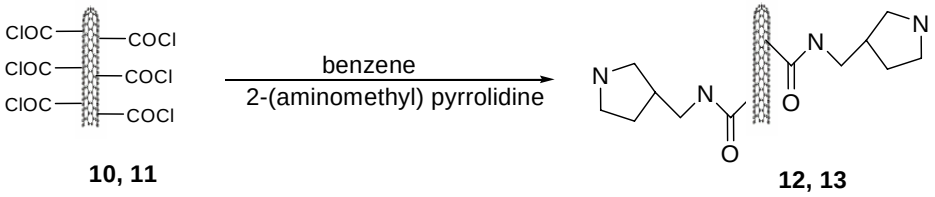

10, 11 **12, 13**

Scheme 3.4

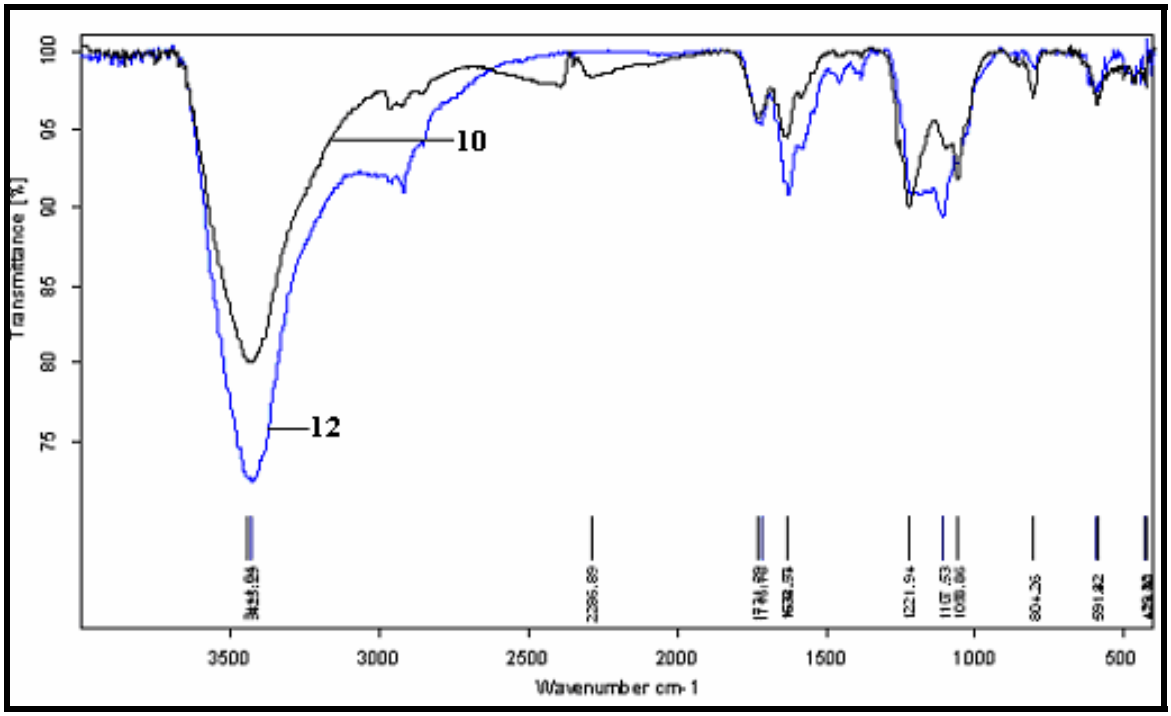

Figure 3.55 IR spectra of SWCNTs acyl chloride intermediate **10** and after amidation reaction **12**, a distinctive band at 3425 cm^{-1} shows the presence of –OH groups while the changes in C=O stretching mode band at around 1630 cm^{-1} and 1730 cm^{-1}, a peak at around 1107 cm^{-1} (C-N stretching mode vibrations) indicates the functionalization to some extent.

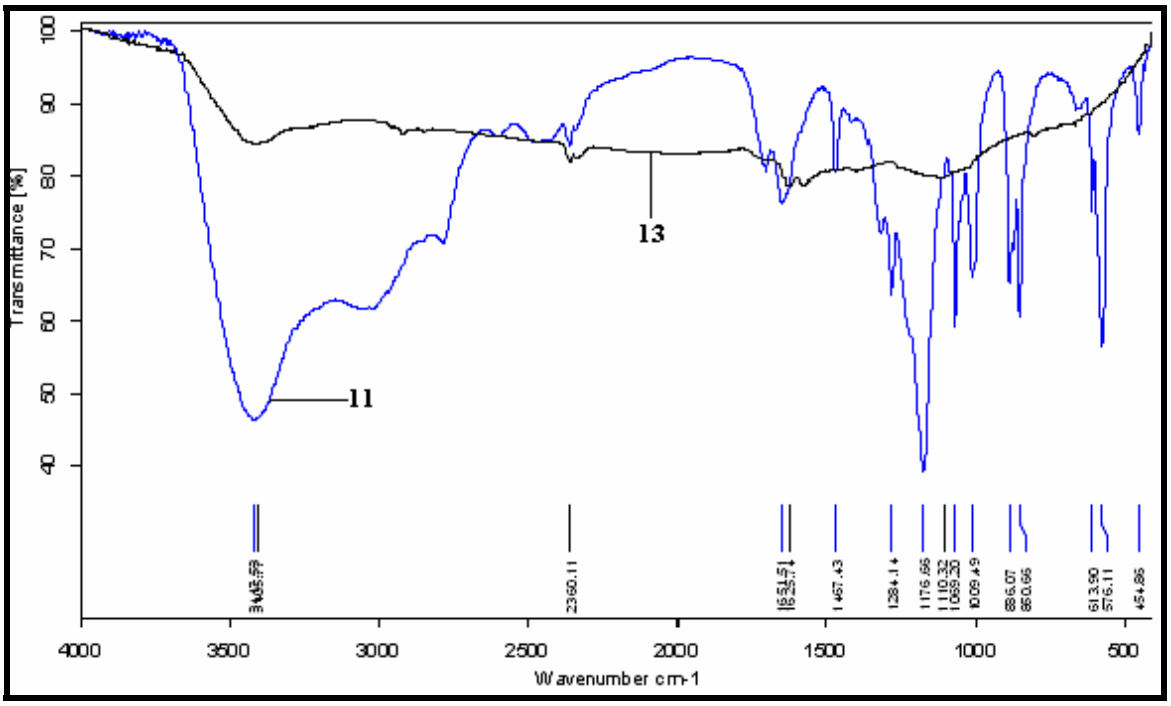

Figure 3.56 IR spectra of MWCNTs acyl chloride intermediate **11** and after amidation reaction **13**, no distinctive peaks could be observed to confirm the functionalization in case of MWCNTs.

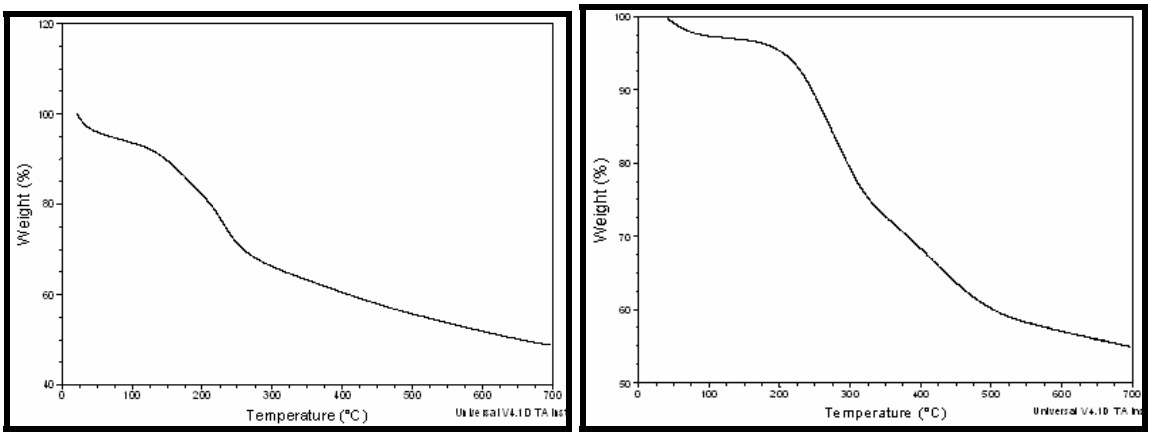

Figure 3.57 TGA spectra of SWCNTs **12** (left) and MWCNTs **13** (right) after amidation reaction, weight loss of about 20% in **12** and 30% in **13** (temp. range: 200-400 ºC) can be attributed to pyrrolidine attached to CNTs.

3.7.3 Brønsted Acid/Base Reaction

Oxidized carbon nanotubes were also subjected to a Brønsted acid/base reaction as shown in Scheme 3.5. Functionalization of carboxy groups of MWCNTs was performed by adding them with (*S*)-1-(2-pyrrolidinylmethyl)pyrrolidine using the following Scheme. Figure 3.58, 3.59 shows IR and TGA spectra of functionalized CNTs.

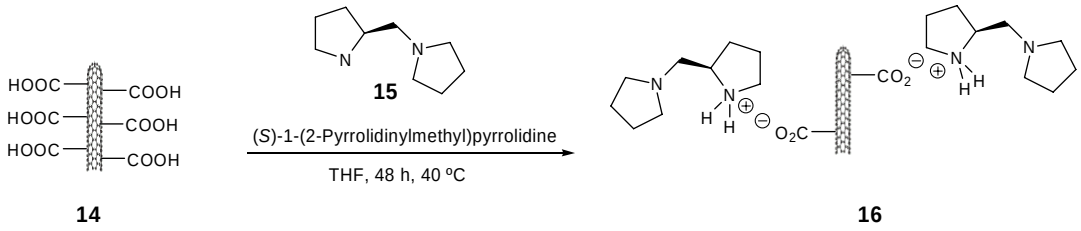

14 **16**

Scheme 3.5

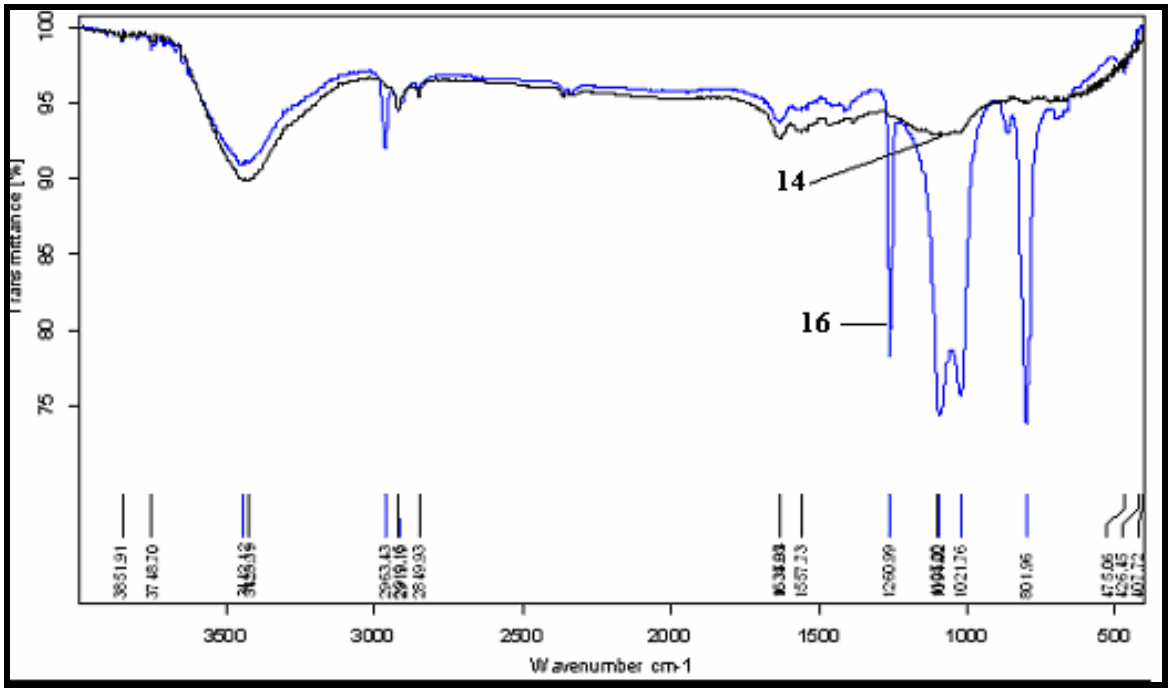

Figure 3.58 IR spectra of oxidized MWCNTs **14** and after functionalization **16**, peaks at 1021, 1096 cm^{-1} (C-N stretching mode vibrations) and at 801 cm^{-1} (N-H bending mode vibrations) confirms the presence of pyrrolidine in **16.**

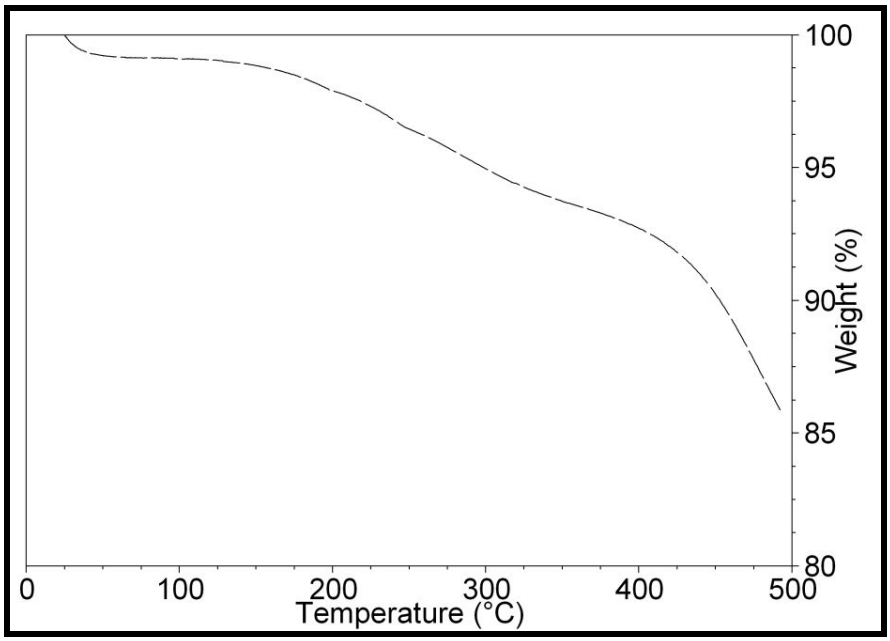

Figure 3.59 TGA of functionalized CNT **16**, approximately 15% weight loss (temp. range: 200-500 °C) can be attributed to the functionalization.

A similar reaction for non-covalent functionalization of MWCNTs was performed with (2*S*,5*S*)-(-)-2-*tert*-butyl-3-methyl-5-benzyl-4-imidazolidinone (see Scheme 3.6). The product was analyzed by IR (Figure 3.60) and TGA (Figure 3.61).

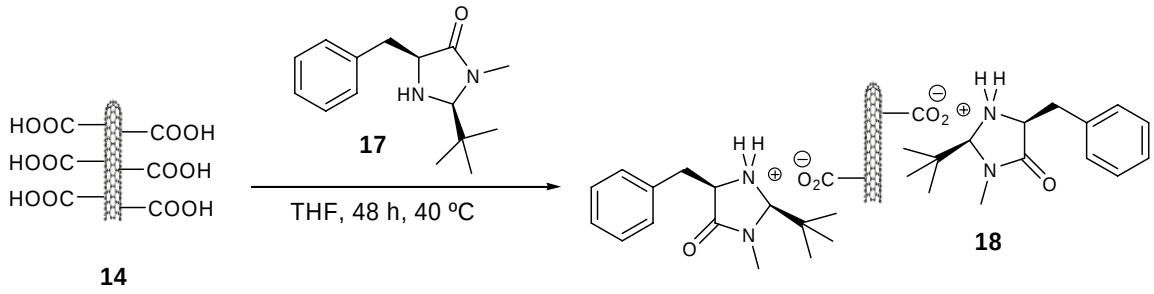

Scheme 3.6

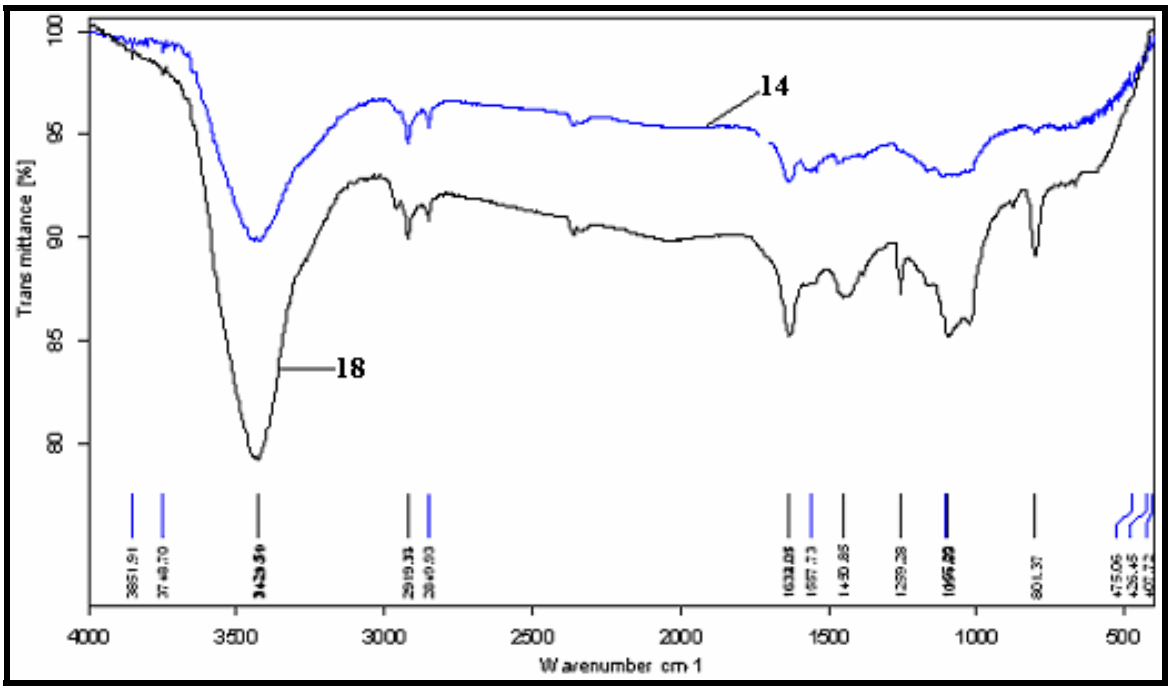

Figure 3.60 IR spectra of oxidized MWCNTs **14** and after functionalization **18**, similar band as seen in **16**, at 1096 cm^{-1} (C-N stretching mode vibrations) and at 801 cm^{-1} (N-H bending mode vibrations) confirms the presence of imidazolidine **18.**

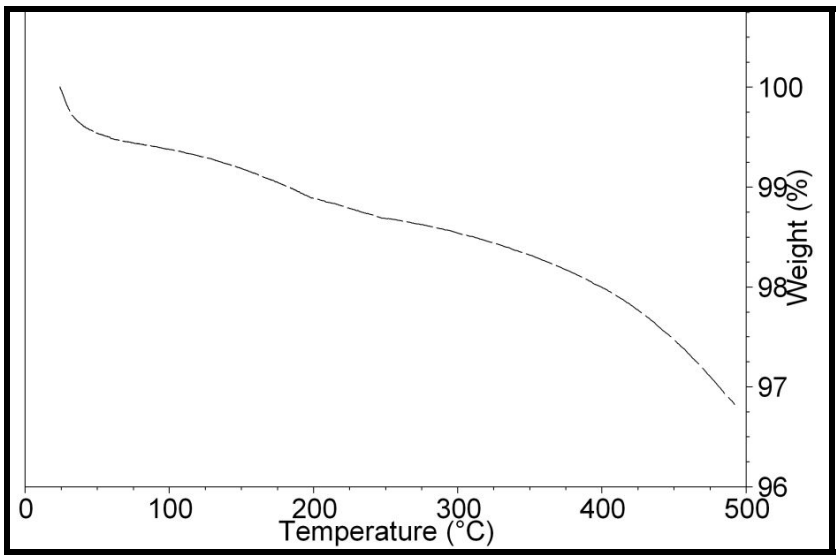

Figure 3.61 TGA of functionalized CNT **18**, less than 5% weight loss (temp. range: 200-300 °C) shows low level of functionalization.

To ensure the functionalization, IR spectra of modified nanotubes (**16**, **18**) were compared with acetyl salts of their corresponding amines prepared by treating them with acetic acid (see Scheme 3.7 and Figure 3.62, 3.63).

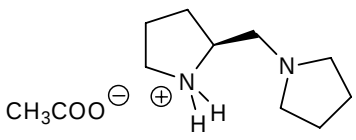

19

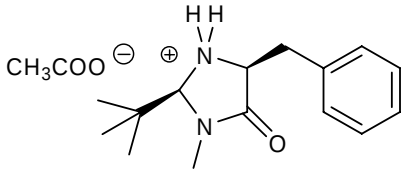

20

Scheme 3.7

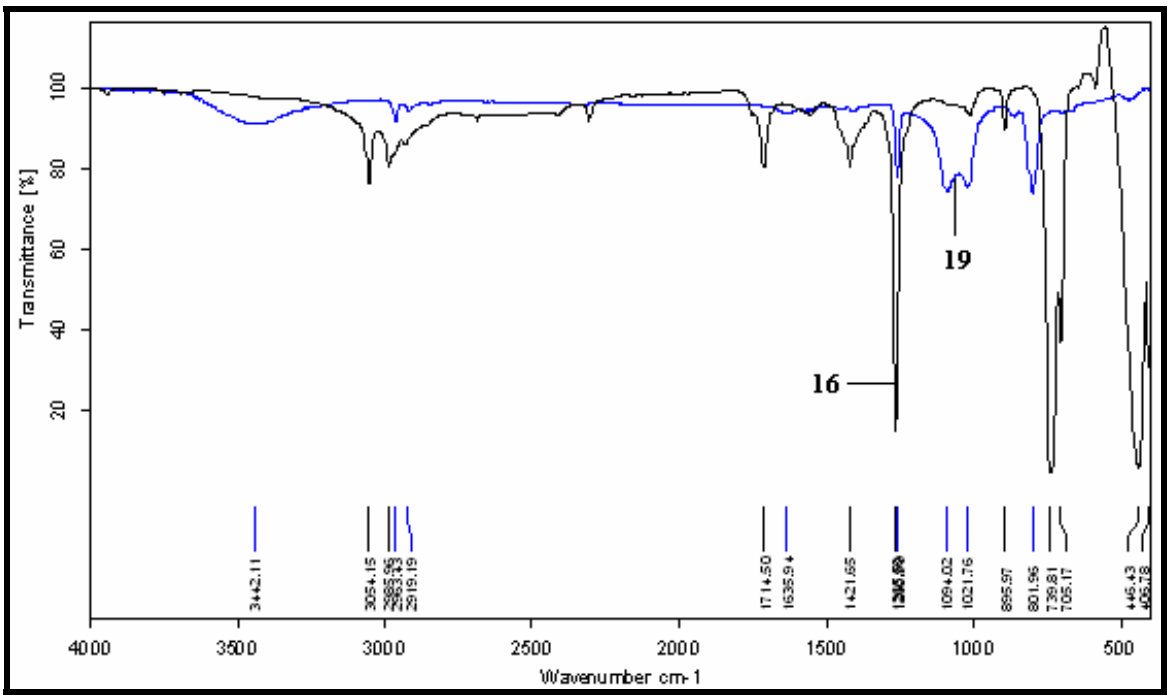

Figure 3.62 Comparative IR spectra of functionalized CNTs (**16**) and its corresponding amine salt **19,** IR spectra of **19** also shows the peaks at 1094, 1015 cm^{-1} (C-N stretching mode vibrations) and at 801 cm^{-1} (N-H bending mode vibrations) as seen in **16.**

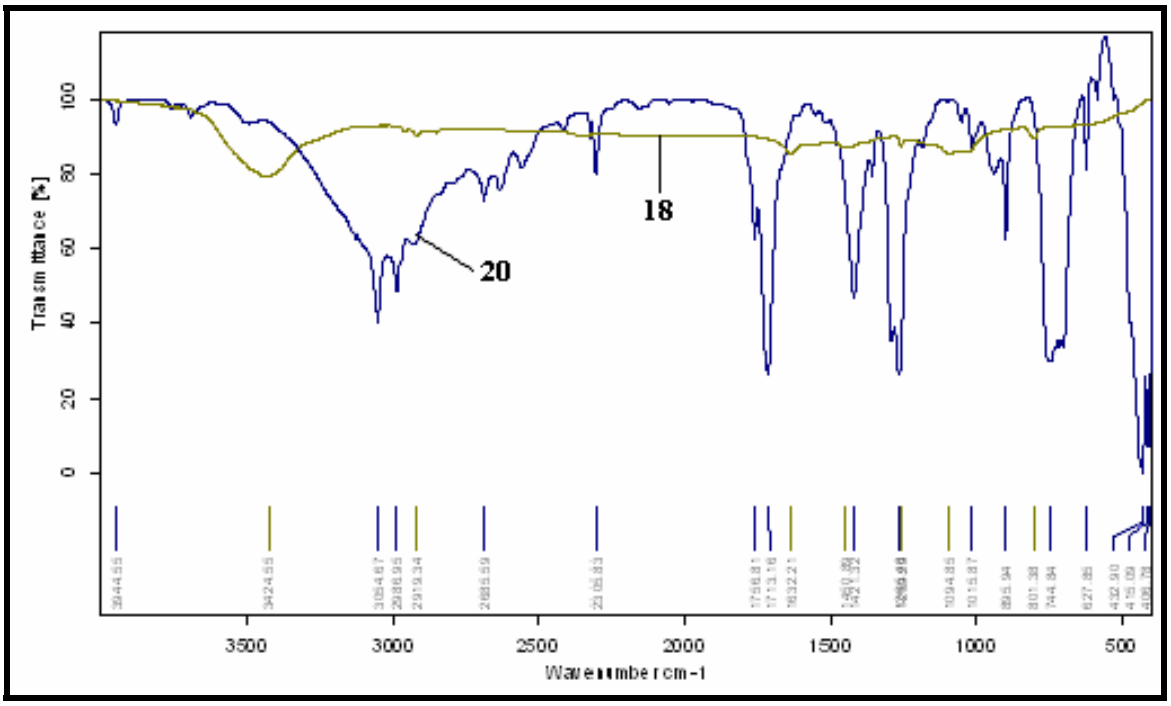

Figure 3.63 Comparative IR spectra of functionalized CNTs (**18**) and its corresponding amine salt **20,** IR spectra of **20** also shows the peaks at 1096 cm^{-1} (C-N stretching mode vibrations) and at 801 cm^{-1} (N-H bending mode vibrations) as seen in **18.**

3.7.4 Immobilization of a Chiral Ligand on Carbon Nanotube Surface

Recycling of catalysts via immobilization by grafting them on heterogeneous supports have been a recent research interest of the scientific communities. Filtration-free recyclable catalysts have been prepared by immobilizing ligands on magnetic mesocellular mesoporous silica.[251] Such catalysts can be recovered by magnetic decantation and hence enable a filtration-free processing. A similar principle was used in the presented work for the immobilization of catalyst by grafting them on carbon nanotubes surface. Carboxy groups on oxidized nanotubes were first reduced to alcohol by treating them with $LiAlH_4$. Reduced carbon nanotubes were further functionalized with a chloride linker as shown in Scheme 3.8. The product was analyzed by IR and TGA (see Figure 3.64, 3.65).

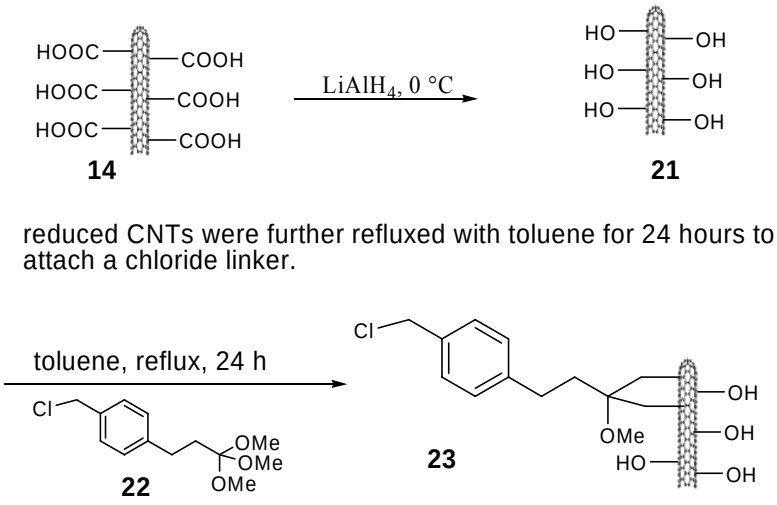

reduced CNTs were further refluxed with toluene for 24 hours to attach a chloride linker.

Scheme 3.8

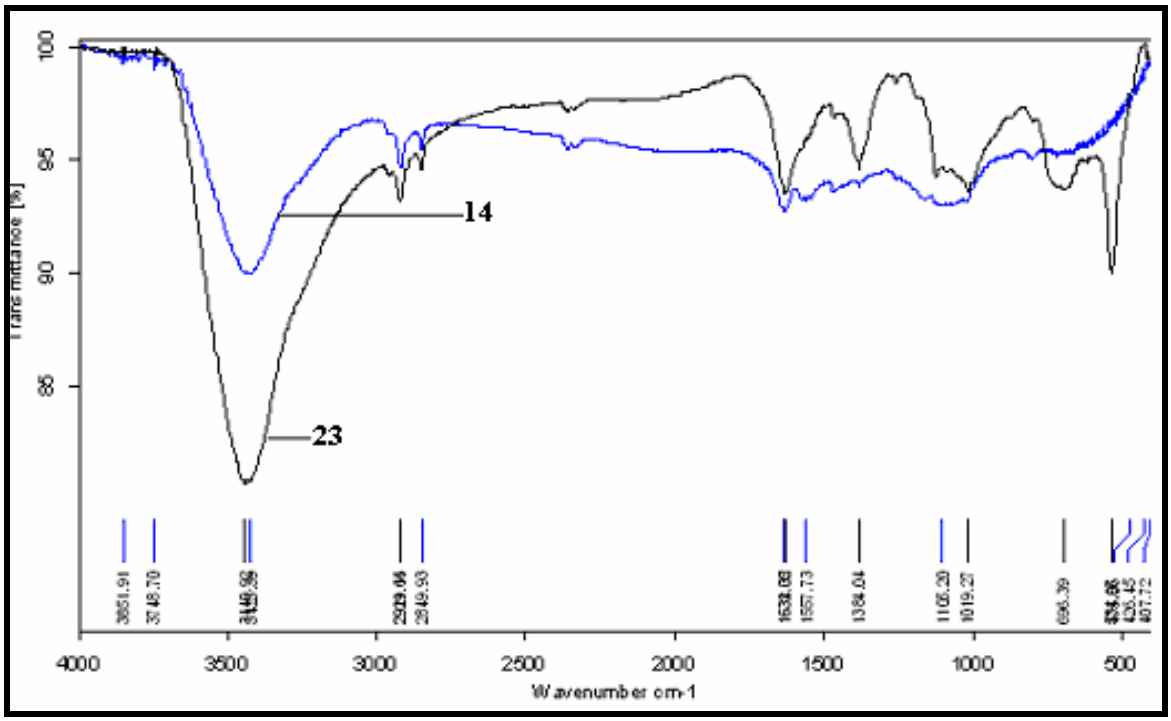

Figure 3.64 IR spectra of carboxylated MWCNTs **14** and after attaching a chloride linker **23**, IR spectra of **23** differs from **14** but no distinctive peaks were observed to conclude any result.

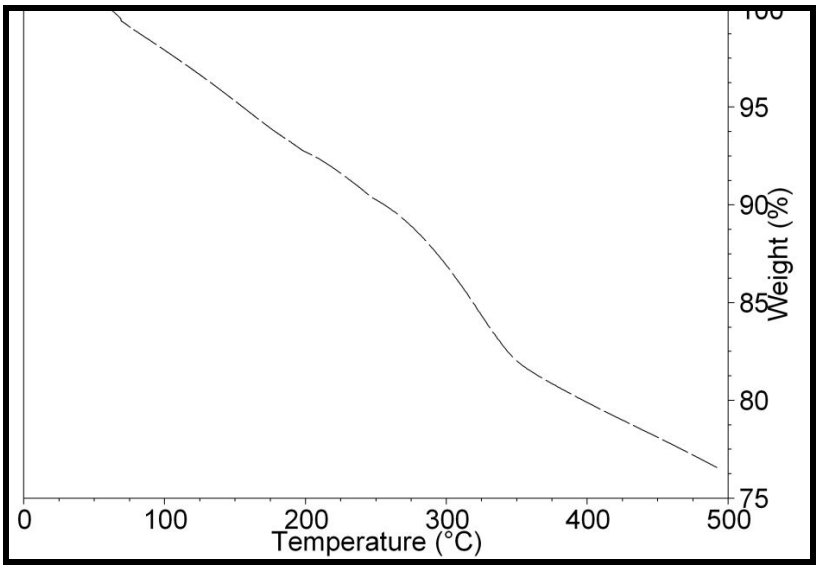

Figure 3.65 TGA of functionalized CNT **21**, about 20% weight loss (temp. range: 200-400 °C) can be attributed to functionalization.

3.7.5 Grafting of A Radical Polymerization Initiator (V501)

The group of R. Jerome have reported the attachment of magnetite nanoparticles via attaching a commercially available radical polymerization initiator 4,4′-azobis(4-cyanovaleric acid) (V501).[252] Using a similar protocol 4-4′- azobis(4-cyanopentanoic acid) (V501) was attached to α-Fe filled MWCNTs (Scheme 3.9). The product was analyzed by IR (Figure 3.66) TGA (Figure 3.67) and TEM (Figure 3.68).

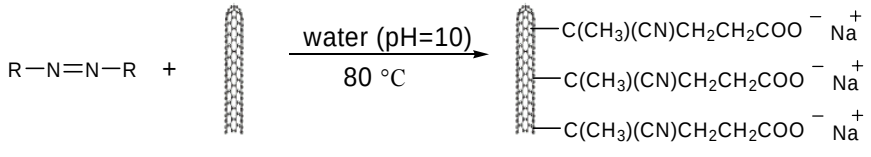

25

24

R = —C(CH$_3$)(CN)CH$_2$CH$_2$COO$^-$ Na$^+$

Scheme 3.9

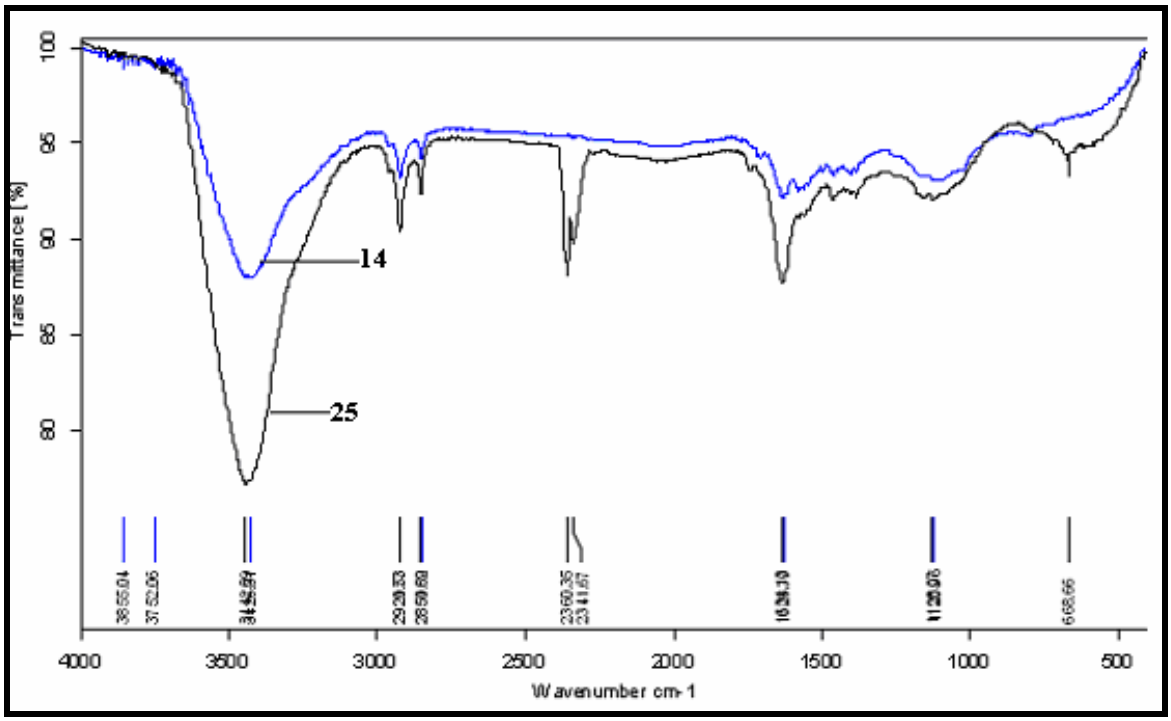

Figure 3.66 IR spectra of raw MWCNTs and functionalized nanotubes **25**, the spectra of **25** differ from raw MWCNTs but no distinctive peaks were observed to conclude any result.

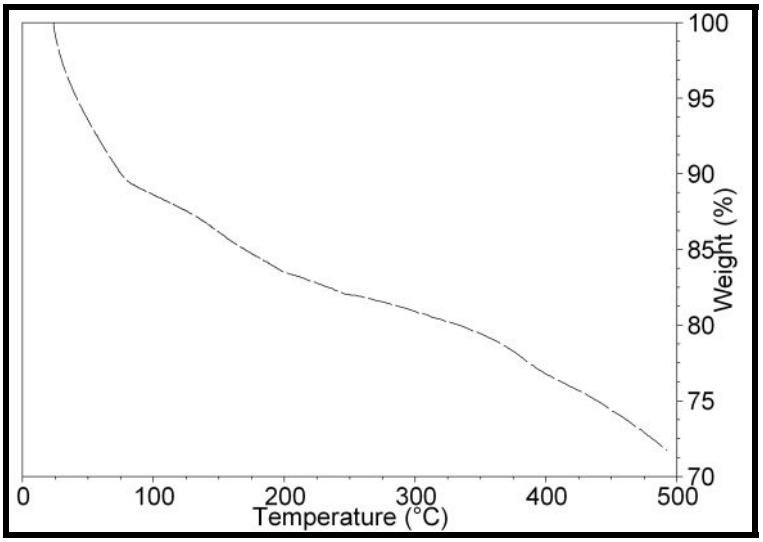

Figure 3.67 TGA spectra of functionalized nanotubes **25**, about 10% weight loss in the temperature range (200-300 °C) can be attributed to functionalization.

It was observed that after the reaction functionalized nanotubes were not attracted towards a magnet. The loss of ferromagnetic behavior in CNTs suggested, it was possible that in such grafting reactions α-Fe filled nanotubes became empty during the reaction. Below are TEM images of such empty MWCNTs after the functionalization reaction according to Scheme 3.9. This suggested that it is necessary to close the α-Fe filled nanotubes before performing any reaction on them.

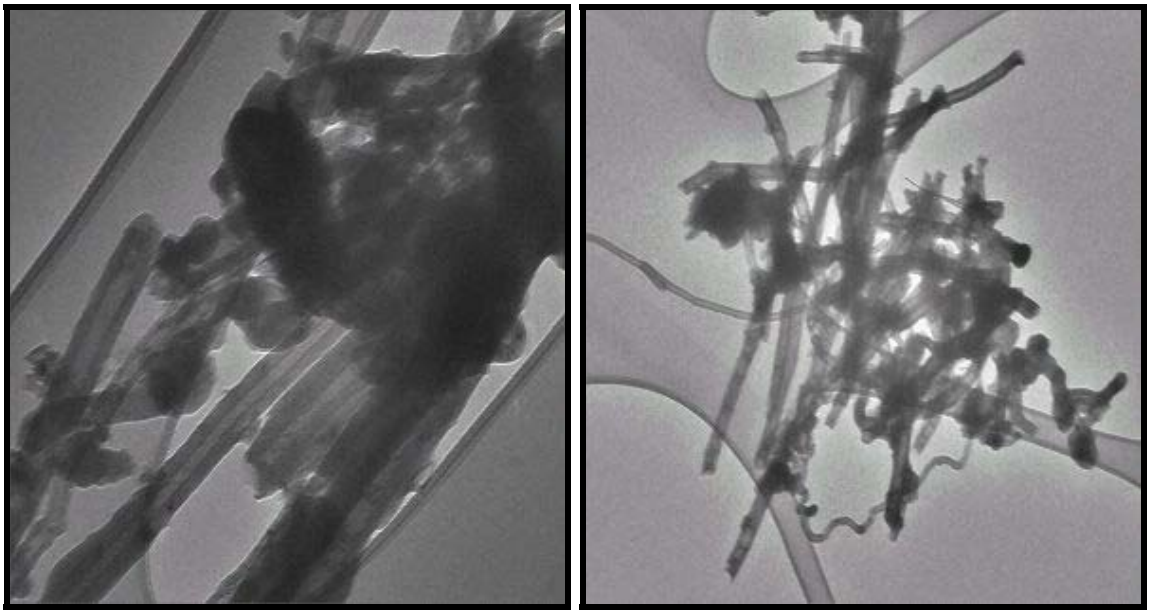

Figure 3.68 TEM images of MWCNTs **25** obtained after the functionalization reaction.

3.7.6 Reaction with Diazonium Salts

A functionalization with diazonium salts of aniline and toluidine using the procedure reported by R. G. Compton *et al.*[253], was also carried out (see Scheme 3.10). The α-Fe filled functionalized tubes were further subjected to chloromethylation. The preparation of diazonium salts and chloromethylation reaction was performed using standard procedures (see Scheme 3.10).[254, 255] The products were analyzed by IR and TGA (see Figure 3.69 and 3.70).

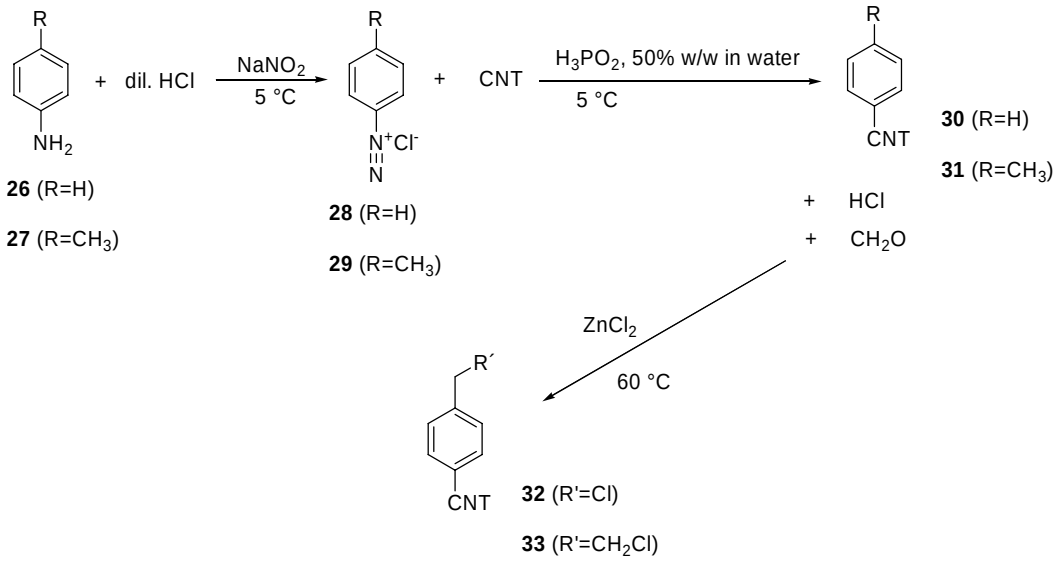

Scheme 3.10

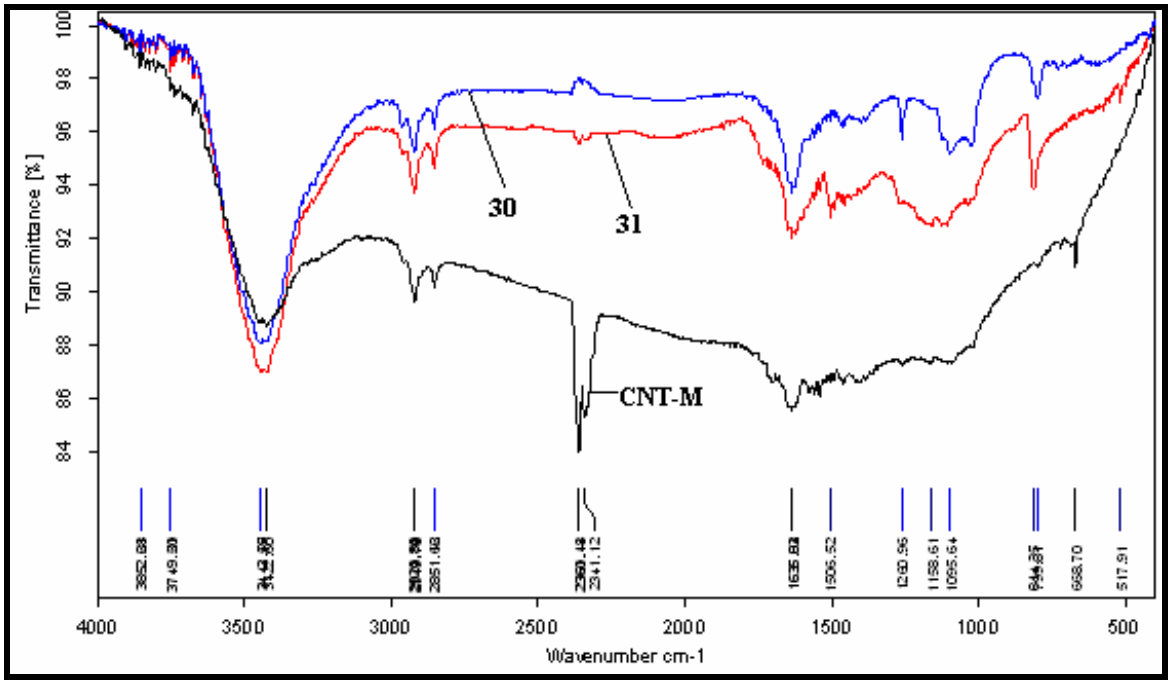

Figure 3.69 IR spectra of raw MWCNT (CNT- M) and CNTs functionalized with diazonium salts of aniline **30** and toluidine **31**, no distinctive peaks were observed to conclude any result.

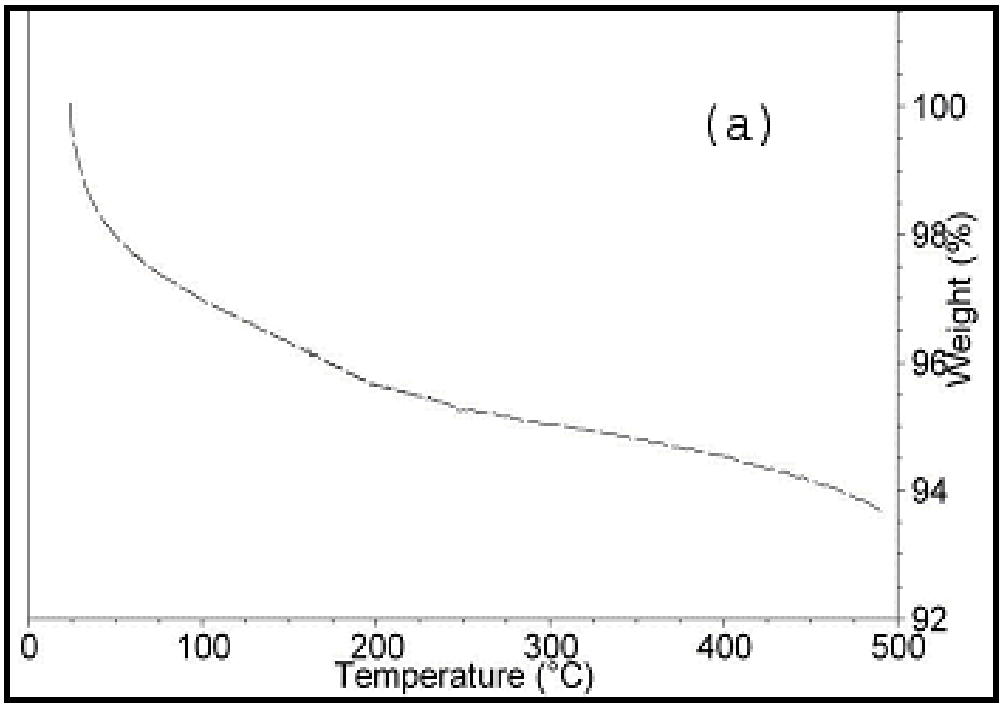

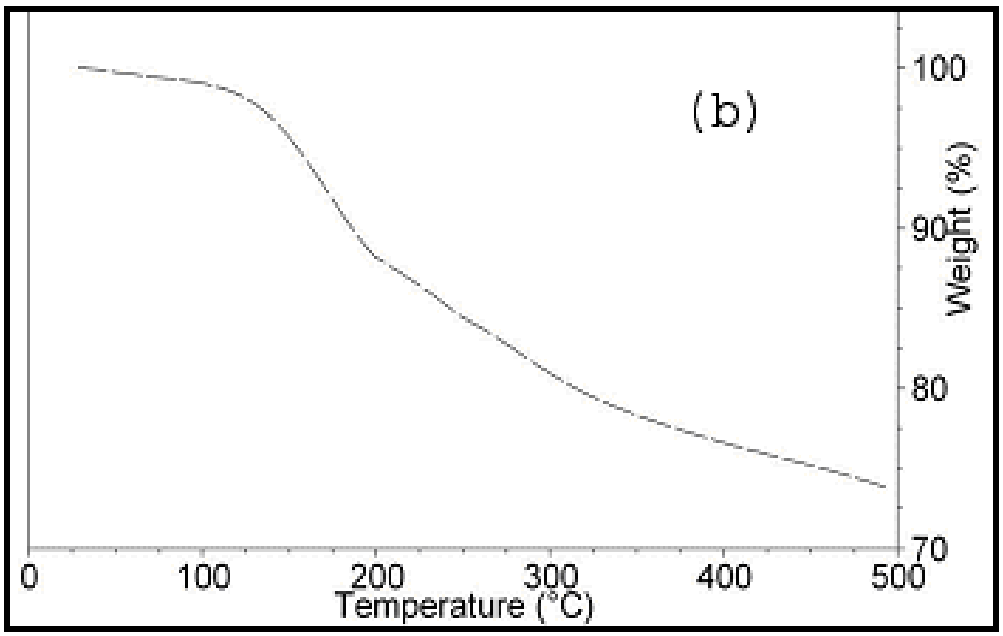

Figure 3.70 TGA spectra of CNTs functionalized with diazonium salts of aniline **30** (a), and toluidine **31** (b), less than 5% weight loss (temp. range: 200-300 °C) in case of **30** shows low level of functionalization, while about 25% weight loss in case of **31** can be attributed functionalization.

3.7.7 [3+2] Reaction

Functionalization of SWCNTs and MWCNTs by the application of a [3+2] reaction as described by the group of Prato *et al.* (Scheme 3.11)[256] was also performed. However, the observed level of functionalization was not useful for the desired applications. The products were analyzed by IR (Figure 3.71, 3.72) and TGA (Figure 3.73).

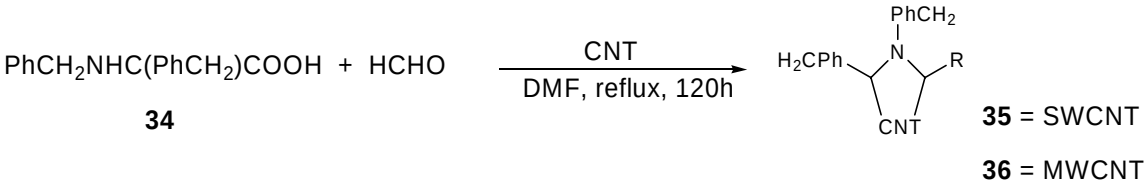

Scheme 3.11

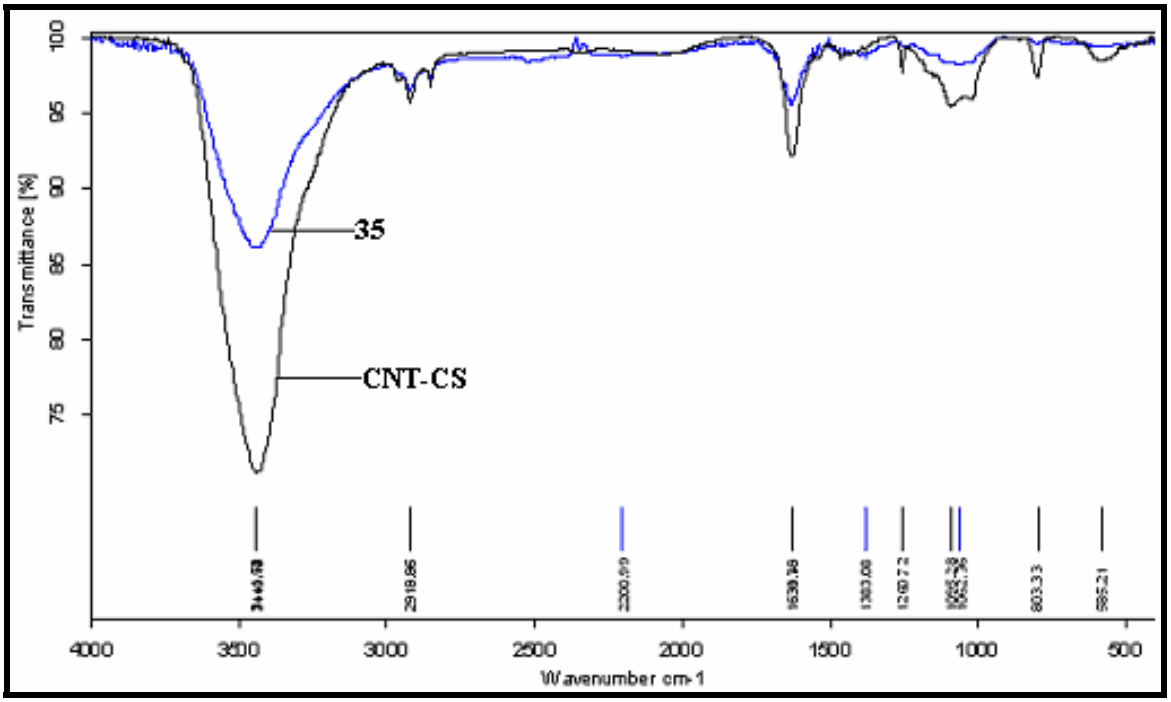

Figure 3.71 IR spectra of raw SWCNTs (CNT-CS) and functionalized nanotube **35**, C-N stretching mode vibrations bands at 1062 cm^{-1} and a weak N-H bending mode vibrations at 845 cm^{-1} can be attributed to the functionalization.

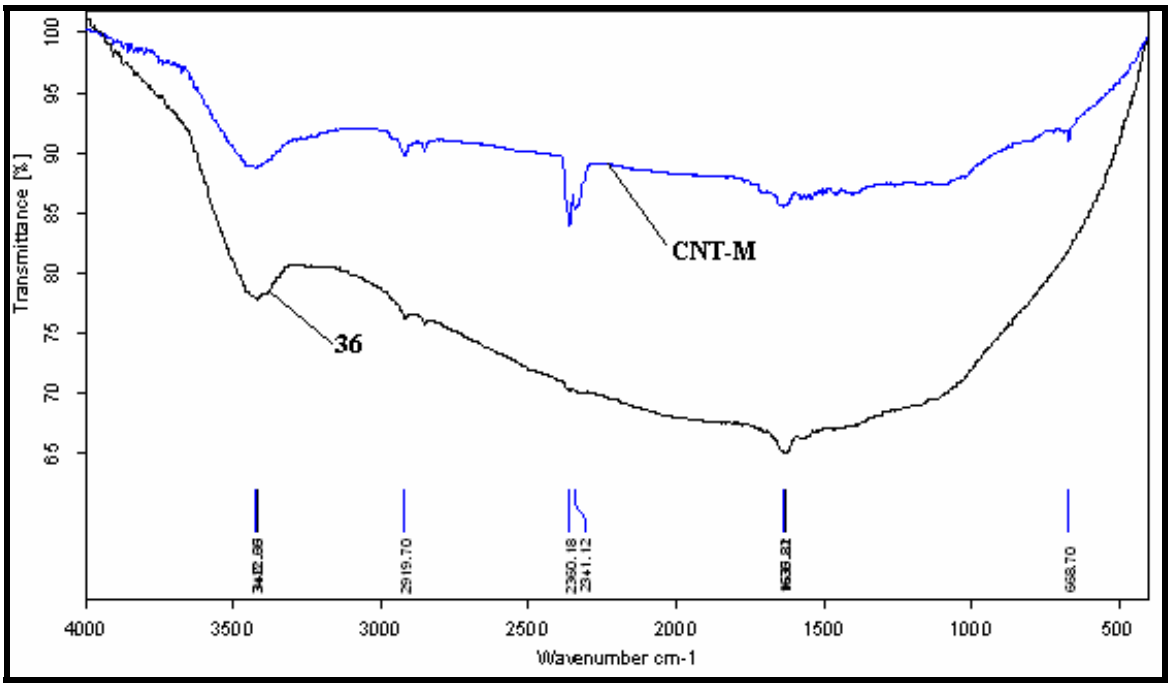

Figure 3.72 IR spectra of raw MWCNTs (CNT-M) and functionalized nanotube **36**, IR spectra of **36** differs from raw MWCNTs but no distinctive peaks were observed to conclude any result.

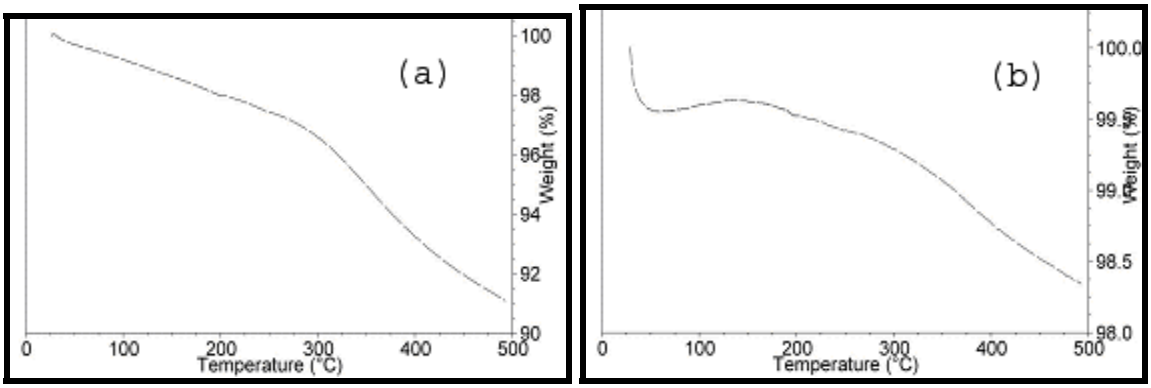

Figure 3.73 TGA spectra of functionalized nanotubes **35** (a) and **36** (b), less than 8 % weight loss up to 500 °C predicts a low level of functionalization.

3.7.8 Arylation Reaction

In addition an attempt was made to prepare aryl group functionalized MWCNTs by the method described by W. E. Billups *et al*. for SWCNTs (Scheme 3.12).[257] The arylation reactions were carried out by replacing the reported SWCNTs with the filled MWCNTs (**37**). However this method was not useful, since the obtained material was not ferromagnetic anymore. The product was analyzed by IR (Figure 3.74) and TGA (Figure 3.75).

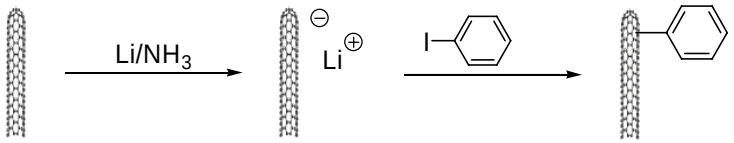

37 **38** **39**

Scheme 3.12[257]

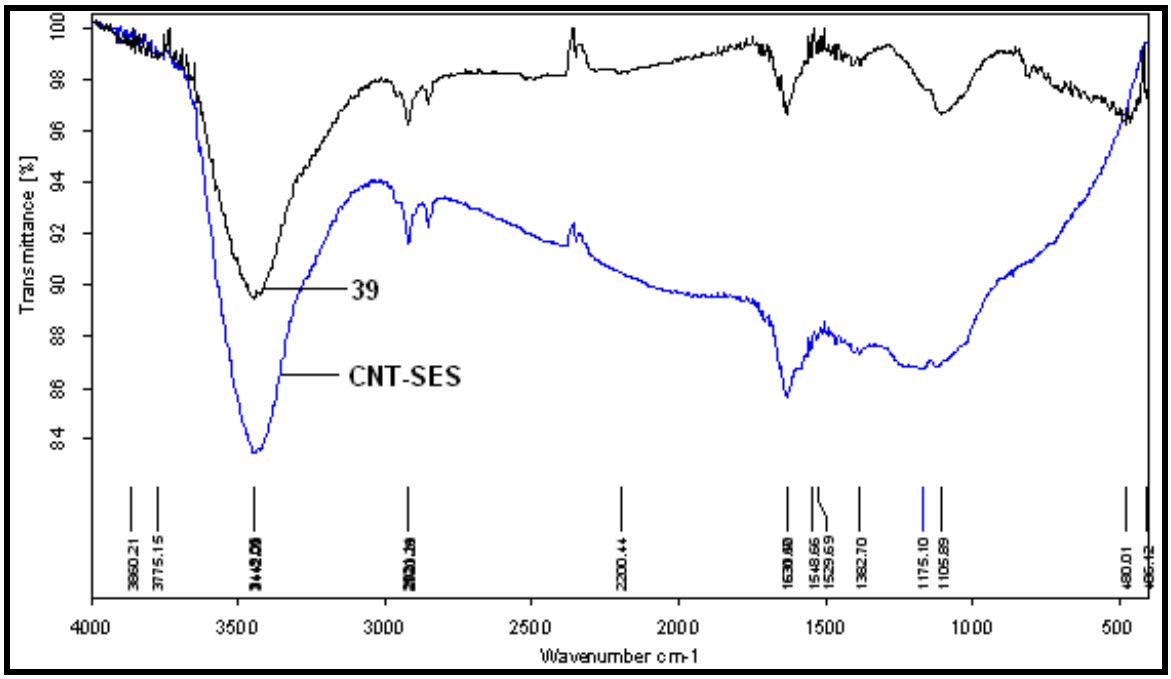

Figure 3.74 IR spectra of raw MWCNTs (CNT-SES) and functionalized nanotubes **39**, IR spectra of **39** differs from MWCNTs but since C=C stretching mode vibrations at 1630 cm^{-1} are present in both so the spectra shown does not conclude any result.

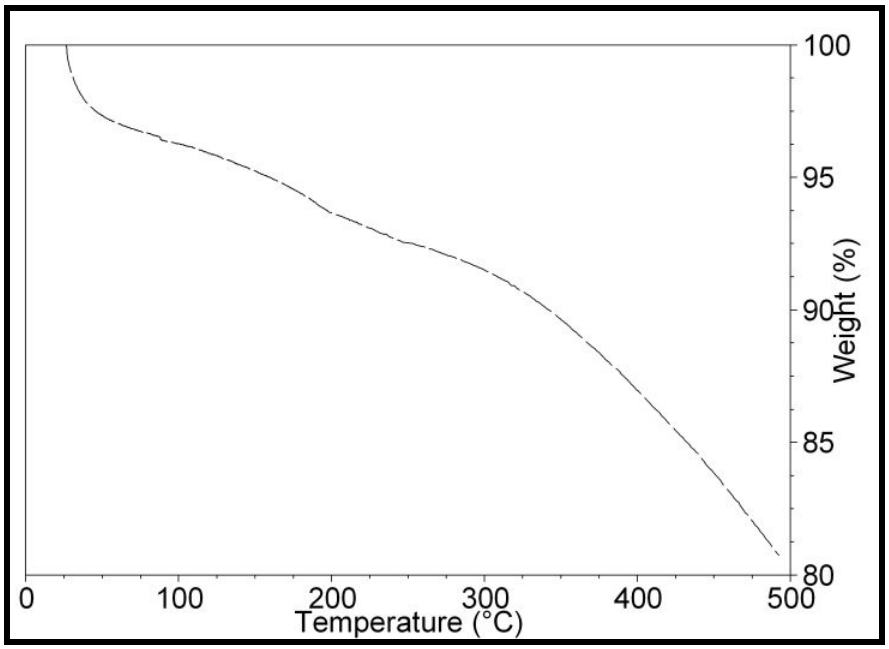

Figure 3.75 TGA spectra of functionalized nanotubes **39**, less than 10 % weight loss up to 300 °C predicts a low level of functionalization.

3.8 Application of Modified Carbon Nanotubes

3.8.1 Epoxide Ring Opening Reaction of Epoxycyclohexane with Aniline[258]

Carboxylated ferromagnetic MWCNTs were used as a catalyst for a prototype ring opening reaction of epoxides as shown in the scheme 3.13. The reaction was observed to be catalyzed by CNTs and after 4 days it afforded the product **42** with 75% yield with 80% conversion of aniline (calculated by GC, internal standard - cyclododecane).

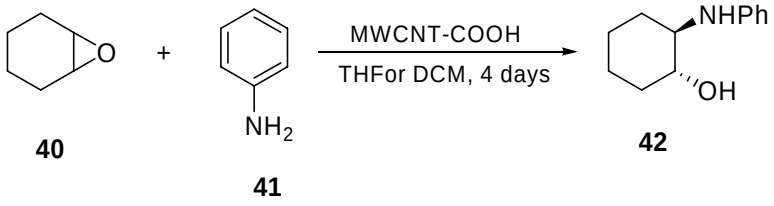

40 **41** **42**

Scheme 3.13

In such reactions ferromagnetic heterogeneous catalyst (modified CNTs) was easily removed from the reaction mixture using a magnet (see Figure 3.76).

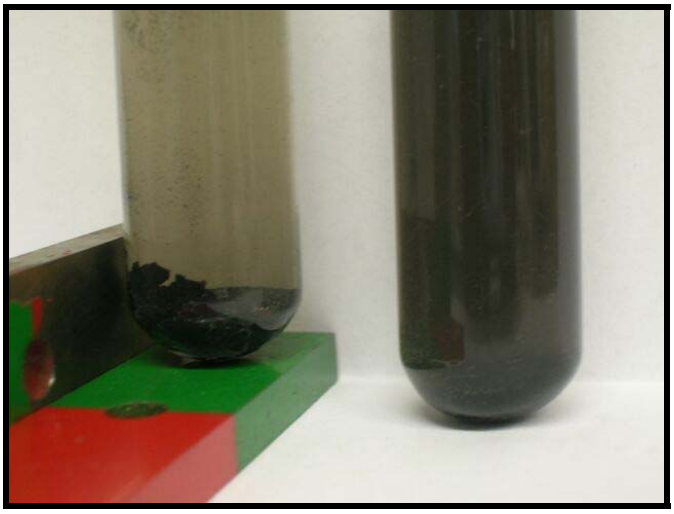

Figure 3.76 Carbon nanotubes attracted towards a magnet (left), nanotubes dispersed in the reaction mixture (right).

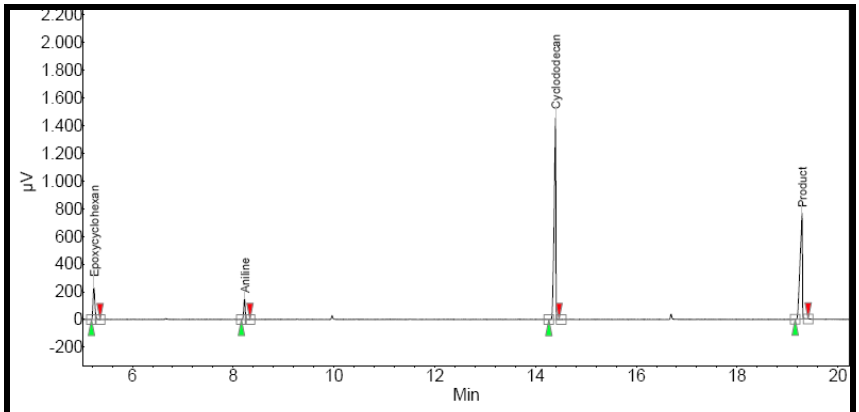

Peak results :

Index	Name	Time [Min]	Quantity [% Area]	Height [µV]	Area [µV.Min]	Area % [%]
1	Epoxycyclohexan	5,24	8,69	228,7	10,0	8,693
2	Aniline	8,23	4,31	147,8	4,9	4,311
3	Cyclododecan	14,40	50,80	1454,9	58,2	50,795
4	Product	19,29	36,20	764,6	41,5	36,200
Total			100,00	2596,1	114,7	100,000

Figure 3.77 A typical chromatogram of the reaction mixture after 4 days showing the product with 75% yield.

To ensure the catalytic activity of iron filled CNTs, reactions were also performed with pristine MWCNT, CNT-COONa, ferrofluid and without catalyst in THF using cyclododecane as an internal standard. The reaction mixture was analyzed every 24 hours by GC and the reaction was continued for 4 days when an optimal yield of the product was reached. When DCM was used as a solvent, the product yield was lower than in THF as solvent. Results observed after 4 days are summarized in Table 3.1.

Table 3.1 Epoxide ring opening reaction of Epoxycyclohexane with aniline in THF or DCM.

Entry no.	**Catalyst**	**Solvent**	**% Conversion of 40** (2 eq.)	**% Conversion of 41** (1 eq.)	**% Yield of 42**
1	CNT-COOH-filled	THF	78	80	75
2	Pristine MWCNTs	THF	0	0	0
3	CNT-COONa	THF	7	20	21
4	Ferrofluid	THF	25	70	13
5	-	THF	0	0	0
6	CNT-COOH-filled	DCM	40	65	60
7	-	DCM	<< 1	<< 1	<< 1

Table 3.2 Summary of epoxide ring opening reaction (Table 3.1, entry 1, 5, 6 and 7).

Entry no.	**Catalyst (Solvent)**	**% Yield of 42 (time interval)**			
		3 h	**24 h**	**72 h**	**96 h**
1	CNT-COOH-filled (THF)	<< 1	11	66	75
2	- (THF)	0	0	0	0
3	CNT-COOH-filled (DCM)	<< 1	9	39	60
4	- (DCM)	0	<< 1	<< 1	<< 1

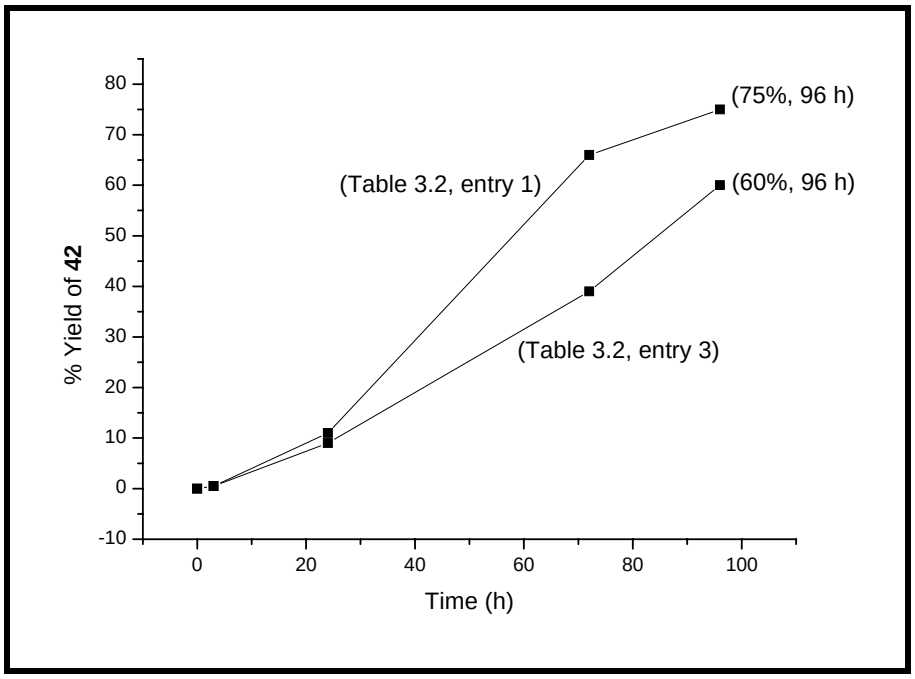

Figure 3.78 A plot against % yield of product (**42**) at different time intervals.

After the reaction was completed, recovered catalyst (CNT-COOH-filled) was once again used for the same reaction and the product was obtained with 72% yield (estimated by GC). This indicates that the catalyst can be recovered after 4 days and re-used multiple times.

3.8.2 Diels-Alder Reaction[259]

Diels-Alder reaction with a simple α,β-unsaturated ketone (4-hexen-3-one) was performed using modified CNT **18** as a catalyst (Scheme 3.14).

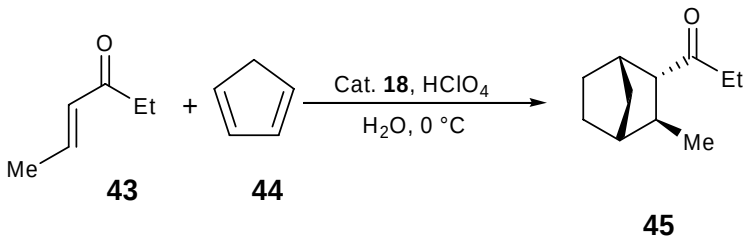

Scheme 3.14

It has been shown by the group of MacMillan that (2*S*, 5*S*)-(-)-2-*tert*-butyl-3-methyl-5-benzyl-4-imidazolidinone when used as a catalyst for the Diels-Alder reaction between 4-hexen-3-one and cyclopentadiene, gave the product with 27% yield (with less than 30% conversion in 48 hours) and 0% ee.[259] For the presented work similar reaction conditions were used while as a catalyst, modified CNTs **18** were applied. After 48 hours 17% product was obtained with 0% ee. After completion of the reaction, the recovered catalyst was used once again for the same reaction and the product was obtained with 15% yield, which indicates that the recovered catalyst can be re-used multiple times.

Although the yield obtained in the reaction was not satisfying but such reactions are a start up towards the use of carboxylated nanotubes as a Brønsted acid solid support for several catalysts (eg. MacMillan type catalysts). The catalytic activity shown by the nanotubes gives an indication that it might be possible to obtain better results when reaction conditions are optimized and nanotubes are modified with a more suitable catalyst. Modified nanotubes still serve the advantage of their easy removal from the reaction mixture by filtration or decantation.

4. Summary and Future Directions

During this work various aspects related to single and multi walled carbon nanotubes were studied. Chemical vapor deposition and solid state synthesis methods were studied for optimization. In the present work it has been shown that the [CpFe(arene)] derivative **3** yielded unique carbon structures in near quantitative yield upon pyrolysis. No other catalyst material was required in such experiments. These structures contained iron and phosphorus, which are present in the derivative **3**. It was further shown that the resulting nanostructures are highly dependent on the starting material that was employed. Such unique iron encapsulated carbon nanostructures may find a potential role in nanoscale applications. Ti and V complexes were also shown to yield TiC and VC nanospheres when subjected to pyrolysis in a sealed tube. More experiment in the same direction may reveal the pyrolysis behavior of other simple organometallic complexes.

Effect of various reported purification methods were studied on carbon nanotubes obtained from different sources and a multistep purification method was found to give better results for the purification.

Opened carbon nanotubes were filled with Ru, Pd and Fe. A simple wet chemical route was developed to fill commercially available multiwalled carbon nanotubes with magnetic Fe_3O_4 particles. Further reduction of the filled MWCNTs resulted in tubes filled with α-iron. These α-iron-filled MWCNTs may have potential applications in chemistry as catalyst support. Also they might be found useful for drug delivery and other biomedical applications.[218-220]

A simple route was developed to solubilize single or multi walled carbon nanotubes by treating them with a urea solution. Solubilization, precipitation and closing and opening of the ends of nanotube based on hydrogen bonding with urea molecules was shown to be pH dependent.

Fe filled magnetic CNTs and unfilled nanotubes were modified by using various functionalization methods for using them as a catalyst support in a variety of chemical reactions. Purified carbon nanotubes having carboxy groups were shown to be an effective catalyst for epoxide ring opening reactions. Also the catalytic activity of COOH containing CNTs **18** was studied for Diels-Alder reaction by attaching MacMillan type catalysts using a Brønsted acid/base reaction.

5. Experimental Section

5.1 General Procedure

Pyrolytic combustion experiments were performed in an alumina work tube placed horizontally in a Carbolite Gmbh (CTF 18/300) furnace. Chemical reactions were carried out in open air atmosphere unless otherwise stated. When needed, an atmosphere of pure nitrogen was used by applying standard schlenk techniques.[260] Handling of Ti (**5**, **6**)[233] and V (**7**)[234] complexes was done in a glovebox where O_2 and H_2O level was maintained usually below 1 ppm. Sonication was performed using Bandelin Sonorex (RK-52) ultrasonic bath and for centrifuge purposes Hettich EBA 20 centrifuge was used.

Toluene (Na/benzophenone ketyl), benezene (Na/benzophenone ketyl), diethyl ether (Na/benzophenone ketyl), dichloromethane (calcium dihydride) and tetrahydrofuran (Na/benzophenone ketyl) were dried and distilled under nitrogen and degassed prior to use. Deionized water was obtained by Deionizer Bohropur (B-5).

5.2 Physical Measurements

General morphology and microstructures of the samples obtained was observed using electron microscopy.

SEM images were obtained on a Leo Gemini S-25 (operated at 50 kV) scanning electron microscope. Powder samples were kept on HOPG for observing them on SEM.

TEM images were observed on a Philips CM200 FEG (operated at 120 kV) and Philips CM 400 (operated at 200 kV) transmission electron microscope equipped with an energy-dispersive x-ray spectrometer (EDS). Samples for TEM were prepared by dispersing the nanotubes in 2-propanol and then placing them onto a copper grid coated with a holey carbon film.

The XRD pattern of the composites were collected on a Röntgen Seifert (type ISO-Debyeflex 2002) diffractometer operated at 35 kV and 35 mA with Cu-K_α radiation.

Thermo gravimetric measurements (TGA) were performed on HIRES-2950.

FTIR spectra of derivatized CNTs were obtained on a Bruker Vektor 22 spectrometer in the range of 400 to 4000 cm^{-1} using a KBr pallet.

GC analyses were performed on a Varian 3900 GC instrument.

Raman spectra were recorded on Dilor LabRam Raman spectrometer. A red laser or green laser was used as an excitation source. Samples were taken in powder form on a glass plate for the observation.

5.3 Materials Used

All chemicals used in the experiments were bought from Merck, Fluka, Aldrich or Lancaster and were used as received without further purification.

MWCNTs were bought form SUN Nanotech Co Ltd, China (produced by CVD method), Material and Electrochemical Research (MER) Corporation, Tucson, Arizona, USA (produced by arc discharge method), SES Research, Houston, Texas, USA (produced by CVD method), and Cheap Tubes Inc., Brattleboro, Vermont, USA (produced by CVD method and SWCNTs were purchased from Carbon Solutions Inc., Riverside, California, USA (produced by arc discharge method).

5.4 Catalyst Preparation

Synthesis of Carbon nanotubes were performed using five different catalysts, Ni-Mo/MgO, Fe-Mo/MgO, Co-Mo/Mgo, Fe-Mo/Al_2O_3 and Co-Mo/Al_2O_3. These catalysts were prepared using two different methods – combustion method as used by Li *et al*.[261] or

by simply mixing metal salts in deionized water as reported by C. J. Lee *et al*.[222] Both procedures are summarized below.

5.4.1 General Procedure – Combustion Method

The Ni-Mo/MgO catalyst was prepared by a combustion method as used by Y. Li *et al*.[261] Typical amounts of $Mg(NO_3)_2{\cdot}6H_2O$, $(NH_3)_6Mo_7O_{24}{\cdot}4H_2O$ and $Ni(NO_3)_2{\cdot}6H_2O$ were dissolved in polyethylene glycol 200 (PEG200, a liquid with molecular weight of 200). Amounts of salts were chosen to yield molar ratios Mg/Mo/Ni/PEG200 = 1.0/1.2/0.1/1.0. After mixing them well, the obtained solution was placed in a furnace heated at 650 °C. The material immediately ignited and the fire lasted for about 5 minutes. The material was kept at 650 °C for an additional 5 minutes. Faintly green, foamy material obtained was then ground to fine powders. Powdered material was used as a catalyst for the CVD growth of carbon nanotubes.

5.4.2 General Procedure – Mixing Metal Salts in Water

For making other bimetallic catalysts the same procedure as used by Lee *et al*.[222] was followed. In one experiment a mixture of metal salt $Fe(NO_3)_3{\cdot}9H_2O$ (99.99%, Aldrich) and Mo solution (Adlrich, ICP/DCP standard solution, 9.8 mg/mL of Mo in H_2O) was dissolved in deionized water for 1 hour. The mixture was then introduced to the suspension of MgO powder and deionized water and was further sonicated for an hour. The weight ratio was maintained at Fe:Mo:MgO = 1:0.1:11 to fabricate Fe-Mo bimetallic catalyst on support material MgO. So formed material was then dried under vacuum. Dried material was baked at 150 °C for 15 hours in vaccum and then ground in mortar to break the chunks in powder.

A similar procedure was used for making other bimetallic catalyst. Metal salts $Ni(NO_3)_2{\cdot}6H_2O$ and $Co(NO_3)_2{\cdot}6H_2O$ were used in place of $Fe(NO_3)_3{\cdot}9H_2O$. In case of Al_2O_3 supported catylsts, Al_2O_3 powder was used in place of MgO powder.

5.5 Synthesis of Carbon Nanotubes

5.5.1 CVD synthesis of Carbon Nanotubes

Carbon nanotubes were synthesized using catalysts mentioned in the previous section. C_2H_2 or CH_4 were used as carbon feedstock. For the synthesis the procedure similar to the one described by Li *et al.*[261] or by Lee *et al.* was used.[262]

In a typical experiment for the synthesis of MWCNTs using Ni-Mo/MgO catalyst, approximately 60 mg of the catalyst was sprayed uniformly into an alumina boat. The boat was then placed at the center into a horizontal tube of the furnace. The material was then heated up to 1000 °C at a rate of 25 °C per minute under an Ar atmosphere. A mixture of CH_4/H_2 (900/100, v/v) was then introduced into the alumina tube at a flow rate of 1000 mL/min. and the flow of gases was maintained at 1000 °C for 30 and 60 minutes respectively. The furnace was then allowed to cool to room temperature under an Ar atmosphere. As prepared samples were then collected and analyzed without further purification. The same procedure was applied for the synthesis with other catalysts.

In other experiments, where C_2H_2 was used as a carbon feed stock, experimental conditions similar to the one reported by Lee *et al.*[262] were applied. Approximately 60 mg of the catalyst (Fe-Mo/Al_2O_3) was sprayed uniformly into an alumina boat. The boat was then placed at the center into a horizontal tube of the furnace. The material was then heated up to 950 °C at a rate of 25 °C per minute under an inert atmosphere of Ar. A mixture of Ar/ C_2H_2 (500/70, v/v) was then introduced into the alumina tube at a flow rate of 570 mL/min. and the flow of gases was maintained at 950 °C for 10 and 30 minutes respectively. The furnace was then allowed to cool to room temperature under an Ar atmosphere. As prepared samples were then collected and analyzed without further purification. The same procedure was applied for the synthesis with other catalysts.

5.5.2 Solid State Synthesis of Carbon Nanotubes

Co filled MWCNTs were prepared as described by K. P. C. Vollhardt *et al*.[109] through the pyrolysis of a cobalt complex **2**[111] at 700 °C in a sealed quartz tube. Co-complex **2** was prepared by mixing 1 gm of dicobaltcarbonyl with 0.83 gm of diphenylacetylene (**1**) in hexane.[111] The mixture was then stirred overnight. A dark reddish solid was obtained after flash column chromatography.

50 mg of so obtained Co-complex **2** was then sealed in a quartz tube under high vacuum. The sealed quartz tube was then kept in a horizontal tube furnace. Temperature of the furnace was raised to 700 °C at a rate of 10 °C per minute. Furnace temperature was maintained at 700 °C for 2 hours. It was then allowed to cool to room temperature. The obtained carbon soot was stirred overnight in conc. HCl (aq.) to wash off metal particles remained outside. The material was then washed several times with deionized water until the filtrate had a neutral pH. The sample was then dried in an oven at 60 °C overnight. Dried samples were then used for the analysis by TEM (see Fig. 3.3, pg. 66 and Fig. 3.4, pg. 67).

5.5.3 Solid State Synthesis of Carbon Nanocapsules

For the synthesis of carbon nanocapsules ferrocene derivatives were prepared and used as a carbon precursor for the pyrolysis experiments.

5.5.3.1 Synthesis of Ferrocene Derivative **3**[229]

Ferrocene derivative **3**[229] was prepared according to Scheme 5.1 (see next page).

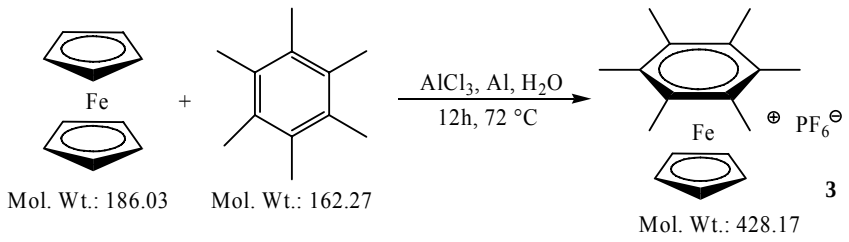

Scheme 5.1

In a typical experiment ferrocene (2.80 gm, 15 mmol), hexamethyl benzene (3.25 gm, 20 mmol), aluminium chloride (8 gm, 60 mmol), aluminium powder (0.4 gm, 15 mmol) and water (0.27 mL, 15 mmol) were mixed under a nitrogen atmosphere and heated for 12 hours at 72 °C. After cooling to ambient temperature, ice water (250 mL) was added to the mixture which was then sonicated for 5 minutes. Ammonia was added until pH = 9 and the precipitated aluminium hydroxide was filtered off and washed successively with water. Washing and filtrate were combined and hexafluoro phosphoric acid (2.75 mL, 11 mmol) was added dropwise. The precipitate was filtered off, washed with water and dried. The solid was extracted with dichloromethane. The addition of excess diethyl ether caused the crude product to precipitate. The obtained product was then dried, washed with pentane and dried again under high vacuum. After recrytallization in acetone:diethyl ether (1:1) a pale yellow solid was obtained (620 mg, 10%).

^{1}H-NMR (200 MHz, acetone-d_6) δ : 2.59 (s, 18H, $6CH_3$), 4.78 (s, 5H, C_5H_5) ppm.
Anal Calcd. for $C_{17}H_{23}F_6FeP$: C, 49.69; H, 5.41. Found: C, 47.88; H, 5.46.

Spectral data were consistent with literature values.[229]

5.5.3.2 Synthesis of Ferrocene Derivative **4**[230]

Ferrocene derivative **4**[230] was prepared according to Scheme 5.2 (see next page).

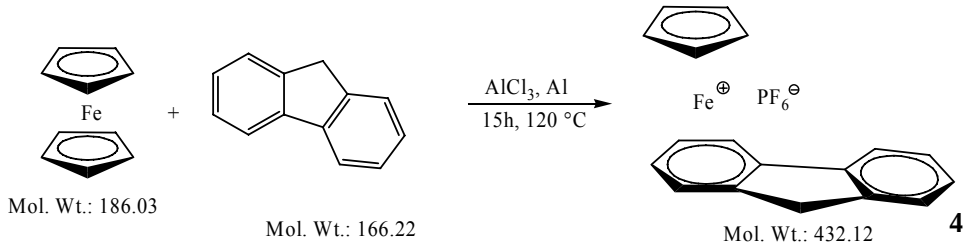

Scheme 5.2

In a typical experiment ferrocene (2 gm, 10.8 mmol), fluorene (0.36 gm, 2.2 mmol), aluminium chloride (1.4 gm, 10.5 mmol) and aluminium powder (0.06 gm, 2.2 mmol) were mixed under a nitrogen atmosphere and heated for 15 hours at 120 °C. After cooling to ambient temperature, ice water (250 mL) was added to the mixture which was then sonicated for 5 minutes. Ammonia was added until pH = 9 and the precipitated aluminium hydroxide was filtered off and washed successively with water. Washing and filtrate were combined and hexafluoro phosphoric acid (0.55 mL, 2.2 mmol) was added dropwise. The precipitate was filtered off, washed with water, dried, washed again with pentane and then dried under high vacuum. After recrystallization in acetone:diethyl ether 1.1 a brown solid was obtained (312 mg, 32.8%).

Anal. Calcd. for $C_{18}H_{15}F_6FeP$: C, 50.03; H,3.50. Found: C, 49.23; H, 3.54.

Spectral data was consistent with literature values.[230]

5.5.3.3 Pyrolysis of Complexes **3** and **4**

Complex **3** or **4** was sealed under vacuum in a quartz tube while keeping the lower part of the tube in liquid nitrogen to prevent decomposition. The sealed tube was placed at the center into a horizontal tube of the furnace. The temperature was then raised up to 700 °C and 900 °C in two different experiments at a rate of 25 °C per minute and maintained for 2 hours before cooling down to room temperature. The isolated crude black soot was then stirred overnight in conc. HCl and then washed several times with deionized water until

the filtrate had a neutral pH. The sample was then dried overnight in an oven at 60 °C. Dried samples were dispersed in isopropanol and a drop of the dispersion was placed on a holey carbon coated copper grid for analyzing the morphology of the sample by TEM. Dried samples were further annealed in H_2/Ar atmosphere at 1100 ºC for 12 hours and analyzed again by TEM (see Fig. 3.5; pg. 69, Fig. 3.6, pg. 70 and Fig. 3.7, pg 71).

5.5.4 Solid State Synthesis of TiC and VC Carbon Nanospheres

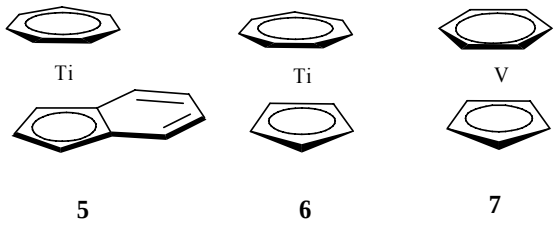

Figure 5.1

50 mg of each complex (**5**, **6** and **7**) was sealed in a quartz tube as described before. Samples were then heated in a horizontal tube furnace at 700 ºC and 900 ºC for 2 hours. These samples were further annealed in a H_2/Ar atmosphere at 1100 ºC for 2 hours. Morphology of the samples before and after annealing was analyzed by TEM (see Fig.3.12, pg. 75; Fig. 3.13, pg. 76 and Fig. 3.14, pg. 77). Raman spectra and XRD of powder samples were also taken (see Fig. 3.15, pg.78; Fig. 3.16, pg. 79 and Fig. 3.17, pg.80).

5.6 Purification Methods

Several oxidative purification methods were investigated for the purification of crude nanotubes and for opening their ends at the same time.

5.6.1 Acid Treatment

Acid treatment is the most common method for the removal of metal particles and other impurities from the crude CNT sample. In a typical experiment 100 mg of the CNT sample was dispersed in 200 mL of 65% HNO_3. The dispersion was refluxed in a 250 mL round bottomed flask fitted with a reflux condenser for 48 hours. After cooling down the dispersion to room temperature 2 liter of deionized water was added and the solid was filtered through a G4 glass filter (pore size 10-16 mm). The solid was then washed several times with deionized water until the filtrate had a neutral pH. The filtered solid was then dried in an oven at 60 °C for 20 hours prior to further use. The dried sample was used for TEM and TGA analysis and for further experiments (see Fig. 3.19, pg. 82 and Fig. 3.20, 3.21 on pg. 83).

5.6.2 Acidic $KMnO_4$ Solution

Purification of crude CNT products by a strong oxidant, potassium permanganate in acidic solution, has been suggested and described by Hiura *et al.*[122] For such purification, 250 mg of crude CNT soot (CNT-M) was dispersed in 50 mL of 1 N sulfuric acid. The dispersion was placed in a two necked round bottomed flask fitted with a reflux condenser. 4.95 gm (1.5 molar excess in terms of atomic carbon content) of $KMnO_4$ was separately dissolved in 50 mL of 1 N sulfuric acid and placed in a dropping funnel fitted to the side neck of the flask. The dispersion was subsequently heated to 150 °C in an oil bath with vigorous stirring. $KMnO_4$ solution was then added drop by drop through the funnel in 5 hours. The mixture was then refluxed for additional 5 hours before cooling to room temperature. The solid obtained by filtering the mixture through a G4 glass filter (pore size 10-16 mm) was washed with deionized water and then with conc. HCl to remove MnO_2 (reduced from $KMnO_4$) until all the MnO_2 was washed away. Subsequently the solid was washed several times with deionized water before drying under vacuum for several hours. The dried sample (170 mg) was used for TEM analysis and for further experiments (see Fig. 3.22, pg. 84).

5.6.3 Sulfidative Purification

In a sulfidative purification method as reported by Park *et al.*,[242] a mixture of CNT sample (50 mg, CNT-M) and elemental sulfur (133 mg, equi molar amount according to atomic carbon content in a crude CNT sample) was placed in an alumina crucible and heated to 300 °C in an oven at a rate of 20 °C per minute under vacuum. The temperature was maintained at 300 °C for 30 minutes before cooling it down to room temperature. Carbonaceous impurities present in the nanotube sample were removed by the following sulfidation reaction:

$$C + S \rightarrow CS_2 \quad \text{(at 300 °C)}$$

The material obtained (43 mg) was used for TEM observations (see Fig. 3.23a, pg. 85).

5.6.4 Oxidation in Air

A simple oxidation of crude CNT soot was performed. 50 mg of CNT sample (CNT-M) was placed on an alumina boat and heated in a furnace to 500 °C at a rate of 25 °C per minute in air. The material was subsequently cooled down to room temperature and used as obtained (36 mg) for further analyses (see Fig. 3.23b, pg. 85).

5.6.5 Multi-Step Purification

A combination of oxidative purification by acid and subsequent reduction by H_2 was used for such purification.[263] 100 mg of crude CNT sample (CNT-S or CNT-CS) was first refluxed with 200 mL of conc. HCl for 18 hours. The solid was then filtered and washed several times with deionized water. An oven dried sample was then placed in a furnace on an alumina boat and heated to 800 °C at a rate of 25 °C per minute under H_2 for 12 hours. After washing the sample with conc. HCl and deionized water it was further dried in an oven and the obtained sample was then reduced under H_2 at 1200 °C for 5 hours. After cooling down the furnace to room temperature, obtained sample was washed with

conc. HCl followed by repeated washing with deionized water and finally with EtOH and then dried under vacuum at 60 °C. The dried samples were used for TEM observations and for further experiments (see Fig. 3.24, pg. 86).

5.7 Oxidative Cutting and Shortening of Carbon Nanotubes

5.7.1 Oxidative Cutting

For shortening of CNTs, using the method as described by Smalley *et al.*,[243] 100 mg of purified CNTs sample (CNT-CS) was dispersed in 100 mL of freshly prepared piranha solution (4:1, v/v, 96% H_2SO_4/30% H_2O_2) maintained at 70 °C. The mixture was then stirred for 7-9 hours maintaining the temperature of the reaction at 70 °C. The reaction proceeded with the evolution of gases. After the completion, the reaction was quenched with 2 L of deionized water and the solid was filtered and dried in an oven at 60 °C for 15 hours. The dried sample was then reduced under H_2 at 500 °C for 1 hour. The obtained sample was used for TEM analyses and further experiments (see Fig. 3.25, pg. 87).

5.7.2 Ball Milling[244, 245]

Purified CNT samples (CNT-M) were subjected to ball milling for different time durations (15, 30 and 60 minutes) and analyzed by TEM as obtained (see Fig. 3.26, pg. 88).

5.8 Filling of Carbon Nanotubes

5.8.1 Filling of Carbon Nanotubes with Pd and Ru

For filling CNTs (CNT-M or CNT-CS) with Ru or Pd, 50 mg of purified nanotube samples were mixed with 15 mg of $PdCl_2$ or $RuCl_3$ and dispersed in 1 mL of deionized water. The mixture was sonicated on an ultrasonic bath for 30 minutes and left with stirring for 20 hours. The mixture was then filtered and the solid was washed several

times with deionized water before drying in an oven at 60 °C for 12 hours. Samples obtained were investigated for the level of filling with TEM (see Fig.3.27, pg. 89; Fig. 3.28, pg. 90 and Fig. 3.29, pg. 91).

5.8.2 Filling of Carbon Nanotubes with Fe

5.8.2.1 Using Iron Salts

Iron salts $Fe(NO_3)_2$ and $FeCl_3$ were used for filling nanotubes. A purified sample of MWCNTs (50 mg, CNT-S) was mixed with a saturated salt solution (2 mL, in water) and sonicated for 20 minutes. Subsequently the mixture was left to stir for 20 hours and then dried in an oven at 80 °C for 12 hours. A dry sample was then washed several times with deionized water to remove excess iron salts followed by washing with ethanol. Washed samples were further dried in vacuum for several hours. After drying the sample, it was reduced under a stream of hydrogen at 600 °C for 2 hours. The obtained samples were characterized with TEM for the level of filling (see Fig.3.30, pg. 93 and Fig. 3.31, pg. 94).

5.8.2.2 Using Ferrofluid

As a source of iron, commercially available organic solvent based and water based ferrofluid (EMG 911 and EMG 508 respectively, Ferrotec Corporation) were used. Purified and opened MWCNTs were purchased from SES Research (TX, USA) (formed by arc discharge, with a diameter ranges from 2 to 20 nm) and used as received. Crude MWCNTs were purchased from Sun Nano (China) (formed by CVD process, with a diameter ranges from 20 to 70 nm) and were purified by acidic $KMnO_4$ solution prior to use. In a typical experiment 50 mg of purified and opened MWCNTs sample was kept in a 25 mL round bottomed flask and made wet by adding a few drops of ferrofluid (EMG 911 or EMG 508). The mixture was then sonicated for 30 minutes on an ultrasonic bath and then left for 20 hours. Samples were then washed thoroughly with acetone and further with toluene (in case of EMG 911) or with deionized water and ethanol (in case of

EMG 508). Washed samples were dried in an oven at 60 °C for 12 hours. Dry samples were then reduced under a stream of H_2/Ar (100/500 ccm) at 645 °C for 20 hours. The microstructures and composition of the samples obtained before and after reduction were analyzed with TEM and EDX (see Fig. 3.32, pg. 95; Fig. 3.33. 3.34 on pg. 96; Fig. 3.35, pg. 97). To analyze the state of iron present in the sample, XRD patterns of the composites were also recorded (see Fig. 3.36, pg. 103).

5.9 Closing the Open Ends of Carbon Nanotubes

In one experiment 25 mg of iron filled MWCNTs (CNT-S) were suspended in 2 mL of propan-1,3-diol for 20 hours. Samples were then carefully washed with acetone to remove excess alcohol and dried under vacuum. In another experiment polyethylene glycol (PEG) was used in place of propane-1,3-diol and samples were washed with acetone, diethyl ether and ethanol successively prior to drying under vacuum. Microstructures of the samples obtained after drying, were observed with TEM (see Fig.3.42, pg. 105 and Fig. 3.43, pg. 106). In another attempt of closing 50 mg of iron filled CNTs (CNT-S) were heated to 900 °C in a horizontal tube furnace on a quartz boat. Subsequently a stream of benzene vapour, Ar and H_2 was passed for 30 minutes. CNTs were then brought to room temperature in an Ar atmosphere.

5.10 Treating Carbon nanotubes with Urea Solution

Carbon nanotubes used for this experiment were purified using the method described in section 5.6.5. Nanotube samples (CNT-S, CNT-CT and CNT-CS) were further oxidized by refluxing them in 65% HNO_3 solution for 48 hours (CNT-S, CNT-CT) or for 24 hours (CNT-CS). 100 mg portions of oxidized nanotube sample were dispersed in 20 mL of urea solutions in deionized water with 6 different concentrations 4 gm, 2 gm, 1 gm, 0.5 gm, 0.25 and 0.10 gm each in 20 mL deionized water (approximately 3 M, 1.5 M, 0.75 M, 0.375 M, 0.1875 M and 0.075 M respectively). Mixtures were sonicated for 10 minutes and then left to stir using a magnetic stirrer for 48 hours. Each solution was then filtered on a whatman filter paper. The filtrate was collected and a drop of it was placed

on a copper grid coated with holey carbon and the morphology was observed on TEM. The solid left on the filter paper was washed 3 times with 40 mL of deionized water and washings were collected separately and used directly for preparing the samples on carbon coated copper grid for TEM observations. 3 mL portions of the first filtrate of each were collected in 2 different test tubes and 2 mL of saturated Na_2O_3 (aq.) solution or 2 mL of 3 M HCl solution was added to each sample. A clear precipitation of black solid was observed. The dispersion was centrifuged and washed with deionized water. Centrifugation and washing with water was repeated 5 times and finally obtained samples were dried in an oven at 60 °C for 12 hours before dispersing them in isopropenol for observation on TEM (see Fig. 3.45, 3.46 on pg. 109; Fig. 3.49, pg. 113, Fig. 3.50, pg. 114, Fig. 3.51, pg. 115 and Fig. 3.52, pg. 116).

The amount of CNTs dissolved in the solution was calculated by making saturated solution of CNTs. An excess amount of CNTs (300 mg of CNT-S, CNT-CT and CNT-CS) was added to 3 mL of 0.075 molar solution of urea. Mixtures were sonicated for 10 minutes and then left with stirring using a magnetic stirrer for 48 hours. Dispersions were then filtered through a whatman filter paper. Nanotubes were precipitated from 1 mL of each filtrate by adding dil. HCl and precipitates were washed thoroughly with deionized water and then dried in an oven at 60 °C for 12 hours before measuring the exact mass of CNTs dissolved per mL in a urea solution (CNT-S: 11 mg/mL, CNT-CT-2.6 mg/mL and CNT-CS: 3.8 mg/mL).

5.11 Functionalization Reactions

5.11.1 Acylation Reaction

A 100 mg pre-purified and oxidized CNT sample **8**, **9** (CNT-CS, CNT-M) was placed in a 50 mL two necked round bottomed flask fitted with a reflux condenser and kept under a nitrogen atmosphere. 20 mL of $SOCl_2$ was slowly added to the solid under nitrogen. After addition of 0.1 mL dry DMF, the mixture was refluxed for 48 hours. After cooling down the black solid was washed several times with dry THF while maintaining the whole

system under a nitrogen atmosphere. The washed solid was then dried under vacuum for several hours. IR of the sample obtained (**10**, 60 mg; **11,** 72 mg) mgwas recorded as a KBr pallet. Also TGA for acylated SWCNTs **10** and MWCNTs **11** samples was recorded (see Fig. 3.53, pg. 118 and Fig. 3.54, pg. 119).

IR of **10** (KBr) : 3440, 2918, 2285, 1731, 1420, 1221, 1095, 1058, 802, 581, 424 cm^{-1}.
IR of **11** (KBr) : 3422, 2919, 2360, 2341, 1651, 1457, 1284, 1176, 1069, 1009, 886, 860, 668, 613, 576, 454 cm^{-1}.

5.11.2 Acylation – Amidation Reaction

A 50 mg acylated sample of SWCNTs **10** or MWCNTs **11** as obtained by previous step was placed in a 25 mL two necked round bottomed flask fitted with a reflux condenser and kept under a nitrogen atmosphere. 2 mL of dry DCM was added to the solid and the mixture was sonicated for 5 minutes. Further 0.02 mL of 2-(aminomethyl) pyrrolidine was added to the dispersion and the mixture was stirred for 48 hours. The solid was then filtered and washed several times with dry DCM. Washed solid was then dried in vacuum for several hours and the obtained sample (**12**, 32 mg; **13**, 40 mg) was analyzed by IR as a KBr pallet. TGA for functionalized SWCNTs **12** and MWCNTs **13** samples was also recorded (see Fig. 3.55, pg. 120 and Fig. 3.56, 3.57 on pg. 121).

IR of **12** (KBr) : 3426, 2286, 1751, 1632, 1221, 1107, 1020, 804, 591, 429 $cm^{-1.}$
IR of **13** (KBr) : 3405, 2360, 1651, 1625, 1467, 1284, 1176, 1110, 1069, 1009, 886, 860, 613, 576, 454 cm^{-1}.

5.11.3 Brønsted Acid/Base Reaction

150 mg of pre-purified and oxidized MWCNTs (CNT-CT) filled with α-iron **14** were placed in a 25 mL round bottomed flask. 10 mL of dry THF was added to the mixture and it was sonicated for 10 minutes. 70 mg of (*S*)-1-(2-pyrrolidinylmethyl)pyrrolidine was then added to the suspension and it was refluxed for 24 hours. The solid was filtered and

washed several times with water before drying in vacuum. A similar procedure was followed with (2*S*,5*S*)-(-)-2-*tert*-butyl-3-methyl-5-benzyl-4-imidazolidinone. Dry samples **16** (100 mg) and **18** (140 mg) were analyzed by IR and TGA (see Fig. 3.58, pg. 122; Fig. 3.59, pg. 123 and Fig. 3.60, 3.61 on pg. 124).

IR of **16** (KBr) : 3428, 2983, 2919, 1611, 1557, 1260, 1104, 1021, 801, 476 cm^{-1}.
IR of **18** (KBr) : 3425, 2919, 1611, 1557, 1450, 1260, 1096, 801, 475 cm^{-1}.

To ensure the functionalization, amines **15** and **16** were treated with 1 eq. acetic acid to form their acetyl salts. IR spectra of these salts (**19**, **20**) were recorded and compared with functionalized functionalized nanotube **16** and **18** (see Fig. 3.62, pg. 125 and Fig. 3.63, pg. 126).

IR of **19** (in DCM, NaCl) : 3054, 2985, 1714, 1421, 1265, 895, 739, 705, 446 cm^{-1}.
IR of **20** (in DCM, NaCl) : 3054, 2986, 2919, 2685, 2306, 1713, 1425, 1265, 895, 744, 627 cm^{-1}.

5.11.4 Immobilization of a Chiral Ligand on Carbon Nanotube Surface

38 mg of $LiAlH_4$ was suspended in 2.5 mL of dry THF in a 100 mL round bottomed flask under nitrogen atmosphere. The solution was then cooled to 0 °C. Subsequently 50 mg of pre-purified and oxidized MWCNTs (CNT-CT) **14** dispersed in 2 mL THF was added to the stirred solution and it was brought to room temperature after 30 minutes. The mixture was stirred for 20 hours at room temperature. $LiAlH_4$ was then hydrolyzed by adding water, diethyl ether and diluted HCl. The solid was filtered off with a whatman filter paper and was washed several times with deionized water before drying in vacuum. 45 mg of the obtained nanotube sample was then mixed with 32 mg of 2-(4-chloromethylphenyl)ethyltrimethoxysilane with 20 mL of toluene and refluxed for 24 hours. The solid was then filtered and washed with toluene, MeOH, ether and hexane. The filtered solid was dried under vacuum and the obtained sample **23** (27 mg) was analyzed by IR as a KBr pallet (see Fig. 3.64, pg. 127 and 3.65, pg. 128).

IR of **23** (KBr) : 3440, 2919, 1631, 1384, 1105, 686, 423 cm^{-1}.

5.11.5 Grafting of a Radical Polymerization Initiator (V501)

Iron filled MWCNTs (CNT-CT) **14** (10 mg) were heated with 4-4′-azobis(4-cyanopentanoic acid) (V501) (10 fold by wt., excess compared to MWCNTs) in basic water at 80 °C for 20 hours and then filtered and repeatedly washed with basic water. The solid was dried under high vacuum and the obtained product **25** (9 mg) was analyzed by IR, TGA and TEM (see Fig.3.66 and Fig. 3.67 on pg. 129 and Fig. 3.68, pg. 130).

IR of **25** (KBr) : 3449, 2920, 2360, 2341, 1625, 1120, 668 cm^{-1}.

5.11.6 Reaction with Diazonium Salts

10 mg of Fe filled MWCNTs (CNT-M) was added to the diazonium salt solution of aniline **26** or toluidine **27**, followed by the addition of hypophosphorous acid (H_3PO_2, 50% w/w in water). The solution was then allowed to stand at 5 °C for 30 minutes with a gentle stirring. The solution was filtered, washed with deionized water to remove an excess of acid and finally washed with acetonitrile to remove any unreacted diazonium salt. The functionalized nanotubes were then dried in air for 12 hours. Dried samples (**30**, 7 mg; **31**, 6 mg) were analyzed by IR and TGA (see Fig. 3.69, pg. 131 and Fig. 3.70, pg. 132).

IR of **30** (KBr) : 3442, 2915, 2851, 1620, 1260, 1095, 668, 517 cm^{-1}.
IR of **31** (KBr) : 3440, 2915, 2841, 1622, 1260, 1095, 814 cm^{-1}.

5.11.7 [3+2] Reaction[179]

For a [3+2] reaction of amino acid **32** with CNTs (CNT-M, CNT-CS) a method described by Prato *et al.*[179] was used (see Scheme 5.3). 30 mg of CNTs and 100 mg of paraformaldehyde were suspended in 100 mL DMF. The mixture was heated at 130 °C

while a solution of amino acid in DMF (100 mg in 8 mL of solvent) was added in portions (4 x 2 mL every 24 hours) and the reaction was continued for 5 days. The reaction mixture was then centrifuged and the organic phase was separated from the solid. The solid was washed with DMF and DCM and dried in oven at 60 °C for 12 hours. The obtained products (**35**, 18 mg; **36,** 12 mg) were analyzed by IR and TGA (see Fig. 3.71, pg. 133 and Fig.3.72, 3.73 on pg. 134).

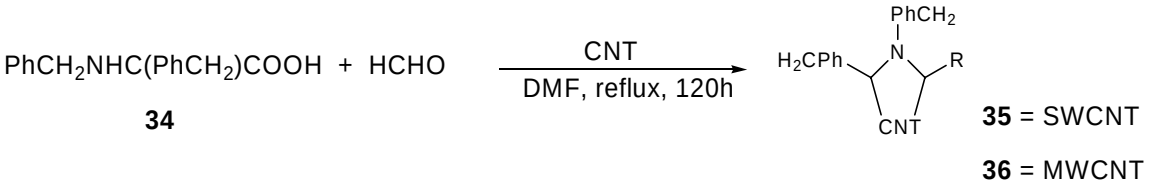

Scheme 5.3

IR of **35** (KBr) : 3445, 2918, 2300, 1635, 1095, 803 585 cm^{-1}.
IR of **36** (KBr) : 3418, 2919, 2360, 1639 cm^{-1}.

5.11.8 Arylation Reactions[257]

The arylation reactions of CNTs (CNT-SES) with iodobenzene were performed using a procedure described by Billups *et al.*[257] In a typical reaction 20 mg (1.6 mmol carbon) of CNT was kept in a flame dried 100 mL three necked flask. 60 mL NH_3 was then condensed into the flask followed by the addition of Li metal (231 mg, 33 mmol). Iodobenzene (1.3 mg, 6.4 mmol) was then added and the reaction mixture was stirred overnight. The flask was then cooled in an ice bath and 10 mL methanol was added to the reaction mixture followed by water (20 mL). After acidification (10% HCl) nanotubes were extracted with hexane and washed several times with water. The hexane layer was then filtered off and the solid was dried in vacuum at 80 °C for 12 hours. The product obtained (**39,** 12 mg) was analyzed by IR and TGA (see Fig. 3.74, pg. 135 and Fig. 3.75, pg. 136).

IR of **39** (KBr) : 3442, 2920, 2200, 1548, 1382, 1175, 480 cm^{-1}.

5.12 Application of Modified Carbon Nanotubes

Iron filled and functionalized carbon nanotubes were tested as a catalyst for a Brønsted acid catalyzed epoxide ring opening reaction and a Diels-Alder reaction.

5.12.1 Epoxide Ring Opening Reaction[258]

A prototype epoxide ring opening reaction of epoxide (cyclohexene oxide) with aniline (see Scheme 3.12, pg. 136) was chosen for studying the catalytic behavior of iron filled carboxylated CNTs (CNT-M). Reactions were performed on an automatic synthesizer (Heidolph Synthesis 1) and the conversion of aniline and the yield of product was estimated by gas chromatography. Cyclododecane was used as an internal standard for GC analysis. In a typical reaction, aniline (60 mg, 1 eq.), cyclohexene oxide (126 mg, 2 eq.), cyclododecan (108 mg, 1 eq.) and iron filled carboxylated CNTs (90 mg) were mixed in a glass tube of the synthesizer. 6 mL of solvent (THF) was added to the mixture and the synthesizer was set to wobble. The reaction was observed after every 24 hours GC. For a comparison in place of iron filled carboxylated CNTs similar amounts of just carboxylated CNTs, CNT-COONa, pristine CNT-M and ferrofluid (0.3 mL) were also used for the reaction and the yields were determined by GC (see Table 3.1 and 3.2, pg.138). Recovered catalyst (CNT-COOH-filled) was used once again for the same reaction.

5.12.2 Diels-Alder Reaction[259]

The Diels-Alder reaction was performed according to the procedure described by MacMillan *et al.*[259] The effect of modified CNTs **18** was studied in the Diels-Alder reaction between 4-hexen-3-one and cyclopentadiene (see Scheme 3.14, pg. 139). In a typical reaction 150 mg of the catalyst **18** was kept in a 10 mL round bottomed flask with a magnetic bar and 0.3 mL of water was added to the flask. The mixture was sonicated for 10 minutes and then cooled to 0 °C. To the resulting suspension was added 100 mg of α,β-unsaturated ketone (4-hexen-3-one, 1 eq.) followed by 70% perchloric acid (0.2 eq.).

After stirring for 5 minutes, freshly distilled and pre-chilled cyclopentadiene (1.5 eq.) was added dropwise. The resulting suspension was stirred at constant temperature for 48 hours. The solid was filtered off and washed several times with ethyl acetate. The organic layer was concentrated and the product **45** was obtained after purification by silica gel flash column chromatography (28 mg, 17%). The catalyst **18** used in the reaction was recovered and used once again for the same reaction.

^{1}H NMR (400 MHz, $CDCl_3$) δ : 6.26 (m, 1H), 5.93 (m, 1H), 3.16 (m, 1H), 2.49–2.46 (m, 4H), 1.94 (m, 1H), 1.48 (d, 1H), 1.46 (br, 1H), 1.19 (d, 3H), 1.05 (t, 3 H).
^{13}C NMR (400 MHz, $CDCl_3$) δ : 211.75, 138.55, 132.53, 60.66, 48.99, 46.31, 35.69, 34.75, 21.07, 7.84.

Spectral data were consistent with previously reported literature values.[264]

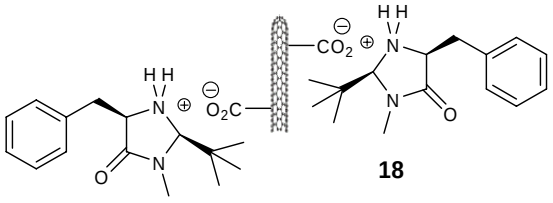

18

Figure 5.2

6. References

[1] H. W. Kroto, D. R. M. Walton, *The Fullerenes, New Horizons for the Chemistry, Physics and Astrophysics of Carbon, Cambridge University Press, New York, USA*. **1997**.

[2] M. S. Dresselhaus, G. Dresselhaus, P. C. Eklund, *Science of Fullerenes and Carbon Nanotubes, Academic, New York.* **1996**.

[3] H. W. Kroto, J. R. Heath, S. C. Obrien, R. F. Curl, R. E. Smalley, *Nature* **1985**, *318*, 162-163.

[4] W. Kratschmer, L. D. Lamb, K. Fostiropoulos, D. R. Huffman, *Nature* **1990**, *347*, 354-358.

[5] S. Iijima, *Nature* **1991**, *354*, 56-58.

[6] S. Iijima, T. Ichihashi, *Nature* **1993**, *363*, 603-605.

[7] D. S. Bethune, C. H. Kiang, M. S. Devries, G. Gorman, R. Savoy, J. Vazquez, R. Beyers, *Nature* **1993**, *363*, 605-607.

[8] A. Thess, R. Lee, P. Nikolaev, H. J. Dai, P. Petit, J. Robert, C. H. Xu, Y. H. Lee, S. G. Kim, A. G. Rinzler, D. T. Colbert, G. E. Scuseria, D. Tomanek, J. E. Fischer, R. E. Smalley, *Science* **1996**, *273*, 483-487.

[9] M. Reibold, P. Paufler, A. A. Levin, W. Kochmann, N. Patzke, D. C. Meyer, *Nature* **2006**, *444*, 286-286.

[10] O. L.V. Radushkevich and V.M. Lukyanovich, *Zurn. Fisic. Chim.* **1952**, *28*, 88-95.

[11] M. Monthioux, V. L. Kuznetsov, *Carbon* **2006**, *44*, 1621-1623.

[12] J. A. E. Gibson, *Nature* **1992**, *359*, 369-369.

[13] R. T. K. Baker, P. S. Harris, R. B. Thomas, R. J. Waite, *J. Catal.* **1973**, *30*, 86-95.

[14] R. T. K. Baker, P. S. Harris, S. Terry, *Nature* **1975**, *253*, 37-39.

[15] A. Oberlin, M. Endo, T. Koyama, *J. Cryst. Growth* **1976**, *32*, 335-349.

[16] G. G. Tibbetts, *Abstr. Pap. Am. Chem. Soc.* **1984**, *187 (Apr.)*, 79.

[17] G. G. Tibbetts, *Carbon* **1984**, *22*, 234-234.

[18] G. G. Tibbetts, *J. Cryst. Growth* **1984**, *66*, 632-638.

[19] H. G. Tennent, *"Carbon fibrils, method for producing same and compositions containing same", U.S. Patent 4663230* **May 5, 1987**.

[20] T. C. Maganas, A. L. Harrington, *"Intermittent film deposition method and system", U.S. Patent 5143745* **September 1, 1992**.

[21] Y. Ando, S. Iijima, *Jpn. J. Appl. Phys. 2* **1993**, *32*, L107-L109.

[22] C. H. Kiang, W. A. Goddard, R. Beyers, D. S. Bethune, *Carbon* **1995**, *33*, 903-914.

[23] D. S. Bethune, *Tsukuba Symposium on Carbon Nanotube, Tsukuba, Japan.* **October 3-5, 2001**, *Physica B 323 (1-4), 90-96*.

[24] W. L. Guo, Y. F. Guo, H. J. Gao, Q. S. Zheng, W. Y. Zhong, *Phys. Rev. Lett.* **2003**, *91*, 125501.

[25] Z. G. Mao, A. Garg, S. B. Sinnott, *Nanotechnology* **1999**, *10*, 273-277.

[26] E. D. Minot, Y. Yaish, V. Sazonova, J. Y. Park, M. Brink, P. L. McEuen, *Phys. Rev. Lett.* **2003**, *90*, 156401.

[27] R. Krupke, F. Hennrich, H. von Lohneysen, M. M. Kappes, *Science* **2003**, *301*, 344-347.

[28] R. Krupke, F. Hennrich, H. B. Weber, M. M. Kappes, H. von Lohneysen, *Nano Lett.* **2003**, *3*, 1019-1023.

[29] *Tests Verify Carbon Nanotube Enable Ultra High Performance Transistor, NEC Press Release* **(September 19, 2003)**.

[30] J. Q. Wei, H. W. Zhu, D. H. Wu, B. Q. Wei, *Appl. Phys. Lett.* **2004**, *84*, 4869-4871.

[31] L. X. Zheng, M. J. O'Connell, S. K. Doorn, X. Z. Liao, Y. H. Zhao, E. A. Akhadov, M. A. Hoffbauer, B. J. Roop, Q. X. Jia, R. C. Dye, D. E. Peterson, S. M. Huang, J. Liu, Y. T. Zhu, *Nat. Mater.* **2004**, *3*, 673-676.

[32] M. Freitag, J. Chen, J. Tersoff, J. C. Tsang, Q. Fu, J. Liu, P. Avouris, *Phys. Rev. Lett.* **2004**, *93*, 076803.

[33] M. F. Yu, O. Lourie, M. J. Dyer, K. Moloni, T. F. Kelly, R. S. Ruoff, *Science* **2000**, *287*, 637-640.

[34] S. Frank, P. Poncharal, Z. L. Wang, W. A. de Heer, *Science* **1998**, *280*, 1744-1746.

[35] S. Sanvito, Y. K. Kwon, D. Tomanek, C. J. Lambert, *Phys. Rev. Lett.* **2000**, *84*, 1974-1977.

[36] J. W. Che, T. Cagin, W. A. Goddard, *Nanotechnology* **2000**, *11*, 65-69.

[37] W. A. Deheer, A. Chatelain, D. Ugarte, *Science* **1995**, *270*, 1179-1180.

[38] E. Bekyarova, M. E. Itkis, N. Cabrera, B. Zhao, A. P. Yu, J. B. Gao, R. C. Haddon, *J. Am. Chem. Soc.* **2005**, *127*, 5990-5995.

[39] B. W. Smith, M. Monthioux, D. E. Luzzi, *Nature* **1998**, *396*, 323-324.

[40] X. L. Zhao, Y. Ando, Y. Liu, M. Jinno, T. Suzuki, *Phys. Rev. Lett.* **2003**, *90*, 187401-187404.

[41] S. Iijima, M. Yudasaka, R. Yamada, S. Bandow, K. Suenaga, F. Kokai, K. Takahashi, *Chem. Phys. Lett.* **1999**, *309*, 165-170.

[42] D. Ugarte, *Nature* **1992**, *359*, 707-709.

[43] R. S. Ruoff, D. C. Lorents, B. Chan, R. Malhotra, S. Subramoney, *Science* **1993**, *259*, 346-348.

[44] E. M. Brunsman, R. Sutton, E. Bortz, S. Kirkpatrick, K. Midelfort, J. Williams, P. Smith, M. E. Mchenry, S. A. Majetich, J. O. Artman, M. Degraef, S. W. Staley, *J. Appl. Phys.* **1994**, *75*, 5882-5884.

[45] X. W. Wei, G. X. Zhu, C. J. Xia, Y. Ye, *Nanotechnology* **2006**, *17*, 4307-4311.

[46] M. Schlatter, *Diamond Relat. Mater.* **2002**, *11*, 1781-1787.

[47] M. Shimada, S. Takigami, Y. Nakamura, Y. Abe, T. Iizuka, N. Makiyama, *J. Appl. Polym. Sci.* **1993**, *48*, 1121-1126.

[48] M. Bockrath, D. H. Cobden, P. L. McEuen, N. G. Chopra, A. Zettl, A. Thess, R. E. Smalley, *Science* **1997**, *275*, 1922-1925.

[49] J. W. G. Wildoer, L. C. Venema, A. G. Rinzler, R. E. Smalley, C. Dekker, *Nature* **1998**, *391*, 59-62.

[50] T. W. Odom, J. L. Huang, P. Kim, C. M. Lieber, *Nature* **1998**, *391*, 62-64.

[51] P. J. F. Harris, *Carbon nanotubes and related structures, Cambridge University Press, Cambridge, United Kingdom.* **1999**.

[52] E. Dujardin, T. W. Ebbesen, H. Hiura, K. Tanigaki, *Science* **1994**, *265*, 1850-1852.

[53] A. W. Scott, *Understading Microwaves, Wiley, New York.* **1993**.

[54] P. M. Ajayan, S. Iijima, *Nature* **1993**, *361*, 333-334.

[55] S. Amelinckx, D. Bernaerts, X. B. Zhang, G. Vantendeloo, J. Vanlanduyt, *Science* **1995**, *267*, 1334-1338.

[56] O. Zhou, R. M. Fleming, D. W. Murphy, C. H. Chen, R. C. Haddon, A. P. Ramirez, S. H. Glarum, *Science* **1994**, *263*, 1744-1747.

[57] E. Flahaut, R. Bacsa, A. Peigney, C. Laurent, *Chem. Commun.* **2003**, 1442-1443.

[58] N. Yao, V. Lordi, *J. Appl. Phys.* **1998**, *84*, 1939-1943.

[59] A. Krishnan, E. Dujardin, T. W. Ebbesen, P. N. Yianilos, M. M. J. Treacy, *Phys. Rev. B* **1998**, *58*, 14013-14019.

[60] H. Ajiki, T. Ando, *J. Phys. Soc. Jpn.* **1996**, *65*, 505-514.

[61] H. Ajiki, T. Ando, *J. Phys. Soc. Jpn.* **1993**, *62*, 1255-1266.

[62] C. Dekker, *Physics Today* **1999**, *52*, 22-28.

[63] S. Berber, Y. K. Kwon, D. Tomanek, *Phys. Rev. Lett.* **2000**, *84*, 4613-4616.

[64] P. G. Collins, P. Avouris, *Nanotubes for Electronics, Scientific American* **December 2000**, *69*.

[65] C. M. Niu, E. K. Sichel, R. Hoch, D. Moy, H. Tennent, *Appl. Phys. Lett.* **1997**, *70*, 1480-1482.

[66] J. H. Kim, K. W. Nam, S. B. Ma, K. B. Kim, *Carbon* **2006**, *44*, 1963-1968.

[67] I. H. Kim, J. H. Kim, B. W. Cho, K. B. Kim, *J. Electrochem. Soc.* **2006**, *153*, A1451-A1458.

[68] I. H. Kim, J. H. Kim, B. W. Cho, Y. H. Lee, K. B. Kim, *J. Electrochem. Soc.* **2006**, *153*, A989-A996.

[69] L. Su, F. Gao, L. Q. Mao, *Anal. Chem.* **2006**, *78*, 2651-2657.

[70] X. Murata, S. Yoshimoto, M. Kishida, D. Maeda, T. Yasuda, T. Ikuno, S. Honda, H. Okado, R. Hobara, I. Matsuda, S. Hasegawa, K. Oura, M. Katayama, *Jpn. J. Appl. Phys. 1* **2005**, *44*, 5336-5338.

[71] J. M. Singer, J. Grumer, *Proc. Combust. Inst.* **1959**, 559-569.

[72] A. A. Puretzky, D. B. Geohegan, X. Fan, S. J. Pennycook, *Appl. Phys. Lett.* **2000**, *76*, 182-184.

[73] A. A. Puretzky, D. B. Geohegan, X. Fan, S. J. Pennycook, *Appl. Phys. A* **2000**, *70*, 153-160.

[74] A. A. Puretzky, H. Schittenhelm, X. D. Fan, M. J. Lance, L. F. Allard, D. B. Geohegan, *Phys. Rev. B* **2002**, *65*, 245425.

[75] S. Iijima, *Mater. Sci. Eng., B* **1993**, *19*, 172-180.

[76] M. Endo, H. W. Kroto, *J. Phys. Chem.* **1992**, *96*, 6941-6944.

[77] A. Yasuda, N. Kawase, F. Banhart, W. Mizutani, T. Shimizu, H. Tokumoto, *J. Phys. Chem. B* **2002**, *106*, 1247-1251.

[78] A. Yasuda, N. Kawase, F. Banhart, W. Mizutani, T. Shimizu, H. Tokumoto, *J. Phys. Chem. B* **2002**, *106*, 1849-1852.

[79] A. Yasuda, W. Mizutani, T. Shimizu, H. Tokumoto, *Physica B* **2002**, *323*, 269-271.

[80] R. J. Andrews, C. F. Smith, A. J. Alexander, *Carbon* **2006**, *44*, 341-347.

[81] R. Andrews, D. Jacques, A. M. Rao, F. Derbyshire, D. Qian, X. Fan, E. C. Dickey, J. Chen, *Chem. Phys. Lett.* **1999**, *303*, 467-474.

[82] A. M. Cassell, J. A. Raymakers, J. Kong, H. J. Dai, *J. Phys. Chem. B* **1999**, *103*, 6484-6492.

[83] M. Chen, C. M. Chen, C. F. Chen, *J. Mater. Sci.* **2002**, *37*, 3561-3567.

[84] T. Guo, P. Nikolaev, A. Thess, D. T. Colbert, R. E. Smalley, *Chem. Phys. Lett.* **1995**, *243*, 49-54.

[85] W. K. Hsu, M. Terrones, J. P. Hare, H. Terrones, H. W. Kroto, D. R. M. Walton, *Chem. Phys. Lett.* **1996**, *262*, 161-166.

[86] T. W. Ebbesen, P. M. Ajayan, *Nature* **1992**, *358*, 220-222.

[87] M. Ushio, *Pure Appl. Chem.* **1988**, *60*, 809-814.

[88] http://www.iljinnanotech.co.kr.

[89] T. W. Ebbesen, *Annu. Rev. Mater. Sci.* **1994**, *24*, 235-264.

[90] M. Cadek, R. Murphy, B. McCarthy, A. Drury, B. Lahr, R. C. Barklie, M. Panhuis, J. N. Coleman, W. J. Blau, *Carbon* **2002**, *40*, 923-928.

[91] T. W. Ebbesen, H. Hiura, J. Fujita, Y. Ochiai, S. Matsui, K. Tanigaki, *Chem. Phys. Lett.* **1993**, *209*, 83-90.

[92] G. H. Taylor, J. D. Fitz Gerald, L. Pang, M. A. Wilson, *J. Cryst. Growth* **1994**, *135*, 157-164.

[93] D. D. Cheng, R. Q. Yu, Z. Y. Liu, Q. Zhang, Y. H. Wang, R. B. Huang, M. X. Zhan, L. S. Zheng, *Chem. J. Chinese U.* **1995**, *16*, 948-949.

[94] X. Zhao, M. Ohkohchi, M. Wang, S. Iijima, T. Ichihashi, Y. Ando, *Carbon* **1997**, *35*, 775-781.

[95] X. L. Zhao, M. Wang, M. Ohkohchi, Y. Ando, *Jpn. J. Appl. Phys. 1* **1996**, *35*, 4451-4456.

[96] S. B. Sinnott, R. Andrews, D. Qian, A. M. Rao, Z. Mao, E. C. Dickey, F. Derbyshire, *Chem. Phys. Lett.* **1999**, *315*, 25-30.

[97] Z. F. Ren, Z. P. Huang, J. W. Xu, J. H. Wang, P. Bush, M. P. Siegal, P. N. Provencio, *Science* **1998**, *282*, 1105-1107.

[98] Z. F. Ren, Z. P. Huang, D. Z. Wang, J. G. Wen, J. W. Xu, J. H. Wang, L. E. Calvet, J. Chen, J. F. Klemic, M. A. Reed, *Appl. Phys. Lett.* **1999**, *75*, 1086-1088.

[99] Z. P. Huang, D. Z. Wang, J. G. Wen, M. Sennett, H. Gibson, Z. F. Ren, *Appl. Phys. A* **2002**, *74*, 387-391.

[100] M. Yudasaka, R. Yamada, N. Sensui, T. Wilkins, T. Ichihashi, S. Iijima, *J. Phys. Chem. B* **1999**, *103*, 6224-6229.

[101] P. C. Eklund, B. K. Pradhan, U. J. Kim, Q. Xiong, J. E. Fischer, A. D. Friedman, B. C. Holloway, K. Jordan, M. W. Smith, *Nano Lett.* **2002**, *2*, 561-566.

[102] A. P. Bolshakov, S. A. Uglov, A. V. Saveliev, V. I. Konov, A. A. Gorbunov, W. Pompe, A. Graff, *Diamond Relat. Mater.* **2002**, *11*, 927-930.

[103] W. K. Maser, E. Munoz, A. M. Benito, M. T. Martinez, G. F. de la Fuente, Y. Maniette, E. Anglaret, J. L. Sauvajol, *Chem. Phys. Lett.* **1998**, *292*, 587-593.

[104] R. L. V. Wal, G. M. Berger, L. J. Hall, *J. Phys. Chem. B* **2002**, *106*, 3564-3567.

[105] R. L. V. Wal, T. M. Ticich, *J. Phys. Chem. B* **2001**, *105*, 10249-10256.

[106] R. L. Vander Wal, L. J. Hall, G. M. Berger, *J. Phys. Chem. B* **2002**, *106*, 13122-13132.

[107] C. J. Lee, S. C. Lyu, H. W. Kim, C. Y. Park, C. W. Yang, *Chem. Phys. Lett.* **2002**, *359*, 109-114.

[108] M. H. Ge, K. Sattler, *Appl. Phys. Lett.* **1994**, *64*, 710-711.

[109] V. S. Iyer, K. P. C. Vollhardt, R. Wilhelm, *Angew. Chem., Int. Ed.* **2003**, *42*, 4379-4383.

[110] J. L. Bahr, J. P. Yang, D. V. Kosynkin, M. J. Bronikowski, R. E. Smalley, J. M. Tour, *J. Am. Chem. Soc.* **2001**, *123*, 6536-6542.

[111] H. Pepermans, R. Willem, C. Hoogzand, *B. Soc. Chim. Belg.* **1987**, *96*, 563-574.

[112] W. K. Hsu, J. P. Hare, M. Terrones, H. W. Kroto, D. R. M. Walton, P. J. F. Harris, *Nature* **1995**, *377*, 687-687.

[113] P. M. Ajayan, T. W. Ebbesen, T. Ichihashi, S. Iijima, K. Tanigaki, H. Hiura, *Nature* **1993**, *362*, 522-525.

[114] S. C. Tsang, P. J. F. Harris, M. L. H. Green, *Nature* **1993**, *362*, 520-522.

[115] J. L. Zimmerman, R. K. Bradley, C. B. Huffman, R. H. Hauge, J. L. Margrave, *Chem. Mater.* **2000**, *12*, 1361-1366.

[116] T. W. Ebbesen, P. M. Ajayan, H. Hiura, K. Tanigaki, *Nature* **1994**, *367*, 519-519.

[117] I. D. Rosca, F. Watari, M. Uo, T. Akaska, *Carbon* **2005**, *43*, 3124-3131.

[118] L. A. Montoro, J. M. Rosolen, *Carbon* **2006**, *44*, 3293-3301.

[119] K. C. Hwang, *J. Chem. Soc., Chem. Commun.* **1995**, 173-174.

[120] A. R. Harutyunyan, B. K. Pradhan, J. P. Chang, G. G. Chen, P. C. Eklund, *J. Phys. Chem. B* **2002**, *106*, 8671-8675.

[121] O. Zhou, H. Shimoda, B. Gao, S. J. Oh, L. Fleming, G. Z. Yue, *Acc. Chem. Res.* **2002**, *35*, 1045-1053.

[122] H. Hiura, T. W. Ebbesen, K. Tanigaki, *Adv. Mater.* **1995**, *7*, 275-276.

[123] S. R. C. Vivekchand, R. Jayakanth, A. Govindaraj, C. N. R. Rao, *Small* **2005**, *1*, 920-923.

[124] S. Delpeux, K. Szostak, E. Frackowiak, F. Beguin, *Chem. Phys. Lett.* **2005**, *404*, 374-378.

[125] F. Ikazaki, S. Ohshima, K. Uchida, Y. Kuriki, H. Hayakawa, M. Yumura, K. Takahashi, K. Tojima, *Carbon* **1994**, *32*, 1539-1542.

[126] K. B. Shelimov, R. O. Esenaliev, A. G. Rinzler, C. B. Huffman, R. E. Smalley, *Chem. Phys. Lett.* **1998**, *282*, 429-434.

[127] K. L. Lu, R. M. Lago, Y. K. Chen, M. L. H. Green, P. J. F. Harris, S. C. Tsang, *Carbon* **1996**, *34*, 814-816.

[128] S. Bandow, A. M. Rao, K. A. Williams, A. Thess, R. E. Smalley, P. C. Eklund, *J. Phys. Chem. B* **1997**, *101*, 8839-8842.

[129] H. Zhang, C. H. Sun, F. Li, H. X. Li, H. M. Cheng, *J. Phys. Chem. B* **2006**, *110*, 9477-9481.

[130] H. Kajiura, S. Tsutsui, H. J. Huang, Y. Murakami, *Chem. Phys. Lett.* **2002**, *364*, 586-592.

[131] L. Thien-Nga, K. Hernadi, E. Ljubovic, S. Garaj, L. Forro, *Nano Lett.* **2002**, *2*, 1349-1352.

[132] D. Chattopadhyay, L. Galeska, F. Papadimitrakopoulos, *J. Am. Chem. Soc.* **2003**, *125*, 3370-3375.

[133] B. L. Chen, J. P. Selegue, *Anal. Chem.* **2002**, *74*, 4774-4780.

[134] G. S. Duesberg, J. Muster, V. Krstic, M. Burghard, S. Roth, *Appl. Phys. A* **1998**, *67*, 117-119.

[135] S. Niyogi, H. Hu, M. A. Hamon, P. Bhowmik, B. Zhao, S. M. Rozenzhak, J. Chen, M. E. Itkis, M. S. Meier, R. C. Haddon, *J. Am. Chem. Soc.* **2001**, *123*, 733-734.

[136] E. Farkas, M. E. Anderson, Z. H. Chen, A. G. Rinzler, *Chem. Phys. Lett.* **2002**, *363*, 111-116.

[137] M. Zheng, A. Jagota, E. D. Semke, B. A. Diner, R. S. Mclean, S. R. Lustig, R. E. Richardson, N. G. Tassi, *Nat. Mater.* **2003**, *2*, 338-342.

[138] C. S. László Forró, *Europhysics News* **2001**, *32*.

[139] H. Hiura, T. W. Ebbesen, K. Tanigaki, H. Takahashi, *Chem. Phys. Lett.* **1993**, *202*, 509-512.

[140] J. Kastner, T. Pichler, H. Kuzmany, S. Curran, W. Blau, D. N. Weldon, M. Delamesiere, S. Draper, H. Zandbergen, *Chem. Phys. Lett.* **1994**, *221*, 53-58.

[141] A. M. Rao, E. Richter, S. Bandow, B. Chase, P. C. Eklund, K. A. Williams, S. Fang, K. R. Subbaswamy, M. Menon, A. Thess, R. E. Smalley, G. Dresselhaus, M. S. Dresselhaus, *Science* **1997**, *275*, 187-191.

[142] M. S. Dresselhaus, P. C. Eklund, *Adv. Phys.* **2000**, *49*, 705-814.

[143] M. E. Itkis, D. E. Perea, R. Jung, S. Niyogi, R. C. Haddon, *J. Am. Chem. Soc.* **2005**, *127*, 3439-3448.

[144] Y. Saito, T. Yoshikawa, S. Bandow, M. Tomita, T. Hayashi, *Phys. Rev. B* **1993**, *48*, 1907-1909.

[145] M. Bretz, B. G. Demczyk, L. Q. Zhang, *J. Cryst. Growth* **1994**, *141*, 304-309.

[146] D. Reznik, C. H. Olk, D. A. Neumann, J. R. D. Copley, *Phys. Rev. B* **1995**, *52*, 116-124.

[147] C. H. Kiang, M. Endo, P. M. Ajayan, G. Dresselhaus, M. S. Dresselhaus, *Phys. Rev. Lett.* **1998**, *81*, 1869-1872.

[148] G. Hu, M. J. Cheng, D. Ma, X. H. Bao, *Chem. Mater.* **2003**, *15*, 1470-1473.

[149] J. Sloan, D. M. Wright, H. G. Woo, S. Bailey, G. Brown, A. P. E. York, K. S. Coleman, J. L. Hutchison, M. L. H. Green, *Chem. Commun.* **1999**, 699-700.

[150] R. R. Meyer, J. Sloan, R. E. Dunin-Borkowski, A. I. Kirkland, M. C. Novotny, S. R. Bailey, J. L. Hutchison, M. L. H. Green, *Science* **2000**, *289*, 1324-1326.

[151] C. G. Xu, J. Sloan, G. Brown, S. Bailey, V. C. Williams, S. Friedrichs, K. S. Coleman, E. Flahaut, J. L. Hutchison, R. E. Dunin-Borkowski, M. L. H. Green, *Chem. Commun.* **2000**, 2427-2428.

[152] J. Sloan, M. C. Novotny, S. R. Bailey, G. Brown, C. Xu, V. C. Williams, S. Friedrichs, E. Flahaut, R. L. Callender, A. P. E. York, K. S. Coleman, M. L. H. Green, R. E. Dunin-Borkowski, J. L. Hutchison, *Chem. Phys. Lett.* **2000**, *329*, 61-65.

[153] A. Govindaraj, B. C. Satishkumar, M. Nath, C. N. R. Rao, *Chem. Mater.* **2000**, *12*, 202-205.

[154] K. Hirahara, K. Suenaga, S. Bandow, H. Kato, T. Okazaki, H. Shinohara, S. Iijima, *Phys. Rev. Lett.* **2000**, *85*, 5384-5387.

[155] A. M. Zhang, J. L. Dong, Q. H. Xu, H. K. Rhee, X. L. Li, *Catal. Today* **2004**, *93-95*, 347-352.

[156] J. P. Tessonnier, L. Pesant, G. Ehret, M. J. Ledoux, C. Pham-Huu, *Appl. Catal., A* **2005**, *288*, 203-210.

[157] Z. L. Zhang, B. Li, Z. J. Shi, Z. N. Gu, Z. Q. Xue, L. M. Peng, *J. Mater. Res.* **2000**, *15*, 2658-2661.

[158] B. C. Satishkumar, A. Govindaraj, J. Mofokeng, G. N. Subbanna, C. N. R. Rao, *J. Phys. B: At. Mol. Opt. Phys.* **1996**, *29*, 4925-4934.

[159] M. Monthioux, B. W. Smith, B. Burteaux, A. Claye, J. E. Fischer, D. E. Luzzi, *Carbon* **2001**, *39*, 1251-1272.

[160] C. H. Kiang, J. S. Choi, T. T. Tran, A. D. Bacher, *J. Phys. Chem. B* **1999**, *103*, 7449-7451.

[161] X. Fan, E. C. Dickey, P. C. Eklund, K. A. Williams, L. Grigorian, R. Buczko, S. T. Pantelides, S. J. Pennycook, *Phys. Rev. Lett.* **2000**, *84*, 4621-4624.

[162] J. Sloan, J. Hammer, M. Zwiefka-Sibley, M. L. H. Green, *Chem. Commun.* **1998**, 347-348.

[163] M. Monthioux, *Carbon* **2002**, *40*, 1809-1823.

[164] C. A. Furtado, U. J. Kim, H. R. Gutierrez, L. Pan, E. C. Dickey, P. C. Eklund, *J. Am. Chem. Soc.* **2004**, *126*, 6095-6105.

[165] E. T. Mickelson, C. B. Huffman, A. G. Rinzler, R. E. Smalley, R. H. Hauge, J. L. Margrave, *Chem. Phys. Lett.* **1998**, *296*, 188-194.

[166] E. T. Mickelson, I. W. Chiang, J. L. Zimmerman, P. J. Boul, J. Lozano, J. Liu, R. E. Smalley, R. H. Hauge, J. L. Margrave, *J. Phys. Chem. B* **1999**, *103*, 4318-4322.

[167] P. J. Boul, J. Liu, E. T. Mickelson, C. B. Huffman, L. M. Ericson, I. W. Chiang, K. A. Smith, D. T. Colbert, R. H. Hauge, J. L. Margrave, R. E. Smalley, *Chem. Phys. Lett.* **1999**, *310*, 367-372.

[168] R. K. Saini, I. W. Chiang, H. Q. Peng, R. E. Smalley, W. E. Billups, R. H. Hauge, J. L. Margrave, *J. Am. Chem. Soc.* **2003**, *125*, 3617-3621.

[169] J. L. Stevens, A. Y. Huang, H. Q. Peng, L. W. Chiang, V. N. Khabashesku, J. L. Margrave, *Nano Lett.* **2003**, *3*, 331-336.

[170] L. Zhang, V. U. Kiny, H. Q. Peng, J. Zhu, R. F. M. Lobo, J. L. Margrave, V. N. Khabashesku, *Chem. Mater.* **2004**, *16*, 2055-2061.

[171] E. Unger, A. Graham, F. Kreupl, M. Liebau, W. Hoenlein, *Curr. Appl. Phys.* **2002**, *2*, 107-111.

[172] B. N. Khare, M. Meyyappan, A. M. Cassell, C. V. Nguyen, J. Han, *Nano Lett.* **2002**, *2*, 73-77.

[173] B. N. Khare, M. Meyyappan, J. Kralj, P. Wilhite, M. Sisay, H. Imanaka, J. Koehne, C. W. Baushchlicher, *Appl. Phys. Lett.* **2002**, *81*, 5237-5239.

[174] B. Khare, M. Meyyappan, M. H. Moore, P. Wilhite, H. Imanaka, B. Chen, *Nano Lett.* **2003**, *3*, 643-646.

[175] J. Chen, M. A. Hamon, H. Hu, Y. S. Chen, A. M. Rao, P. C. Eklund, R. C. Haddon, *Science* **1998**, *282*, 95-98.

[176] K. Kamaras, M. E. Itkis, H. Hu, B. Zhao, R. C. Haddon, *Science* **2003**, *301*, 1501-1501.

[177] M. Holzinger, O. Vostrowsky, A. Hirsch, F. Hennrich, M. Kappes, R. Weiss, F. Jellen, *Angew. Chem., Int. Ed.* **2001**, *40*, 4002-4008.

[178] D. Tasis, N. Tagmatarchis, A. Bianco, M. Prato, *Chem. Rev.* **2006**, *106*, 1105-1136.

[179] V. Georgakilas, K. Kordatos, M. Prato, D. M. Guldi, M. Holzinger, A. Hirsch, *J. Am. Chem. Soc.* **2002**, *124*, 760-761.

[180] N. Tagmatarchis, M. Prato, *J. Mater. Chem.* **2004**, *14*, 437-439.

[181] K. S. Coleman, S. R. Bailey, S. Fogden, M. L. H. Green, *J. Am. Chem. Soc.* **2003**, *125*, 8722-8723.

[182] J. L. Delgado, P. de la Cruz, F. Langa, A. Urbina, J. Casado, J. T. L. Navarrete, *Chem. Commun.* **2004**, 1734-1735.

[183] H. Q. Peng, L. B. Alemany, J. L. Margrave, V. N. Khabashesku, *J. Am. Chem. Soc.* **2003**, *125*, 15174-15182.

[184] N. Tagmatarchis, V. Georgakilas, M. Prato, H. Shinohara, *Chem. Commun.* **2002**, 2010-2011.

[185] J. B. Cui, M. Burghard, K. Kern, *Nano Lett.* **2003**, *3*, 613-615.

[186] D. B. Mawhinney, V. Naumenko, A. Kuznetsova, J. T. Yates, J. Liu, R. E. Smalley, *J. Am. Chem. Soc.* **2000**, *122*, 2383-2384.

[187] S. Banerjee, S. S. Wong, *Nano Lett.* **2004**, *4*, 1445-1450.

[188] W. Wu, S. Zhang, Y. Li, J. X. Li, L. Q. Liu, Y. J. Qin, Z. X. Guo, L. M. Dai, C. Ye, D. B. Zhu, *Macromolecules* **2003**, *36*, 6286-6288.

[189] R. Blake, Y. K. Gun'ko, J. Coleman, M. Cadek, A. Fonseca, J. B. Nagy, W. J. Blau, *J. Am. Chem. Soc.* **2004**, *126*, 10226-10227.

[190] J. N. Coleman, M. Cadek, R. Blake, V. Nicolosi, K. P. Ryan, C. Belton, A. Fonseca, J. B. Nagy, Y. K. Gun'ko, W. J. Blau, *Adv. Funct. Mater.* **2004**, *14*, 791-798.

[191] S. S. Wong, E. Joselevich, A. T. Woolley, C. L. Cheung, C. M. Lieber, *Nature* **1998**, *394*, 52-55.

[192] M. A. Hamon, J. Chen, H. Hu, Y. S. Chen, M. E. Itkis, A. M. Rao, P. C. Eklund, R. C. Haddon, *Adv. Mater.* **1999**, *11*, 834-840.

[193] J. Chen, A. M. Rao, S. Lyuksyutov, M. E. Itkis, M. A. Hamon, H. Hu, R. W. Cohn, P. C. Eklund, D. T. Colbert, R. E. Smalley, R. C. Haddon, *J. Phys. Chem. B* **2001**, *105*, 2525-2528.

[194] M. E. Kose, B. A. Harruff, Y. Lin, L. M. Veca, F. S. Lu, Y. P. Sun, *J. Phys. Chem. B* **2006**, *110*, 14032-14034.

[195] Y. P. Sun, K. F. Fu, Y. Lin, W. J. Huang, *Acc. Chem. Res.* **2002**, *35*, 1096-1104.

[196] P. M. Ajayan, O. Stephan, C. Colliex, D. Trauth, *Science* **1994**, *265*, 1212-1214.

[197] G. G. Tibbetts, J. J. McHugh, *J. Mater. Res.* **1999**, *14*, 2871-2880.

[198] B. Z. Tang, H. Y. Xu, *Macromolecules* **1999**, *32*, 2569-2576.

[199] W. Ding, A. Eitan, F. T. Fisher, X. Chen, D. A. Dikin, R. Andrews, L. C. Brinson, L. S. Schadler, R. S. Ruoff, *Nano Lett.* **2003**, *3*, 1593-1597.

[200] M. J. O'Connell, P. Boul, L. M. Ericson, C. Huffman, Y. H. Wang, E. Haroz, C. Kuper, J. Tour, K. D. Ausman, R. E. Smalley, *Chem. Phys. Lett.* **2001**, *342*, 265-271.

[201] J. J. Davis, M. L. H. Green, H. A. O. Hill, Y. C. Leung, P. J. Sadler, J. Sloan, A. V. Xavier, S. C. Tsang, *Inorg. Chim. Acta.* **1998**, *272*, 261-266.

[202] T. Ito, L. Sun, R. M. Crooks, *Chem. Commun.* **2003**, 1482-1483.

[203] A. G. Rinzler, J. H. Hafner, P. Nikolaev, L. Lou, S. G. Kim, D. Tomanek, P. Nordlander, D. T. Colbert, R. E. Smalley, *Science* **1995**, *269*, 1550-1553.

[204] B. Q. Wei, R. Vajtai, P. M. Ajayan, *Appl. Phys. Lett.* **2001**, *79*, 1172-1174.

[205] N. S. Lee, D. S. Chung, I. T. Han, J. H. Kang, Y. S. Choi, H. Y. Kim, S. H. Park, Y. W. Jin, W. K. Yi, M. J. Yun, J. E. Jung, C. J. Lee, J. H. You, S. H. Jo, C. G. Lee, J. M. Kim, *Diamond Relat. Mater.* **2001**, *10*, 265-270.

[206] Y. Saito, S. Uemura, *Carbon* **2000**, *38*, 169-182.

[207] R. Rosen, W. Simendinger, C. Debbault, H. Shimoda, L. Fleming, B. Stoner, O. Zhou, *Appl. Phys. Lett.* **2000**, *76*, 1668-1670.

[208] H. Sugie, M. Tanemura, V. Filip, K. Iwata, K. Takahashi, F. Okuyama, *Appl. Phys. Lett.* **2001**, *78*, 2578-2580.

[209] J. M. Bonard, J. P. Salvetat, T. Stockli, L. Forro, A. Chatelain, *Appl. Phys. A* **1999**, *69*, 245-254.

[210] M. J. Biercuk, M. C. Llaguno, M. Radosavljevic, J. K. Hyun, A. T. Johnson, J. E. Fischer, *Appl. Phys. Lett.* **2002**, *80*, 2767-2769.

[211] D. Qian, E. C. Dickey, R. Andrews, T. Rantell, *Appl. Phys. Lett.* **2000**, *76*, 2868-2870.

[212] B. Gao, C. Bower, J. D. Lorentzen, L. Fleming, A. Kleinhammes, X. P. Tang, L. E. McNeil, Y. Wu, O. Zhou, *Chem. Phys. Lett.* **2000**, *327*, 69-75.

[213] R. H. Baughman, C. X. Cui, A. A. Zakhidov, Z. Iqbal, J. N. Barisci, G. M. Spinks, G. G. Wallace, A. Mazzoldi, D. De Rossi, A. G. Rinzler, O. Jaschinski, S. Roth, M. Kertesz, *Science* **1999**, *284*, 1340-1344.

[214] A. Bachtold, P. Hadley, T. Nakanishi, C. Dekker, *Science* **2001**, *294*, 1317-1320.

[215] R. Martel, T. Schmidt, H. R. Shea, T. Hertel, P. Avouris, *Appl. Phys. Lett.* **1998**, *73*, 2447-2449.

[216] D. A. Walters, M. J. Casavant, X. C. Qin, C. B. Huffman, P. J. Boul, L. M. Ericson, E. H. Haroz, M. J. O'Connell, K. Smith, D. T. Colbert, R. E. Smalley, *Chem. Phys. Lett.* **2001**, *338*, 14-20.

[217] R. H. Baughman, *Science* **2000**, *290*, 1310-1311.

[218] A. Bianco, K. Kostarelos, C. D. Partidos, M. Prato, *Chem. Commun.* **2005**, 571-577.

[219] D. Pantarotto, J. P. Briand, M. Prato, A. Bianco, *Chem. Commun.* **2004**, 16-17.

[220] X. Chen, U. C. Tam, J. L. Czlapinski, G. S. Lee, D. Rabuka, A. Zettl, C. R. Bertozzi, *J. Am. Chem. Soc.* **2006**, *128*, 6292-6293.

[221] K. C. Patil, *Bull. Mater. Sci.* **1993**, *16*, 533-541.

[222] B. C. Liu, S. C. Lyu, S. I. Jung, H. K. Kang, C. W. Yang, J. W. Park, C. Y. Park, C. J. Lee, *Chem. Phys. Lett.* **2004**, *383*, 104-108.

[223] Y. Li, X. B. Zhang, X. Y. Tao, J. M. Xu, W. Z. Huang, J. H. Luo, Z. Q. Luo, T. Li, F. Liu, Y. Bao, H. J. Geise, *Carbon* **2005**, *43*, 295-301.

[224] D. Jain, A. Winkel, R. Wilhelm, *Small* **2006**, *2*, 752-755.

[225] J. S. Wu, B. El Hamaoui, J. X. Li, L. J. Zhi, U. Kolb, K. Mullen, *Small* **2005**, *1*, 210-212.

[226] B. E. Hamaoui, L. Zhi, J. Wu, J. Li, N. T. Lucas, Z. e. Tomovic´, U. Kolb, K. Müllen, *Adv. Funct. Mater.* **2007**, *17*, 1179-1187.

[227] L. J. Zhi, T. Gorelik, R. Friedlein, J. S. Wu, U. Kolb, W. R. Salaneck, K. Mullen, *Small* **2005**, *1*, 798-801.

[228] C. Z. Wu, X. Zhu, L. L. Ye, C. Z. OuYang, S. Q. Hu, L. Y. Lei, Y. Xie, *Inorg. Chem.* **2006**, *45*, 8543-8550.

[229] J. R. Hamon, D. Astruc, P. Michaud, *J. Am. Chem. Soc.* **1981**, *103*, 758-766.

[230] M. Lacoste, H. Rabaa, D. Astruc, A. Lebeuze, J. Y. Saillard, G. Precigoux, C. Courseille, N. Ardoin, W. Bowyer, *Organometallics* **1989**, *8*, 2233-2242.

[231] Y. Derraz, O. Cyrathis, R. Choukroun, V. Valade, P. Cassoux, F. Dahan, F. Teyssandier, *J. Mater. Chem.* **1995**, *5*, 1775-1778.

[232] G. M. Brown, L. Maya, *Inorg. Chem.* **1989**, *28*, 2007-2010.

[233] H. T. Verkouw, M. E. E. Veldman, C. J. Groenenboom, H. O. Vanoven, H. J. Deliefdemeijer, *J. Organomet. Chem.* **1975**, *102*, 49-56.

[234] K. Jonas, W. Russeler, K. Angermund, C. Kruger, *Angew. Chem., Int. Ed.* **1986**, *25*, 927-928.

[235] S. Delpeux-Ouldriane, K. Szostak, E. Frackowiak, F. Beguin, *Carbon* **2006**, *44*, 814-818.

[236] R. Andrews, D. Jacques, D. Qian, E. C. Dickey, *Carbon* **2001**, *39*, 1681-1687.

[237] R. Choukroun, C. Lorber, *Eur. J. Inorg. Chem.* **2005**, 4683-4692.

[238] S. Eroglu, B. Gallois, *J. Mater. Sci.* **1995**, *30*, 1754-1759.

[239] R. Gupta, M. P. Srivastava, *Plasma Sources Sci. Technol.* **2004**, *13*, 371-374.

[240] V. N. Lipatnikov, A. I. Gusev, *Inorg. Mater.* **2006**, *42*, 14-18.

[241] F. Schlottig, J. Schreckenbach, K. Witke, G. Marx, *Mikrochimica Acta* **1997**, *125*, 161-163.

[242] Y. S. Min, E. J. Bae, W. Park, *J. Am. Chem. Soc.* **2005**, *127*, 8300-8301.

[243] K. J. Ziegler, Z. N. Gu, H. Q. Peng, E. L. Flor, R. H. Hauge, R. E. Smalley, *J. Am. Chem. Soc.* **2005**, *127*, 1541-1547.

[244] N. Pierard, A. Fonseca, Z. Konya, I. Willems, G. Van Tendeloo, J. B. Nagy, *Chem. Phys. Lett.* **2001**, *335*, 1-8.

[245] Y. A. Kim, T. Hayashi, Y. Fukai, M. Endo, T. Yanagisawa, M. S. Dresselhaus, *Chem. Phys. Lett.* **2002**, *355*, 279-284.

[246] G. Korneva, H. H. Ye, Y. Gogotsi, D. Halverson, G. Friedman, J. C. Bradley, K. G. Kornev, *Nano Lett.* **2005**, *5*, 879-884.

[247] W. E. Ford, A. Jung, A. Hirsch, R. Graupner, F. Scholz, A. Yasuda, J. M. Wessels, *Adv. Mater.* **2006**, *18*, 1193-1197.

[248] T. P. Murray, E. R. Austin, R. G. Howard, T. J. Bradford, *Abstr. Pap. Am. Chem. Soc.* **1984**, *188 (Aug.)*, 28.

[249] T. P. Murray, E. R. Austin, R. G. Howard, T. J. Bradford, *Ind. Eng. Chem. Prod. Rd.* **1985**, *24*, 420-425.

[250] S. M. Turega, D. Philp, *Chem. Commun.* **2006**, 3684-3686.

[251] D. Lee, J. Lee, H. Lee, S. Jin, T. Hyeon, B. M. Kim, *Adv. Synth. Catal.* **2006**, *348*, 41-46.

[252] F. Stoffelbach, A. Aqil, C. Jérome, R. Jérome, C. Detrembleur, *Chem. Commun.* **2005**, 4532-4533.

[253] C. G. R. Heald, G. G. Wildgoose, L. Jiang, T. G. J. Jones, R. G. Compton, *Chem. Phys. Chem.* **2004**, *5*, 1794-1799.

[254] R. S. Feinberg, R. B. Merrifield, *Tetrahedron* **1974**, *30*, 3209-3212.

[255] J. M. Tedder, *J. Chem. Soc.* **1957**, 4003-4008.

[256] V. Georgakilas, N. Tagmatarchis, D. Pantarotto, A. Bianco, J. P. Briand, M. Prato, *Chem. Commun.* **2002**, 3050-3051.

[257] J. Chattopadhyay, A. K. Sadana, F. Liang, J. M. Beach, Y. Xiao, R. H. Hauge, W. E. Billups, *Org. Lett.* **2005**, *7*, 4067-4069.

[258] N. Azizi, M. R. Saidi, *Tetrahedron* **2007**, *63*, 888-891.

[259] A. B. Northrup, D. W. C. MacMillan, *J. Am. Chem. Soc.* **2002**, *124*, 2458-2460.

[260] D. F. Shriver, M. A. Drezdon, *The Manipulation of Air-Sensitive Compounds, 2nd Edition, McGraw Hill, New York, USA* **1969**.

[261] Y. Li, X. B. Zhang, X. Y. Tao, J. M. Xu, W. Z. Huang, J. H. Luo, Z. Q. Luo, T. Li, F. Liu, Y. Bao, H. J. Geise, *Carbon* **2005**, *43*, 295-301.

[262] S. C. Lyu, B. C. Liu, T. J. Lee, Z. Y. Liu, C. W. Yang, C. Y. Park, C. J. Lee, *Chem. Commun.* **2003**, 734-735.

[263] S. R. C. Vivekchand, R. Jayakanth, A. Govindaraj, C. N. R. Rao, *Small* **2005**, *1*, 920-923.

[264] Z. L. Zhu, J. H. Espenson, *J. Am. Chem. Soc.* **1997**, *119*, 3507-3512.

7. Curriculum Vitae

Name: Dheeraj Jain
Nationality: Indian
Date and Place of Birth: 05th March 1979; Gaya, Bihar, India.

Academic Records

1997-2003	Integrated Masters of Science (Chemistry) from Indian Institute of Technology, Kanpur, U.P., India.
2003-2004	Research Associate, Nanotechnology, Department of Chemistry, Indian Institute of Technology, Kanpur, U.P., India. Supervisor: Prof. Dr. S. Sarkar
2004-2007	Ph.D., Institut für Organische Chemie, Technische Universität Clausthal, Germany. Thesis title: "Modification and Application of Carbon Nanotubes". Supervisor: Prof. Dr. René Wilhelm

---

Research Publications

1. An easy way to produce α-iron filled multiwalled carbon nanotubes. Dheeraj Jain, René Wilhelm, Carbon, (2007), 45, 602-606.

2. Solid-State Synthesis of Well Defined Carbon Nanocapsules from Organometallic Precursors. Dheeraj Jain, Andreas Winkel and René Wilhelm, Small, (2006), 2, 752-755.

3. Rearrangement of 1,4,5,6-tetrahalo-7,7-dimethoxybicyclo[2.2.1]-hept-5-en-2-ones to phenolic derivatives. Faiz Ahmed Khan, Jyotirmayee Dash, Dheeraj Jain and B. Prabhudas J. Chem. Soc., Perkin Trans. 1, (2001), 3132–3134.

---

8. Zusammenfassung (Abastract)

Carbon nanotubes (CNTs) have been a focus of considerable research since their first observation by Iijima. Their remarkable properties include their interesting mechanical, electrical and thermal conductivity behavior. They offer tremendous opportunities for the development of fundamentally new material systems for application in nanoscale devices, materials, chemistry and in bio-nanotechnology. Due to their widely possible applications, functionalization of single walled (SWCNTs) and multiwalled carbon nanotubes (MWCNTs) with various inorganic and organic substances has become a significant topic of current research interest.

Surfaces of Carbon nanotubes can be modified to incorporate desired properties in nanotubes using approaches that involve either covalent linkage (such as defect targeted or side wall targeted) or non covalent interactions (such as polymer wrapping or π-π stacking). Methods for characterization of these modified nanotubes usually include spectroscopic techniques, such as IR, NMR, Raman, x-ray diffraction pattern (XRD) and energy dispersive x-ray analysis (EDX) and solid phase techniques such as thermal gravimetric analysis (TGA). In addition, microscopic tools such as Scanning electron microscopy (SEM), Transmission electron microscopy (TEM) and atomic force microscopy (AFM) provide valuable visual information on the structure of modified nanotubes.

During the presented work, SWCNTs and MWCNTs were synthesized via CVD process using various known catalysts. As synthesized CNTs and nanotubes obtained from other sources were further purified by a multi-step purification method. Several methods were used to fill SWCNTs and MWCNTs with metal particles - Fe, Pt and Ru. Metal filled nanotubes were further explored to investigate their potential in various chemical reactions. Attempts were made to functionalize iron filled ferromagnetic MWCNTs and use them as a catalyst carrier for various reactions. Several amine functionalized (covalent and non-covalent) nanotubes (SWCNTs and MWCNTs) were prepared and their uses as a catalyst were studied for various reactions like the direct asymmetric Aldol

reaction and enantioselective Diels-Alder reaction. Also the catalytic behavior of iron filled oxidized MWCNTs was studied for an epoxide ring opening reaction.

In addition, organometallic precursors in the solid state pyrolysis for the synthesis of novel carbon nanostructures were studied. The pyrolysis of a CpFe(arene)PF_6 complex gave a new from of carbon structures – carbon nanocapsules in near quantitative yield. Observed experimental results showed that the structure of obtained materials were highly dependent on the complex used and pyrolysis parameters chosen for the experiment. When Ti and V complexes were used for pyrolysis experiments, TiC and VC nanospheres were obtained with nearly quantitative yield. Characterization of such new nanostructures was done by HRTEM, EDX and XRD.

9. Acknowledgements

On the first place, I owe a sincere word of gratitude to my supervisor Prof. Dr. René Wilhelm whose excellent guidance and support has made me complete my project. He has been a constant source of inspiration to me. He has also molded my outlook towards chemistry in general and organic synthesis in particular. With all that he gave me even after that if I felt lost or dejected sometime he was always ready to boost my morale and helped me with my work.

I would also like to thank Prof. Dr. Dieter Kaufmann for being a co-referee of this work and for his support during my stay at the Institut für Organische Chemie.

I express my heartfelt thanks to my lab-mates, Vaclav Jurcik, Amélie Blanrue, Nicole Clemens, Christian Torborg, Tobias Berghoff, Andreas Winkel, Oksana Sereda, Dr. Vasu Peddiahgari Reddy, Mazhar Gilani and Sobia Tabassum for the touch of camaraderie they brought to the lab.

I express my thanks to all the coworkers in the Institut für Organische Chemie for their kind cooperation and for making the institute a wonderful place to work.

The technical staff of Institut für Organische Chemie plays an important role in any scientific work performed in the institute, therefore I would like to thank Dr. Jan Namyslo, Claudia Stanitzek and Birgit Stövesant for measuring the NMR spectra. Apart from that I owe sincere thanks to Christian Meyer for helping me out with GC measurement and Frank Stiemke for IR measurements. Special thanks to our glass blower Roland Zain for providing me with the needful glass apparatus and more importantly with quartz tubes for my experiments. I thank to PD Dr. Andreas Schimidt for giving me the friendly moments time to time with his cheerful nature.

I thank to Mr. Nietzel from the Institut für Physik und Physikalische Technologien, Dr. Michael Siemann and Dr. Mikhail Tsypukov from the Institut für

Mineralogie und Mineralische Rohstoffe for XRD and Raman measurements, Dr. Ilya Reviakine and Pattrawin Gasemjit from the Institut für Physikalische Chemie for AFM analyses, Dr. Milos from the Institut für Werkstoffkunde und Werkstofftechnik for TEM measurements and Petra Droettboom also from the Institut für Werkstoffkunde und Werkstofftechnik for TGA measurements. I also extend my word of gratitude to Dr. Wilbrandt and Mr. Hahn from the Institute for Material Physics at the University of Göttingen for the possibility to perform TEM measurements. Moreover, I thank PD Dr. Michael Seibt and Tore Niermann from the Institute of Physics at the University of Göttingen for HRTEM and EDX measurements.

Also financial support by Fonds der Chemischen Industrie and DFG (WI 2147/2-1) is gratefully acknowledged.

I am indebted to the Institut für Organische Chemie for providing me with the best of everything and exposing me to the latest and the city of Clausthal for nourishing me with its beautiful scenic view.

Finally I would like to say an affectionate word of thanks to my family and friends for their love and encouragement. Their contribution is unparallel and indescribable.